Process intensification of biodiesel production from algae using foam flotation column

A thesis submitted by

Salihu Danlami Musa

For the Degree of Doctor of Philosophy

School of Engineering
Newcastle University

January 2020

Abstract

To achieve cost effective biodiesel production from microalgae, the elimination of drying steps (responsible for about 84.1 % of process energy cost) is the single most important strategy to adopt. This project looks at combining three major components of algal biodiesel production, namely: harvesting, oil extraction, and transesterification into a one-unit operation. The intensified process hereby proposed, combines the advantage of three main ingredients to achieve its aim. Cell lysing, frothing and algae cell capture by surfactants; hydrophobicity inducement, cell lysing, as well as catalyst properties of acid; and the oil extraction and reactant properties of methanol, were combined in the process.

The effect of operating condition (airflow), surfactant type (CTAB, MTAB, DAH, & DPC); and concentration, and media chemistry (pH and ionic strength) on the foam flotation harvesting of marine algae (*N. oculata*) was investigated. The impacts of cell properties (size, morphology, hydrophobicity, and surface charge) were also studied. Using 20 mg L^{-1} CTAB, 1.2 L min^{-1} air flow, at pH 6, the highest enrichment ratio of 14 was achieved in 77 % of cells recovered. When airflow and CTAB were 3.6 L min^{-1} and 60 mg L^{-1}, respectively, 83 % of cells were recovered, albeit a low enrichment of 4. Cell properties (morphology, hydrophobicity, and surface charge) and media chemistry (pH and ionic strength) are strong determinants of flotation performance. The results suggest that foam flotation harvesting of *N. oculata* is more collision dependent than attachment controlled and the frequency of collision and attachment can be enhanced by reducing ionic strength as well as pH whilst increasing airflow.

As a prerequisite for biodiesel production from algae in a flotation column, foam stability as well as efficient methanol injection must be guaranteed. The impact of methanol and its injection pattern on flotation process has been investigated. For foam stability to occur, the percentage of methanol in the liquid pool must not exceed 50 % wt./wt. Using 50 % methanol

in a *C. vulgaris* culture, 98 % of cells (CF =18.3) were recovered via cocurrent methanol injection foam floatation, while moisture content (water and methanol) was 156 wt. %. Countercurrent methanol injection into the column top was achieved with the aid of methanol distributors. This countercurrent methanol delivery system guarantees more effective and economic methanol usage than cocurrent methanol injection, delivering methanol at 76 % concentration.

Using the countercurrent methanol feed system in a riser-enabled column, it was possible to convert *D. salina* lipids to biodiesel with yields of 9.3 ± 0.2 and 11.2 ± 0.3% after 1 and 24 h respectively without any additional dewatering processes. Besides the novelty of this process, it has potential for huge reduction in cost of production, due to cost savings by elimination of drying. However, these levels of yield have to be improved on in order to ensure profitability. To this end, it is expected that the concept demonstrated by this work will rekindle hope that was once associated with algal biodiesel as an alternative to liquid fossil fuels.

Dedication

This work is dedicated to Maulana Sheikh Ibrahim Inyass (R T A) and to the memory of my late father, Ret. Navy Lieutenant Salihu Musa Adoga. May your soul rest in eternal peace, daddy (Ameen thumma Ameen).

Acknowledgements

In the first place, all thanks and glory be unto God almighty for the gift of life, health, wisdom, and faith, through which I was able to attain this feat. I would like to express my sincere gratitude and appreciation to Dr. Jonathan Lee and Dr Gary Caldwell for supervising this work and for their guidance and encouragement in the course of this research. Their wealth of experience and expertise; and regular discussions were helpful in finishing up; and I have learnt a great deal from working with them. I would like to thank them for the time taken to read through the first draft of this dissertation and their constructive criticism and recommendations.

I would like to also acknowledge Dr. Jonathan McDonough for his help with 3D printing. Similarly, I wish to thank the entire members of the process intensification group, especially Professor Adam Harvey who has been a major pillar of support right from the beginning of my PhD.

Also, worth mentioning are the technicians like Stewart Latimer, Rob Dixon, Ian Strong, Michael Percival, Paul Sterling, Kevin Brown, Ashley Craig, Peter McParlin, David Whitaker, and the rest of the team for their technical support. I appreciate you all!

Without the sponsorship from the Petroleum Technology Development Fund (PTDF), this research would not have come to pass, so I wholeheartedly thank the organisation and the government of Nigeria for their support.

My sincere gratitude also goes to the SuperGen Bioenergy Hub for supporting my research with a £50,000 in research grant, as a result of which I was able to build the flotation column that was used in this work.

Finally, I would like to say a big thank you to my mum, my wife, my sons, Maulud, and Walid, my daughter Ta'bah, and all my friends for their support, love and encouragement.

Table of contents

Abstract....ii

Dedication....iv

Acknowledgements....v

Table of contents....vi

List of figures....x

List of tables....xv

Chapter 1 Introduction....1

1.1 Project Background....1

1.2 Biofuels....3

1.3 Microalgae as feedstock for biodiesel....6

1.4 Freshwater Vs Marine Algae as potential biodiesel feedstock....8

1.5 Problem statement....9

1.6 Aims and objectives....10

1.7 Dissertation outline and summary of chapters....11

Chapter 2 Literature Review....13

Abstract....13

2.1 Introduction....14

2.2 Algae cultivation process....14

2.3 Harvesting of Algae....15

2.3.1 Flocculation....16

2.3.2 Filtration....18

2.3.3 Centrifugation....19

2.3.4 Flotation....20

2.3.5 Factors affecting dispersed air (foam) flotation....23

2.3.6 Foam Flotation recovery of marine algae....29

2.3.7 The DLVO theory and zeta potential....30

2.4 Drying and processing of microalgae ***34***

2.4.1 Algae cell disruption and Oil extraction 35

2.4.2 Oil extraction from dried feedstock 36

2.4.3 Wet oil extraction process 36

2.5 Biodiesel from algae ***37***

2.5.1 Pyrolysis of biomass or algal oil 38

2.5.2 Transesterification 38

2.6 Alcohol-water- surfactant-air interactions ***41***

2.7 Conversion of wet biomass and the need for an intensified biodiesel production from wet algae ***43***

2.8 Conclusion ***45***

Chapter 3 Foam flotation harvesting of *Nannochloropsis oculata* 47

3.1 Introduction ***48***

3.2 Materials and Methods ***50***

3.2.1 Algae cultivation 51

3.2.2 Foam flotation: Column description 52

3.2.3 Foam flotation: impact of cell size and morphology 54

3.2.4 Surfactant screening and investigation of the impacts of airflow, ionic strength, and pH on foam flotation harvesting of *N. oculata* 56

3.2.5 Effect of CTAB concentration on Zeta (ζ) potential 58

3.2.6 Hydrophobicity as a function of CTAB concentration 59

3.2.7 Surface tension as a function of CTAB 60

3.3 Results and discussion ***60***

3.3.1 Recovery of *N. oculata* in freshwater and seawater 60

3.3.2 Recovery of beads from freshwater, seawater, and *N. oculata* medium 61

3.3.3 Recovery of *C. vulgaris* in seawater and *N. oculata* medium 62

3.3.4 Effect of airflow, surfactant and media chemistry on foam flotation of *N. oculata* 63

3.3.5 Effect of CTAB, pH, and CTAB-organic matter complexes on ζ- potential and hydrophobicity 79

3.3.6 DLVO explanation of foam flotation of *N. oculata* 89

3.4 Conclusion ***92***

Chapter 4 Effective methanol injection - a prerequisite for biodiesel production in a foam column 95

4.1 Introduction 95

4.1.1 Pseudo steady state and methanol balance across a flotation column 100

4.2 Materials and methods 102

4.2.1 Measurement of surface tension, refractive index, density, and pressure 102

4.2.2 Foam flotation experiments 104

4.2.3 Distributor design 113

4.3 Results and discussion 117

4.3.1 Effect of methanol on surface tension 117

4.3.2 Foam stability and algae recovery as a function CTAB and methanol 118

4.3.3 Methanol injection in foam flotation – quantitative and qualitative analysis 120

4.3.4 Improved methanol enrichment using distributors (countercurrent flotation) 129

4.3.5 Methanol balance- effect of contractions on accumulation rate of methanol 134

4.4 Conclusion 137

Chapter 5 Process intensification of biodiesel production: coupling the harvesting and reactive extraction of *Dunaliella salina* within a foam column 139

5.1 Introduction 139

5.2 Materials and method 143

5.2.1 Cultivation of *Dunaliella salina* 143

5.2.2 Flotation harvesting of *Dunaliella salina* 143

5.2.3 Quantification of lipid in *D. salina* and determination of maximum biodiesel yield 145

5.2.4 Analysis of cell lysis by CTAB treatment 146

5.2.5 Combined harvesting and reactive extraction of D. salina using foam flotation 146

5.2.6 Analysis of biodiesel production 147

5.2.7 Cost analysis and process economy 148

5.3 Results and discussion 149

5.3.1 Foam flotation: Effect of column design, CTAB, and airflow 150

5.3.2 Lipid content of *D. salina* 154

5.3.3 Cell lysis: Effect of CTAB 154

5.3.4 Biodiesel production: Effect of reaction time 155

5.3.5 Cost analysis 158

5.4 Conclusions ***160***

Chapter 6 Conclusion and recommendations for future work 162

6.1 Conclusions ***162***

6.2 Recommendations ***166***

References 168

Appendices 188

List of figures

Figure 1.1: 2018 Global energy outlook showing energy consumption based on fuels 2

Figure 1.2: 2018 EU energy outlook showing energy consumption based on fuels 3

Figure 1.3: global consumption of renewable energy in 2017; CIS implies to Commonwealth of Independent States (13.9% of EU's consumption is in the UK) 4

Figure 1.4: Biofuels production by regions in 2018 5

Figure 1.5: : Potentials of microalgae cells *[19]* 8

Figure 2.1: (A)Diagram showing the various components of a raceway according to [25]); B) An example of open raceway pond owned by the Cyanotech Corporation Kona, Hawaii (credited to Cyanotech Corporation) [19] 15

Figure 2.2: Closed systems of cultivation: A) Horizontal tubular (credited to Dan Brookshear); B) Bag culture (Photo by Robert Clark); C) Vertical tubular (Photo by Robert Clark); D) Vertical flat plate at Arizona State University. [19] 15

Figure 2.3: Schematics of the operations of a Dissolved Air Flotation (DiAF) for wastewater treatment; Courtesy chemiocalonline.com (https://www.chemicalonline.com/doc/chem-show-99-pump-eliminates-need-for-daf-air-0001) 21

Figure 2.4: Pictorial representation of Electrocoagulation process credited to Milton Andrade [116] 22

Figure 2.5: Schematics of a simple flotation column for microalgae recovery 23

Figure 2.6: Electrical double layer with respect to a negatively charged particle in a solution 31

Figure 2.7: Illustration of the DLVO theory; V_T=Total potential, V_A= Potential due to attractive Vander Waals forces and V_R= Repulsive double layer (electrostatic coulomb) forces 31

Figure 2.8: Figure 6. Cell disruption methods (Modified from [184]) 35

Figure 2.9: Mechanism of biodiesel production from vegetable oil 39

Figure 3.1: Description of the flotation operation showing a continuous flotation run 53

Figure 3.2: Set up of ZEN 3600 Zetasizer; about 2 mL of sample is injected into the folded capillary and secured with the aid of two provisioned caps for each end before being inserted into the zetsasizer via the sample loader. 58

Figure 3.3: Effect of process conditions on concentration factor using CTAB of varying concentrations with undiluted cultures; n=2, R^2 = 0.978 64

Figure 0.4: Effect of process conditions on recovery using CTAB of varying concentrations with undiluted cultures; n=2, R^2 = 0.988 64

Figure 3.5: Effect of process conditions on concentration factor using MTAB of varying concentrations with undiluted cultures; n=2, R^2 = 0.990 65

Figure 3.6: Effect of process conditions on recovery using MTAB of varying concentrations with undiluted cultures; n=2, R^2 = 0.986 66

Figure 3.7: Effect of process conditions on concentration factor using DAH of varying concentrations with undiluted cultures; n=2, R^2 = 0.993 67

Figure 3.8: Effect of process conditions on recovery using DAH of varying concentrations with undiluted cultures; n=2, R^2 = 0.990 68

Figure 3.9: Effect of process conditions on concentration factor, using DPC of varying concentrations with undiluted cultures; n=2, R^2 = 0.985 69

Figure 3.10: Effect of process conditions on recovery, using DPC of varying concentrations with undiluted cultures; n=2, R^2 = 0.994. 70

Figure 3.11: Effect of process conditions on concentration factor using CTAB of varying concentrations with half diluted culture of *N. oculata*; R^2 = 0.977 71

Figure 3.12: Effect of process conditions on recovery using CTAB of varying concentrations on half diluted culture of *N. oculata*; R^2 = 0.987 72

Figure 3.13: Effect of process conditions on concentration factor using MTAB of varying concentrations with half diluted culture of *N. oculata*; n=2, R^2 = 0.99 73

Figure 3.14: Effect of process conditions on recovery using MTAB of varying concentrations with half diluted culture of *N. oculata*; n=2, R^2 = 0.986 74

Figure 3.15: Effect of process conditions on concentration factor using DAH of varying concentrations with half diluted culture of *N. oculata*; n=2, R^2 = 0.991 75

Figure 3.16: Effect of process conditions on recovery using DAH of varying concentrations with half diluted culture of *N. oculata*; n=2, R^2 = 0.989 75

Figure 0.17: Effect of process conditions on concentration factor using DPC of varying concentrations with half diluted culture of *N. oculata*; n=2, R^2 = 0.99 76

Figure 3.18: Effect of process conditions on recovery using DPC of varying concentrations with half diluted culture of *N. oculata*; n=2, R^2 = 0.994 77

Figure 3.19: Comparison of changes in ζ-potential of beads and *N. oculata* with change in CTAB concentrations; concentration is 1.3 g L^{-1} (DW); B-FW, B-SW, N-FW, and N-F/2 represent beads suspended in freshwater, beads suspended in seawater, *N. oculata* suspended in freshwater, and *N. oculata* in original media, respectively 80

Figure 3.20: Variations in ζ-potential s of beads, *N. oculata*, and *C. vulgaris* in various media with CTAB concentration; colloid concentration is 0.65 g L^{-1}; B-FW, B-NS, B-F/2, C-FW, C-F/2, N-FW, N-F/2, and N-SW represent beads suspended in freshwater, beads suspended in freshwater in *N. oculata* supernatant, beads suspended in f/2, *C. vulgaris* suspended in freshwater, *C. vulgaris* suspended in f/2, *N. oculata* suspended in freshwater, *N. oculata*

suspended in f/2, and *N. oculata* suspended in seawater, respectively 82

Figure 3.21: Effect of pH on ζ-potential of *N. oculata* in f/2 media with respect to changes in CTAB concentration 84

Figure 3.22: Influence of pH on hydrophobicity of *N. oculata*; Fractional distribution is hereby used in order to indicate the interaction between CTAB and salt ions that leaves precipitates that interfere with the absorbance readings 85

Figure 3.23: Hydrophobicity of *N. oculata* as a function CTAB; The effect of salt ions was eliminated by subtracting the absorbance when hexane was added from that in which no hexane was added and presented as deduced hydrophobicity 86

Figure 3.24: Interaction between CTAB and sweater as it affects absorbance; ; N-SW, N-FW, SW, and FW represents mixture of *N.oculata* supernatant and seawater, mixture of *N.oculata* supernatant and freshwater, seawater, and freshwater, respectively 87

Figure 3.25: Suspended CTAB-organic matter complex; at 90 mg L^{-1} (A), there is higher concentration of the suspension than in B)when CTAB concentration was 30 mg L^{-1} 88

Figure 3.26: Surface tension changes with CTAB concentration for seawater and *N. Oculata* medium; NS, SW-HX, SW, and NS-HX represents *N. oculata* supernatant, mixture of seawater and hexane, seawater, and mixture of *N.oculata* supernatant and hexane, respectively 88

Figure 3.27: DLVO interpretation of Nannochloropsis cells under fresh water conditions; ζ potential of -32mV, pH 7; VD, VH, and VT are electrostatic repulsive forces, Vander Waals attractive forces, and Total system energy or potentials, respectively 91

Figure 3.28: DLVO interpretation of Nannochloropsis cells in f/2 medium; ζ-potential 0f -8mV, pH 8; VD, VH, and VT are electrostatic repulsive forces, Vander Waals attractive forces, and total system energy or potentials, respectively 92

Figure 4.1: Process flow diagram for methanol concentration using foam column; ^{M}Methanol, ^{U}Underflow, ^{F}Feed, and ^{T}Top 101

Figure 4.2: Modified flotation column with riser section and methanol injection line; the methanol distributor is connected to methanol feed bottle with the aid of grooves of external diameter equal to the internal diameter of the PVC hose that serves as feed line. 105

Figure 4.3: Process flowsheet for the flotation system; the example here is that of the cocurrent continuous methanol process and it is assumed that no surfactants are found in the underflow 106

Figure 4.4: Cocurrent recovery of *C. vulgaris* and methanol enrichment in a batch operated column of 100 cm height; methanol concentration in the feed was varied from 25 to 75 vol. % at 30-350 mg L^{-1} CTAB, airflow was 1 L min^{-1}, and feed rate was 50 mL min^{-1} 107

Figure 4.5: Countercurrent recovery of *C. vulgaris* and methanol injection in a batch operated column of 100 cm height; methanol concentration in the feed was varied from 25 to 75 vol. % at 30-350 mg L^{-1} CTAB, airflow was 1 L min^{-1}, and feed rate was 50 mL min^{-1} 108

Figure 4.6: Flow diagram for batch flotation of 10 wt. % methanol in water in a cocurrent methanol process; n=2 109

Figure 4.7: Continuous methanol injection in a cocurrent flotation process; Process conditions were varied based on the factorial design in Table 4.2.....111

Figure 4.8: : Methanol injection in a countercurrent continuous flotation process; feed rate was 32 g min^{-1}, liquid level was 30 cm, column height was 135 cm, distributor size 0.5 – 3mm, and 40 - 60 mg kg^{-1} CTAB. 113

Figure 4.9: Formlabs 3D Desktop printer with Form 2 SLA provisions.....114

Figure 4.10: Example of methanol distributor (1mm holes).....114

Figure 4.11: Schematics of glass contraction section fitted to increase methanol concentration and reduce accumulation of methanol 116

Figure 4.12: Measured surface tension as a function of volume fraction of methanol in water at different CTAB concentrations; CMC of surfactant is 360 mg L^{-1} 118

Figure 4.13: Main and interaction effects of major process parameters on the percentage of methanol in the foamate during batch flotation of 10 wt. %; n=2, R^2=0.97.....121

Figure 4.14: Main effects of major process parameters on the mass of methanol in the foamate during batch flotation of 10 wt. % methanol; n=2, R^2=0.99.....122

Figure 4.15: Main and interaction effects of major process parameters on the percentage of methanol in the foamate during batch flotation of 10 wt. %; n=2, R^2=0.97.....124

Figure 4.16: Interaction effects of major process parameters on the mass of methanol in the foamate during batch flotation of 10 wt. % methanol; n=2, R^2=0.99.....123

Figure 4.17: Main effects of some major process parameters on the mass of methanol in the foamate during a continuous flotation of 10 wt. % methanol feed; airflow (0.7- 2.4 L min^{-1}), feed (77-333 g min^{-1}), CTAB (40- 100 mg Kg^{-1}), runtime (15 - 45 min), and column height (60 -120 cm), n=2, R^2= 1 124

Figure 4.18: Main effects of major process parameters on the percentage of methanol in the foamate during a continuous flotation of 10 wt. % methanol feed; airflow (0.7- 2.4 L min^{-1}), feed (77-333 g min^{-1}), CTAB (40- 100 mg Kg^{-1}), runtime (15- 45 min), and column height (60 -120 cm), n=2, R^2=0.99 125

Figure 4.19: Interaction effects of major process parameters on the mass of methanol in the foamate during a continuous flotation of 10 wt. % methanol feed; n=2, R^2=1 126

Figure 4.20: Interaction effects of major process parameters on the percentage of methanol in the foamate during a continuous flotation of 10 wt. % methanol feed; n=2, R^2=0.99 127

Figure 4.21: Plots of main effects of process parameters on mass of methanol at the top during the continuous flotation using methanol distributors at 1.5 g min^{-1}, airflow of 2.4 L min^{-1}, liquid height of 30cm and a column height of 135cm; R^2=98.7, n=2 130

Figure 4.22: Plots of interaction between process parameters on mass of methanol at the top during the continuous flotation using methanol distributors at 1.5 g min^{-1}, airflow of 2.4 L min^{-1}, liquid height of 30cm and a column height of 135cm; R^2=98.7, n=2 131

Figure 4.23: Mass of methanol as a function of CTAB concentration and distributor size during continuous flotation using methanol distributors at 1.5 g min^{-1}, airflow of 2.4 L min^{-1}, liquid height of 30 cm and a column height of 135 cm; R^2=98.7, n=2.....131

Figure 4.24: Plots of main process parameters on percentage of methanol at the top during the continuous flotation using methanol distributors at 1.5 g min^{-1}, airflow of 2.4 L min^{-1}, liquid height of 30 cm and a column height of 135 cm ; R^2=98.3, n=2 132

Figure 4.25: Plots of interaction between process parameters on percentage of methanol at the top during the continuous flotation using methanol distributors at 1.5 g min^{-1}, airflow of 2.4 L min^{-1}, liquid height of 30 cm and a column height of 135 cm; R^2=98.3, n=2.....133

Figure 4.26: Contour plots of the effect CTAB concentration and distributor sizes on percentage of methanol at the top during the continuous flotation using methanol distributors at 1.5 g min^{-1}, airflow of 2.4 L min^{-1}, liquid height of 30 cm and a column height of 135 cm ; R^2=98.3, n=2 133

Figure 4.27: Example of a pressure profile measured at 2 L min^{-1} air; 4.5 g min^{-1} methanol; 100 mg kg^{-1} CTAB; 135 cm column height; 32 g min^{-1} and 16 g min^{-1} feed and bottom rates, respectively. 135

Figure 5.1: Calibration curve for optical density as a function of *D. salina* cell concentration @ 670 nm wavelength: initial cell concentration was 256 mg L^{-1} of culture and was concentrated to 256 mg in 50 mL (20 X) through mild centrifugation @ 1000 rev for 1 minute; the final concentration and 1L of initial sample were diluted serially. The least dilution was obtained at 5 X dilution of initial culture 145

Figure 5.2: *Dunaliella salina* cells (A) without and (B) after treatment with 50 mg L^{-1} CTAB. X100 magnification. 154

List of tables

Table 2.1: Other flotation separation processes 29

Table 3.1: Composite design of experiments for foam flotation of *N. oculata*; liquid height is 20 cm and column height was maintained at 135 cm, flotations were carried out in continuous modes. 58

Table 3.2: Summary of recovery and concentration factor for flotation process using a column height of 135 cm and airflow of 1 L min^{-1} ; B-FW, B-NS, B-F/2, C-FW, C-F/2, N-FW, N, and N-SW represent beads suspended in freshwater, beads suspended in freshwater in *N. oculata* supernatant, beads suspended in F/2, *C. vulgaris* suspended in freshwater, *C. vulgaris* suspended in f/2, *N. oculata* suspended in freshwater, *N. oculata* in original media, and *N. oculata* suspended in seawater, respectively 61

Table 4.1: Composite design for batch flotation of 10 wt. % methanol in water in a cocurrent methanol process; n=2 110

Table 4.2: ½ Factorial design to check the impact of all process parameters on continuous methanol concentration and wt. % in foamate; n=2 112

Table 4.3: Composite design of experiments for countercurrent methanol stream in a continuous flotation system, feed rate was 32 g min^{-1}, liquid level was 30cm, column height was 120 cm when contraction is involved otherwise it is 135 cm ; n=2 115

Table 4.4: Summary of results of foam flotation harvesting of *C. vulgaris* in the presence of methanol; S and NS stand for stable and nonstable foams respectively: Airflow was 1 L $min^{-1}$and the column height was 100 cm. CMC of CTAB is 360 mg L^{-1} 119

Table 4.5: Methanol balance across 135 cm long column at airflow rate of 2 L min^{-1} under continuous process using 2 mm holes distributors, measured at 10 minute of reaction. M – methanol, U – underflow, Acc. – methanol accumulation measured at 12 min 135

Table 4.6: Effect of constriction (1/5) on rate of accumulation in a 120 cm column with constriction between 90 and 105 cm at airflow rate of 2 L min^{-1} using 2 mm holes distributors, measured at 10 minute of reaction. M – methanol, U – underflow, Acc. – methanol accumulation measured at 12 min 136

Table 5.1: Effect of constriction presence on flotation harvest performance; column height was 120 cm with constriction and 135 cm without, feed and bottom rates were 32 and 16 g min^{-1} respectively. Normal material stream compositions were: 20 mg L^{-1} chitosan, 30 mg L^{-1} saponin, 50 mg L^{-1} CTAB, and 1.5 g L^{-1} methanol. 145

Table 5.2: Trial experiments on *D. salina* using a 135 cm height column without a riser and a 120 cm with riser (0.2); airflow of 2.4 L min^{-1} 151

Table 5.3: Effect of contraction on the recovery % and concentration factor (CF) of *D. salina.* Operating conditions of 20 mg L^{-1} chitosan, 30 mg L^{-1} saponin, 50 mg L^{-1} CTAB and 1.5 g L^{-1} methanol. 151

Table 5.4: Effect of mixing pattern with contraction on the recovery and concentration factor

(CF) of *D. salina*. Operating conditions: airflow of 3.6 L min^{-1} with constriction, 20 mg L^{-1} chitosan, 30 mg L^{-1} saponin, 50 mg L^{-1} CTAB and 1.5 g L^{-1} methanol. 152

Table 5.5: Effect of dilution on recovery and concentration factor (CF) of *D. salina* at a reduced CTAB concentration. Operating conditions*:* airflow of 3.6 L min^{-1} with constriction, 20 mg L^{-1} chitosan, 30 mg L^{-1} saponin, 30 mg L^{-1} CTAB and 1.5 g L^{-1} methanol. 152

Table 5.6: Effect of airflow at low CTAB concentration with constriction on the recovery % and concentration factor (CF) of *D. salina.* Operating conditions*:* 20 mg L^{-1} chitosan, 30 mg L^{-1} saponin, 30 mg L^{-1} CTAB and 1.5 g L^{-1} methanol.....153

Table 5.7: Effect of airflow at high CTAB with constriction on recovery and concentration factor (CF) of *D. salina*. Operating conditions*:* 20 mg L^{-1} chitosan, 30 mg L^{-1} saponin, 50 mg L^{-1} CTAB and 1.5 g L^{-1} methanol.....153

Table 5.8: Cost estimation of harvesting 1 m^3 of *D. salina* through foam flotation. The airflow and feedflow were 2.4 L min^{-1} and 0.05 L min^{-1} (32 g min^{-1}).....158

List of Abbreviations and notations

Abbreviations

BSA	Bovine serum albumin
CCD	Central composite design
CF	Concentration factor
CMC	Critical micelle concentration
CTAB	Cetyltrimethylammonium bromide
DAF	Dissolved air flotation
DAG	Diacylglycerol
DAH	Dodecylammonium hydrochloride
DCM	Dichloromethane
DFF	Direct flow filtration
DiAF	Dispersed air flotation
DOE	Design of experiment or US Department of energy
DPC	Dodecyl pyridinium chloride
DW	Dry weight basis
EOM	Extracellular organic matter
EPS	Extracellular polymer substances
FAEE	Fatty acid ethyl ester
FAME	Fatty acid methyl ester
FFA	Free fatty acids
FID	Flame ionisation detector
GHG	Greenhouse gas
HTL	Hydrothermal liquefaction
MAG	Monoacylglycerol
MTAB	Myristyltrimethylammonium bromide
SDS	Sodium dodecylsulphate
SS	Steady state
TAG	Triacylglycerol

Notations

A	Hamaker constant
Acc.	Accumulation rate of methanol
A_{Ei}	Area under the standard peak for FAME
B-F/2	Polystyrene beads suspended in f/2
B-FW	Polystyrene beads suspended in freshwater
B-NS	Polystyrene beads suspended in supernatant recovered from *N. oculata* culture
C	Concentration of FAME in a sample
C_{Ei}	Concentration of standard FAME
CF	Concentration factor
C-F/2	*C. vulgaris* suspended in f/2
C-FW	*C. vulgaris* suspended in freshwater
C-NS	*C. vulgaris* suspended supernatant recovered from *N. oculata* culture
DWC	Dry weight concentration
E	Electrophoretic mobility
e	Charge on an electron
EDL	Electric double layer
F	Feed flow rate
FW	Freshwater
g	Acceleration due to gravity
H	Hydrophobicity
k	Boltzmann's constant
m	Sample mass
M	Methanol injection rate
M_f	Mass of methanol in the column
n	Number of moles of substance
N-FW	*N. oculata* suspended in freshwater
N-SW	*N. oculata* suspended in seawater
P	Total pressure
P_0	Pressure upstream of the compressor
P_1	Pressure of the compressed gas
R	Universal gas constant
RE	Recovery efficiency
SW	Seawater
t	Flotation time
T	Temperature
T_o	Absolute initial temperature
Top	Foamate flow rate
U	Rate of underflow
v	volume of substance
VD	Double layer electrostatic repulsive forces

V_{Ei}	Volume of standard FAME
VH	Vander Waals attractive forces
VT	Total system energy or potentials
W_{comp}	Compressor work
$X_{m,F}$	Composition of methanol in the feed stream
$X_{m,M}$	Composition of methanol in the methanol stream
$X_{m,T}$	Composition of methanol in the top stream
$X_{m,U}$	Composition of methanol in the underflow stream
Z	Column height

Greek letters

Γ	surface excess
ε	Permittivity
ν_i	Electron valency
n_i	Valency number on an ionic specie
k^{-1}	Permittivity of suspension medium
λ	Correlation length of molecules in a suspension medium
ϕ_l	Liquid hold up
ζ	Zeta potential
τ_p	Perimeter of tension probe
μ	Liquid viscosity
η_{is}	Efficiency of air compressor
ρ_l	Liquid density
ρg	Gas density
γ	Surface tension

Chapter 1
Introduction

1.1 Project Background

The industrial economy of the world is predominantly dependent upon fossil fuels (oil, gas and coal) which has been at the centre stage of important geopolitical developments for several decades [1]. In 2019, fossil fuels accounted for 84.3 % (Fig. 1.1) of total global energy consumption [2]. In Europe, 73.6 % of fuels consumed in 2019 were fossils (Fig. 1.2). The heavy reliance of the global economy on fossil fuels is threatened by the dual challenge of supply insecurity and climate change issues. There are projections suggesting that the world's reserve of oil and gas will run out around the middle of this century to be followed by coal sixty years after [3]. Jeffrey Rissman has a contrary and rather optimistic projection of the fate of fossil fuel. He rightly argued that the process of decomposition and eventual conversion of dead organic matter is an ongoing process. Therefore, the prospect of oil discoveries will remain open for the foreseeable future [4]. While it is true that the process of organic matter diagenesis is continuous, the current rate of oil exploration is unprecedented and might outstrip the natural rate of regeneration. In addition, the environmental footprint of fossil fuels is still a growing concern particularly as related to greenhouse gas emissions. This concern has led to the mobilisation of global efforts towards diversification of energy sources and addressing the menace of climate change. The resolution of the COP 21 conference held in Paris [5] and the thrust of goal-7 of the sustainable development goal of the United Nations [6] bears testimony to the global consensus towards mainstreaming renewable energy in the global energy mix. The COP 21 conference represented a major landmark achievement in the effort to combat climate change.

In spite of the global increase (as high as 40 % in some sectors) in CO_2 emission over the last 12 years, the emission in the EU have seen a decline from all the CO_2 indices, namely: power (-21 %); building (-21 %); transport (- 6%); other industrial combustion (-21 %); other sectors (-6 %) [7]. Judging from the trend, it could be said that the UK is committed to reducing its CO_2 emission, but there is always room for improvement especially when the sustainability of fossil fuels is critically looked at. Based on 2018 data,

the UK accounts for 394.1 kilotons (1.2 % of global) CO_2 emission out of 208 countries sampled. While this percentage may appear small, it is one-third of all the CO_2 generated by the African continent.

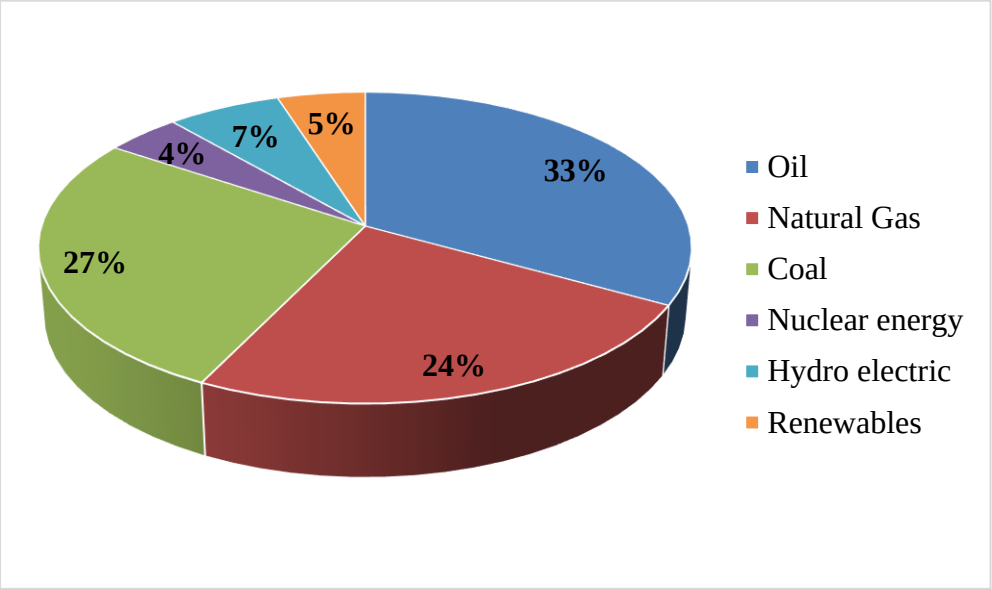

Figure 1.1: 2019 Global energy outlook showing energy consumption based on fuels

Decarbonisation of the transport sector has been a major talking point in every major discuss that is related to environmental safety and CO_2 mitigation. This is rightly so because the transport sector is the biggest contributor after the energy sector, to global warming according to a report by United Nations' Food and Agriculture Organisation (UNFAO) in 2017. This has led to an increase in the number of research works dedicated to finding alternative and renewable sources of energy with potential to cater for the transport sector. But for the prohibitive cost of production, biofuels are one of the most favoured alternatives to liquid fossil fuels. In an effort to make biodiesel commercially viable and sustainable, microalgae as feedstock has received a lot of attention, especially in the last four decades due to their numerous advantages over terrestrial plants. However, the cost of recovering and drying of algal biomass has created an even wider gap in terms of cost competitiveness with fossil fuels. Biomass is seen to be a major source of renewable energy in the EU beyond 2030 because relying on electric cars alone can only account for a mere 3% of renewables in the transport sector, hence the need to pay attention to liquid biofuels as they have the capacity to power the remaining 97% of non-electric cars.

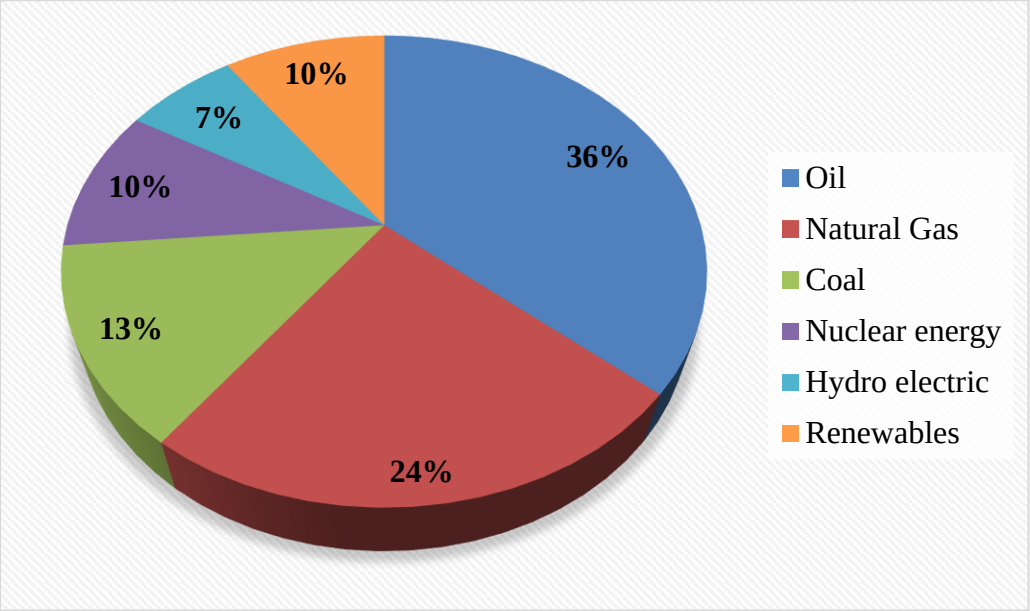

Figure 1.2: 2019 EU energy outlook showing energy consumption based on fuels

1.2 Biofuels

Biofuel refers to any hydrocarbon fuel that is produced from organic matter (living or otherwise) by converting the products of carbon fixation thereof into energy for mechanical, heating, and other purposes. Unlike fossil fuels, biofuels take between days and months to form, making them more sustainable than fossil fuels, which takes millions of years to form. Because they utilise CO_2, biofuels are thought to be cleaner and by this, their use is considered a good way to reducing global warming. Examples of biofuels are: biodiesel, bio-alcohols, biogas, hydrogen, bio-oils, and bio-syngas [8].

Solid biofuels such as wood, charcoal and dung have been used since the discovery of fire and are still being used today in many rural communities for cooking and heating [9, 10]. Liquid biofuels such as plant and animal oils have been used for lighting and transportation. Indeed the first fuel ever tested on a diesel engine, over hundred years ago by Rudolf Diesel, was groundnut oil [11]. The use of liquid biofuel has been gradually phased out with the discovery of petroleum fuel as a readily available, cheaper and more efficient alternative [10, 12]. Interstate wars and geopolitics have at different points in time, generated renewed interest in liquid biofuel especially among less energy secure states [9, 10]. However, this interest rapidly wanes as soon as the cost of oil decreases.

According to the 2020 energy outlook released by BP [2], Europe accounted for 28 % (Fig. 1.3) of total renewable energy consumed and only 16 % of global biofuels production in 2019 (Fig. 1.4).

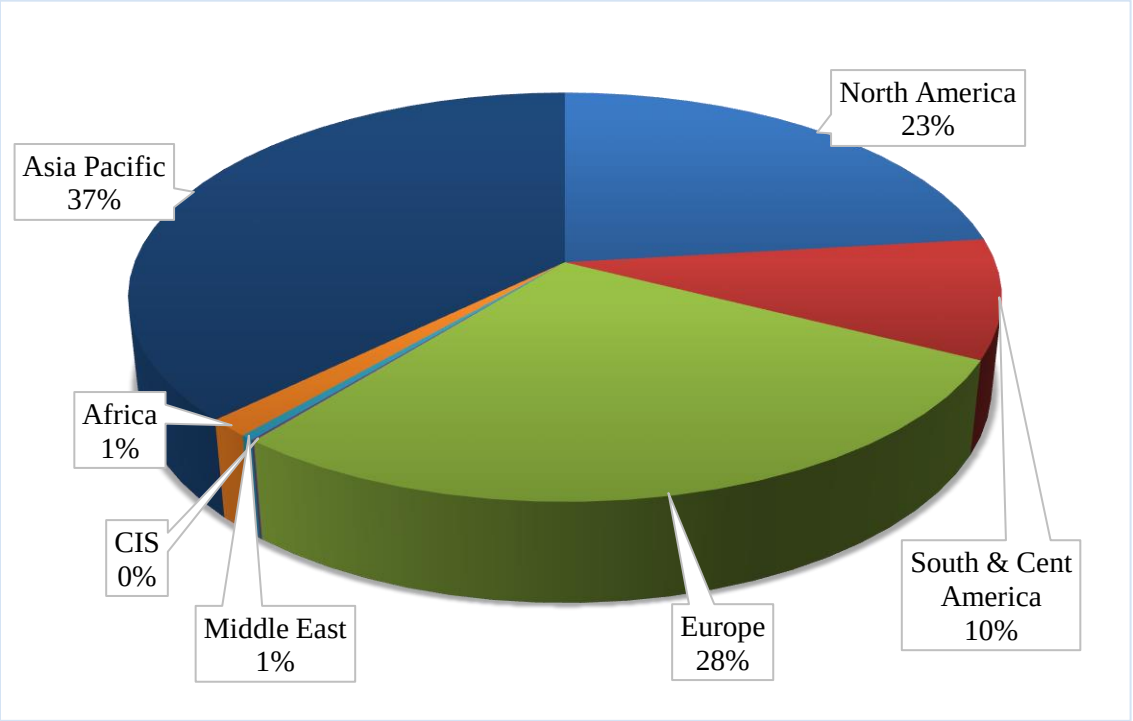

Figure 1.3: global consumption of renewable energy in 2019; CIS refers to Commonwealth of Independent States (13.9% of EU's consumption is in the UK)

"Waste to wealth" is a phrase that is used to describe second generation of biofuels. These are agricultural or forestry wastes or some specially grown non-food feed stocks based on the conversion of cellulose, lignin, and hemicellulose into fuel and chemicals. First generation biofuels on the other hand, are those produced based on conversion of the lipid and starch in food feedstock [13].

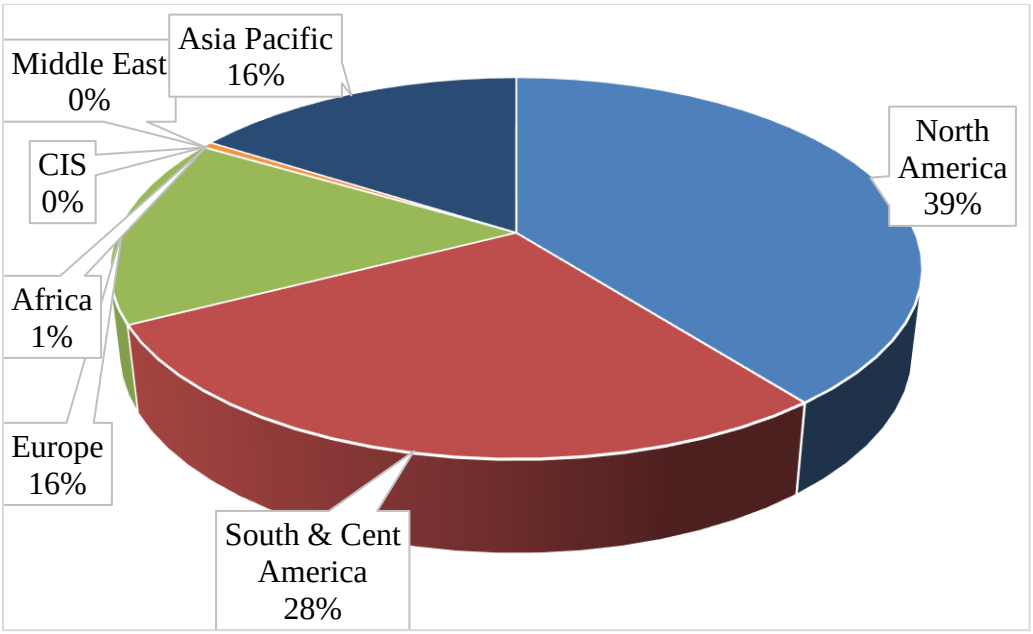

Figure 1.4: Biofuels production by regions in 2019

Global production of biofuels has increased by 9.6 % between 2017 and 2018, which is an improvement from the annual increase of 9 % from the previous ten years. Between 2018 and 2019 however, the growth rate of biodiesel was 3 % which is a reduction from the average values for the previous 10 years (6.8 %). The reduction in the 10-year average is as a result of the sharp drop between 2018 and 2019. This is an indication that the challenges facing the biodiesel industry is on the rise. Therefore, efforts must be made to reduce the cost of production which is the major obstacle in the way of biodiesel venture.

The production of biofuels in Europe has witnessed a decline from the previous 9.7 % per annum between 2009 and 2017, to 4.4% between 2017 and 2018, which further declined by 2.6 % between 2018 and 2019. Again, this can be related to the high cost of production. This is an indication that the hope once associated with biodiesel is starting to wane, in spite of the environmental and safety advantages.

Biodiesel refers to vegetable oil or vegetable oil- derivatives. The revolutionary groundnut oil used by Diesel is a unique example of biodiesel. Besides groundnut oil, other ingredients that have been used for biodiesel are: rapeseed, sunflower seed, Jatropha, soybean, canola, algae, bacteria, fungi, cottonseed, palm, tallow, cocoanut, lard, crambe, corn, etc. [14].

The EU targets to increase its share of global consumption of renewable energy to 34% by the year 2030, which is twice its 2015 figure but this is possible if all renewable transport options (mainly biofuels and electric cars) are included in the objective [15]. About a quarter of the GHG emission from the EU in 2014 came from transportation, 70% of which was associated with road transport [6]. In 2015, 40% of the total 137,430 kilotons of oil equivalence (Ktoe) energy consumed by all sectors in the UK went into transportation [7]. Bioethanol and biodiesel are two renewable alternatives to fossil fuels in the transport sector [8] and with the food crisis affecting bioethanol, biodiesel remains the only option. Besides, biomass is seen to be a major source of renewable energy in the EU beyond 2030 because relying on electric cars alone can only account for a mere 3% of renewables in the transport sector, hence the need to pay attention to liquid biofuels as they have the capacity to power the remaining 97% of non-electric cars [15].

1.3 Microalgae as feedstock for biodiesel

Third generation algae-based biodiesel is being considered as a sustainable alternative to first- and second-generation biofuels. The autotrophic consumption of CO_2, light and nutrients by microalgae provides the source of carbon for conversion to biofuels [13]. Algae feedstock has a number of advantages over other feedstock such as higher photosynthetic efficiency compared to terrestrial crops owing to their simple cells [16-19], rapid growth and harvesting rate [20], high lipid accumulation per body weight (30 times as much oil per acre as oil crop) [20, 21], and have the potential for wastewater treatment and CO_2 capture [19, 22]. In spite of these advantages, algal biodiesel has not been deployed commercially due to the prohibitive cost associated with culturing and harvesting of algae as well as extraction and treatment of algal oil [23, 24].

The development of algal based biofuel has been ongoing for several decades. Between 1976 and 1996 the National Renewable Energy Laboratory (NREL) of the US was involved in a project called “The Aquatic Species Program” ASP, aimed at developing algal based biodiesel. A 2008 joint workshop organized by The Air Force Office of Scientific Research (AFOSR) and the NREL focused on the following topics: general lipid metabolism in algae, triacylglyceride synthesis pathways, bio-prospecting, algal genomics, algal growth and physiology, development of algal genetic tools among others [25]. In

order to improve the economic competitiveness of algal based biofuels all these aspects must be fully exploited.

As stated earlier, one of the motivations for the development of biofuel is the increasing price of crude oil which is decreasing at the moment. This fact has made the previously daunting task of attaining cost parity with crude oil even more difficult. The economic viability of biodiesel can be estimated according to the following formulae [26]

$$C(algal\ oil) = 25.9X10^{-3}C(petroleum) \quad (1.1)$$

Where: C (algal oil) is the cost of algal oil per gallon while C (petroleum) is the cost per barrel of crude oil [27].

Thus, with the current international price of crude oil hovering at $50/barrel, algal oil should be selling at $1.3/gallon for it to compete economically with fossil fuel.

Although there are research articles published with impressive cost reductions [28], Sun et al.[29] noted based on a comparative study consisting of 12 public studies resulted in costs spread over two order of magnitude. The disparate result was due to uncertainties and assumptions. However, a harmonization study by the authors resulted in algal oil production costs ranging from $10.87/gallon to $13.32/gallon [30]. Likewise, Davis et al. [31], estimated $9.84/gal and $20.53/gal for open pond and photo-bioreactor produced algal oil respectively.

Below is a diagram which summarizes some of the major processes involved in converting microalgae to energy and other useful products.

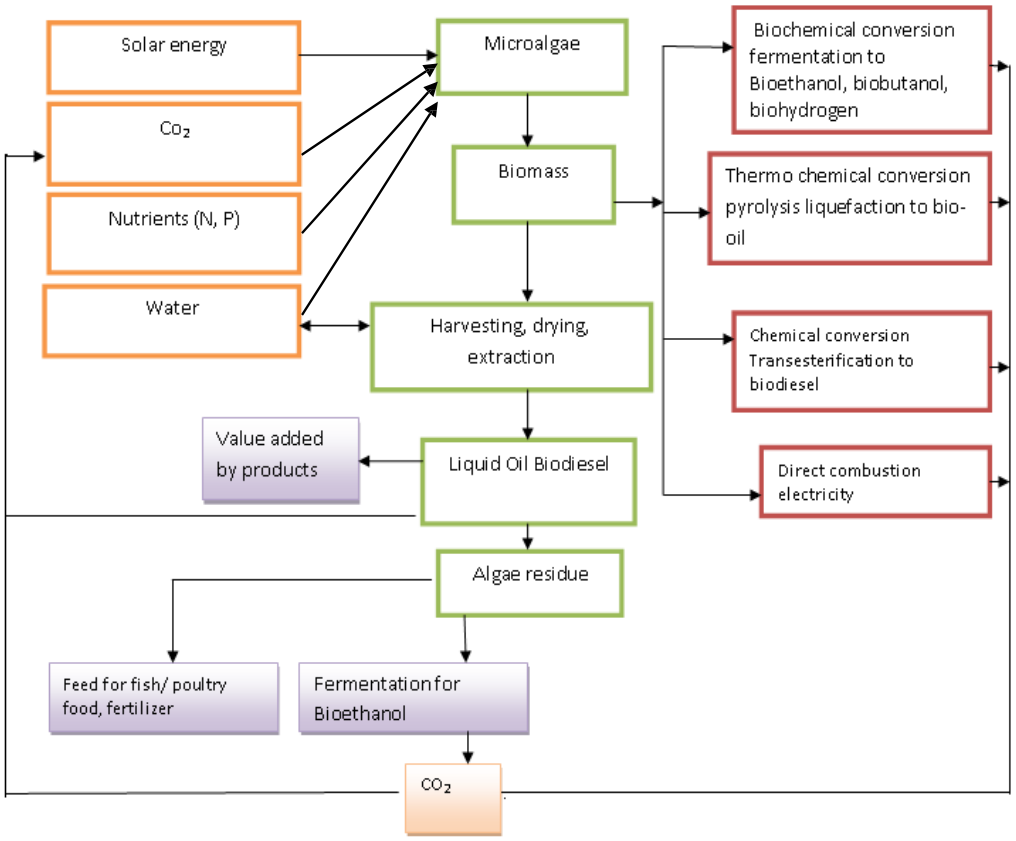

Figure 1.5: : Potentials of microalgae cells *[19]*

1.4 Freshwater Vs Marine Algae as potential biodiesel feedstock

The shortage of freshwater for drinking and growing of plants as food makes the choice of marine species as feedstock for biodiesel production an important one [32] as this also adds to the sustainability of the process since seawater is abundantly available. In addition to being a potential source of biodiesel, marine algae have potential for other renewable energy forms like biogas, bioethanol and hydrogen and boast of additional advantages over their freshwater counterparts because they can grow on non-arable land, hence no competition for resources with conventional agriculture [33].

Given that the world is three-quarter water, most of which is saline, algal biodiesel could gain additional acceptance and cost effectiveness if they emerge through a means that does not threaten freshwater supply which is already a problem in some parts of the world. However, the high ionic strength of seawater has made harvesting more difficult. The interference by salt ions has made it difficult for floatation in particular to be deployed

as a means of harvesting saltwater microalgae. The result is an additional cost added to the already cost inefficient process of algae biodiesel.

1.5 Problem statement

The dilute nature of microalgae culture requires that the biomass be concentrated and dried so that oil extraction can be achieved without water. About 30% of biomass production cost goes to harvesting and dewatering [19, 34]. Lardon et al. [35] reported that 84.9% of process energy is expended on harvesting and drying of microalgae. Two ways of improving the energy balance according to Xu et al. [36] are to use low energy drying methods or the complete avoidance of the drying steps by carrying out oil extraction on the wet biomass. Reactive extraction, otherwise known as in-situ transesterification is a combination of the oil extraction step and the reaction step with the advantages of minimising oil losses, the number of processing steps and the process time, all of which will reduce cost of production. However, the reactive extraction process consumes a large amount of alcohol, leading to additional cost required to recover over 94% excess methanol. But, the excess methanol allows for a more water tolerant process [37] compared to conventional transesterification.

Surfactants have the ability of breaking down the microalgae cell wall [38, 39], an advantage that could be used to reduce the amount of methanol needed as solvent for microalgae oil extraction. Foam flotation is cheap, simple, devoid of moving parts and has been used to achieve up to 90 % recovery of the microalgae during harvesting [40]. these advantages can be combined with that of reactive extraction to reduce the cost of biofuel production. *Nannochloropsis oculata* is a high lipid containing microalgae that is a good candidate for biodiesel production and because it is a salt water species, its usage does not lead to freshwater supply crisis. However, the complex structure of the cell wall hampers their exploitation for biodiesel production. As a marine species the presence of ions was found not to be a limiting factor when FAME was produced using *Nannochloropsis* [32] but with regards to harvesting, salt ions and the cell size of *Nannochloropsis* (2-4 microns), cannot be easily as dismissed as determinants. These and other questions, are what this project seeks to address. As an alternative to *Nannochloropsis oculata*, *Dunaliella salina* will be investigated as a biodiesel feedstock because of their lack of a true cell wall.

1.6 Aims and objectives

The aim of this work is to carry out transesterification of marine algae oil into biodiesel in a foam flotation column. In order to achieve this aim, the following objectives are to be pursued:

1. To establish a foam flotation harvesting of marine microalgae based on a surfactant screening and important operating conditions such as airflow and feedflow
2. To undertake a programme of surfactant screening to establish foam behaviour in the presence of methanol.
3. To understand the balance and fate of methanol and how to best make it available for transesterification in a foam column
4. To device a means by which methanol can be effectively used as a solvent and reactant at the top of the foam column
5. To achieve algae cell disruption using surfactant
6. To combine foam flotation with reactive extraction for process intensification.

This project seeks to focus on the use of foam flotation as a technique for harvesting marine microalgae (e.g. *Nannochloropsis oculata* and *Dunaliella salina*). Combining algae harvest with reactive extraction is to reduce processing steps (particularly the highly expensive drying steps) and oil losses which in turn reduces production cost. The success of this project depends on generating stable foam in the presence of methanol hence making this a key objective. In order to ensure that algal lipid is accessible to injected methanol, cell lysis needs to be achieved. Once access to algal oil is established, oil extraction and eventually transesterification becomes a possibility. The presence of surfactant is expected to contribute to cell lysis in addition to their roles as collectors and frothers. To this end, it is important to carefully screen for the most appropriate surfactant for the task since surfactants are known to be sensitive to cell and medium type. Because water tolerance is a problem during transesterification, the right surfactant will be one with the highest capability for not only cell disruption but high cell enrichment.

1.7 Dissertation outline and summary of chapters

The chapters in this thesis are presented in a format that conforms to journal publication style. As the author of the thesis, I have also conducted all the experiments described in this work. The current chapter is a brief introduction to the work and it focuses on the global energy nexus and the role that biodiesel has to play in shaping the future of sustainable and renewable energy for a better and safer environment.

In chapter 2, a literature review was conducted to critically investigate the journey so far with algal biodiesel production in particular. The literature review begins with a brief overview of the merits and demerits of using algae as a raw material and goes ahead to highlight the various means through which algae can be converted to biodiesel, while the advantages and disadvantages associated with each method is focused to justify the choice of technique. Because of the importance of harvesting and drying on the economics of algal biodiesel, the different approaches towards achieving them was critically discussed, touching on culturing process, even though this project was not focused on culturing. Nevertheless, the role of culture media was discussed due to the negative impact of ionic strength particularly on foam flotation harvesting technology. All of these critical analyses were aimed at justifying the eventual choice of methods.

Chapter 3 details the design and application of the foam flotation column that was used in this project. The role of airflow, surfactant type and concentration on the flotation of *N. oculata* was examined based on a composite design of experiments. In addition to process parameters and surfactant, cell properties such as size, morphology, surface charge, and hydrophobicity, as well as media chemistry (pH and ionic strength), were equally investigated.

Chapter 4 is dedicated to building a foundation upon which chapter 5 of this project is laid. It investigates the pros and cons of the addition of methanol as an additional feed to the already established foam flotation process of harvesting microalgae. In order to establish a trade-off between foam stability and the possibility of concentrating methanol at the top of the column, this chapter looks at how best to introduce methanol into the system. The impact of process parameters (airflow, column height, and feedflow), surfactant concentration, and ionic strength of media on the enrichment of methanol at the column top was investigated and established in this chapter.

Chapter 5 explores the possibility of biodiesel production in a foam column; starting with establishing cell lysis as a precondition for converting *Dunaliella salina* into biodiesel. A constricted version of the column fitted with methanol distributors was designed and commissioned. This is to serve as a tool for not just harvesting *D. salina* cells but converting them into biodiesel via transesterification. The crucial role of moisture content and temperature on biodiesel conversion and yield was hereby discussed. A cost analysis of the proposed technology is also presented in this chapter.

In Chapter 6, a summary of the main deliverables from this project is presented. This chapter captures the possibility of optimising the new findings in order to chart a course for further research. Genetic modification, the use of freshwater algae as feedstock, and a closer look at the acid-base interaction component of marine colloidal system, are some of the main suggestions. The potential of applying the proposed technology in water treatment was also proposed.

Chapter 2

Literature Review

Abstract

The possibility of achieving biofuel production from algae, through a process that eliminates the drying steps is key to reducing production cost and thereby offering an opportunity for the commercialisation of algal biofuels. To this end, previous investigations aimed at reducing the overall cost of producing algal biodiesel have been critically reviewed.

Some industrial scale harvesting technologies like centrifugation, flocculation/coagulation, filtration, and modifications thereof have been studied. Flotation technologies that have been applied in related fields like water treatment have also been discussed to see if these technologies particularly the low-cost ones, can be adapted either as they are or with modifications to the field of microalgae harvesting. Bearing in mind process safety and sustainability, and selectivity to algae as a feedstock as opposed to current materials. Based on the analysis of harvesting processes, foam flotation was chosen because of its relatively cheap cost so that its application with two marine species *Nannochloropsis oculata* and *Dunaliella salina* may be established. The literature review established that the two selected strains have never been harvested through foam flotation; hence, a knowledge gap was established. A huge knowledge gap also exists in terms of the principles of operation of the foam flotation technology especially as it affects algae harvesting. Another gap established by this work, is the fact that the flotation harvesting of marine algae is poorly understood. One unique feature of this work is that it tries to couple harvesting and biodiesel production in one-unit operation in a way that is new to literature. The interplay between water, methanol, algae, salt ions, and air was reviewed in order to achieve an intensified process of producing biodiesel from algae using the flotation column for harvesting as well as a reaction vessel.

Keywords: Algae harvesting, process intensification, foam flotation, algal biodiesel, transesterification, wet reactive extraction.

2.1 Introduction

The process of converting microalgae oil into biodiesel begins with the selection of a strain, which is cultivated under defined conditions of nutrient, light and time. At the end of a chosen cultivation period, cultivated microalgae are harvested and dried before being converted to biodiesel after oil extraction and refining. Dried microalgae cells can be converted into biodiesel via three major processes, namely: pyrolysis, microemulsification, and transesterification. The biggest obstacles to the commercialisation of algal biofuel from any of the aforementioned processes, is the cost of drying, followed by harvesting. Because of the importance of these two process steps, it is necessary to take a critical look at them with the aim of reducing their share of the entire process duty. This can be achieved by: using low energy harvesting and drying technologies and/or reactive extraction of wet biomass after the application of low energy harvesting/drying technology. In place of centrifugation, the combination of flocculation and rotary press is said to be capable of increasing the algae concentration from 500 g m^{-3} to 200 kg m^{-3} [35]. Even with this strategy, drying still accounted for 85 % of energy cost. Therefore, not only should driving be avoided, the combination of transesterification with harvesting (in situ) would go a long way in reducing the production cost of biodiesel from algae. This would however require the selection of the appropriate harvesting technology.

2.2 Algae cultivation process

Cultivation of microalgae is usually done through closed or open systems. The open systems refer to open ponds while in the closed system photo-bioreactors are employed. While the open system may appear cheaper, the invasion and contamination of the culture as well as the inability to control nutrient supply, results in a low yield. The closed system on the other hand, has better control of nutrients and predators / pathogens but is more expensive to build and operate than the open system and hence there is an ongoing discussion as to which of the two approaches could be used for the commercial production of biofuels from algae [40]. Basic challenges as highlighted by Kumar et.al [41] are: Temperature, pH, light, mixing and substrate inhibition. Some examples of open ponds include: raceway ponds, paddle-wheel-driven open raceway ponds, sump-assisted raceway ponds and airlift/split sump-assisted raceways [41]. Photobioreactors include:

vertical tubular, horizontal tubular, helical tubular, and flat panel Photo-bioreactors [41].

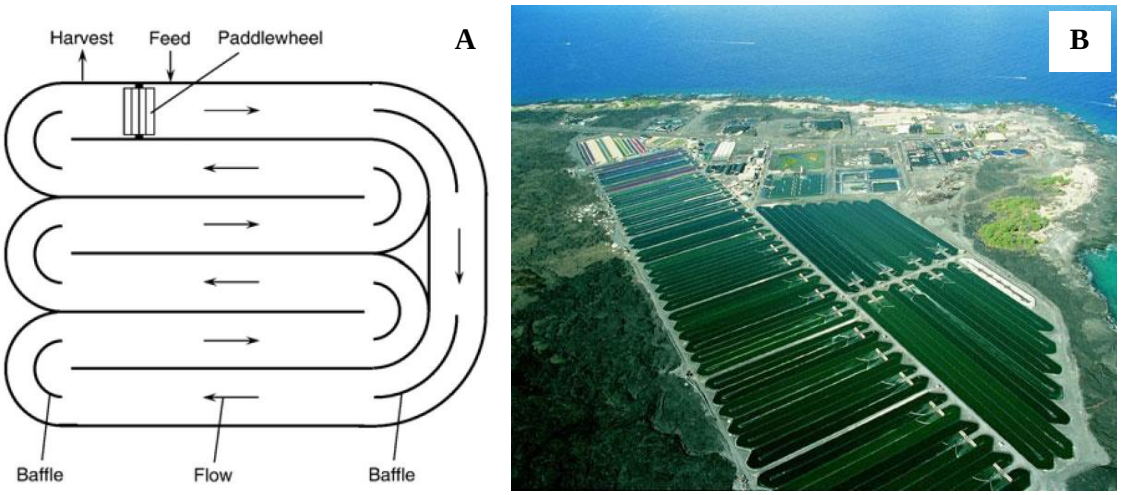

Figure 2.1: (A)Diagram showing the various components of a raceway according to [25]); B) An example of open raceway pond owned by the Cyanotech Corporation Kona, Hawaii (credited to Cyanotech Corporation) [19]

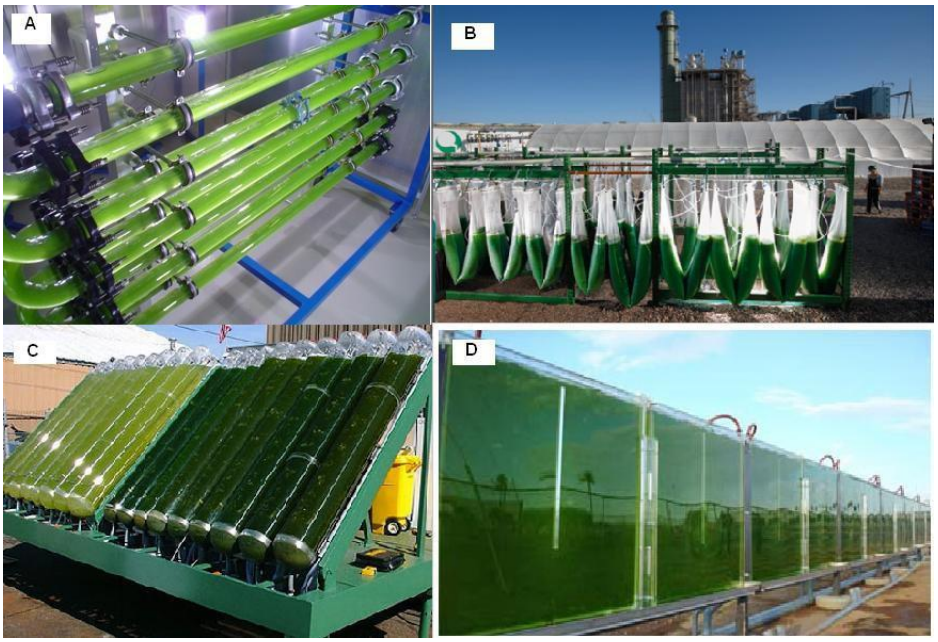

Figure 2.2: Closed systems of cultivation: A) Horizontal tubular (credited to Dan Brookshear); B) Bag culture (Photo by Robert Clark); C) Vertical tubular (Photo by Robert Clark); D) Vertical flat plate at Arizona State University. [19]

2.3 Harvesting of Algae

Harvesting may account for at least 25% of the production costs [42, 43], due to the dilute nature of the culture medium and the fact that the specific gravity of the cells is close to

that of the water in which they are suspended [34, 43]. Another factor is the repellent force generated from the negative charge on the cell surface that constrains the effectiveness of settlement as a collection option [40]. Particles in aqueous medium are negatively charged and the ability of these negatively charged surfaces to keep particles as far apart as possible, ensure that the colloid remains stable. In order for flotation to be successful, colloid instability has to be achieved by overcoming the electric double layer repulsive energy barrier that holds the particles apart.

Common harvesting techniques include; coagulation/flocculation, auto and bio-flocculation, gravity sedimentation, flotation, electro-filtration, and centrifugation [44-46]. Wechsler et al. [47] concluded that combining flocculation with a chamber filter press had the best energy footprint, although their analysis did not consider foam flotation.

2.3.1 Flocculation

Flocculation is one of the most popular technologies for algae removal from suspension because of its ability to handle a wide range of species [48]. It is well established as a water treatment procedure and is usually followed by sedimentation or flotation [49]. Flocculation and coagulation are sometimes used interchangeably but while flocculation is reversible, coagulation is not. Because of the negatively charged nature of solid surfaces and microalgae cells in particular in suspension [43, 50, 51], they tend to stay separated or dispersed, making them difficult to collect. The essence of flocculation is to bring the cells together into larger flocs by breaking the energy barrier that keeps them apart. Further details on how the different energies in a colloidal system affects flocculation is given in the section 2.3.8. the role of media chemistry is also discussed. Flocculation can be achieved through chemical, electrical, biological, or a combination thereof.

Chemical flocculation

Chemical flocculation refers to the use of either organic or inorganic chemicals to achieve cell aggregation. Inorganic flocculants are usually in the form of multivalent metallic salts (moistly of iron and aluminium) and they have the ability to either reduce or nullify the negative charge around microalgae cells by forming polyhydroxy complexes at the appropriate pH [52]. This allows the cells to come together to form aggregates that can easily be collected [42]. Salts with lower solubility and higher electronegativity have been

reported to be more efficient and rapid, respectively as flocculants [44].

Cationic flocculants and high molecular weight polymers (polyelectrolytes) are deployed as organic flocculants for wastewater treatment as well as algae recovery. They usually form a bridge between individual cells by electrostatic attachment. Although they are available in cationic, anionic, and non-ionic forms, only the former has proven useful as coagulants. This is due to the attractive forces between the polymers and negatively charged algae cells. Their effectiveness increases with charge density while dosage requirement decreases with increasing molecular weight [53]. In comparison with metallic salts, organic salts were reported to have higher ability (35-fold) to concentrate biomass [53].

Due to their non-eco-friendliness, biomass contamination, colouration and degradation of growth media, the use of metal salts as flocculants or coagulants for harvesting microalgae for biodiesel and animal feed is not recommended [54].

Electro-Flocculation

Electrofloucculation (EF) involves the in-situ production of coagulants through electrolysis where an oxidised electrode is used to break the energy barrier between cells thereby disrupting the colloidal stability. The resulting flocs are positively charged and are as a result, electrostatically attracted to the anode, where they are collected. Between 80 to 98% recovery has been reported using this process. Common electrodes are aluminium and iron, aluminium being the better option. Factors like pH, runtime, current, and algae medium composition [55, 56] could affect electro-flocculation. Some advantages of this process include: low power consumption compared to centrifugation, specie-independence, ease of control, low electrode demand, and lack of anionic (chloride and sulphate for example) waste [48, 55]. However, this process suffers from the high cost of replacing and maintaining the electrodes, as it also leads to an increase in medium temperature, pH variation and deposition of waste metals in the recovered algae [57].

Autoflocculation

This is a process whereby microalgae cells, in response to changes in pH and/or nitrogen and dissolved oxygen levels, settles naturally in the absence of any chemical treatment. The advantage of this process lies in its simplicity, rapidness, and when compared with

centrifugation, it is less destructive to the algae calls [58]. pH induced autoflocculations have been reported for high and low pH values [59]. High pH processes [58-63] where the hydrolysis of Mg^{2+} to MgOH, are more popular, probably because of the acid toxicity on cells and equipment. Nevertheless, high pH induced flocculation was reported to produce less compact flocs that are easily resuspended for recycle [59].

Bio-Flocculation

The production of extracellular polymers usually in the form of exopolysaccharides by bacteria and algae, and fungi [64], is exploited based on the flocculant properties due to their adhesive nature [65]. Microorganisms obtained from soil and activated sludge, produce the best form of extracellular polymers, where extracts from such organisms are introduced into the algae culture [66-68]. They have also been produced from bacterial glucose [69, 70], acetate, and glycerine [64]. The need for metallic flocculants in addition to the already painstaking and expensive processes of producing bioflocculants has however limited their use for microalgae harvesting in biodiesel production process, bearing also in mind that they produce low lipid. Being specie-dependent [71], also counts against their robustness for batch processing, given the fact that microalgae usually exist in colonies. Nevertheless, it is adjudged to be a promising technology for algae harvesting if complimented with other harvesting processes, especially flotation [72].

2.3.2 Filtration

Filtration is best suited for laboratory scale operations, especially where larger cell sizes (>70 μm) are involved [49, 73, 74]. In order to reduce the rate of membrane fouling, filtration is carried out via tangential flow of fluid across the filter medium as opposed to the dead-end approach [72]. Another approach towards mitigating the problem of fouling has been reported by Hwang et al., where a cross flow with anti-fouling agent, yielded almost 100% recovery of *Chlorella* sp. KR-1at a maximum concentration factor of 77 [75]. Other modifications to improve the cost efficiency and operational bottlenecks of filtration are vibrating screens and microstrainers [76]. However, fouling remains a problem, particularly where large cells are involved. As a corrective measure, micro-straining is preceded by flocculation [34].

When combined with other fabrics, like polyester-linen, satin-polyester, and silk,

cotton membrane was reported to have the highest recovery of between 66 and 93% [77]. Other filtration related methods for harvesting microalgae include: sand filtration [78], a combination of sand filtration with drum drying [79], and the combination of filtration with ozonisation [80]. High maintenance cost in addition to other operational challenges, as membrane fouling are some of the disadvantages of filtration as a microalgae separation process. Nevertheless, filtration remains one of the most favoured technologies currently applied in microalgae harvesting, particularly the cross-flow technology due to their ability to minimise fouling of the membrane [81]. Other advantages include lack of chemical contaminants, ability to produce up to 15% total solids suspension (TSS) [82], ease of separation [83] and potential for scale up if modified [84].

2.3.3 Centrifugation

Centrifugation is a process that uses centrifugal force to separate solid particles from liquid suspension based on size and density of the solids involved [85]. Depending on centrifugation speed (500 to 13000 g), a recovery efficiency of between 80 and 100% can be achieved using centrifugation [34]. This makes it by far the most efficient in terms of solid capture, particularly when the relative similarity in density between algae and water as well as small particle size is brought to bear. It is a very unsustainable process with a Net Energy Return (NER) of 0.4 [77]. However, Heasman et al [86] have indicated that centrifugation depends on cell type and the kind of centrifuge (disk stack, perforated/imperforated basket). In order to improve on the NER, centrifugation can be preceded by flotation or sedimentation, taking advantage of the low energy consumption of these pre-processing steps. Also, processing large amount of algae was said to have to have reduced the energy cost of centrifugation by 82 % [73]. Another disadvantage is that centrifugation can be greatly destructive of algal cells [87], particularly fragile ones like *Dunaliella salina* which can only withstand mild conditions of centrifugation. Although this might not matter, if this was done at the oil extraction stage, using centrifugation to harvest such algae cells can lead to loss of cellular content and hence a reduction in yield, if biodiesel production is intended. Overall, centrifugation is not cost effective and hence not compatible with cost effective algal biofuel.

2.3.4 Flotation

Flotation as a separation process has been applied in mineral processing for about a century and a half [88].The application of foam flotation in water treatment to remove surface active chemicals has been reported as well as for biofuels [38, 40, 51, 89-96]. As an algal separation process, foam flotation was first investigated in 1961 by Levin et al [97]. While Levin's work relied on the natural surfactant production capacity of algae [98] to drive the separation, most others [38, 40, 51, 92, 94, 99-102] have utilised the action of surfactants or polymers as frothers and collectors. Nevertheless, the self-settling characteristics that was exploited by Levin, gave flotation its advantage of rapidness and effectiveness over sedimentation [103]. Recently, foam fractionation was combined with dispersed air flotation to achieve up to 90 % algae recovery of *C. Vulgaris* using Cetyltrimethylammonium bromide (CTAB) [40]. In related work, Coward et al. [102] reported that the lipid content of biomass concentrated using foam fractionation was higher than concentrated biomass obtained from centrifugation. This observed increase in lipid profile is because CTAB has the same ester functional group as lipid, and a higher lipid profile can be an additional benefit especially when high value products like phospholipids are desired as food supplements [104]. Foam flotation has the ability to handle a diverse collection of species, making them suitable for combined harvesting within the confines of optimisation [105], particularly as algae are sometimes found to live in colonies. Although it is a potentially low cost process, there is a need for improvement in design that would allow for scale up [104].

Generally, flotation can be divided into two main types, namely; dissolved air flotation (DAF) and induced air flotation (IAF), part of which is the dispersed air flotation (DiAF) [106]. Other types of IAF are: nozzle flotation; jet flotation; centrifugal flotation; and cavitation air flotation [106]. While dispersed air flotation processes generally are devoid of mechanical or moving parts [40], a high speed mixer combined with an air injection nozzle has been reported [106].

Dissolved air flotation (DAF)

Dissolved air flotation, like DiAF has gained some commercial popularity among flotation processes [107]. However, the two processes differ in terms of the mechanism by which air bubbles are generated, and to this end, the size of bubbles in DAF are much smaller,

ranging from 20 to 100µm [52, 108]. In order to generate such microbubbles, the suspension media is supersaturated with air to allow for air dissolution, at pressures above atmospheric pressure (>500 kPa), which comes at a higher energy cost (7.6 kWh/m^3) [109] in comparison to DiAF (0.003-0.015 kWh/m^3) [40, 110]. Although high capture efficiency of more than 90 % [111] is said to be associated with smaller bubbles, the addition of surfactant in DiAF is capable of creating smaller bubbles [91]. From economic point of view, DiAF has more potential as a microalgae recovery technique for biodiesel production. A variation of DAF where microbubbles are generated via fluidic oscillation is called Microflotation. Although micrloflotation is said to be cheaper and could be more efficient than DAF due to the generation of smaller bubbles [112-114], it is not as cheap as DiAF [40].

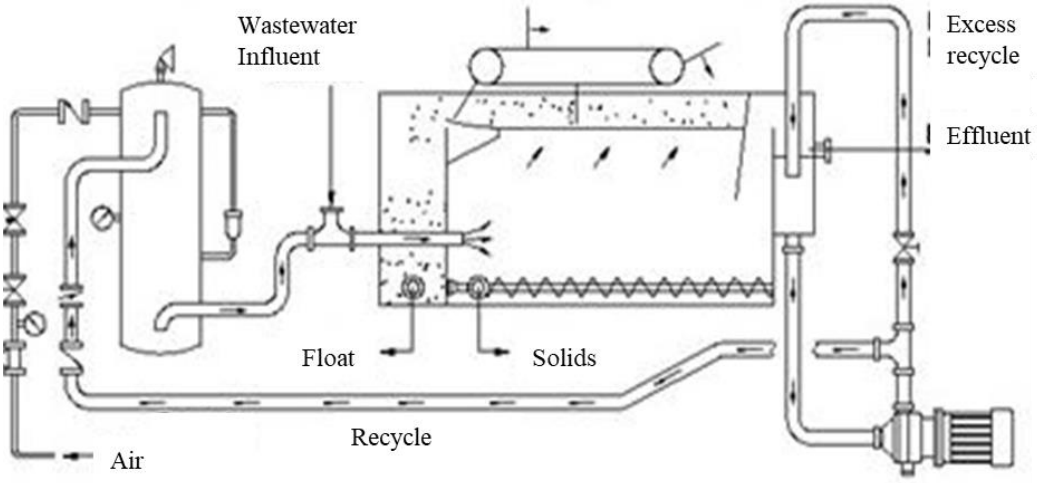

Figure 2.3: Schematics of the operations of a Dissolved Air Flotation (DiAF) for wastewater treatment; Courtesy chemiocalonline.com (https://www.chemicalonline.com/doc/chem-show-99-pump-eliminates-need-for-daf-air-0001)

Electrocoagulation flotation (ECF)

This is a combination of the earlier described electroflocculation with DiAF flotation in order to improve on the efficiency of EF through creation of more bubbles [95]. Because EF is an electrolysis process, the deposition of flocculants is a function of current density [95], which in turn determines the efficiency of the process by producing flocs at higher rates. The result is a rather expensive process particularly when seawater species are

involved, owing to the high medium conductivity, although small bubbles (22-50µm) are produced [91]. A major drawback for the ECF is the cost of electrodes in addition to the safety-related problem of H_2 emission. Further operating cost may be required from the use of polarity exchange to mitigate the problem of film formation on the electrodes [115], which otherwise reduces efficiency [104]. In the area of water treatment, this processes was said to be better than conventional coagulation by 20%, given the same amount of Al [106].

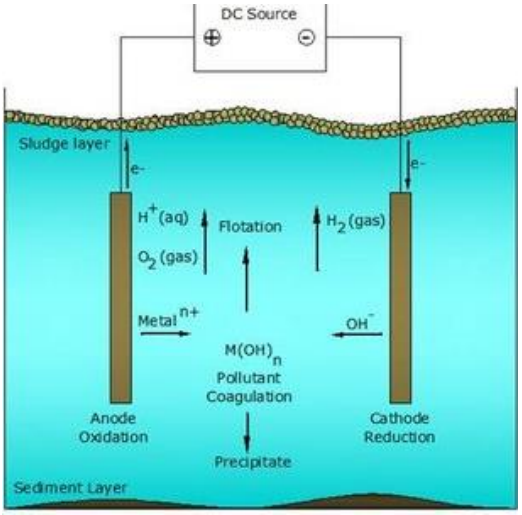

Figure 2.4: Pictorial representation of Electrocoagulation process credited to Milton Andrade [116]

Dispersed air flotation (DiAF)

Dispersed air flotation is sometimes referred to as froth flotation or foam flotation, particularly in the mineral industry where it originated [117]. In DiAF, air is dispersed into a slurry with the aid of a mechanical disperser or compressed through a porous material to generate air bubbles that will collect suspended particles. The collected particles are transferred from the bulk suspension into the rising foam through collision and attachment mechanisms.

In foam flotation, frothers are needed to generate froth or foams while collectors are used to collect or transport the solid particles from the bulk solution to foam phase. Most surfactants are capable of acting both as frothers and as collectors.

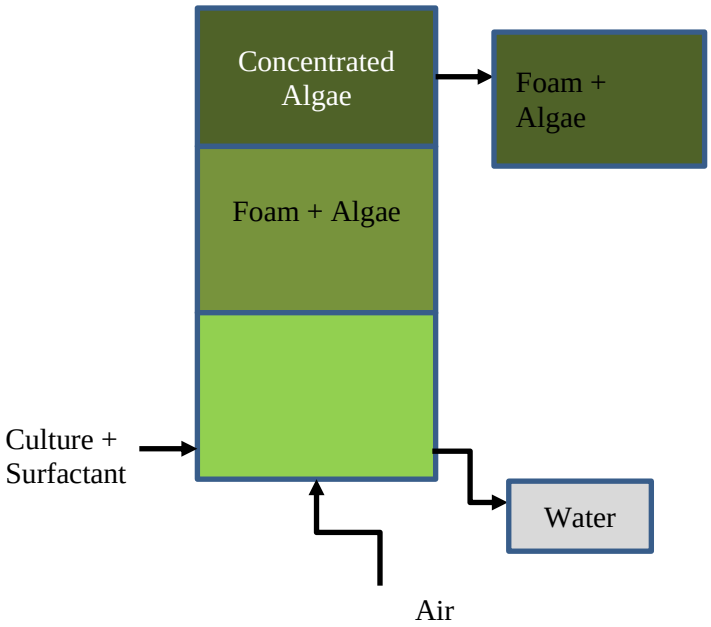

Figure 2.5: Schematics of a simple flotation column for microalgae recovery

Factors that have been identified to affect the efficiency of dispersed air flotation for microalgae harvesting are: microalgae cell properties; surfactant (collector) type and concentration; bubble characteristics; media chemistry; and operational parameters [118].

2.3.5 Factors affecting dispersed air (foam) flotation

Collector or surfactant type and concentration

The type of collector (surfactants or flocculants) that is used during foam flotation has a major role to play in terms of not only the efficiency of the process but also on the end use for which the recovered algae is desired. Collectors or surfactants are used to generate air bubbles that would in turn to attach to microalgae, making them hydrophobic (attracted to air bubbles as opposed to water) [119]. Cationic surfactants for example, have the ability to modify the negative charge of microalgae [42]or air bubble [120] to positive [100]. The use of metallic (particularly ion and aluminium) salts [121, 122], for example has been reported to have health related disadvantages such as toxicity [123] and carcinogenesis [124] in addition to high dosage demand, pH dependence, and incompatibility with certain microalgae [124]. This is in spite of their economic advantage, making them more suitable for wastewater treatment [52]. The concentration factor of *C. vulgaris* was said to be better

when lower concentration of Ecover© (0.1 mL L^{-1}) was used as against a higher concentration (0.2 mL L^{-1}), consequent of increased water content in the foam [40]. In other words, the success of flotation process also depends on collector concentration. Increase in surfactant concentration was said to have led to an increase in recovery and when the appropriate airflow is combined with surfactant concentration, both recovery and concentration factor can be increased with long column height [19]. According to how the bubbles are been produced, flotation has been classified as: dissolved air flotation (DAF), dispersed air flotation (DiAF), electrolytic flotation (EF), ozonation-dispersed flotation (ODF) [52, 125]. Usually, a single collector is enough for effective flotation harvesting, although there have been cases where a mixture of collectors was used to achieve better recovery. For example, in order to correct the effect of ions on the recovery of Cd (II), non-ionic surfactants, namely; octanol, dodecanol, and tetradecanol were added to the ionic sodium lauryl sulphate and sodium laurate with compositions ranging between 8.3% to 55.5% [98]. The concept of mixed surfactants has also been reported for microalgae recovery [51, 93] where recovery efficiency of more than 93% was recorded. In general, high cell recovery rates of between 70 and 99% have been reported based on microalgae flotation [38, 40, 89, 94, 100, 103, 110, 126, 127].

Some collectors that have been investigated for microalgae harvesting are: aluminium sulphate (Al2(SO4)3), iron (III) sulphate (Fe2(SO4)3), CTAB, chitosan, sodium dodecyl sulphate (SDS), myristyltrimethylammonium bromide (MTAB), iron (III) chloride (FeCl3), Saponin, dodecylammonuim hydrochloride (DAH), and dodecylpyridinium chloride (DPC).

Surfactants facilitate the generation of bubbles and these bubbles make it possible for particles (microalgae) to be separated from the bulk liquid by bubble-particle collision which is usually followed by bubble- particle attachment [128]. Collision may occur between bubbles and particles as a result of interception of the particles along the fluids streamline and such collision is expected to be followed with attachment [129]. The attachment process between algae cells and bubbles has been described by Shen et al [130], as follows: 1. Cationic surfactant attaches electrostatically to a negatively charged algae through its hydrophilic (positively charged) end, leaving the hydrophobic end protruding away from water and towards bubbles. Because bubbles are being constantly separated from the bulk liquid so does the algae that has been attached through the link with

surfactant. 2. The surfactant first attaches to a bubble through its hydrophobic end modifying the bubbles charge from negative to positive. Positively charged bubbles then attach electrically to negatively charged bubbles.

Media chemistry (PH and ionic strength)

pH has a logarithmic relationship with the activity of H_3O^+ ion in solution [131]. Due to the sensitivity to pH of surfactants, coagulants, and other chemicals, certain collectors are likely to perform optimally at certain pH or pH ranges. pH is also reported to affect interfacial properties [51]. According to Liu et al. [51, 90], flotation of microalgae was not affected by pH values between 5 and 8 but away from this range in either directions, recovery efficiency of metal salts was improved. It was argued that at acidic pH, excess H^+ ions caused further release of metal cations by reacting with salts whereas, at elevated pH, metals oxides result and larger flocs are formed [103]. Hence it is noteworthy in the case of flotation that, as flocs become more dense, they become harder to lift and that will reduce recovery [115]. For both cationic CTAB and anionic SDS, acidic pH was reported to increase yeast recovery to about 86 and 80 % respectively [132]. This can be explained by the fact that the yeast that was used in the process was highly hydrophobic and hence all that was needed was a frother at the appropriate pH. Cationic surfactants (long-chain amines and their salts) are said to be more soluble and stable in acidic environments while quaternary ammonium surfactants are stable to acid [133]. Hence, when quaternary ammonium salt (surfactants) like CTAB are used, only the cells and their double layer according to the content of the medium feel the effect of pH.

While some researchers [127, 134] argue that salinity favours the production of smaller bubbles due to reduced coalescence, and hence more efficient floatation, it is reported elsewhere [51], that salinity has a negative impact on flotation efficiency. The role of salinity in determining flocculation is equally contradicting, particularly in terms of EFC where one investigation [123], claims that high energy demand for EFC for rapid flocculation of seawater species was because of high conductivity, another investigation [135], reported lower electrical energy demand when seawater species were harvested. Perhaps the ambiguity here lies in the fact that salinity and ionic strength are misinterpreted. While salinity refers to the concentration of NaCl in a medium, ionic strength includes the concentrations of other ions other than Na^+ and Cl^-. Nevertheless,

whether translated as ionic strength or salinity, the surface characteristics i.e. net charge and hydrophobicity of cells is a function of the ions present in solution [136-138]. While cations have been said to favour flotation [40, 139, 140], the reason why they behave contrary in other cases [93, 141], cannot be explained through simple performance analysis [142]. It is also noteworthy that the production of small bubbles does not always translate to higher recovery and concentration factor as claimed by Barrut et al. [127]. Other factors like cell morphology and differences between the treated cells may have not been taken into account, and hence the resulting ambiguity. It is therefore necessary to consider other factors like the production of extracellular materials by the microalgae, which is likely to have an effect in terms of cellular and surface charge behaviour.

Bubbles

Because of the important role of bubbles as particle carriers in flotation, their characteristics such as size, shape and stability can affect their ability to capture cell particles. Bubble size has been found to generally affect flotation efficiency with higher efficiency associated with smaller bubbles. In terms of surface charge, bubbles are negatively charged [143]and that explains why they naturally would not attach to negatively charged microalgae[144], unless they are modified [100, 145, 146]. As stated above, the surface properties of the bubbles and particles to be separated, particularly their zeta potentials, needs to be minimal [120]. Nevertheless, smaller bubbles means more of them are available for individual particle collision [100], and it also allows for easier rise to the column top which could translate to better efficiency [102].

Microalgae cell properties

The diversity of microalgae cells in terms of size, morphology, hydrophobicity, surface charge, functional group, and growth media, is bound to play some roles in the recovery and concentration of the affected specie. While most microalgae are known to be hydrophilic, some organisms are not and the fact that a specie is highly hydrophobic does not necessarily translate to good recovery [132]. This is because of the presence of certain extracellular components that could be responsible for their perceived hydrophobicity. It was noticed during the flotation of *Saccharomyces cerevisiae* that when the yeast was resuspended in water, it failed to float, even though they showed very high cell

hydrophobicity [132]. This is possibly because the extracellular material that has been isolated from the cells by centrifugation, conferred on the yeast cells, their ability to float, which lead to the conclusion that the flotation of the yeast was more dependent on the extracellular components that had been transferred in to the supernatant of the yeast. It should be noted, that marine phytoplankton are known to produce insoluble surfactants [147] whose surface activity are capable of interfering with added surfactants [148] and this could either inhibit or complement the added surfactants, depending on the exact type of surfactant that is produced by the cells and the introduced collector. For example, the addition of surfactant did not show significant improvement on DAF recovery because the seawater medium already contained surface active salts [149]. However, it has been reported elsewhere [150] that the production of extracellular materials can lead to additional dosage of flocculants. These extracellular compounds are responsible for their functional groups. Microalgae cells just like most solid surfaces are negatively charged. This explains why cationic surfactants have become more popular in the foam flotation of microalgae. Although there have been cases where anionic surfactants have been used, this happens when cationic surfactants are used as frothers as well as ion switchers by way of which the microalgae are no longer negatively charged. This is the idea behind using multiple and zwitterionic surfactants.

Operational parameters

Operating conditions that are associated with foam flotation are: duration of flotation; airflow; foam height; column height; and liquid pool. In the work of Coward et al. [19] for example, at constant bubble sizes, surfactant concentration, airflow, surfactant type, and column height, were said to affect the recovery and concentration factor of the processes. Increase in surfactant concentration and airflow had positive effect on the recovery but reduces concentration factor [40].

Other types of flotation

Other types of flotation that are not as popular as DiAF and DAF are in the table below:

Method	Summary	Pros and cons	Reference

Nozzle flotation	Uses gas aspiration nozzles to draw air into the suspension that will later mix with the latter to produce froth, which is collected as an overflow.	Less expensive compared to other induced air flotation methods but a vacuum is needed which increases the operating cost.	[106, 107]
Jet flotation	Air jet is bubbled through an aqueous medium to generate froth, which overflows into a collector along with captured solid particles.	Efficient but expensive and not appropriate for solids in the size range of microalgae.	[106, 108, 151]
Gas aphrons-based flotation	The use of a venturi generator to introduce gas into surfactants solutions at high velocity and low pressure, to produce special types of microbubbles that are highly stable, allowing their diffusion into aqueous medium in order to achieve particle removal by attachment.	It is expensive in terms of downstream treatment of algae for biodiesel production and process cost. It is however, effective in solid capture and can be applied to microalgae.	[108, 152-154]
Ion flotation	The use of surfactant to float an oppositely charged ion by transferring the ions from the bulk liquid to the froth.	This is suitable for metals recovery but require an additional process for selective release of spent ions.	[106, 108]
Centrifugal flotation	Pressure drop is exploited in generating a tangential flow of liquid stream that obey a centrifugal rotation in the presence of sparged air, causing the generation of bubbles that collects hydrophobic particles to the top via a vortex finder.	Expensive and selective in action. It is highly efficient but complex with high maintenance cost. Efficiency depends on flocculants dosage and vortex finder clearance.	[106, 108, 155]
Ballasted flotation	The use of low-density microspheres that allow for easy flotation of flocs aimed at reducing cost of aeration.	Up to 60% reduced cost compared with DAF however not as cheap as DiAF.	[104, 156, 157]
Ozone flotation	In place of air in DAF and DiAF, ozone is used due to the added advantage of cell lysis.	More expense in terms of ozone and air or oxygen but capable of cell lysis.	[104]

Positive dissolved air flotation (PosiDAF)	This is a modified DAF where the production of positively charged bubbles without the need for coagulants.	Reduced coagulant dosage compared with DAF but specie dependent and not as cheap as DiAF	[99, 100, 145, 146]

Table 2.1: Other flotation separation processes

2.3.6 Foam Flotation recovery of marine algae

The use of foam flotation as a tool for harvesting marine microalgae has received very little attention. This is because of the higher ionic strength of seawater, which leads to a compact electrical double layer (EDL) surrounding the cells and therefore decreases the Debye length, making it difficult for collectors to interact with cells. One reason why microalgae are generally difficult to recover are their small cell sizes; the smaller the cell size, the less probable it is for air bubble to collide with cells [158]. The production of extracellular compounds like algaenan as well as surfactants by marine algae [159] are capable of controlling the interaction between the cells and collectors and hence bringing about a low recovery efficiency. The chemistry of algaenan (a hydrophobic trilaminar non-hydrolysable biopolymer) [160] around the cell wall of certain microalgae, is barely understood. Besides their hydrophobicity [160], algaenan also tends to reduce the effect of collectors, by limiting their access to cell wall polysaccharides [161] and the formation of a bond with them [162]. In addition to the production of extracellular materials, the presence of multivalent ions, i.e. Mg^{2+} and Ca^{2+} in seawater are capable of reducing sorption capabilities of seawater organism [163].

For algal biodiesel to be sustainable and widely acceptable there is the need to concentrate on marine species due to the advantage of lack of competition with portable water. This sustainably advantage, if combined with the use of low energy technology like flotation, is capable of lowering the harvesting cost. Sourabh et al [92, 94] have recently reported the flotation harvesting of marine algae, *Tetraselmis* sp. (*M8*) by tuning the medium pH to induce cell hydrophobicity. pH-induced hydrophobicity has been reported for both freshwater and marine algae [104, 164, 165] and the impact of pH is said to be specie and surfactant dependent [166]. However, *M8* as a specie, is not a favoured biodiesel candidate, partly due to the low average lipid content (20-30%) [167]. The work of Sourabh et al involves the use of Jameson's cell to generate bubbles through a high energy intensive

mechanical process [108], which may not be economically wise. One of the most favoured marine species for biodiesel production based on lipid content (20 -56%) and FAME productivity [168, 169] is *Nannochloropsis oculata*. *N. oculata* also has high specific growth rate of 0.27 day^{-1} and doubling time of 2.59 days compared with *Dunaliella salina* (0.18 and 3.85), *S. obliquus* (0.22 and 3.15), and *C. vulgaris* (0.14 and 4.95), respectively [170]. It is important to state that the recovery of *N. oculata* or *Dunaliella salina* using foam floatation has never been reported and considering how important both species potentially are to biodiesel production, an attempt to harvest them should be worthwhile.

2.3.7 The DLVO theory and zeta potential

Increases in ionic strength of solutions which in turn leads to an increased electric double-layer (EDL), can be unfavourable for absorbance of organisms onto surfaces by maintaining a finite repulsion and this can occur at ionic concentrations similar to those of seawater [163]. The balance between the attractive Vander Waals force and the ionic strength-dependent EDL (Fig. 6) repulsion force can explain this sorption. The electric double layer refers to the stern layer, which is a stationary layer (formed of oppositely charged ions around a particle) and the mobile diffused layer (made up of a mix of oppositely charged ions interacting according to Brownian diffusion). DLVO theory [171] credited to Derjaguin-Landau [172] and Verwey-Overbeek [173] who separately developed the theory was proposed to define the attachment of particles in suspension (colloid) to solid substrates. According to DLVO, the potential energy of a colloidal system is the sum of these two opposing forces and whichever is greater, shall determine the possibility or otherwise of the particles to floc. If repulsive force is completely overcome, then coagulation, which is the irreversible stage of flocculation, may occur (Fig. 7).

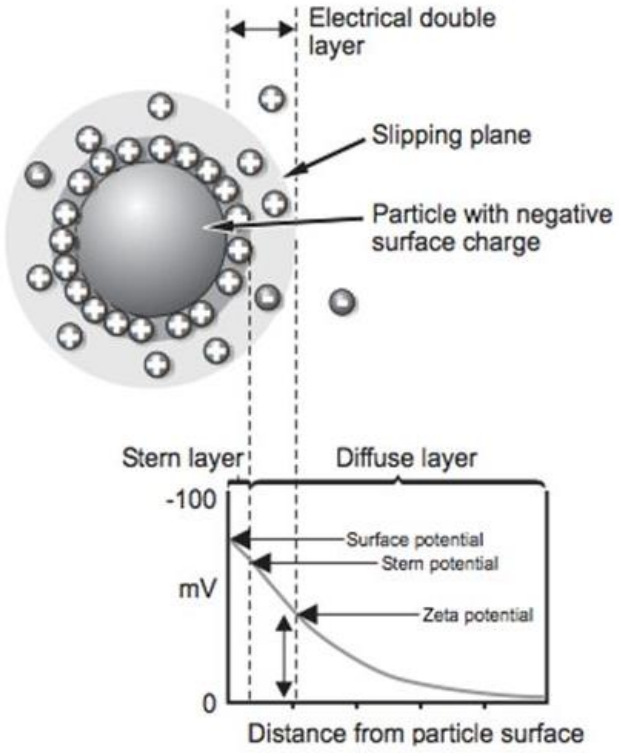

Figure 2.6: Electrical double layer with respect to a negatively charged particle in a solution

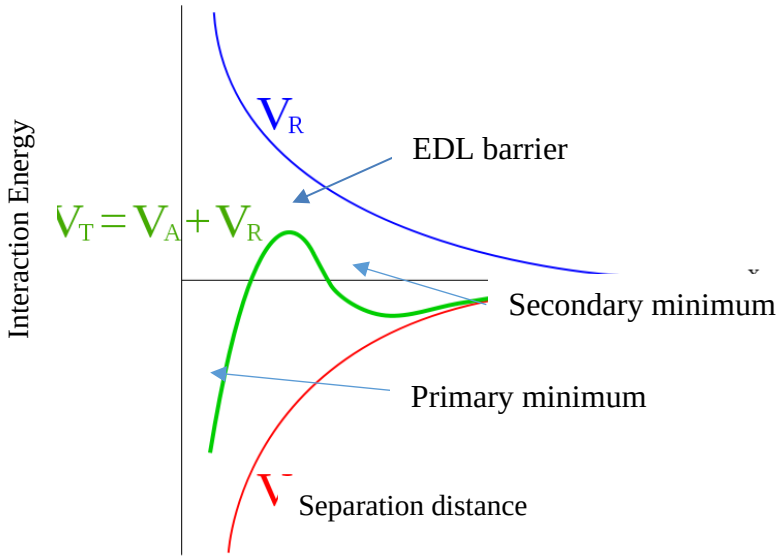

Figure 2.7: Illustration of the DLVO theory; V_T=Total potential, V_A= Potential due to attractive Vander Waals forces and V_R= Repulsive double layer (electrostatic coulomb) forces

From the diagram, according to the DLVO theory, as the distance between particles decrease the Vander Waals forces of attraction increases as well as the repulsive double layer electrostatic force. If the particles become close enough, the attractive forces could overcome the repulsive forces and particles may begin to aggregate, resulting in an unstable colloid. In order to achieve colloid instability which is the goal of foam flotation and flocculation or coagulation, the repulsive electric double layer force V_R must be overcome. Because V_R is favoured by high surface charge density and low electrolyte concentration, a common strategy known as "salting out" is applied, where the increase in ionic concentration caused by the introduction of salt ions, to break the EDL barrier (Fig. 2.7). If, however, the ionic strength and valency of the media is reversed, the attractive forces could be overcome and colloid stability is regained. The secondary minimum is a point after which colloid stability can be regained. As particles get closer, a point is reached beyond which permanent aggregation or coagulation occurs. This is called the primary minimum.

The higher flocculation efficiency of two strains of algae, *Scenedesmus dimorphus and Nannochloropsis oculata*, at lower total DLVO interaction energy, could be an indication of the ability of the DLVO model to qualitatively predict the flocculation of the two algae [174]. Although the changes in pH and ionic strength could not be so easily explained for the marine species (*N. oculata*) as, flocculation increased with increased ionic strength, as long as extreme (low or high) pH values were maintained. This is a sharp contrast to the case of the freshwater *Scenedesmus* which follows the DLVO model where isotonic point (zero net charge) combines with either low ionic strength or average pH (pH 7.5) to bring about increased flocculation.

The extended DLVO or XDLVO was proposed by Van Oss et al. [175] to account for the polar (acid–base) interfacial energy. In the classical DLVO, only the electrostatic repulsive forces and the Vander Waals attractive forces terms are defined as responsible for the total energy of colloidal systems. For colloidal system where the suspension medium is other liquids but water, steric interactions are considered in place of the electrostatic interactions because of the likelihood that the dielectric constant of such liquid is not as high as that of water and hence not enough to cause stabilisation.

The mathematical expression of the XDLVO is as shown in Eqn. 2.1.

$$\Delta G^{TOT} = \Delta G^{LW} + \Delta G^{EL} + \Delta G^{AB} \quad (2.1)$$

WhereΔG^{LW}, ΔG^{EL} and ΔG^{AB} denotes Lifshitz-van der Waals, electrostatic, and Lewis acid–base interaction energies respectively.

For a spherical particle such as *N. oculata* cells, opposed to a semi-infinite plate by distance d, $\Delta G^{LW}(d)$, $\Delta G^{EL}(d)$, and $\Delta G^{AB}(d)$ are then expressed as:

$$\Delta G^{LW}(d) = -\frac{A}{6}\left[\frac{a}{d} + \frac{a}{d+2a} + ln\left(\frac{d}{d+2a}\right)\right] \quad (2.2)$$

$$\Delta G^{EL}(d) = \pi\varepsilon a(\xi_1^2 + \xi_2^2)\left[\frac{2\xi_1\xi_2}{\xi_1^2+\xi_2^2} + ln\frac{1+exp\,(-kd)}{1-exp\,(-kd)} + ln\{1 - exp\,(-2kd)\}\right] \quad (2.3)$$

$$\Delta G^{AB}(d) = 2\pi a\lambda\Delta G_{adh}^{AB} exp\left[\frac{(d_0-d)}{\lambda}\right] \quad (2.4)$$

$$A = -12\pi d_0^2 \Delta G_{adh}^{LW} \quad (2.5)$$

where *a* is the radius of a sphere.

For two interacting spherical particles with radii a_1 and a_2 separated by the distance *d*, $\Delta G^{LW}(d)$, $\Delta G^{EL}(d)$, and $\Delta G^{AB}(d)$ are then expressed as:

$$\Delta G^{LW}(d) = -\frac{A(a_1a_2)}{6d(a_1+a_2)} \quad (2.6)$$

$$\Delta G^{EL}(d) = \frac{\pi\varepsilon a_1a_2(\xi_1^2+\xi_2^2)}{(a_1a_2)}\left[\frac{2\xi_1\xi_2}{\xi_1^2+\xi_2^2} + \ln\frac{1+\exp\,(-kd)}{1-\exp\,(-kd)} + \ln\{1 - \exp\,(-2kd)\}\right] \quad (2.7)$$

For particles with same radius, $\Delta G^{AB}(d)$ has been derived as follows:

$$\Delta G^{AB}(d) = \pi\lambda\Delta G_{adh}^{AB} exp\left[\frac{(d_0-d)}{\lambda}\right] \quad (2.8)$$

In Eqns. 2.2 – 2.8, A is the Hamaker constant, while ε, ζ, and κ^{-1} are the permittivity of the medium, the zeta potential of the particles, and the double-layer thickness, respectively. In addition, the correlation length of molecules in a suspension medium is λ and d_0 is the distance of the closest approach between the plate and the sphere in Eqns. 2.2-2.4 or between 2 spherical particles in Eqns. 2.7 and 2.8. The term ε is usually expressed as the product of the permittivity of a vacuum (ε0, 8.854 × 10-12 C2·J-1·m-1) and the

relative permittivity (dielectric constant) of the medium εr, which is 80 for water at 20°C.

$$\frac{1}{k} = \left[\frac{(\varepsilon kT)}{(e^2 \sum v_i^2 n_i)}\right]^{1/2} \quad (2.9)$$

where k and e are Boltzmann's constant ($k = 1.38X10^{-23}J/K$) and the charge of an electron ($e = 1.602X10^{-19}C$), respectively; T is the absolute temperature in K; v_i and n_i are the valency and the number density (per mL of bulk liquid) of each ionic species, respectively.

In summary, the larger the zeta potential, the greater the repulsive force and the more stable the particle suspension system will be [176]. Zeta (ζ) potential is defined as the potential between the stationary surface (stern layer) of a particle in a suspension and the mobile phase located anywhere from the slipping plane and it changes as you move further away from the slip plane into less dilute parts of the suspension (Fig. 6) [177].

The XDLVO [178, 179] proposes, 0.6 nm and 0.157 nm as values of λ and d_0, respectively and the application thereof by Nabweteme et al [180] on the flocculation of the freshwater (*Microcystis sp*) and marine (*P. minimum*) suggested that the process was controlled by electrostatic repulsive forces. In the literature, there has not been a mention of DLVO as a tool to explain the process of flotation in general, and microalgae flotation in particular. In other to further expand the limited knowledge about microalgae flotation in order to take advantage of the cost effectiveness it boasts of, it is necessary to explore the possibility of using the DLVO and/or the XDLVO.

Even though the contribution of the polar acid-base component of surface tension is much greater than the contribution by the non-polar interactions (London, Keesom, and Debye), they are generally short-ranged [175, 181, 182] but these could extend beyond several molecular diameters when the suspension medium is water or other polar liquids [183]. For monopolar surfaces (having acid or base group), monopolar repulsion energies between surfaces can be much stronger than the attractive Lifshtz-Van der Waals, the electrostatic repulsion as well as steric repulsion [183]. Hence the inability of the classical DLVO to explain the colloidal behaviour of systems involving monopoles or acid-base groups (bipoles).

2.4 Drying and processing of microalgae

Drying technologies based on waste heat, solar, and other technologies like spray drying, drum drying, multi-stage drying, freeze-drying or ovens are available for achieving > 85% biomass concentration. However, heating is an energy intensive process, and even when waste heat is used, there is need to put in place extra infrastructure in order to collect and channel the heat which is expensive to install and maintain [184]. However, drying duty can be reduced or eliminated if cell lysis can be achieved in the wet algae cells [36].

2.4.1 Algae cell disruption and Oil extraction

The complexity of the microalgae cell wall makes access to their oil problematic. Several techniques have been developed to facilitate cell disruption as shown in Figure 6. The complexity and toughness of *Nannochloropsis oculata* cell wall, for example is because of the presence of an aliphatic polymer known as known as algaenan. The cell wall of *Chlorella vulgaris* however, is made of microfibrils of glucosamine polymers [185]. In order to maximize biofuel production from microalgae, selecting a microalgae species with high oil content should be matched with the right cell disruption technique [185].

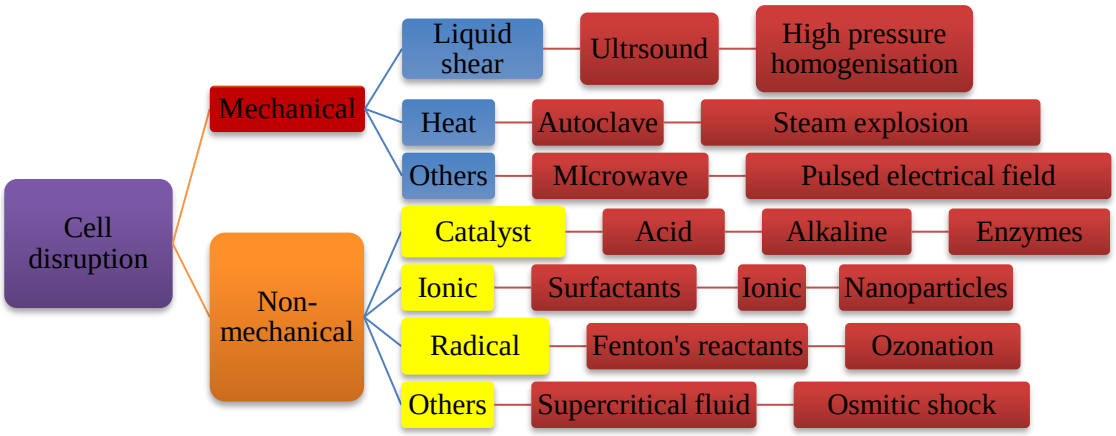

Figure 2.8: Figure 6. Cell disruption methods (Modified from [185])

The higher the degree of cell disruption, the more efficient is the lipid or oil extraction [186] that can be achieved by physical or chemical means, or a combination of both [187]. The use of surfactant to achieve cell disruption on *Chlorella* vulgaris and *Nannochloropsis*

oculata has been reported by Velasquez-Orta et al. [32] and Salami et al. [188]. In addition to surfactants, pulsed electrical fields [189], electroflocculation by alternating currents, autoclave, and osmotic shock [190] are some other cell lysing techniques. Others are functional polymeric membrane [191], nanoparticles [192, 193]; Fenton's reactant [194], ozonation [195], steam explosion fractionation [196], hot water [197-200], and subcritical organic solvent extraction [201]. A comparative study of the cell disruption efficiency of sulphuric acid, glass beads, high-pressure homogeniser, and ultrasonicator on wet *Chlorococcum* cells revealed that high-pressure homogeniser was the most efficient while no cell disruption occurred with ultrasonication [202].

2.4.2 Oil extraction from dried feedstock

Oil extraction from microalgae is traditionally based on solvent extraction. Recently, advance methods like microwave irradiation, ultrasound, supercritical fluids and ionic liquids are been deployed, mainly as a cell disruption mechanism to allow for more efficient solvent extraction [203] . The most popular solvent- based oil extraction method for dry biomass is the Bligh and Dyer [204] even though the Folch et al. [205] method existed earlier. Modified versions of the Bligh and Dyer method exists such as: Bligh-Dyer ultrasonic bath, Bligh-Dyer ultrasonic probe, the miniaturized Bligh-Dyer [206], and Halim et al. [207]. Guldhe at al [187] reported a 28.33% yield of lipid per dry cell weight of *Scenedesmus* sp using microwave for cell disruption while the yield from sonication was 9.43 % less. In another investigation using *Nannochloropsis* [208], 90.21 % lipid recovery was achieved using subcritical ethanol.

2.4.3 Wet oil extraction process

The presence of water has the tendency to improve or influence cell wall components (phospholipids and glycolipids) extraction [209], without which it is not easy to access the fatty acids layer within the cells. In this regards, wet oil extraction could be seen as more advantageous in comparison with dry approach. It is noteworthy however, that water interference can negatively affect the process of oil extraction, notably is the fact that the strength or concentration of the extracting agent or solvent is reduced. This implies that the more water there is, the more the quantity of the extracting agent that would be needed and hence the more expensive is the process of oil extraction. All of the extraction methods

used for dry microalgae can also be used to extract oil from wet microalgae. However, the advanced technologies are preferred because of the extreme conditions that allows for less water interaction as compared to when dry biomass are used. Huang and Kim [210] reported that at 80 % water content, 100 % oil extraction was achieved on *Chlorella vulgaris* using cationic surfactant CTAB in a process said to improve energy intensity of biofuel production step. Without heating, wet microalgae containing 90 wt. % water was made to dissolve in 1-Ethyl-3-methylimidazolium methylphosphate ($C_{13}H_{25}N_4O_3P$), a polar ionic liquid that was recoverable and reusable [211]. Other surfactant-based methods for oil extraction include: [193-195]. During the hot water approach of Park et al. (2014) [198], SDS was also involved as a cell disruption agent resulting in a reduction of the amount of acid catalyst needed for the esterification of FFA.

2.5 Biodiesel from algae

Biofuel derived from algal lipids are considered good replacements for liquid fossil fuels [1, 42, 212], having similar combustion properties to traditional fossil oil and thus reducing the need for major changes to combustion engines [213, 214]. However, algal biodiesel has not been commercially deployed due to the prohibitive costs associated with culturing and harvesting the algae, and the subsequent extraction and treatment of the oil [23, 24].

The use of algae for biodiesel production is one of several other ways through which algae biomass can be used for energy. Other process for converting the biomass include anaerobic digestion to produce methane, gasification to produce syngas fermentation to ethanol and direct combustion to produce steam for the production of electricity [18]. It has been possible to use vegetable oil directly in the diesel engine invented by Rudolph Diesel in 1897 and demonstrated during the 1900 World Fair with peanut oil [11]. However, due to the low volatility and high viscosity of algal oil (10 times the viscosity of Petro diesel) because they are approximately 20 times as light as diesel, it needs to be modified in order to work in current diesel engines. The specified legal requirements for biodiesel viscosity is 1.9 - 6.0 $mm^2\ s^{-1}$ for the American ASTM D6751 standard and 3.5 - 5.0 $mm\ s^{-1}$ according to the EN 14214 European standard) [19]. For heating purposes, EN14213 and ASTM D396 are the European and American standards, respectively [215]. Some of the processes through which the fuel properties of biodiesel can be improved to meet required standards are pyrolysis, micro-emulsification, and

transesterification. Of these three, transesterification is the most widely accepted because it produces biofuels with properties similar to those of petrol-diesel.

2.5.1 Pyrolysis of biomass or algal oil

The term cracking is usually used when pyrolysis (thermal break down of large molecules into smaller parts in an air-tight vessel) is done in the presence of catalysts. Pyrolysis involves the heating of biomass to produce liquid, gaseous, and solid products in an oxygen free environment and depending on the type of pyrolysis, operating temperature is between 350 $^{\circ}$C and 1000 $^{\circ}$C. although the short residence time of less 1 sec in flash pyrolysis results to high liquid yield and reduced accumulation of energy [216], the process is disadvantaged by poor thermal stability and corrosiveness of the oil produced, dissolved solids, eventual increase in viscosity, alkali dissolution, and formation of pyrolytic water [217]. Eterigho et al. [218] and Lima et al. [219] reported the catalytic cracking of vegetable oil to produce biodiesels with advantages such as: low viscosity, non- gumming, and non- coking. However, these type of biodiesels are usually characterised by acid values (0.50 mg. KOH g^{-1}) higher than required by the European and American standards [220]. Immiscible vegetable oil and short or medium chain alcohol can be mixed in the presence of surfactants to improve stability [221]. Although this method eliminates the need to recover impurities of glycerol [19], improved viscosity, and octane number, it is however accompanied by incomplete combustion, carbon deposition, and sticking of injector needle as some of its problems [14, 222].

2.5.2 Transesterification

During the transesterification of lipid to biofuel (fatty acid methyl ester), three steps (Figure 5) are involved, namely: conversion of triglycerides (TG) (oil) to diglycerides (DG), conversion of diglyceride to monoglyceride (MG), and finally the conversion of monoglyceride to glycerol by-product, producing fatty acid methyl ester (FAME) at each stage. Homogeneous (acid, base, or enzymes) and heterogeneous catalysts can be used in the process of conversion of oil or fat to fuel [215]. Non-catalysed transesterification of oil to FAME can also be achieved through supercritical fluid technology [185, 223], the use of co-solvents like chloroform and hexane, microwave, and ultrasound [185].

The most commonly used transesterification process is the base catalysed type with

NaOH or KOH because it is faster than the acid catalysis, where reaction times of as long as 2 days have been reported, and the catalyst is not as corrosive. Sometimes alkoxides are used to prevent water formation [215]. However, this process does not favour oils with a free fatty acid (FFA) content above 2 % [19], due to the conversion of the FFA to soap and water, hence preventing the forward reaction that favours FAME production.

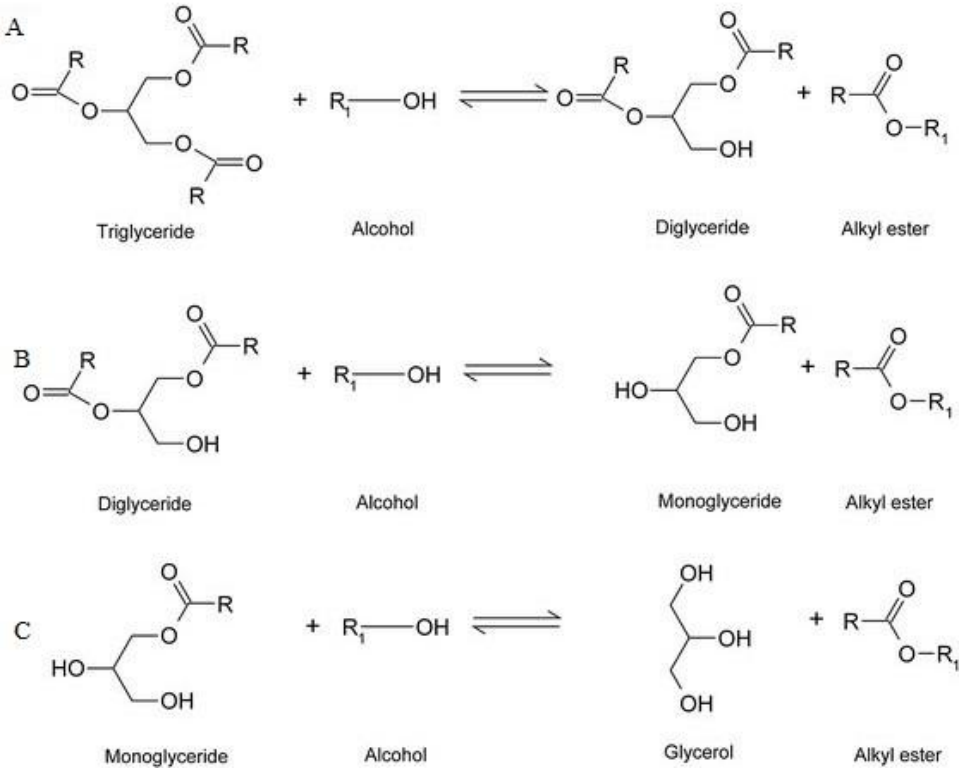

Figure 2.9: Mechanism of biodiesel production from vegetable oil

Acid catalysis has the capacity to deal with the FFA contents of above 2 %, converting them to alkyl esters which is why acid pre-treatment is sometimes applied before a base catalysis is carried out [224-227].

Homogeneous catalysts (acid or base) have the tendency to be dissolve in the glycerol and FAME layers respectively and this makes them difficult to recover and reuse as opposed heterogeneous catalysts [228].

The traditional biodiesel production via transesterification involves a two-step process, namely: oil extraction and transesterification as separate operating units. On the other hand, direct or in situ transesterification requires that both oil extraction and

transesterification be performed in a single operating unit. Using soybean as feedstock, Hass and Wagner estimated an 88 %v reduction in biodiesel production cost when in situ or direct transesterification was used as opposed to the traditional approach [229].

In situ transesterification of dry algae

In situ transesterification requires large methanol to oil molar ratios (52:1-1277:1). That is because methanol is not only acting as a reactant but also as a solvent or lysing agent for breaking of algal cell walls. Tran et al. (2011) [230] reported higher biofuel conversion of 97.3 wt. % oil from disrupted cells of *Chlorella* vulgaris when compared to 72.1 wt. % obtained when extracted oil from the same species was transesterified enzymatically with immobilised lipase that was effective even at about 71% moisture. Indeed, the submission by Tran et al. is in line with that of Park et al. (2015) that; combining the wet process with advanced technology such as supercritical fluids, co-solvents (e.g. hexane), microwave, ultrasound, surfactants, nanoparticles, switchable solvents, and hydrothermal treatment has the tendency to make biodiesel production from wet algae commercially viable [185]. It is important to note that the use of soybean as feedstock, for example, requires little or no drying compared to microalgae feedstock. The cost of oil extraction from soybean is estimated based on 90 % solid content. Therefore, for cost comparison, between algae biodiesel and biodiesel from soybean, the cost of drying the algae up to 90 % solid has to be considered in addition to the cost of oil milling [35]. Hence algal biodiesel is less cost effective than biodiesel from soybean, albeit algal biodiesel is more sustainable and greener.

In situ (direct) transesterification of wet algae

Owing to the high cost of drying microalgae biomass, recent research has been focused on conversion of wet biomass in an attempt to reduce the drying duty of algal biodiesel. Kim et al [231] investigated the possibility of using wet biomass (80 wt.%) at 95 ^{O}C and reported over 90 % FAME yield using hydrochloric acid (HCl) as catalyst. Teixeira [232], proposed an experimental model that will allow for biofuels to be produced from algae based on the dissolution and hydrolysis of the wet algae in ionic liquids in the absence of acid or base catalyst. Inoculum *Nannochloropsis* containing about 90 % water was converted to FAME using supercritical methanol at 255 ^{O}C for 25 minutes, using a 1:9 wet

algae to methanol ratio [233]. Likewise, reactive extraction has been carried out at 80 % water content on *Nannochloropsis oceania* [231]. By comparing energy balances between dry and wet routes for biodiesel production from microalgae, Xu et al. (2011) [36] demonstrated that the wet route has more potential for high value biofuels (Green diesel and H_2) as main products. Sills et al. (2013) [234] supported this argument upon the premise that high energy co-products of anaerobic digestion such as methane be incorporated into an integrated biorefinery.

2.6 Alcohol-water- surfactant-air interactions

Surface tension can be determined by two main methods namely: the Du Noüy [235] method where the pull on a metal ring by a liquid, is used as a measure of the tension force on the surface of the liquid, and the method of Padday et al [236], whereby a rod is used in place of the ring.

The relationship between surface tension and the force of pull exerted by the fluid on the probe is given by:

$$\gamma = \frac{F_{max}}{\tau_P} \tag{2.10}$$

where τ_P is the perimeter of the probe (mm), F_{max} is the maximum pulling force (N), and γ is surface tension (mN m^{-1}).

Unlike a Du Noüy ring, no correction factors are required when calculating surface tensions. Due to its small size the rod can be used in high throughput instruments that use a 96-well plate to determine the surface tension. The small diameter of the rod allows its use in a small volume of liquid with 50 µL samples being tested in a particular case [237]. In addition, the rod also allows use for the Wilhelmy method because the rod is not completely removed during measurements. For this reason, the dynamic surface tension can be used for accurate determination of surface kinetics on a wide range of timescales.

The Padday technique also offers low operator variance and does not need an anti-vibration table. This advantage over other devices allows the Padday devices to be used in the field easily. The rod, when made from composite material is also less likely to bend and therefore cheaper than the more costly platinum rod offered in the Du Noüy method. In a typical experiment, the rod is lowered using a manual or automatic device onto the surface being analysed until a meniscus is formed, and then raised so that the bottom edge

of the rod lies on the plane of the undisturbed surface. One disadvantage of this technique is that it cannot bury the rod into the surface to measure interfacial tension between two liquids.

Surfactants are used in motor oils, lubricants, detergents, soap, pulp and ink to reduce the relatively high surface tension of water and in most cases co-surfactants or additives are applied in order to modify interfacial properties even when bulk concentrations are low [238]. Due to their cell lysing capacities [239], surfactants have been reported to be s useful means to reducing the amount of acids needed for transesterification [198] and this comes as an advantage considering cost and safety implication of acid.

The CMC of a surfactant is that concentration of the surfactant above, which micelles form. Huang et al. [240] reported that the addition of ethanol caused an increase in the critical micelle concentration (CMC) of ionic surfactant in water. This decrease was however, preceded by an increase when non-ionic surfactant was involved. They further reported that the γcmc (surface tension at CMC) of the system decreased or increased depending on whether the saturation adsorption was small and γcm of aqueous solution in the absence of methanol was big, or the other way around [240]. Indeed, the findings of Huang et al. was in agreement with an earlier report by Iyota and Motomura [241] [242] and so many others [238, 243-249] that; interfacial interactions play a major role in determining the interfacial tension, i.e. surface tension depends on alcohol concentration. In fact, research along this area, dates as far back as the work of Hardy [250] in 1912 and A. F. H. Ward [251] at Manchester University in 1940. In the work of Ward, he examined the behaviour of SDS in water and noted that above a certain concentration, C= 0. 00722N, known as the critical micelle concentration (CMC), micelles were formed with a sudden drop in equivalent conductance and these micelles were affected by the presence of methanol, so much so that when the amount of methanol reached 40%, no micelles formed [251]. Equivalent or molar conductance of a substance is a measure of the ability of the ions of that substance to conduct electricity when one gram is dissolved in an equivalent electrolyte.

Considering the dynamic and complex nature of the interactions between surfactants and alcohol as evident from above, there is need to screen for an appropriate surfactant and to determine the concentrations in relation to methanol are required to

effectively achieve algae separation in a methanol environment. This is necessary because depending on whether a surfactant is non-ionic or ionic (anionic, cationic, or zwitterionioc) their behaviour, keeping everything else constant, will not be the same. For example, cationic surfactants have been used extensively to recover microalgae from aqueous medium, relying on the attractive forces between the negatively charged algae and the positive charge carrying surfactant. In a contrary manner, anionic surfactants have also proved to be useful in algae recovery. Other works have also indicated the possibility of harvesting microalgae using zwitterionic (with positive and negative ligands) surfactants. Depending also on whether the medium in which the algae is suspended is freshwater or seawater. The latter, is difficult or almost impossible when it comes to flotation technology. This is because of the interference of salt ions in the interplay between the medium and the suspended algae with respect to the high ionic charge as a result of salt ions (mainly Na and Cl) that controls the electric double layer.

The presence of a second liquid phase (Methanol) can have a very significant impact on the overall process dynamics. Alcohols have the tendency to prevent bubble coalescence, subject to concentration [252]. Higher concentrations do not only result in wet bubbles but they can also reduce their stability. The ability of alcohols to enhance bubble formation is born out of their relatively low surface tensions and hence the tendency to lower the surface tension of water. The lower the surface tension, the easier it is to generate bubbles. The presence of methanol brings about competition between methanol and surfactant at the air-liquid interface reducing the hydrophobicity and adsorption capacity of surfactant as concentration increases leading to low adsorption of surfactant on the water surface [240]. Moreover, there is a reduction in H bond between water molecules due to the presence of methanol [253, 254].

2.7 Conversion of wet biomass and the need for an intensified biodiesel production from wet algae

One of the reasons microalgae are classified as a “third generation” source of biofuels is because they grow mostly on water but this huge “benefit” is not without a “cost” and that is the fact that biodiesel and oil extraction yield is lowered by water interference. If this water growth media can be manipulated so that drying and hexane extraction which accounts for about 92.2 % of energy cost [35] is reduced considerably, production cost will

be greatly reduced. This explains why a lot of research effort has been devoted to investigating ways of eliminating the drying steps.

Efforts to develop a cost-effective algal biodiesel are focused on the improvement of processing mechanisms (cultivation and harvesting technologies) as well as genetic modification of algal strains in order to selectively improve on their oil production and ease with which the extraction and conversion of the produced oil can be achieved. As an integrated biodiesel production process from algae, reactive extraction has been carried out through elimination of the oil extraction steps that may otherwise lead to additional material cost and oil losses. This is a step in the right direction as it seeks to the reduce process and material costs [255] and also increase yield [256]. However, the highly expensive process of drying (~85 % of total energy cost) [35], remain unchanged by the conventional reactive extraction process.

In order to eliminate this drying cost, other researchers have investigated the possibility of converting wet biomass into biodiesel. Furthermore, a comparison between the dry and wet processes were made and it was concluded that the wet process is more has the higher tendency of economic viability, if combined with advanced oil extraction technologies [185]. Essentially, there was no significant reduction in cost as most of these processes, involve high energy and material input and sometimes involves multiple processing stages like dewatering and pre-treatment, making scale-up difficult [48]. A scalable process would be that which eliminates extreme conditions such as high temperature and pressures as well as expensive chemicals. Hence, there is the need to further intensify the algal biodiesel production process such that the number of unit operations are not only reduced but that they are also carried out under ambient conditions. This presents some great potential to enhance the cost effectiveness of algal biodiesel.

The need to achieve biofuel production through a process that eliminates the drying steps is key to reducing production cost and thereby offering an opportunity for the commercialisation of algal oil biofuels. Because of the interference of water, which may lead to saponification, oil hydrolysis, as well as reduced FAME production, most attempts at converting wet biomass to biodiesel were based on acid catalysis since the base reaction is less tolerant to moisture. One peculiar characteristic of the production of biodiesel from wet biomass is the high methanol demand, leading to high cost of recovery and other downstream processes. For example, achieving 69 % biodiesel yield in 20 min, from

Chaetoceros gracilis cells with 400 % moisture, 3460:1 methanol to oil molar ratio was needed [257]. Within a reaction time of 20 hrs, 98 % biodiesel conversion was reported by Liu and Zhao [258], based on methanol to oil ratio of 868:1 involving a mixed culture of algae and cyanobacteria. Also, after 20 hrs, 97% biodiesel conversion was recorded from wet *C. vulgaris*, according to Velasquez-Orta et al. [32] when 600:1 methanol to oil ratio was used. In spite of the progress made in producing biodiesel from wet algae, there is still a lot to be done if the promise of a cost-effective biodiesel production from wet biomass, is to be actualised. Therefore, if the demand for methanol as a solvent for oil extraction is reduced by using a strain that is less compact in terms of cell wall, there might be an opportunity to comparatively lower the amount of methanol and hence the process cost. This cell wall advantage may also lead to a reduction in the reaction time [188].

A recent technology that attempted to use wet biomass directly without prior drying was proposed by Sitepu et al [259]. Although an intensified process, the feedstock that was used in this process was harvested by centrifugation at 8000g for 10 min to lower the moisture contents to 67.7 %, making it rather energy intensive, although conversion to biodiesel was achieved at ambient conditions of temperature and pressure. Another downside of this work is that hexane was used to extract biodiesel, which is not safe, not to mention the fact that the reaction rig itself is based on rotating reactor operated at about 6000 rpm.

2.8 Conclusion

It is obvious that there is a significant research gap existing in the field of foam flotation in spite of the progress made. As far as microalgae harvesting through foam flotation is concerned, there is still a lot to understand in relation to the process parameters as well as media properties and cell morphology. As it stands now, foam flotation of marine microalgae has received very little attention and this is because of the challenge of salt ions interfering with the separation process. This challenge is also an opportunity for further investigation into the foam flotation of marine species of algae, especially because of the comparative advantage that they have over their freshwater counterparts.

Sustainable and cost-effective biodiesel from algae is possible and one way to achieve this is to reduce the process steps to minimise biomass losses and by reducing or eliminating biomass drying stages. Foam floatation has the capacity to achieve that feat once the

process regime is better understood.

Process intensification has the potential to change the narrative of prohibitive cost of biodiesel especially if it is applied to foam flotation where harvesting, cell disruption, oil extraction, as well as biodiesel production is achievable in one-unit operation. The main cost saving strategies in this research include but not limited to: reduced cost of harvesting, reduced cost of cell disruption, reduced cost of oil extraction, and reduced cost of transesterification, mainly due to the simplicity of design and ambient operating conditions. Most importantly, this work intends to eliminate the drying steps, which contributes a major bottleneck to the commercialisation of algal biodiesel process.

Chapter 3

Foam flotation harvesting of *Nannochloropsis oculata*

Abstract

Marine algae claim an advantage over their fresh water counterparts because the better outlook of their energy-food nexus. The lack of competition between energy and food is made better by the fact that brackish and ocean water which are not needed for food and are available in excess of freshwater, making the production of biodiesel from marine algae more sustainable than that involving freshwater species. *Nannochloropsis oculata* (*N. oculata*) being one of the most favoured species for biodiesel production (20 -56% lipid content) was chosen for this work.

The success (96 % recovery and 132 concentration factor) of batch flotation conducted with polystyrene beads of similar size as model is a good indication that within the context of operating conditions (airflow: 1 $Lmin^{-1}$, and CTAB concentration of 30 mg L^{-1}), size of *N. oculata* cells (3 µm) should not be a limiting factor to its recovery. However, it was discovered that factors other than size are equally important to the successful foam flotation recovery of *N. oculata*, as only 2 % of cells were recovered under the same conditions even with twice as much surfactant. One such factor is the production of extracellular materials such as algaenan. This theory is supported by the high recovery (92 %) of polystyrene beads suspended in f/2 medium as opposed to the zero-recovery recorded when beads were suspended in supernatant recovered from the centrifugation of *N. oculata* culture in similar concentration. In f/2 medium, however, the concentration factor reduces to 89 due to more foam being produced in seawater than freshwater.

Based on a composite design of continuous flotation experiments involving three variables (airflow, surfactant concentration, and pH), attempt was made at improving the poor performances recorded in harvesting *N. oculata*. This time, higher airflow was relied on to increase bubble-particle collision while acidic pH was meant to increase bubble-particle attachment. In addition, diluted cultures were used in order to examine the role of salt ions in the foam flotation of *N. oculata*. Results suggests that foam flotation of *N. oculata* is more collision dependent than attachment controlled and the frequency of collision and attachment can be enhanced by reducing ionic strength as well as pH whilst increasing

airflow.

The process hereby proposed, is less expensive and guarantees higher delivery of lipids than previous cases in literature where *Tetraselmis sp. M8* (20-30 % lipid) was recovered at an airflow of 5 L min^{-1} with the support of a comparatively expensive mechanical Jameson's cell. To this end, this work has the potentials for reduced cost of production, which has been in the way of a successful commercialisation of algal biodiesel.

Keywords: Surfactant screening, flotation of marine algae, Algaenan, Design of experiments, polystyrene beads

3.1 Introduction

For algal biodiesel to be sustainable and widely acceptable there is the need to pay close attention to marine species due to the advantages of seawater not being required as a source for drinking water and its much greater abundance compared to freshwater. However, if the recovery of such marine microalgae cannot be achieved via a cost-effective process like flotation, as opposed to current methods of flocculation and centrifugation, prohibitive production cost and lack of scalability would remain as obstacles. The use of foam flotation as a tool for harvesting marine microalgae has received very little attention. This is because the high ionic strength of seawater ensures a more compact electrical double layer around the cells and therefore decreases Debye length. This phenomenon makes it difficult for the positively charged surfactant to interact electrically with the negatively charged algae cells. Sourabh et al [92, 94] have recently reported the flotation harvesting of marine algae, *Tetraselmis sp*. (*M8*) by tuning the medium pH to induce cell hydrophobicity. pH-induced hydrophobicity has been reported for both freshwater and marine algae [104, 164, 165] and the impact of pH is said to be specie and surfactant dependent [166]. However, *M8* as a specie, is not a favoured candidate for biodiesel, partly due to the low average lipid content (20-30%) [167]. One of the most favoured marine species for biodiesel production is *Nannochloropsis* based on lipid content (20 -56%) and FAME productivity [168, 169]. *N. oculata* also has high specific growth rate of 0.27/day and doubling time of 2.59 days compared with *Dunaliella salina* (0.18 and 3.85), *S. obliquus* (0.22 and 3.15), and *C. vulgaris* (0.14 and 4.95), respectively [170], which indicates higher sustainability since this would ensure regular feedstock availability. *N. oculata* also enjoys the advantage of

having a very high biodiesel yield (97.5 wt.%) [260]. However, the few reported cases of harvesting *N. oculata* were based on flocculation [61, 159, 261, 262], which is a non-environmentally friendly process. Although bioflocculants are sometimes used [263], they are not cheap.

One of the reasons why microalgae are generally difficult to recover is their small cell sizes; the smaller the cell size, the less probable it is for air bubbles to collide with and capture the cells on their way up the column [158]. The production of extracellular compounds like algaenan (in *N. oculata* for example) as well as biological surfactants by marine algae is capable of controlling the interaction between the cells and collectors in such manner that results in low recovery efficiency. The chemistry of algaenan (a hydrophobic trilaminar non-hydrolysable biopolymer) [160], found around the cell wall of certain microalgae, is hardly understood. Besides their hydrophobicity [160], algaenan also tends to reduce the effect of collectors, by limiting their access to cell wall polysaccharides [161] as well as the formation of H-bond with same [162]. In addition to the extracellular materials, multivalent ions, i.e. Mg^{2+} and Ca^{2+} in seawater are capable of reducing sorption capability of seawater organism [163] due to their interference with colloid stability.

Because of their similarity with algae cells in terms of density and availability in different sizes [264], the use of polystyrene beads as model microalgae and bacteria has been reported in earlier works [265, 266]. Polystyrene beads have also been used in metallurgy to examine the effect of surface properties and hydrodynamic conditions on metal removal through flotation. One of such is the work of Okada et al in 1990 [120] where beads were used to gain some insight into the interplay between particles floatability and pH in air flotation process. Previous works [267, 268] had highlighted the role of hydrodynamic interactions between particles and the interactions between surface chemicals [269-272], but the work by Okada et al [120] is a combination thereof, just like that of Derjaguin et al. [273], three years later. In the work of Okada et al [120], 0.913 μm sized polystyrene beads and bubbles generated from different surfactants, namely: DAH, SDS, and polyoxyetylene lauryl ether (POE), were tested for ζ-potential as a function of pH. Flotation efficiency was reported to be a function of the surface properties of bubbles and polystyrene beads and the best conditions were achieved when the surface charges were minimum [120]. In a related work, Yoon and Yordan [274] investigated the change in ζ-potential of microbubbles generated by different surfactants and their conclusions

were the same as those of Okada et al [120], including the idea that when non-ionic surfactants were used, the charge carried by the bubbles, be it negative or positive (modified), was a function of pH. According to both works, isoelectric point (pH) is alkaline with cationic surfactants but acidic with anionic surfactants. Although they are similar to microalgae in many ways, the fact that they are non-organic makes them less dynamic and complex than algae cells. This is becasue they are inert to most of the chemical processes that occur within the medium and hence would not matter whether or not the medium is freshwater or seawater. Therefore, the only basis for comparison against a particular biological specie would be size, density, and shape. The task of the researcher therefore is to select particle size and shape that is similar to the modelled cells. This work seeks to use polystyrene beads as model *N. oculata* cells based on size to see if the comparatively small size of *N. oculata* cells could be an impediment to cell recovery. The beads would also be used to investigate the importance of particle surface charge on flotation performance.

Screening for surfactants will be conducted to decide on which surfactant is best suited for the foam flotation of *N. oculata*. In this work, five different surfactants namely; cetyltrimethylammonium bromide (CTAB), sodium dodecyl sulphate (SDS), myristyltrimethylammonium bromide (MTAB), dodecylammonuim hydrochloride (DAH), and dodecylpyridinium chloride (DPC), will be investigated. This will also allow for the impact of air flow to be investigated, in addition to surfactant type and dosage.

In addition to deciding the best surfactant in terms of type and concentration, other objectives of this research are to study the role of cell properties (size, morphology, hydrophobicity, surface charge) as well as media chemistry (pH and ionic strength) in the foam flotation process of *N. oculata.* The impact of surfactants on cell hydrophobicity and surface charge and how they relate with cell morphology, as well as interfacial properties, will also be investigated.

The aim is to define a path through which *N. oculata* can be recovered via foam flotation. This is not only because this has not been investigated before, but to also take advantage of the cost advantage of this technology, bearing in mind the eventual goal of producing algal biodiesel from *N. oculata*.

3.2 Materials and Methods

3.2.1 Algae cultivation

N. oculata (CCAP 849/1) was batch cultivated at 19 ºC in f/2 medium without silicate (F/2-Si) [275]. F2-Si was prepared by adding 1 mL of each of the following stock solutions: (A) 880 mM $NaNO_3$ [sodium nitrate]; (B) 47 mM NaH_2PO_4 [sodium dihydrogen orthophosphate]; and (C) 1 mL Trace Elements Solution; per Litre of the final volume of fresh natural seawater and micro-algal inoculum (20 %) to be added. Therefore, 1mL of the three feedstock and 1 mL of trace elements solution per 800 mL of natural seawater is used at preparation stage. The trace elements and their concentrations per Litre are as follows: Na_2-EDTA (4.16 g); $FeCl_3.6H_2O$ (3.15 g); $CuSO_4.5H_2O$ (0.01 g); $ZnSO_4.7H_2O$ (0.022 g); $CoCl_2.6H_2O$ (0.01 g); $MnCl_2.4H_2O$ (0.18 g); $Na_2MoO_4.2H_2O$ (0.006 g); Vitamin B12 (0.0005 g); Vitamin B1 (0.1 g); and Biotin (0.0005 g). Cultivation was done in a 40 L polycarbonate Nalgene carboy under a 16 L: 8 D photoperiod (2200–2800 lux) using a mixture of warm and cold fluorescent tubes. In order to reach the final culture volume of 40 L, 50 mL of master culture in a tube was transferred into a 200 mL media containing all the nutrients and cultured in an Erlenmeyer flask for two weeks. 200 mL culture was then transferred from the 250 mL into 1 L bottle containing 800 mL of media, and cultured for another two weeks. This process was repeated according to the 20 - 80 % culture- media composition earlier described until the final stage where 8 L culture was used to cultivate 40 L culture that was eventually used. Mixing and gas exchange was facilitated by bubbling HEPA filtered (0.2 µm) air through the culture.

C. vulgaris (CCAP 211/63) was cultured in a BG11 medium [276] in a 20 L carboy under the same conditions as *N. oculata*. The BG 11 medium is comprised of 10 mL per Litre of feedstock and 1 mL per Litre of trace elements solution. The feedstock composition per 500 mL is: (1) $NaNO_3$ (75.0 g); (2) K_2HPO_4 (2.0 g); (3) $MgSO_4.7H_2O$ (3.75 g); (4) $CaCl_2.2H_2O$ (1.80 g); (5) Citric acid (0.30 g); (6) Ammonium ferric citrate green (0.30 g); (7) $EDTANa_2$ (0.05 g); and (8) Na_2CO_3 (1.00 g). The trace elements per Litre are: H_3BO_3 (2.86 g); $MnCl_2.4H_2O$ (1.81 g); $ZnSO_4.7H_2O$ (0.22 g); $Na_2MoO_4.2H_2O$ (0.39 g); $CuSO_4.5H_2O$ (0.08 g); and $Co(NO_3)_2.6H_2O$ (0.05 g). The sequence of culturing was the same as described for *N. oculata.* Once prepared, F2-Si or BG 11 (without the micro-algal inoculum which is added later) were sterilised by autoclaving at 121℃ for 30 min. All chemicals were purchased from Sigma Aldrich UK.

3.2.2 Foam flotation: Column description

The column (Fig. 3.1.) is made of glass with adjustable total column height of up to 135cm and a fixed internal diameter of 5 cm. The air chamber is a 10 cm section located below the liquid and foam chamber with both sections separated by a porous polystyrene (6 µm Ø) air disperser. Liquid is fed at 7.5 cm above the air chamber while air supply is through the base of the column. Foam is collected at the top of the column along with the algae.

The air inlet at the bottom of the column allows the steady generation of bubbles, made possible as a result of the surfactant in the feed. Bubbles generated are carried upward in the column, carrying with it, attached particles that were made possible due to the hydrophobicity induced by the amphiphilic nature of surfactant. Acting as a bridge, the surfactant molecule attaches its hydrophilic end to macroalgae particles while the hydrophobic end is linked to the bubbles. As the bubbles rise, they do so, carrying along particles by way of attachment and/ or collision. At the top of the column is the foam outlet where captured particles are collected as foamate. The mechanism of bubble-particle infarctions has been described in the literature section of this dissertation.

The 5 cm ID column, just like any typical flotation column, is made up of three major sections, namely: the air chamber, the collection or mixing zone, and the separation or frothing zone. The air chamber is 10 cm long, and just like the column height, the liquid chamber or height of the liquid pool can be varied. The froth zone also varies according to the selected column height, liquid pool, airflow feed flow, and surfactant type and concentration. The maximum height of the column with exception of the air chamber, is 135 cm. The plastic coupling assembly allows for column heights of 45 cm, 60 cm, 90 cm, and 120 cm to be selected. The entire column is made of high-grade Pyrex to reduce particle drag that could result from plastic column while the inverted U-shaped top is for easy foamate collection. Bubble-particle collision and bubble-particle attachment occur in the collection zone. The collected particles are then transferred to the froth zone away from the bulk solution. The air chamber is filled with only air which are dispersed through the sparger into the main column where bubbles are generated.

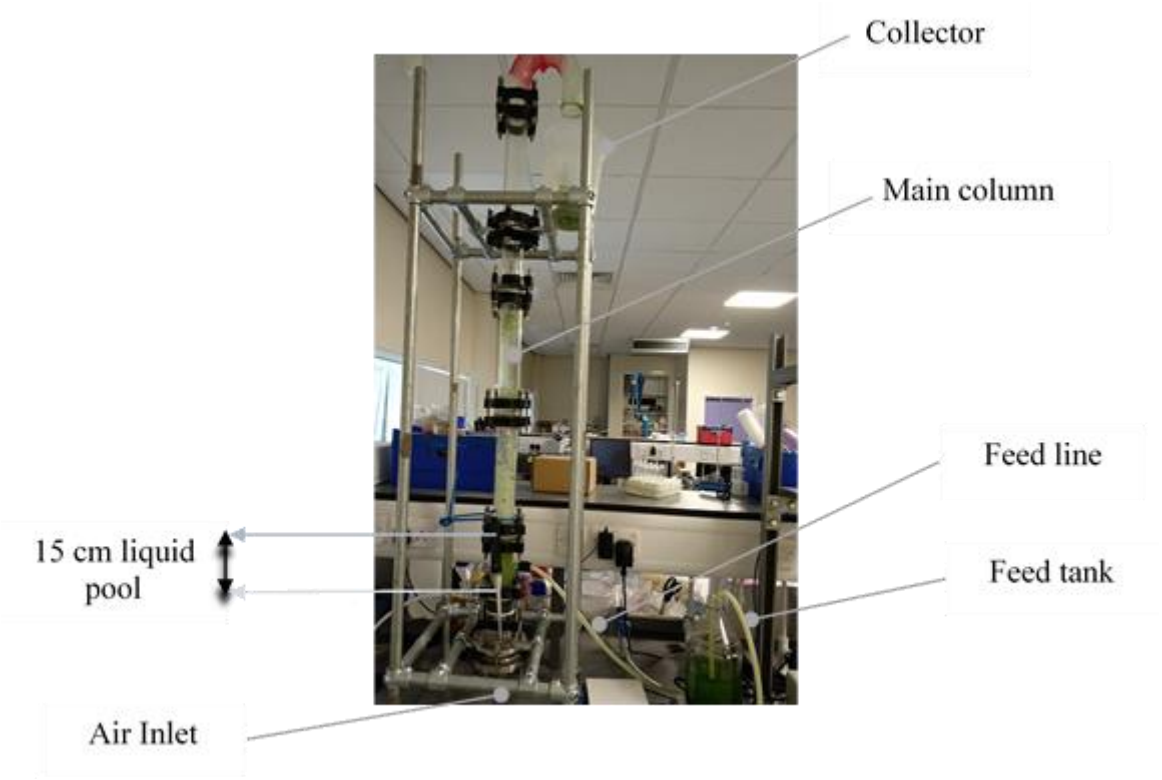

Figure 3.1: Description of the flotation operation showing a continuous flotation run

A 2 L bottle was used as a feed tank from which microalgae culture various of various surfactant concentrations were fed into the mixing zone of the column via a peristaltic pump (Masterflex 7720160 fitted with a Masterflex - 77201-60 head). The mixing zone or liquid chamber of the column is located just above the air chamber and compressed air was supplied into the air chamber through a ¼" hose fitted to the centre of the bottom plate. Between the liquid and air chamber, was a porous (6 µm) polystyrene sparger, which diffuses air through the liquid and thereby creating bubbles that in turn, rose along the column. Foamate was then collected at the top of the column and analysed.

Batch experiments were conducted to investigate the role of media chemistry (salt ions and pH), cell properties (size, morphology, and surface charge). In order to study the impact of surfactant (type and concentration), media pH and operating conditions of airflow, continuous operations were conducted. During batch experiments, the required amount of feed to be treated was fed into the column whilst maintaining around 0.5 L min^{-1} of air to keep the liquids from crossing from the liquid chamber into the gas chamber. Once all the liquid had been fed to the column, the airflow was then set at 1 L min^{-1} with

the aid of flowmeter and the timing of the experiment began. The process is allowed to continue until all the foamate has been collected. Collected foamate is then analysed for recovery and concentration factor. During continuous flotation, once the feed is introduced into the column to a desired liquid level, the airflow was then set to the desired value while simultaneously opening the underflow, which marks the beginning of the continuous process. The continuous flow could be allowed to go on over a specific time or until a certain amount of feed is supplied (with time noted). The airflow is then turned down to 0.5 L min^{-1}(just to prevent liquid from draining down the sparger) while simultaneously stopping the underflow, bringing the process to an end. Collection of foamate was allowed to stop naturally.

3.2.3 Foam flotation: impact of cell size and morphology

Feeds and samples preparation

Feed concentrations of approximately 1.3 g L^{-1}. (DW) and a liquid height of 30 cm was maintained for all feeds throughout the experiment. The feeds were original *N. oculata* culture (N); *N. oculata* in seawater (N-SW); *N. oculata* suspended in freshwater (N-FW); polystyrene latex beads (Alfa Aesar) suspended in freshwater (B-FW); polystyrene latex beads suspended in f/2 (B-F/2); *C. vulgaris* suspended in freshwater media (C-FW) as control; beads suspended in supernatant recovered from *N. oculata* (B-NS); *C. vulgaris* suspended in supernatant recovered from *N. oculata* (C-NS); and *C. vulgaris* suspended in f/2 (C-F/2).

Density (1050 kg m^{-3}) of the beads used in this work is close to the average density of algae (1020 kg m^{-3}) [19]. Polystyrene beads vary in size and hence it is important to make sure that the selected size of beads (2 µm) is a good representation of the microalgae to be modelled. One millilitre of beads of initial concentration of 2.5 wt. % was suspended in 19 mL of either seawater (B-SW) or freshwater (B-FW) to a concentration of 1.25 wt. % which is close to the concentration of algae culture (1.2 ± 0.1 g L^{-1}) based on dry weight analysis. To prepare resuspended samples of *N. oculata* (N-FW, N-F/2 and N-SW), washing of original culture (*N. oculata* or *C. vulgaris*) with DI water, was done by Sigma type centrifuge (Model 2-6). The same centrifugation process was used to acquire *N. oculata* supernatant in which beads and *C. vulgaris* were suspended to obtain B-NS and C-NS, respectively.

Maintaining a constant column height of 135 cm, CTAB (Sigma-Aldrich, UK)

concentration was kept at 60 mg L^{-1} when NS or F/2 were the suspension media, except for when SDS was added or when B-F/2 was the feed. When SDS was used as a complimentary surfactant to bridge between algae cells and CTAB in the presence of HCl (Sigma Aldrich), 30 mg L^{-1} each of CTAB and SDS were used. With B-F/2 and the rest of the feed, 30 mg L^{-1} of CTAB were used. The increase of CTAB to as much as 60 mg L^{-1} in those cases was because 30 mg L^{-1} of CTAB was not enough to cause any meaningful cell recoveries.

In order to investigate the impact of cell morphology and size, *N. oculata*, C. vulgaris, and Polystyrene beads were used as feed. *C. vulgaris* was hereby used as a control due to its popularity in algae flotation [19, 40, 102, 277, 278]. The airflow rate was maintained at 1 L min^{-1} for 6 min per batch operation. Each experiment was repeated two more times and the average of three results recorded with standard deviation.

Recovery efficiency was calculated according to the following expression;

$$RE = \frac{number\ of\ cells\ in\ the\ foamate}{number\ of\ cells\ in\ the\ original\ culture} \tag{3.1}$$

Concentration factor is estimated based on the expression below:

$$CF = \frac{number\ of\ cells\ per\ ml\ of\ \ foamate}{number\ of\ cells\ per\ ml\ of\ the\ original\ culture} \tag{3.2}$$

Cell count was achieved with the aid of a Haemocytometer (Reichert) combined with light microscope (Leica DM 500) at 40X/0.65 magnification. Whatman filter paper (11cm Ø) was used for dry weight analysis in combination with Memmert oven and a precision analytical balance (RadWag, model As220/C/2, Poland) to 4 decimal places accuracy. Cells and beads dry weight measurements were done in triplicate by filtering 10 mL of culture or beads suspension onto a pre-dried and pre-weighed filter paper (Whatman quantitative filter paper, grade 42), rinsed with 20 mL of 0.5 M ammonium formate (Sigma-Aldrich, UK) solution and dried overnight to constant weight in an oven at 60 °C. The filter papers were dried at 103 °C for 3 h then left to cool in a desiccator over silica gel until use. The dried filtrate was then placed in a desiccator to cool after which they were reweighed to calculate the cell dry weight per unit volume of medium. Samplings were done in triplicates to ensure accuracy and repeatability of results.

The dried paper was weighed to 4 decimal places and the dry weight concentration DWC determined according to equation 3.3:

$$DWC = \frac{\text{weight of dried paper containing algae} - \text{weight of filter paper}}{volume\ (v)} \quad (3.3)$$

3.2.4 Surfactant screening and investigation of the impacts of airflow, ionic strength, and pH on foam flotation harvesting of *N. oculata*

In order to screen for the best surfactant and at what conditions they operate best, CTAB, MTAB, DPC, and DAH were tested for foam flotation experiments according to a composite design of experiments as obtained from Minitab®. Table 3.1 below contains details of the continuous flotation processes. Each experiment was carried out twice to ensure data repeatability. Similar experiments were later conducted using *N. oculata* cultures that were diluted by adding equal volume of freshwater to reduce the ionic concentration of the media. This was in order to study the impact of ionic strength, as a function surfactant type and concentration. pH adjustment was done using 0.1 M HCl. In order to bring the original culture from pH 8 to pH 6, 1.5 mL of 0.1 M HCl was used while 2.5 mL was needed to reduce the pH to 4. The column height was maintained at 135 cm throughout the experiments. All experiments were conducted in continuous mode with feed flow of 100 mL min^{-1} while the underflow was 50 mL min^{-1} and the rate of foamate was 50 mL min^{-1}. Higher airflow compared to the batch experiments were used in order to increase the collision probability between cells and air bubbles. SDS was avoided because of its high foaming rate which may affect cell concentration.

Airflow (L min^{-1})	CTAB (mg L^{-1})	pH
1.2	20	6
3.6	20	6
1.2	60	6
3.6	60	6
1.2	40	8
3.6	40	8
1.2	40	4
3.6	40	4
2.4	20	8
2.4	60	8
2.4	20	4
2.4	60	4
2.4	40	6
2.4	40	6
2.4	40	6
Airflow (L min^{-1})	MTAB (mg L^{-1})	pH

1.2	20	6
3.6	20	6
1.2	60	6
3.6	60	6
1.2	40	8
3.6	40	8
1.2	40	4
3.6	40	4
2.4	20	8
2.4	60	8
2.4	20	4
2.4	60	4
2.4	40	6
2.4	40	6
2.4	40	6
Airflow (L min^{-1})	DPC (mg L^{-1})	pH
1.2	20	6
3.6	20	6
1.2	60	6
3.6	60	6
1.2	40	8
3.6	40	8
1.2	40	4
3.6	40	4
2.4	20	8
2.4	60	8
2.4	20	4
2.4	60	4
2.4	40	6
2.4	40	6
2.4	40	6
Airflow (L min^{-1})	DAH (mg L^{-1})	pH
1.2	20	6
3.6	20	6
1.2	60	6
3.6	60	6
1.2	40	8
3.6	40	8
1.2	40	4
3.6	40	4
2.4	20	8
2.4	60	8

2.4	20	4
2.4	60	4
2.4	40	6
2.4	40	6
2.4	40	6

Table 3.1: Composite design of experiments for foam flotation of *N. oculata*; liquid height is 20 cm and column height was maintained at 135 cm, flotations were carried out in continuous modes.

3.2.5 Effect of CTAB concentration on Zeta (ζ) potential

Based on the screening conducted, CTAB was selected as the best candidate and therefore, further investigation on the role of CTAB in modifying cell properties such as surface charge was conducted. Zeta (ζ) - potential was measured using a ZEN 3600 Zetasizer (Malvern, UK) at room temperature according to the Smoluchowski formula (Eqn. 3.6) and in line with manufacturer's recommendation for microalgae. The zetasizer (Fig. 3.2) has the capacity to measure ζ potential, particle size, molecular weight, and other properties.

$$E = \frac{\varepsilon \xi}{\mu} \tag{3.4}$$

Where E, ε, ξ, and μ are electrophoretic mobility, permittivity, ζ-potential, and viscosity, respectively.

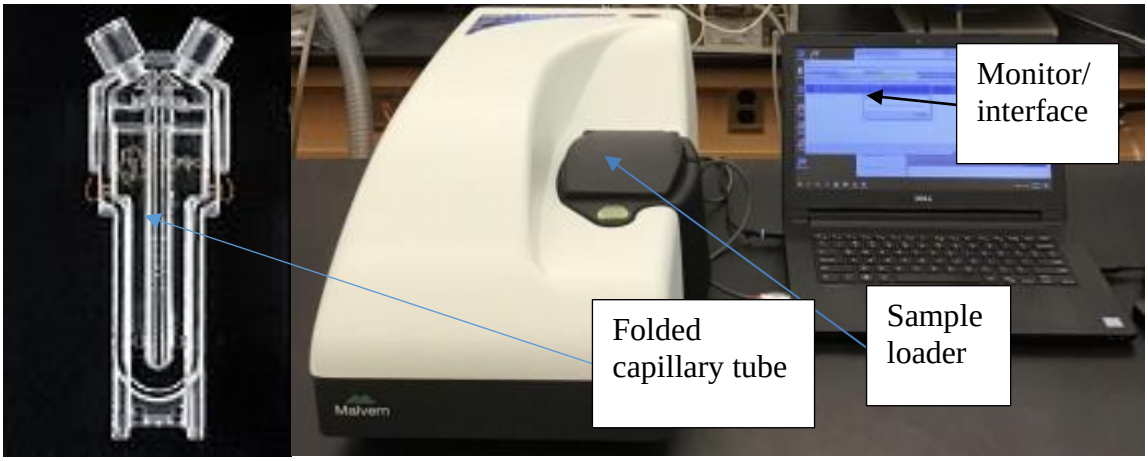

Figure 3.2: Set up of ZEN 3600 Zetasizer; about 2 mL of sample was injected into the folded capillary and secured with the aid of two provisioned caps for each end before being inserted into the zetasizer via the sample loader.

The effect of CTAB concentration on ζ-potential was investigated for beads in seawater (B-SW), beads in freshwater (B-FW), *N. oculata* cells in freshwater (N-FW), *N.*

oculata cells in seawater (N-SW), *C. vulgaris* in freshwater (C-FW), and C. vulgaris in f/2 (C-F/2). CTAB concentration was varied between 20 mg L^{-1} and 90 mg L^{-1} of suspension medium. In order to examine how ζ-potential changes with concentration, half the initial concentrations (0.65 g L^{-1}) of B-FW, B-NS, B-F/2, C-FW, C-F/2, N-FW, N-F/2, and N-SW were investigated as a function of CTAB concentration. The ZEN 3600 has a measurement range of 5 nm – 10 microns (particle diameter) with accuracy of 0.12 μm.cm $V.s^{-1}$ for aqueous systems using NIST SRM1980 standard reference material when temperature is kept between 2 °C – 90 °C. Sampling was done using the folded capillary sampler.

All zeta potential results were obtained in triplicates and the standard error in each measurement is recorded. Furthermore, it was ensured that all samples extracted for zeta potential analysis had been exposed to the surfactant for at least 7 minutes. Previous research has demonstrated that zeta potential can take up to 7 minutes to stabilize after surfactant addition in algae systems depending on the dose administered [279]. No difference was observed between zeta potential measurements obtained during the initial tests and those obtained after 1 hr, which is the estimated flotation time.

3.2.6 Hydrophobicity as a function of CTAB concentration

The fractional distribution of cells in the aqueous or organic phase in the presence of CTAB, was examined using 98 %+ hexane (Sigma-Aldrich, UK). At various CTAB concentration, 2 mL of hexane was added to 8 mL of sample in a test tube. The mixture was hand-shaken for 60 s and allowed to settle for another 20 s. CTAB was selected based on screening results. Using an automatic pipette, 2 mL of the aqueous phase was carefully withdrawn and analysed for absorbance at 685nm in a JENWAY spectrophotometer (Model number 7315). The affinity of the algae cells to hexane described their hydrophobicity (Eqn. 3.5).

$$H = \frac{A_I - A_h}{A_I} X100\% \tag{3.5}$$

where;

H = hydrophobicity (%), A_I = initial absorbance, and A_h = absorbance after hexane addition.

Because the methodology was based on spectrophotometry, we suspect that

scattered rays from suspended particles rather than absorbance were measured and so instead of hydrophobicity, the term “fractional absorbance” (FA) will be used.

3.2.7 Surface tension as a function of CTAB

Surface tension was determined with a Kibron AquaPi tensiometer according to the modified Du Noüy method as described by Padday et al [236], whereby the ring in the Du Noüy [235] apparatus is replaced with a thin rod. The equipment has a measuring range of 10-100 mN m^{-1} and accuracy/sensitivity of 0.1 mN m^{-1}, and it takes an average of 30 sec per measurement.

The equipment was calibrated using deionised water at room temperature (=72.32 ± 0.05 mN m^{-1}). Calibration was made possible as a result of the in-built calibration system that allows for the accuracy of the tensiometer to be measured against known liquids. Surface tension measurements in the presence and absence of CTAB were carried out for SW, seawater-hexane mixture (SW-HX). This investigation was aimed at examining the action of CTAB in both media in order to correct the ambiguities associated with hydrophobicity measurement using and hexane. Same procedures were repeated using supernatant recovered from *N. oculata* culture (NS) and NS-HX, where SW is replaced by NS. Each measurement was done three times to ensure accuracy of results.

3.3 Results and discussion

3.3.1 Recovery of *N. oculata* in freshwater and seawater

A summary of the results from preliminary tests is shown in Table 3.2. With *N. oculata* (N) as feed, using the batch operating conditions (1 L min^{-1} airflow, 60 mg L^{-1} CTAB, pH 8, and column height of 135 cm), very negligible recovery (1.5 %) and a concentration factor (0.5) were recorded. The low concentration factor seem to suggest that there is a stronger affinity between bubbles and CTAB than there is between algae and CTAB, owing to the stronger negative charge on bubbles than on algae [280]. However, when 30 mg L^{-1} each of SDS and CTAB were used at pH value of 4, 20 % of cells were recovered at CF of 11. Introduction of H^+ ions by acidification leads to a further compression of the diffused layer than already created by salt ions, causing a decrease in entropy of the system. The presence of anionic SDS also leads to even further compression and hence limiting the

entropy (freedom) of the charged particles in the diffused layer. To this end, SDS molecules become attracted to Na^+ and H^+ to Cl^-. The result is increased probability of CTAB-microalgae cells attachment [128]. Furthermore, when N-FW of the same concentration as N was foam floated under the same process conditions, 86 % recovery was achieved at a concentration factor of 65, with 30 mg $L^{-1}$of CTAB without SDS. The improved recovery that followed the replacement of NS with FW was partly due to the absence of shielding effect of salt ions, mainly Na^+ [98, 148, 165]. It could also be due to cell biochemistry of *N. oculata*, for example, the production of algaenan, which may have been lost during centrifugation [174] and therefore absent in N-FW.

Sample	Surfactant concentration (mg L^{-1})	Recovery (%)	Concentration factor
N + CTAB	60	1.5 ±0.5	0.5 ±0.1
N+CTAB + SDS	(30 + 30)	20 ±3	11 ±1
N-FW + CTAB	30	86 ±3	65 ±2
B-F/2 + CTAB	30	92 ±1	89 ±1
B-FW + CTAB	30	95 ±1	132 ±2
B-NS + CTAB	60	0	0
C-FW + CTAB	30	97 ±2	137 ±2
C-F/2 + CTAB	60	15 ±2	2.3 ±0.2
C-NS + CTAB	60	0	0

Table 3.2: Summary of recovery and concentration factor (average ± standard deviation) for flotation process using a column height of 135 cm and airflow of 1 L min^{-1} ; B-FW, B-NS, B-F/2, C-FW, C-F/2, N-FW, N, and N-SW represent beads suspended in freshwater, beads suspended in freshwater in *N. oculata* supernatant, beads suspended in F/2, *C. vulgaris* suspended in freshwater, *C. vulgaris* suspended in f/2, *N. oculata* suspended in freshwater, *N. oculata* in original media, and *N. oculata* suspended in seawater, respectively.

The presence of algaenan and other extracellular compounds may also result in the formation of CTAB-organic matter complexes [148]. Nevertheless, as a mechanism of flotation, bubble-particle attachment has been reported to play a stronger role than bubble-particle collision [128]. This does not however rule out the importance of bubble-particle collision especially given the comparatively small cell size of *N. oculata* as bubble-particle collision is a function of particle size [128, 281]. Besides, collision probability increases with increase air flow [128]. It is therefore possible to increase bubble-particle collision by increasing air flow since doing so would allow more bubbles to be generated. Hence, in order to harvest *N. oculata* cells without resuspension in FW, increasing the airflow beyond the current 1 L min^{-1} is necessary. The reduction in pH (from 8 to 7) as a result of resuspension in freshwater is another likely factor responsible for the better performance of CTAB as collector [94, 282].

3.3.2 Recovery of beads from freshwater, seawater, and *N. oculata* medium

B-FW, B-F/2, and B-NS were subjected to the same flotation conditions as with *N. oculata*

cells, at natural pH, with the aim of checking the impact of size and suspension media on recovery of beads. Both B-FW and B-F/2 show very high recoveries (95 % and 92 %) and high CF (132 and 89) (Table 3.2). B-NS on the other hand, could not be recovered even when CTAB was 60 mg L^{-1}. As mentioned earlier, the transfer of the released algaenan from NS as well as Na^+ and other salt ions present in F/2, could have interfered with the adsorption of beads particles onto CTAB or CTAB-modified bubbles and hence the lack of recovery of beads from F/2 and supernatant recovered from *N. oculata* culture (NS). These results are confirmations that, within the limits of experimental conditions, comparatively smaller cell size of *N. oculata* is not responsible for the difficulty in harvesting *N. oculata* through foam flotation. Compared to N-FW, B-FW and B-F/2 had higher recoveries and CF. This further confirms the importance of cell morphology and the fact that there are other extracellular compounds in original *N. oculata* medium that are lacking in fresh F/2 media. Besides, the interaction between organic cells of *N. oculata* and their environment is not the same with "non-organic" beads. The better performance by the control experiment (C-FW) compared to B-FW could be as a result of the larger average particle size of 6 µm in *C. vulgaris* as opposed to 2 µm-sized beads. Higher bubble-particle attachment and bubble-particle collision probabilities are obtainable with increased particle size [281]. In contrast, N-FW had a lower CF than both C-FW and B-FW because of difference in particle properties (functional groups, organic matter, size, morphology). Even though B-FW and N-FW are of approximate particle sizes, the rather stable benzene functional group in polystyrene beads means they are not likely to be affected by media chemistry as would be, algae cells. This is because *N. oculata* cells are composed of multiple functional groups like -OH, carbonyl C=O, $-CH_2/-CH_3$, amide, carbon C-O, P=O, and carboxyl COO- groups [283]. The presence of multiple functional groups has the tendency to affect the steric potential in line with the DLVO theory [284]. The lesser value of CF from N-FW compared C-FW could be as a result of the larger particles in *C. vulgaris* than *N. oculata* which translates to higher collision probability [128, 281].

3.3.3 Recovery of *C. vulgaris* in seawater and *N. oculata* medium

C-FW is used as a control experiments based on previous research [19]. Having ruled out the possibility of cell size as a constraint to harvesting *N. oculata* cells, further evidence based on material composition, became important [49] in order to substantiate the role of

algaenan and/or Na^+ and other ions. In place of B-F/2 and B-NS, C-F/2 and C-NS, respectively, were tested for foam harvesting because the latter are more similar in terms of materials composition (being living cells) to *N. oculata*, than the former. Compared to C-F/2, better process performance was recorded with B-F/2 even though 60 mg L^{-1} of CTAB was used in the case of C-F/2. This is a strong indication of interactions between the functional groups of algae cells and their environment and how important these interactions are, to the harvesting process. Just like the beads, *C. vulgaris* could not be recovered from B-NS and C-NS respectively. This is a confirmation that in addition to salt ions, algaenan covering and other extracellular compounds are strong determinants of a successful foam flotation of microalgae.

3.3.4 Effect of airflow, surfactant and media chemistry on foam flotation of *N. oculata*

Based on results of batch flotation in Table 3.2, the limit of bubble-algae collision was identified. The results have identified that that cell morphology and media chemistry were limiting factors to achieving good recovery of *N. oculata* cells. To this end, instead of relying on bubble-particle attachment mechanism which is highly dependent on media chemistry and cell morphology [130], bubble-particle collision mechanism was exploited. Therefore, in order to increase the probability of collision between algae cells and bubbles, higher airflows (1.2 – 3.6 L min^{-1}) were used, compared to batch operations (1 L min^{-1}).

Figures 3.3 -3.10 below represent the recovery and concentration factors obtained from original cultures under various continuous operations.

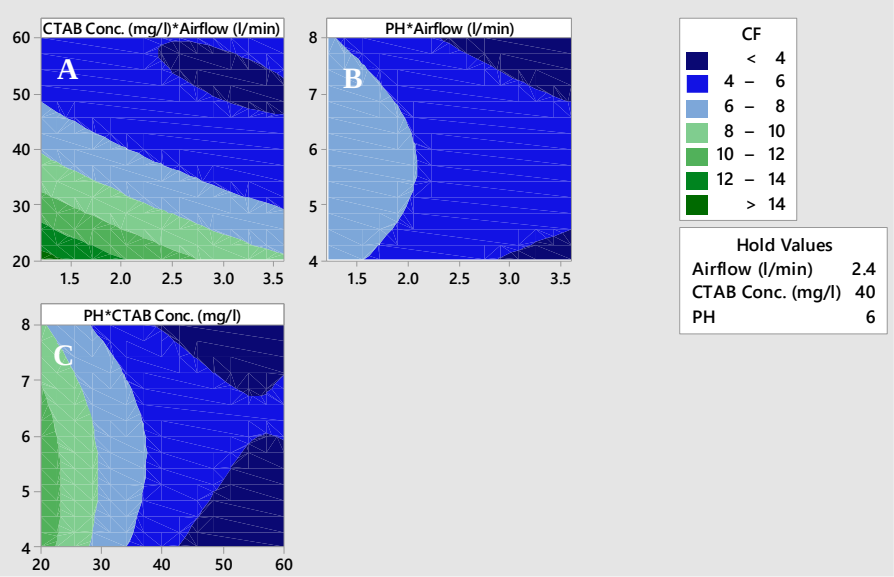

Figure 3.3: Effect of process conditions on concentration factor using CTAB of varying concentrations with undiluted cultures of *N. oculata*; n=2, R^2 = 0.978

In Fig. 3.3; A, B, and C represents the Y-X relationships between CTAB concentration (mg L^{-1}) and airflow (L min^{-1}), pH and airflow (L min^{-1}), and pH and CTAB (mg L^{-1}), respectively. The hold values are the mid values of the third variable (Z-axis) at which the X-Y was plotted. Therefore, A, B, and C were plotted at pH 6, CTAB concentration of 40 mg L^{-1}, and airflow of 2.4 L min^{-1}. From Fig. 3.3, in order to maintain CF ≥12, pH should be kept neutral (7) while airflow and CTAB should be kept below 2.0 L min^{-1} and 25 mg L^{-1}, respectively.

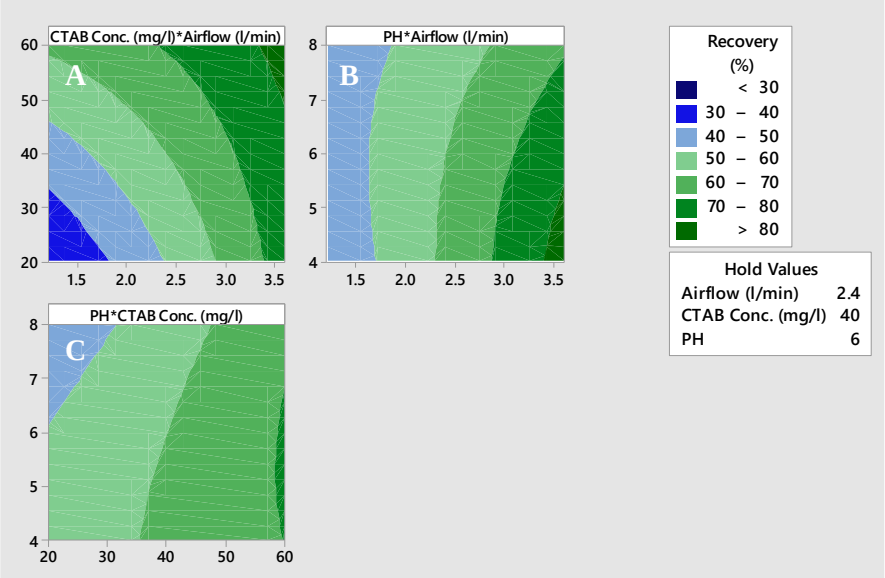

Figure 3.4: Effect of process conditions on recovery using CTAB of varying concentrations with undiluted cultures of *N. oculata*; n=2, R^2 = 0.988

In Fig. 3.4; A, B, and C represents the Y-X relationships between CTAB concentration (mg L^{-1}) and airflow (L min^{-1}), pH and airflow (L min^{-1}), and pH and CTAB (mg L^{-1}), respectively. The hold values are the mid values of the third variable (Z-axis) at which the X-Y was plotted. Therefore, A, B, and C were plotted at pH 6, CTAB concentration of 40 mg L^{-1}, and airflow of 2.4 L min^{-1}. In agreement with literature, high airflow and CTAB under acidic pH allows for better algae capture. From Fig. 3.4, it can be deduced that keeping the recovery above 70 % would require that airflow be higher than 3.4 L min^{-1} with CTAB above 50 mg L^{-1} and pH ≤ 6.

Compared to the batch operations in Table 3.2, Fig. 3.3, indicates better flotation performance (CF) in terms of harvesting *N. oculata* cells. Similarly, the recovery % from the continuous operations, as shown in Fig. 3.4 indicates better process performance. This was made possible as a result of increased airflow. By increasing airflow from 1 L min^{-1} to 3.6 L min^{-1}, it has been possible to increase particle-bubble collision, therefore leading to over 70 % recovery. Although it was possible to increase the recovery from 0 to over 70%, it is important to know that there has been an increase in airflow by three-fold. However, 5 L min^{-1} of air combined with the influence of mechanical components, has been reported elsewhere [92]. It is important to note that these results were achieved without having to combine multiple surfactants which would otherwise complicate the surfactant recovery process.

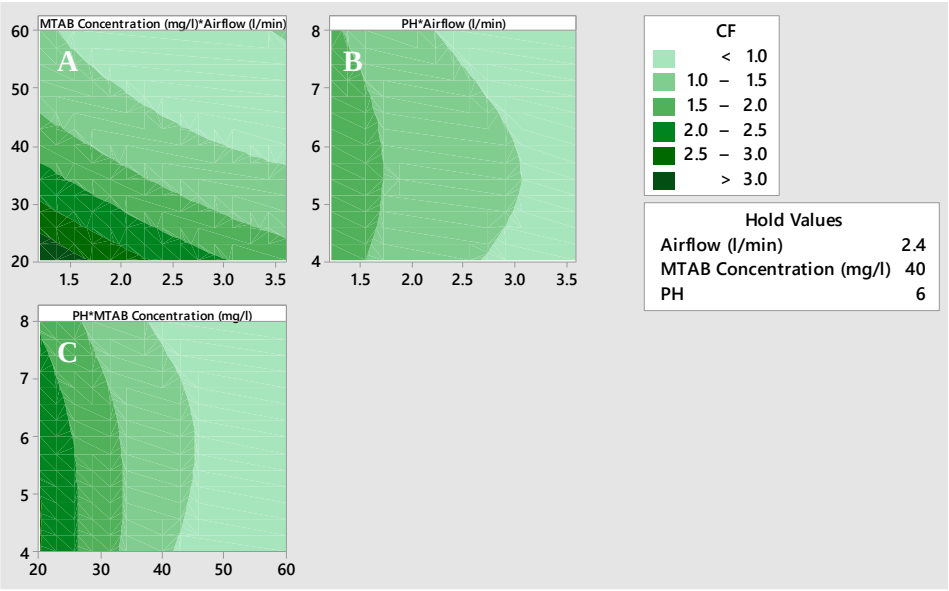

Figure 3.5: Effect of process conditions on concentration factor using MTAB of varying concentrations with undiluted cultures of *N. oculata*; n=2, R^2 = 0.990

In Fig. 3.5; A, B, and C represents the Y-X relationships between MTAB concentration (mg L^{-1}) and airflow (L min^{-1}), pH and airflow (L min^{-1}), and pH and MTAB (mg L^{-1}), respectively. The hold values are the mid values of the third variable (Z-axis) at which the X-Y was plotted. Therefore, A, B, and C were plotted at pH 6, MTAB concentration of 40 mg L^{-1}, and airflow of 2.4 L min^{-1}. The response of CF to operating conditions is similar to what was obtained with CTAB, which agrees with literature [40]. Maintaining and airflow less than 2.0 L min^{-1}, CTAB below 30 mg L^{-1}, and pH ≤ 6, could allow for CF ≥ 2.5.

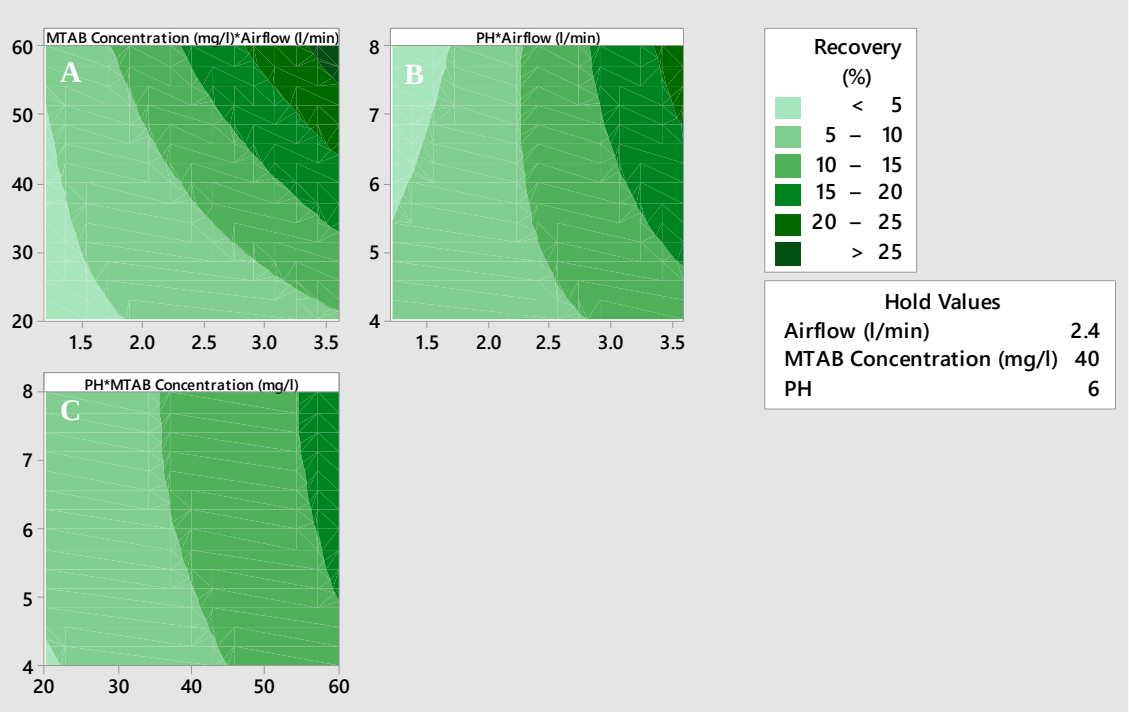

Figure 3.6: Effect of process conditions on recovery using MTAB of varying concentrations with undiluted cultures of *N. oculata*; n=2, R^2 = 0.986

In Fig. 3.6; A, B, and C represents the Y-X relationships between MTAB concentration (mg L^{-1}) and airflow (L min^{-1}), pH and airflow (L min^{-1}), and pH and MTAB (mg L^{-1}), respectively. The hold values are the mid values of the third variable (Z-axis) at which the X-Y was plotted. Therefore, A, B, and C were plotted at pH 6, MTAB concentration of 40 mg L^{-1}, and airflow of 2.4 L min^{-1}. Similar to the case with CTAB, increased airflow and MTAB leads to increased recovery with pH dependence. For cell recovery of 25 % or more, CTAB concentration and airflow ≥ 50 mg L^{-1} and ≥ 3.0 L min^{-1}, respectively, is recommended. In a manner similar to CTAB, recovery with MTAB is

pH dependent. This is because like CTAB, the surface activity of MTAB increases under acidic pH, thereby resulting in more foam with increased airflow and surfactant.

The flotation performance of MTAB was less than that of CTAB as seen from figures 3.5 and 3.6. This is because the free energy of binding ΔG^b for MTAB (18.72 kJ mol^{-1} protein) is higher than of CTAB (7.72 kJ mol^{-1} protein) [285]. This implies that CTAB has higher tendencies to bind with surrounding particles. This ease of binding is associated with the length of carbon ($-CH_2$) chain present in individual surfactants. The longer the carbon chain, the less the energy required for binding. Therefore, it is expected that CTAB with 16 ($-CH_2$) in its carbon tail, should bind easier than MTAB with 14 ($-CH_2$).

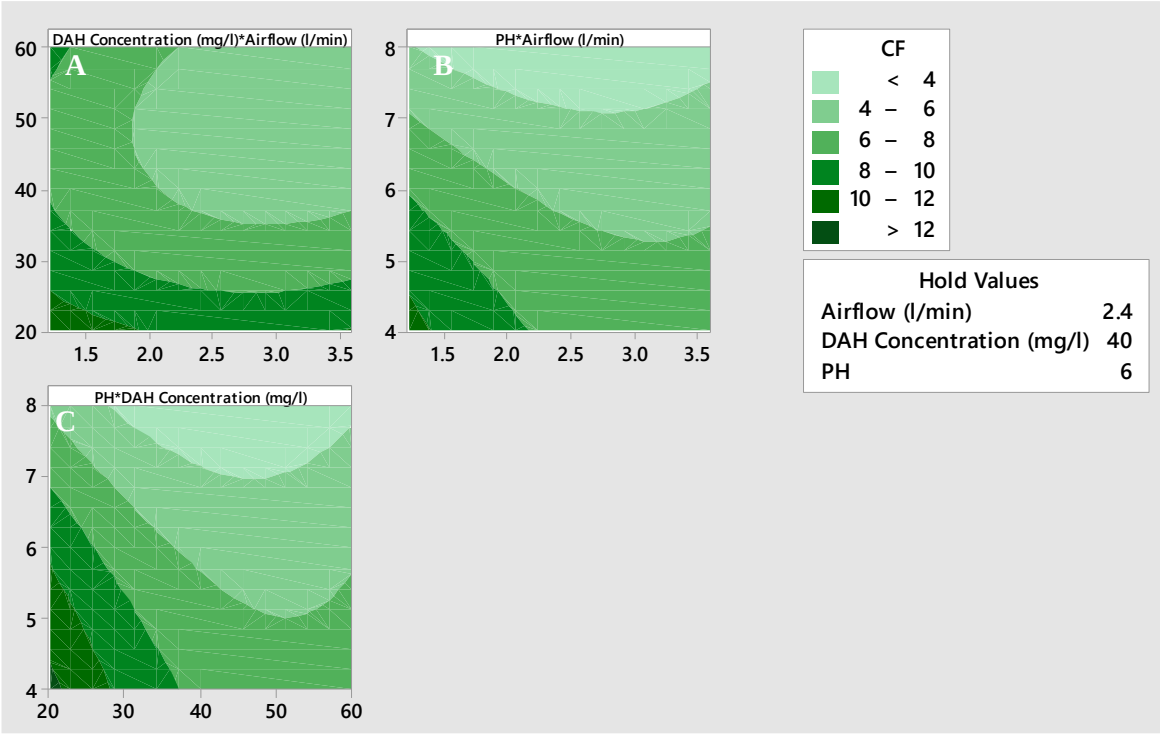

Figure 3.7: Effect of process conditions on concentration factor using DAH of varying concentrations with undiluted cultures of *N. oculata*; n=2, $R^2 = 0.993$

In Fig. 3.7; A, B, and C represents the Y-X relationships between DAH concentration (mg L^{-1}) and airflow (L min^{-1}), pH and airflow (L min^{-1}), and pH and DAH (mg L^{-1}), respectively. The hold values are the mid values of the third variable (Z-axis) at which the X-Y was plotted. Therefore, A, B, and C were plotted at pH 6, DAH concentration of 40 mg L^{-1}, and airflow of 2.4 L min^{-1}. For increase in enrichment to occur, reduced airflow, CTAB concentration, and pH are essential. Contrary to what was obtained with CTAB and MTAB, CF is dependent on pH when DAH is the surfactant, with acidic

pH favouring higher CF. This means that acidic pH enhances bubble- particle attachment when DAH is used as surfactant.

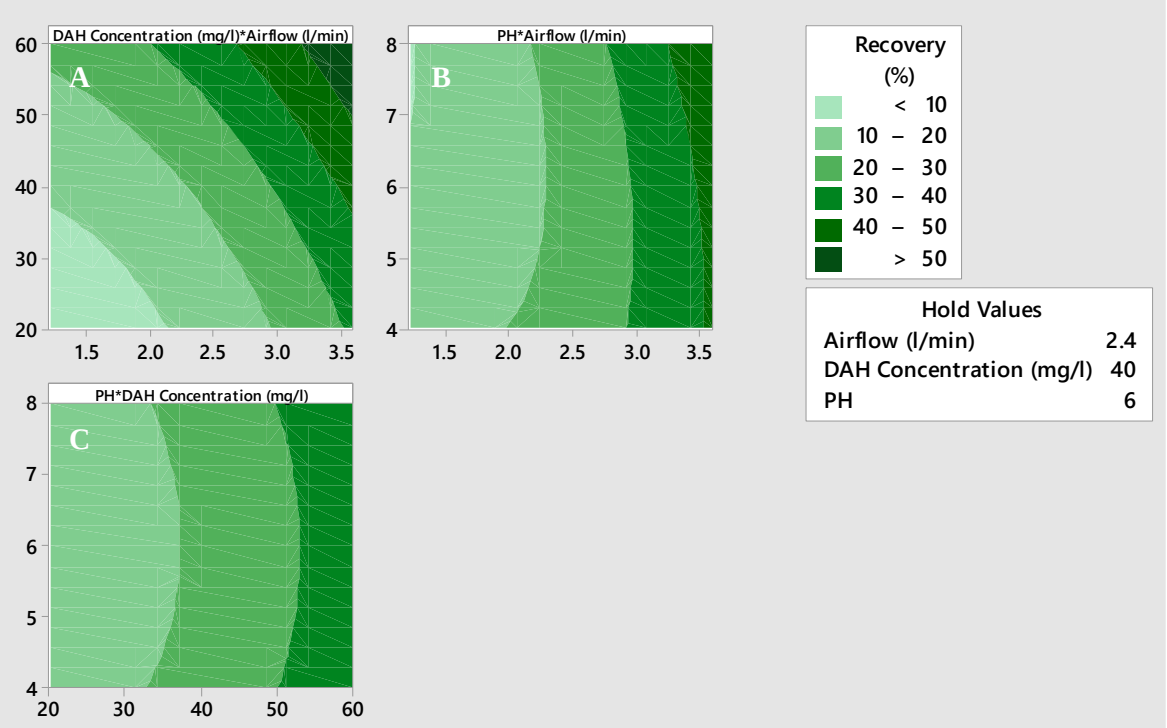

Figure 3.8: Effect of process conditions on recovery using DAH of varying concentrations with undiluted cultures of *N. oculata*; n=2, R^2 = 0.990

In Fig. 3.8; A, B, and C represents the Y-X relationships between DAH concentration (mg L^{-1}) and airflow (L min^{-1}), pH and airflow (L min^{-1}), and pH and DAH (mg L^{-1}), respectively. The hold values are the mid values of the third variable (Z-axis) at which the X-Y was plotted. Therefore, A, B, and C were plotted at pH 6, DAH concentration of 40 mg L^{-1}, and airflow of 2.4 L min^{-1}. The results in Fig. 3.8 tends to suggest that cells recovery is pH neutral when DAH is used as surfactant as opposed to what obtains when CTAB or MTAB were used. This is because there is a higher dependence of recovery on airflow than on DAH concentration.

Although the length of the carbon structure in DAH is the same as that in CTAB, the difference in head groups between the two surfactants may have been responsible for the lower values of CF and recovery % recorded for DAH [285]. The head group in CTAB contains Br^- while that in DAH is Cl^-. Cl^- is higher in the Hoffman's series [286] than Br^- and therefore has a higher tendency to salt out algae cells. The salting out phenomenon is synonymous with coagulation which is the opposite of flotation. Hence, the favouring of coagulation by DAH has a negative impact on flotation. This is because as particles

coagulate, they become more difficult to recover by flotation [104].

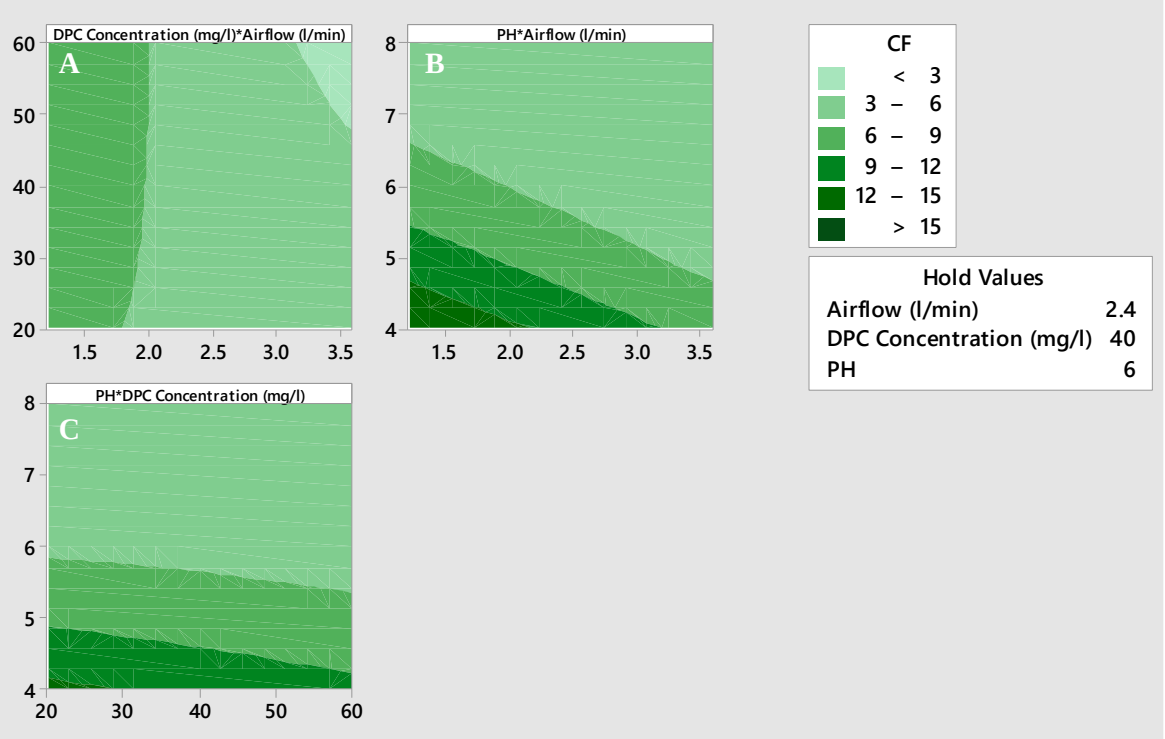

Figure 3.9: Effect of process conditions on concentration factor, using DPC of varying concentrations with undiluted cultures of *N. oculata*; n=2, R^2 = 0.985

In Fig. 3.9; A, B, and C represents the Y-X relationships between DPC concentration (mg L^{-1}) and airflow (L min^{-1}), pH and airflow (L min^{-1}), and pH and DPC (mg L^{-1}), respectively. The hold values are the mid values of the third variable (Z-axis) at which the X-Y was plotted. Therefore, A, B, and C were plotted at pH 6, DPC concentration of 40 mg L^{-1}, and airflow of 2.4 L min^{-1}. The response of CF to pH change is similar to what obtains when DAH was used as surfactant. This is probably due to the similarity in the chloride functional groups present in both surfactants. The response to airflow and CTAB concentration, however, remains similar.

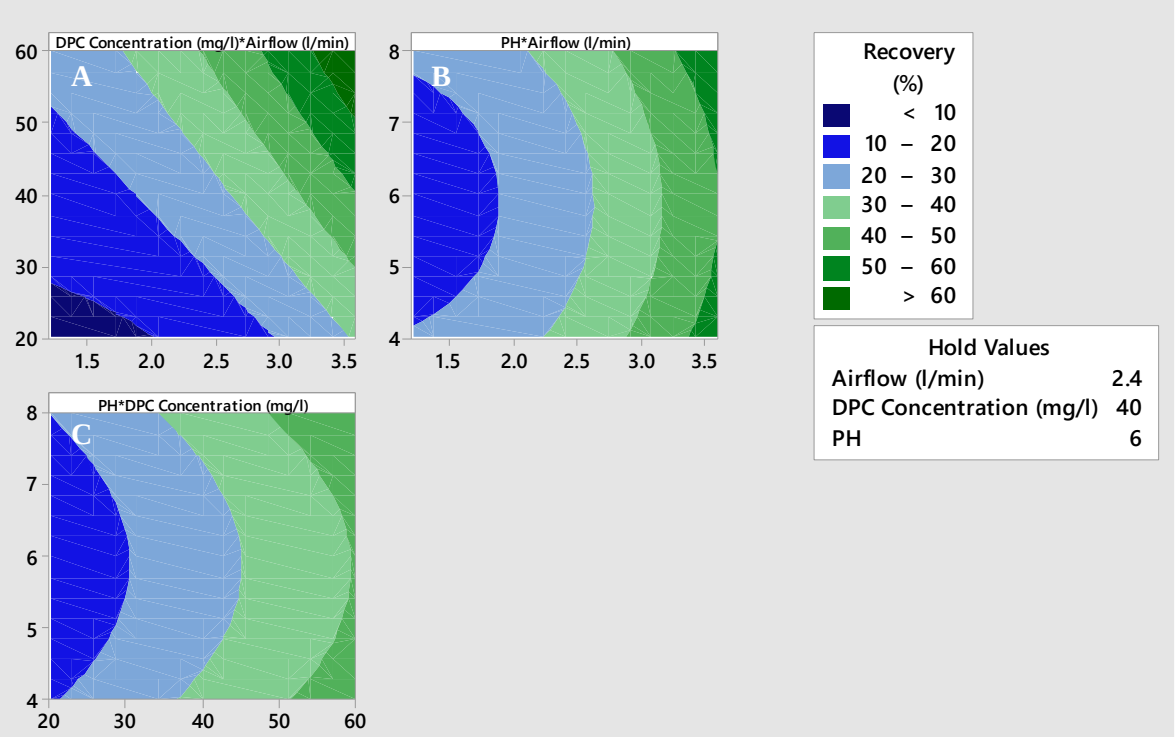

Figure 3.10: Effect of process conditions on recovery, using DPC of varying concentrations with undiluted cultures of *N. oculata*; n=2, R^2 = 0.994.

In Fig. 3.10; A, B, and C represents the Y-X relationships between DPC concentration (mg L^{-1}) and airflow (L min^{-1}), pH and airflow (L min^{-1}), and pH and DPC (mg L^{-1}), respectively. The hold values are the mid values of the third variable (Z-axis) at which the X-Y was plotted. Therefore, A, B, and C were plotted at pH 6, DPC concentration of 40 mg L^{-1}, and airflow of 2.4 L min^{-1}.

Just like CTAB, the length of the CH_2 chain in DPC is 16 and that explains the similarity in performance. Because the amino head group in CTAB is not the same as the pyridinium head group in DPC, there is a lower binding energy (412 kJ mol^{-1} BSA) in DPC (Bovine serum albumin) compared to 541 kJ mol^{-1} BSA [285]. The difference in binding energy is hereby a reflection of the seemingly better CF compared to CTAB but the influence of the head group seems to be stronger.

In summary, figures 3.3 to 3.10 above all indicated an increase in bubble-particle collision as a result of increased airflow. As earlier suggested, the bubble-algae attachment is weak. This is due to the negative impacts of ionic strength and cell morphology of *N. oculata*. The cell morphology, in particular the algaenan covering as well as other extracellular components present in *N. oculata* are responsible for the poor flotation

performance. The response of CF to airflow and surfactant concentrations remains the same for all surfactant, i.e. increase in surfactant concentration and airflow causes a decrease in CF. The response of CF to pH tends to depend on the functional groups present. With Br- functional group in CTAB and MTAB, CF was pH-neutral but with Cl- functional group in DPC and DAH, CF increased with low pH. The response of recovery on the other hand is opposite of what they were with CF. In CTAB and MTAB, recovery was pH-dependent but pH-neutral with DPC and DAH. Increase in airflow and CTAB concentration on the other hand, results in increase in recovery for all four surfactants.

Figures 3.11 – 3.18 represents results obtained when original cultures of *N. oculata* were diluted to half the original concentration and treated under the same conditions as before in order to investigate the influence of ionic strength on the flotation of *N. oculata* as a function of surfactant type and concentration.

From the measurements of ζ-potential it can be seen that, within the operating feed concentrations, colloid concentration had little impact on ζ potential of *N. oculata* and we can conclude that only the impact of ionic concentration and/or pH is measured. This is also justified by the fact that the conductivity of the culture was almost constant at 30 mS cm^{-1} even when the culture was half diluted.

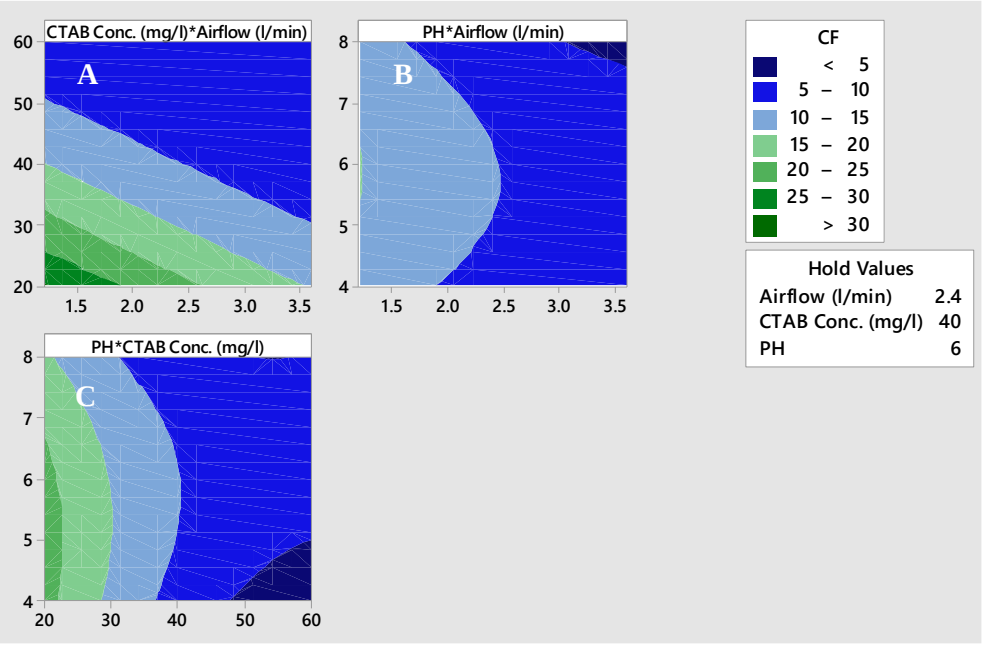

Figure 3.11: Effect of process conditions on concentration factor using CTAB of varying concentrations with half diluted culture of *N. oculata*; $R^2 = 0.977$

In Fig. 3.11; A, B, and C represents the Y-X relationships between CTAB concentration (mg L^{-1}) and airflow (L min^{-1}), pH and airflow (L min^{-1}), and pH and CTAB (mg L^{-1}), respectively. The hold values are the mid values of the third variable (Z-axis) at which the X-Y was plotted. Therefore, A, B, and C were plotted at pH 6, CTAB concentration of 40 mg L^{-1}, and airflow of 2.4 L min^{-1}. Compared to the original culture, there is an increase in CF values. This is due to the reduced ionic strength.

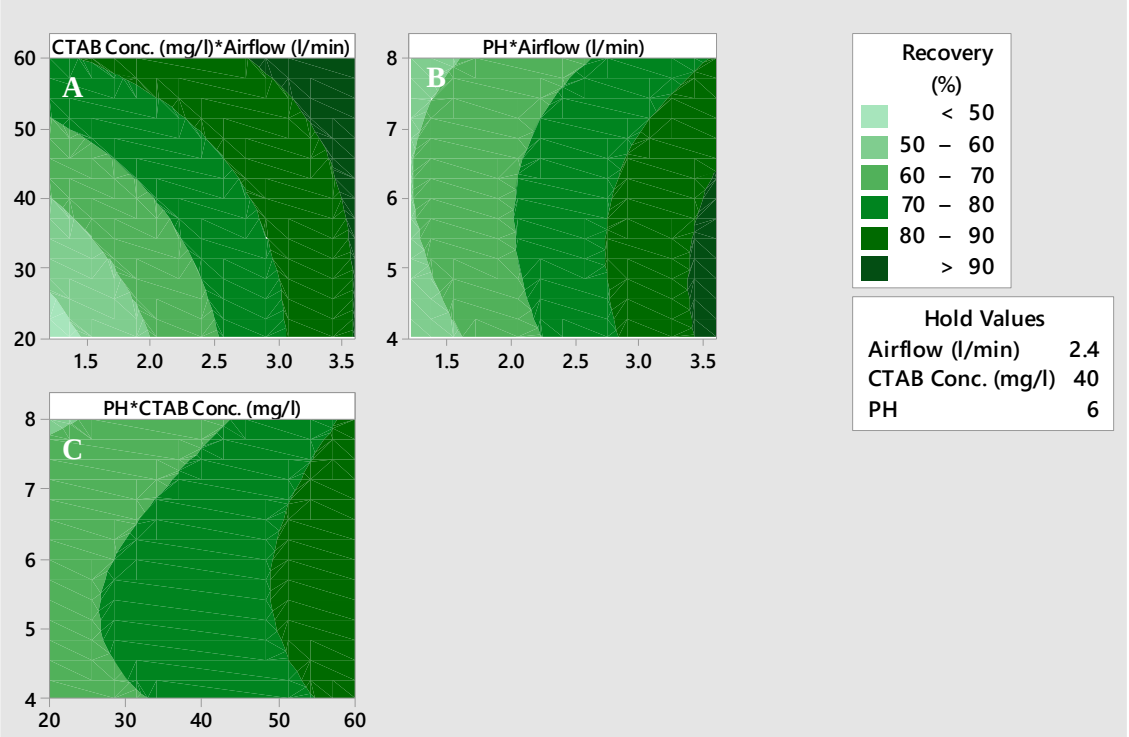

Figure 3.12: Effect of process conditions on recovery using CTAB of varying concentrations on half diluted culture of *N. oculata*; $R^2 = 0.987$

In Fig. 3.12; A, B, and C represents the Y-X relationships between CTAB concentration (mg L^{-1}) and airflow (L min^{-1}), pH and airflow (L min^{-1}), and pH and CTAB (mg L^{-1}), respectively, as they affect the recovery of *N. oculata*. The hold values are the mid values of the third variable (Z-axis) at which the X-Y was plotted. Therefore, A, B, and C were plotted at pH 6, CTAB concentration of 40 mg L^{-1}, and airflow of 2.4 L min^{-1}. The increase in recovery from between 70 and 80 % to above 90 % is a direct consequence of the reduced ionic strength. The results in fig. 3.11 and 3.12 are true representations of why it is difficult to harvest marine algae using foam floatation technology. The need to reduce pH below pH 6 in order to achieve higher recoveries, is also reduced as a result of

reduced ionic strength.

Compared to the original culture, there is an increase in recovery and CF when ionic strength was reduced by half (Fig. 3.11 & 3.12). However, in actual sense the reduction in number of cells by half as a result of the dilution, means that more cells were actually recovered from the original culture. Nevertheless, the product that resulted in this case, is much concentrated due to the reduced influence of salt ions against CF.

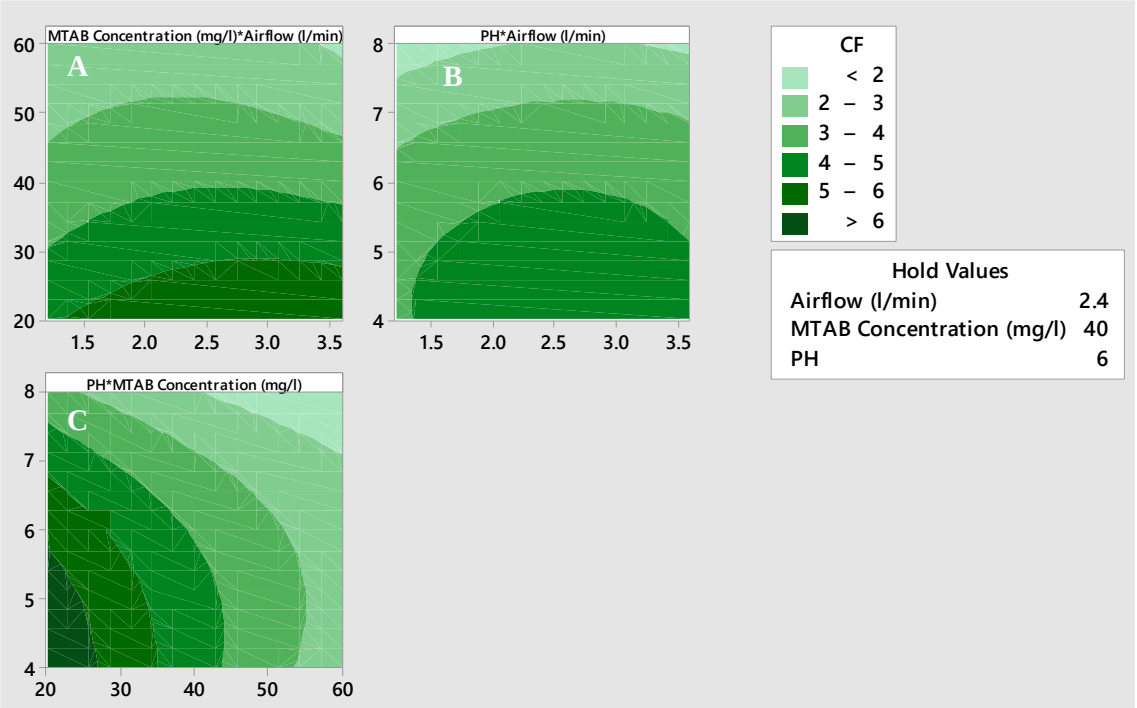

Figure 3.13: Effect of process conditions on concentration factor using MTAB of varying concentrations with half diluted culture of *N. oculata*; n=2, R^2 = 0.99

In Fig. 3.13; A, B, and C represents the Y-X relationships between MTAB concentration (mg L^{-1}) and airflow (L min^{-1}), pH and airflow (L min^{-1}), and pH and MTAB (mg L^{-1}), respectively. The hold values are the mid values of the third variable (Z-axis) at which the X-Y was plotted. Therefore, A, B, and C were plotted at pH 6, MTAB concentration of 40 mg L^{-1}, and airflow of 2.4 L min^{-1}. It can be seen from Fig. 3.13, that ≤ pH6 is needed in addition to maintaining ≤ 35 mg L^{-1} CTAB and airflow between 1.5 and 3.6 L min^{-1}, in order to maintain a CF ≥ 6. The reduced ionic strength has made it possible to achieve increased CF. The fact that reduced ionic strength allows for increased airflow is an indication of reduced foaming as ionic strength reduces.

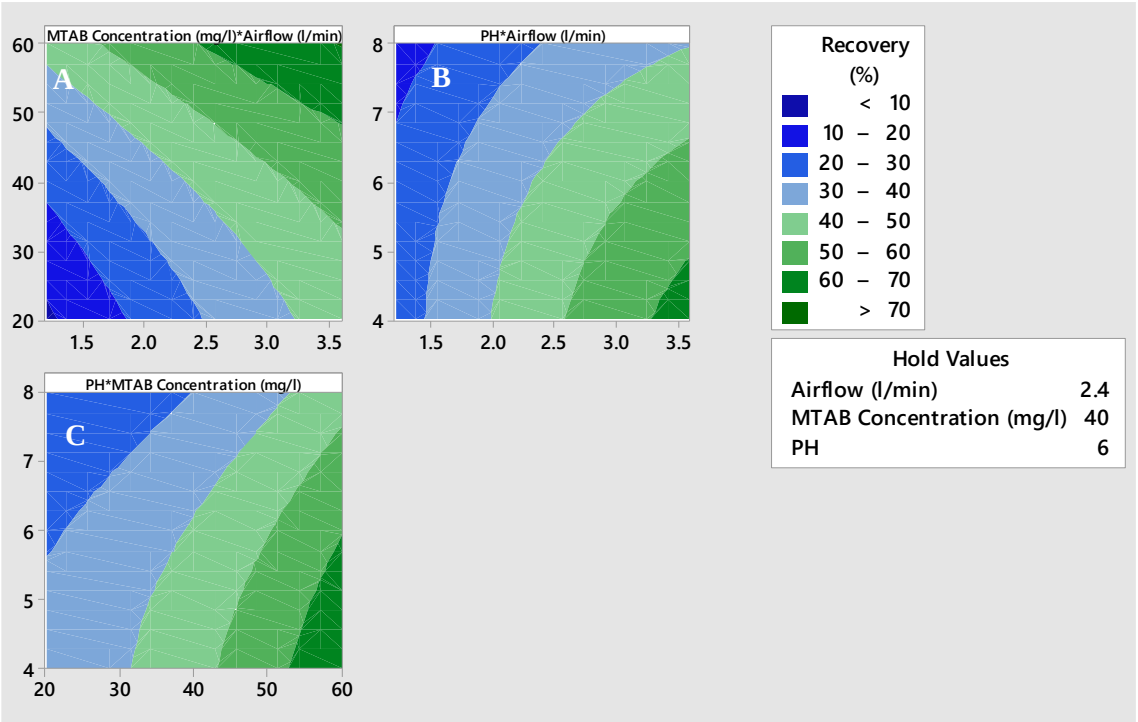

Figure 3.14: Effect of process conditions on recovery using MTAB of varying concentrations with half diluted culture of *N. oculata*; n=2, R^2 = 0.986

In Fig. 3.14; A, B, and C represents the Y-X relationships between MTAB concentration (mg L^{-1}) and airflow (L min^{-1}), pH and airflow (L min^{-1}), and pH and MTAB (mg L^{-1}), respectively. The hold values are the mid values of the third variable (Z-axis) at which the X-Y was plotted. Therefore, A, B, and C were plotted at pH 6, MTAB concentration of 40 mg L^{-1}, and airflow of 2.4 L min^{-1}.

From Fig. 3.14, the recovery of *N. oculata* using MTAB has also shown some increase due to reduced ionic concentration. While there was an increase in recovery from 60 to 70%, CF was increased from 3 to 6. Compared to CTAB, MTAB was less performing as a surfactant than CTAB, just as was the case in original cultures of *N. oculata*. This is an indication that, had freshwater been the media, CTAB would still outperform MTAB.

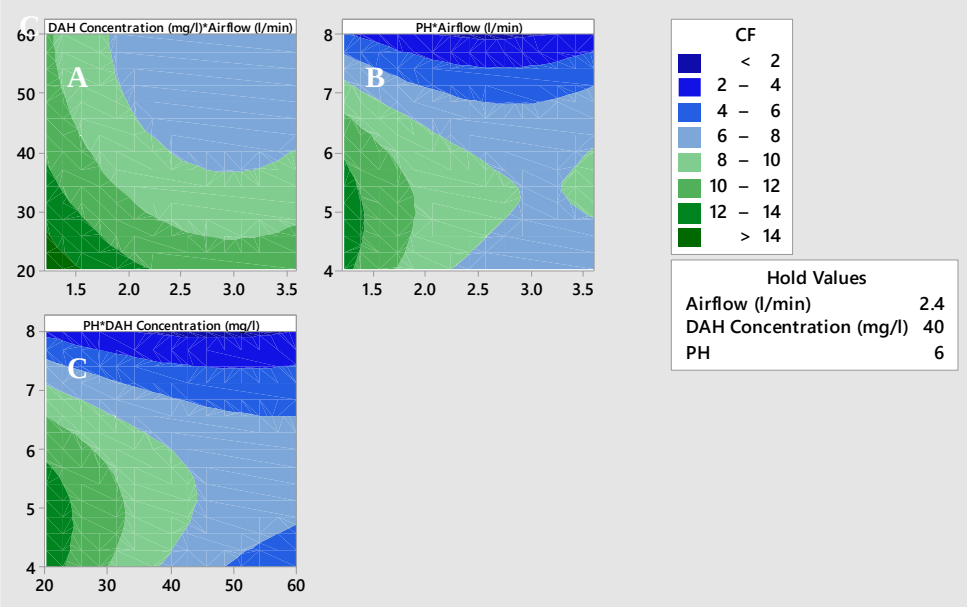

Figure 3.15: Effect of process conditions on concentration factor using DAH of varying concentrations with half diluted culture of *N. oculata*; n=2, R^2 = 0.991

In fig. 3.15; A, B, and C represents the Y-X relationships between DAH concentration (mg L^{-1}) and airflow (L min^{-1}), pH and airflow (L min^{-1}), and pH and DAH (mg L^{-1}), respectively. The hold values are the mid values of the third variable (Z-axis) at which the X-Y was plotted. Therefore, A, B, and C were plotted at pH 6, DAH concentration of 40 mg L^{-1}, and airflow of 2.4 L min^{-1}.

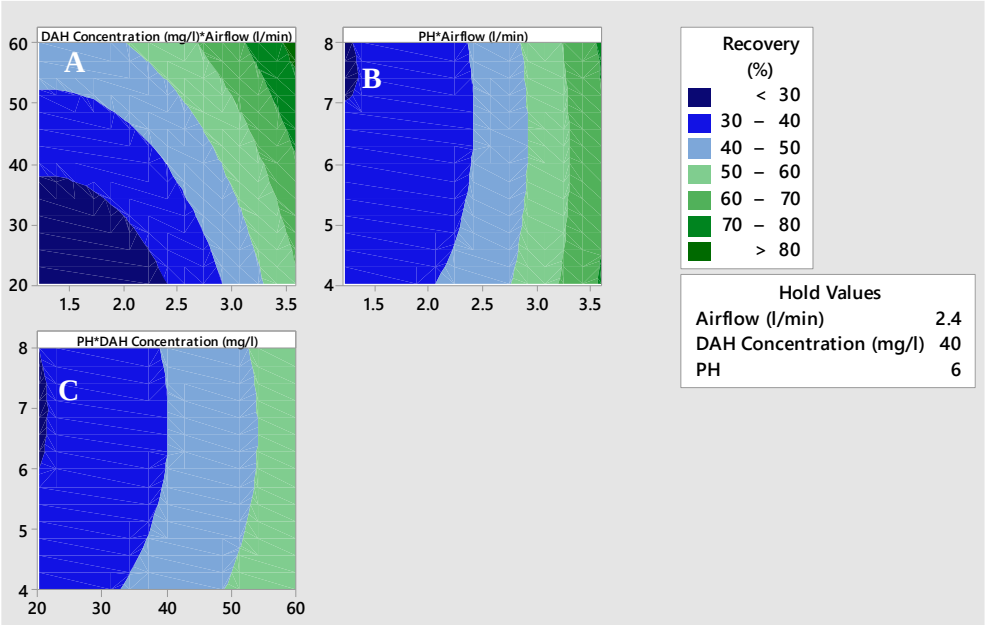

Figure 3.16: Effect of process conditions on recovery using DAH of varying concentrations with half diluted culture of *N. oculata*; n=2, R^2 = 0.989

In fig. 3.16; A, B, and C represents the Y-X relationships between DAH concentration (mg L^{-1}) and airflow (L min^{-1}), pH and airflow (L min^{-1}), and pH and DAH (mg L^{-1}), respectively. The hold values are the mid values of the third variable (Z-axis) at which the X-Y was plotted. Therefore, A, B, and C were plotted at pH 6, DAH concentration of 40 mg L^{-1}, and airflow of 2.4 L min^{-1}.

From figures 3.15 and 3.16 above, both recovery and concentration factor have increased from 25 to 80 % and from 12 to 14, respectively. The results are in agreement with those obtained when CTAB and MTAB were used as surfactants, all indicating the negative impact of salt ions on flotation process.

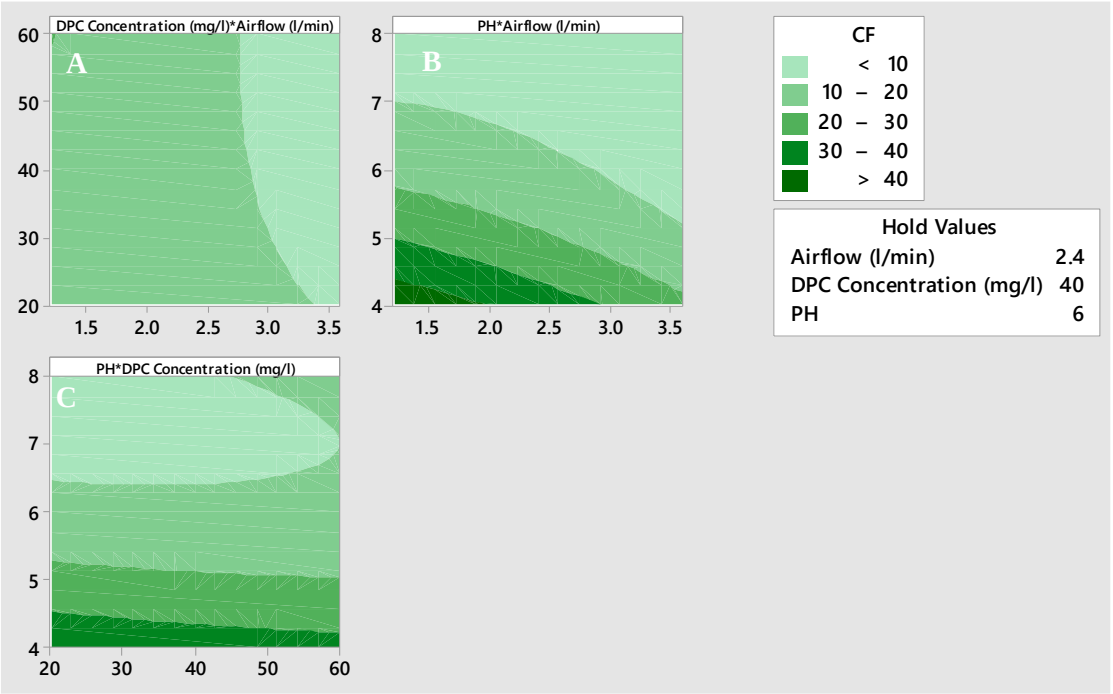

Figure 3.17: Effect of process conditions on concentration factor using DPC of varying concentrations with half diluted culture of *N. oculata*; n=2, R^2 = 0.99

In fig. 3.17; A, B, and C represents the Y-X relationships between DPC concentration (mg L^{-1}) and airflow (L min^{-1}), pH and airflow (L min^{-1}), and pH and DPC (mg L^{-1}), respectively. The hold values are the mid values of the third variable (Z-axis) at which the X-Y was plotted. Therefore, A, B, and C were plotted at pH 6, DPC concentration of 40 mg L^{-1}, and airflow of 2.4 L min^{-1}.

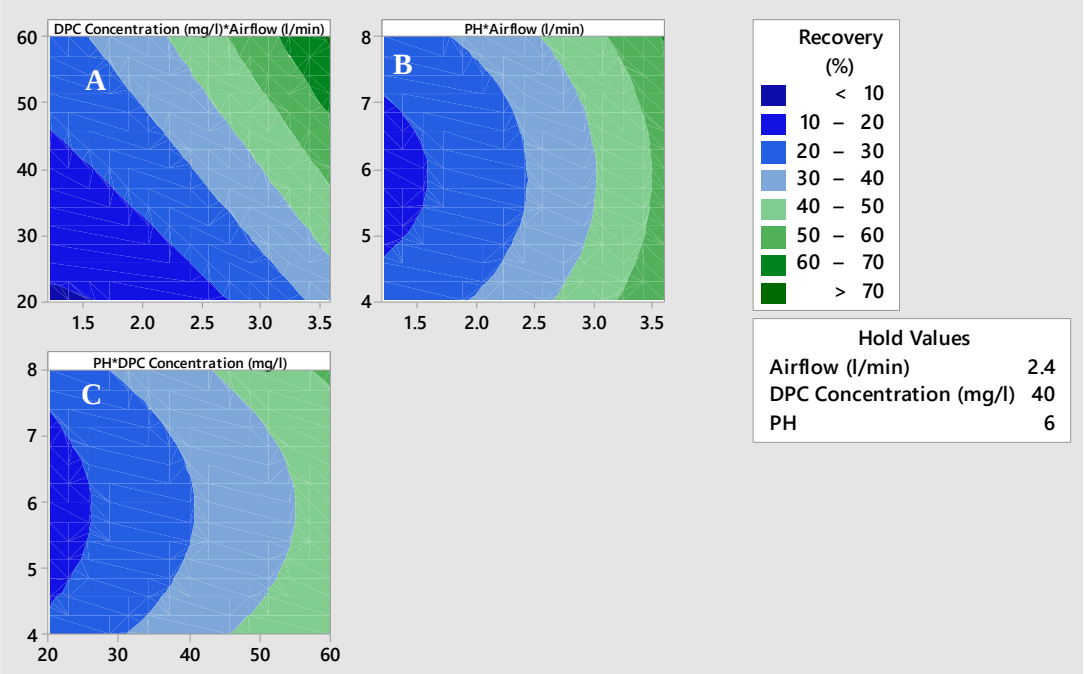

Figure 3.18: Effect of process conditions on recovery using DPC of varying concentrations with half diluted culture of *N. oculata*; n=2, R^2 = 0.994

In Fig. 3.18; A, B, and C represents the Y-X relationships between DPC concentration (mg L^{-1}) and airflow (L min^{-1}), pH and airflow (L min^{-1}), and pH and DPC (mg L^{-1}), respectively. The hold values are the mid values of the third variable (Z-axis) at which the X-Y was plotted. Therefore, A, B, and C were plotted at pH 6, DPC concentration of 40 mg L^{-1}, and airflow of 2.4 L min^{-1}.

The CF and recovery of *N. oculata* using DPC increased from 15 and 60 % to 40 and 70 % respectively. This is yet another evidence that media chemistry plays an important role in the success of harvesting microalgae via foam flotation.

In summary, airflow and surfactant concentration increases recovery while CF is increased by a decrease in airflow and surfactant concentration. This is in agreement with most literature on foam flotation and creating the most beneficial middle ground between these two parameters (recovery and CF) has been the subject of recent investigations into algal foam flotation. The presence of H^+ results in further compression of the diffused layer than already created by salt ions, causing a decrease in entropy of the system. The reduction in entropy limits the freedom of individual particles to stay apart. As the distance between individual particle becomes smaller, the tendency for oppositely charged particles to attract. Eventually there is higher probability for bubbles to attach and/or collide with algae particles which results in higher recovery and CF. However, details of these acid-

base interactions need to be investigated.

The results show that higher ionic strength is a major setback to the success of foam flotation of marine algae in general and in particular, *N. oculata*. Even though seawater possesses higher surface tension and viscosity than freshwater and should produce bigger bubbles [134], there is a reduction in the rate of bubble coalescence and rising speed, and hence smaller bubbles. The presence of salt in the liquid film (plateau) located in between adjacent bubbles, makes stronger the hydrogen bond (repulsive hydration force) and hence overcoming the otherwise prevalent Laplace pressure which could have caused bubble coalescence as a result of collapsed plateau if freshwater were to be involved [134].

The presence of extracellular components like algaenan around *N. oculata* cell walls play another important role in reducing the performance of foam flotation as a tool for harvesting *N. oculata*. However, the addition of freshwater to cultures before dewatering, amounts to reduced productivity since that would also imply a reduction in actual recovery by half. This is besides the fact that it is not a good engineering practice. For the same operating conditions that warranted a 96% recovery using CTAB on diluted culture, 83 % recovery was recorded when undiluted cultures were used. This essentially means that more cells were recovered in the undiluted culture. This is true because 96% recovery from diluted feed is equivalent to 48 % if feed concentrations were the same as with original culture. Although the recovered cells from diluted feed were more concentrated than those from original culture, the latter is more favourable for biodiesel conversion. This is because less energy would be required for further processing. Nevertheless, there is an offset to these reduced cost of further processing by the additional incurred due to initial dilution. Ultimately, the results have confirmed the negative impact of salt ions on bubble-particle attachment. However, within the operating airflow, more cells are recoverable without feed dilution and this is a confirmation of the role of airflow in enhancing bubble-particle collision.

Of the four surfactants (CTAB, MTAB, DAH, and DPC) screened, CTAB was the best in terms recovery and concentration factor. At pH 6 and airflow of 3.6 L min^{-1}, the highest recovery of 83% was obtained using 60 mg L^{-1} of CTAB. However, at pH 4 and airflow of 1.2 L min^{-1}, the highest concentration of 15 was achieved using 40 mg L^{-1} of DPC although similar concentration was achieved using 20 mg L^{-1} CTAB at same airflow but pH 6. When cultures with half the ionic strength of original cultures were foam

harvested, higher recoveries and concentration factors resulted. The highest recovery (96 %) was achieved by CTAB (3.6 L min^{-1}; pH6; 60 mg L^{-1}) but this time, DPC had the highest concentration factor of 40 (1.2 L min^{-1}; pH 4; 40 mg L^{-1}) and this was followed by CTAB with concentration factor of 32 (1.2 L min^{-1}; 20 mg L^{-1}; pH 6). Hence, the conclusion that ionic strength was partly responsible for the low recovery and concentration of *N. oculata*.

In comparison with literature, the continuous flotation hereby proposed is a more economically viable process than the only two available cases in literature where flotation was used to recover *Tetrsselmis sp.* (*M8),* another marine species. This is true because there is additional process cost as a result of higher airflow of 5 L min^{-1} with the support of a comparatively expensive mechanical Jameson's cell. In addition, the lower lipid content in *M8* than in *N. oculata* implies that even if process energy were to be the same, the delivery of lipid is higher when *N. oculata* is harvested.

3.3.5 Effect of CTAB, pH, and CTAB-organic matter complexes on ζ- potential and hydrophobicity

Having decided on CTAB as the most suitable surfactant, further analyses were carried out to understand how particle (cell) properties (hydrophobicity and surface charge) were affected by CTAB and media pH. This would allow for a better understanding of the role of CTAB, pH and cell morphology on the flotation results reported in subsections 3.3.1 - 3.3.4. Hydrophobicity and ζ-potential are two very important determinants of a successful foam flotation, with hydrophobicity having the greater influence [287]. Microalgae cells like most solid surfaces in aqueous suspensions, are negatively charged [43, 50, 51, 89]. The lower the ζ-potential of particles, the less stable is the colloid suspension [288], hence the more likely they are to settle.

From figure 3.19, when B-FW (beads suspended in freshwater), B-SW (beads suspended in seawater), N-FW *(N. oculata* suspended in freshwater), and N-F/2 (original *N. oculata* culture) were treated with 20 mg L-1 CTAB, only B-FW and B-SW underwent a charge transition. B-FW responded better as its ζ-potential went from -45 ±0.2 mV to +47.5 ±1 mV compared to B-SW where the transition was from -28.3 ±0.3 mV to +20.3 ±0.1 mV.

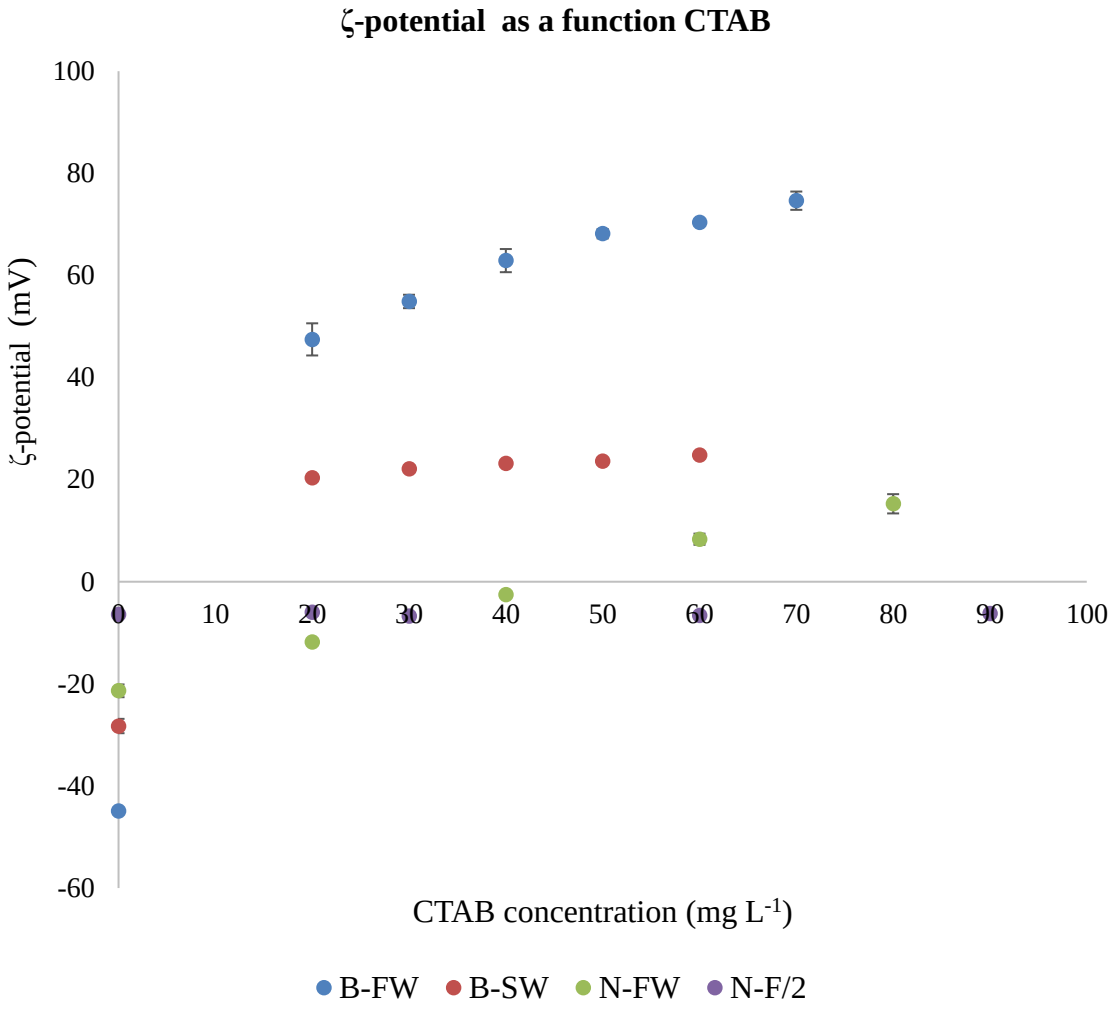

Figure 3.19: Comparison of changes in ζ-potential (average ± standard deviation) of beads and *N. oculata* with change in CTAB concentrations; concentration is 1.3 g L^{-1} (DW); B-FW, B-SW, N-FW, and N-F/2 represent beads suspended in freshwater, beads suspended in seawater, *N. oculata* suspended in freshwater, and *N. oculata* in original media, respectively

The difference in the initial values of ζ-potential between B-FW and B-SW is a clear indication of the compressed diffused layer occasioned by the presence of salt ions in B-SW. The difference in the final values of ζ-potential implies that the electrostatic attraction between CTAB and polystyrene particles is greatly reduced by salt ions present in seawater. Compared to B-FW and B-SW, 60 mg L-1 of CTAB were needed to change the ζ-potential of N-FW from -21.4 ±0.1 mV to +8.3 ±0.2 mV. As explained in section 3.3.1, the difference in physical characteristics, especially functional groups, in addition to a lower value of initial ζ-potential in N-FW as opposed to B-FW or B-SW, is responsible

for the lower value of final ζ-potential in N-FW. This is an indication of the limited electrostatic attraction between CTAB and *N. oculata* cells, even as CTAB concentration of 60 mg L-1 were used in N-FW compared to the 20 mg L-1 in B-FW. On the other hand, N-F/2 did not show any significant change from its ζ-potential value of -6.4 ±0.5 mV, even when CTAB concentrations were increased to 90 mg L-1. The difference in initial values of ζ-potential between N-FW and N-F/2 is an indication of the impact of salt ions in F/2 as earlier explained. Because there are additional metal ions in F/2 compared to seawater, it could be suggested that these extra ions had additional role to play in reducing the ζ-potential of *N. oculata* from -21.4 ±0.1 mV to -6.4 ±0.5 mV. The presence of salt and other metal ions in F/2 media has played a major role in limiting the infarction between CTAB and *N. oculata*. It is interesting to note that about 10 mg L-1 CTAB was needed for B-FW to reach isoelectric point while 42 mg L-1 CTAB was needed for N-FW. Comparing initial values of ζ-potential of the original samples tends to suggest that the more negative the ζ-potential of the cells, the higher the possibility of charge neutralisation. The relatively more negative value of ζ-potential recorded for N-FW (-21.4 ±0.1 mV), which is in agreement with literature value [262], suggest that ζ-potential values recorded for N-F/2 were not true values due to the interference of salt ions and the shielding effect of algaenan. Hence, ζ-potential measurement alone is not sufficient to explain the effect of CTAB in salt media (SW or F/2). Besides, isoelectric point does not necessarily have to be reached in order to have a successful recovery as we have seen in the case of C. vulgaris (Fig. 3.20).

Due to the importance of colloid concentration on ζ-potential, more data was acquired based on 0.65 g L^{-1} colloid concentration, which is half the colloid concentrations in the former samples. The outcomes of these tests are shown in Fig. 3.20. However, N-F/2 in Fig 3.20 represents *N. oculata* cells suspended in F/2 media. Fig. 3.20 also compares the performance of CTAB as a function of cell morphology. As can be seen, the values of ζ-potentials at half concentrations were approximately half what they were for beads (-45 ±0.2 mV to -20.4 ±1 mV) while those of *N. oculata* had increased slightly (-6.4 ±0.5 mV to -11.8 ±0.8 mV. Compared to N-FW at original concentration of 1.3 g L^{-1}, 0.65 g L^{-1} of N-FW has higher negative ζ-potential (-32.7 ±0.9). This is due to the loss of algaenan and other extracellular components during the washing process This contrary behaviour with respect to beads, of the beads, is because higher dilution rate means less activity of

accompanying salt ions as well as algaenan from the original culture. As expected however, 30 mg L^{-1} was enough to reach isoelectric point when half the original concentrations were used (Fig 3.20) as opposed to 44 mg L^{-1} needed in the original culture (Fig. 3.19).

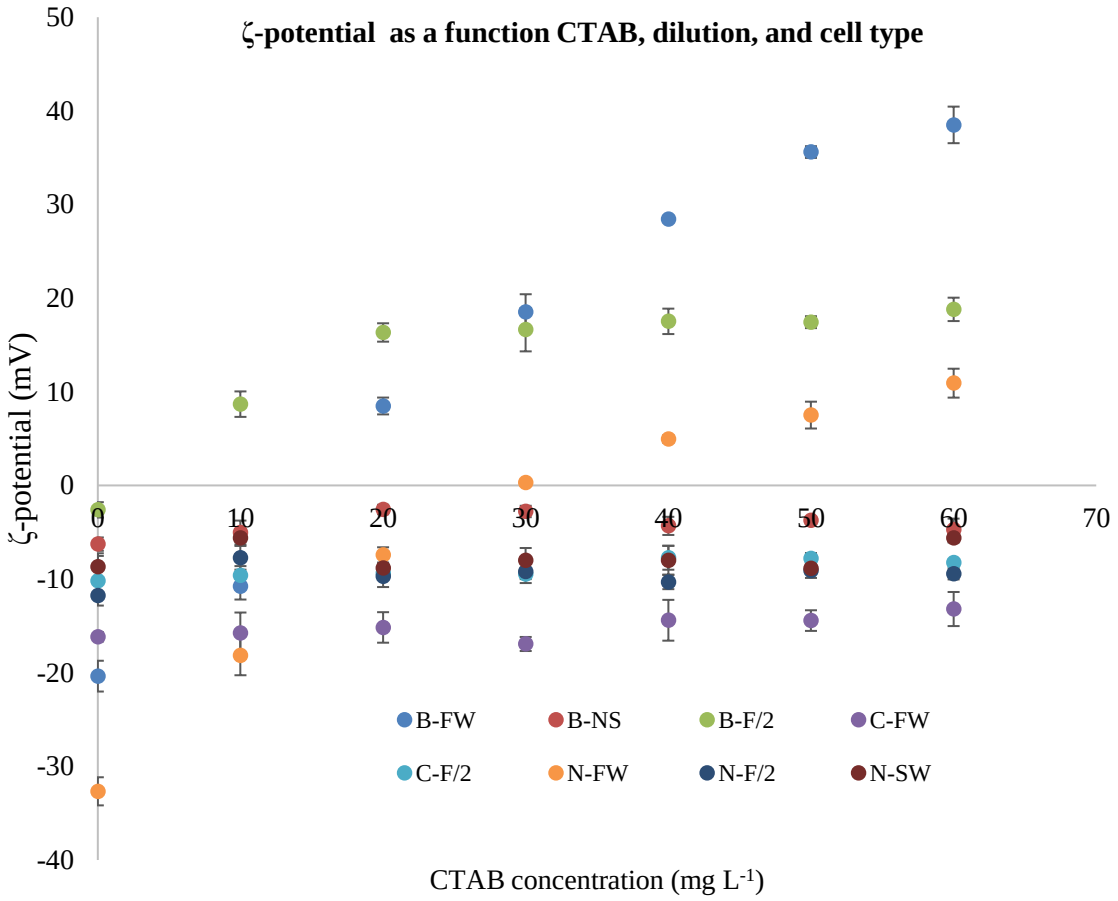

Figure 3.20: Variations in ζ-potential (average ± standard deviation) of beads, *N. oculata*, and *C. vulgaris* in various media with CTAB concentration; colloid concentration is 0.65 g L^{-1}; B-FW, B-NS, B-F/2, C-FW, C-F/2, N-FW, N-F/2, and N-SW represent beads suspended in freshwater, beads suspended in freshwater in *N. oculata* supernatant, beads suspended in f/2, *C. vulgaris* suspended in freshwater, *C. vulgaris* suspended in f/2, *N. oculata* suspended in freshwater, *N. oculata* suspended in f/2, and *N. oculata* suspended in seawater, respectively

Of all the colloid media (B-FW, B-NS, B-F/2, C-FW, C-F/2, N-FW, N-F/2 and N-SW), B-F/2 had the lowest value of -2.6 ±0.9 mV as ζ-potential. However, upon the addition of 10 mg L-1 of CTAB, there was a quick charge transformation in B-F/2, to 6.9 ±0.8 mV. 20 and 30 mg L^{-1} of CTAB respectively were needed to transform the charges in B-FW and N-FW respectively. Although the initial charge in N-FW was the highest, more CTAB was needed to transform its charge due to the actions of multiple functional groups already identified. From Table

3.2, it could be concluded that low initial value of zeta potential translates to poor flotation performance, unless the addition of CTAB is able to cause a charge transformation. If, however, the particle surface charge is large, charge transformation is not a condition for flotation to occur. Such was the case with *C. vulgaris* (C-FW), B-FW, N-FW and N in Table 3.2. It is possible to define a threshold for ζ-potential, below which, even if isoelectric point is not reached, the possibility or otherwise of particle flotation, without using elevated airflow, can be deduced.

The value of ζ-potential of -6.3±0.4 mV recorded in B-NS is similar to that of original *N. oculata* media. Judging from this value, one might suggest that the ζ-potential being measured in B-NS was mostly that of algaenan layer. This explains why beads and *chlorella*, suspended in NS were not recoverable. The behaviour of B-NS curve is similar to that of N-F/2 (original *N. oculata* culture) in Fig. 3.19. Therefore, B-NS and C-NS would have been recovered had the same operating conditions in the continuous flotation, applied.

C. vulgaris cells seem to not respond much (-16 ±0.3 mV to -13.2 ±1 mV) when CTAB concentration increased from 0 to 60 mg L^{-1}. However, the strong negative value means that there is a high level of dispersion of the cells, making it possible for CTAB to attach, which explains why their flotation recovery was very successful. Hence, isoelectric point (zero ζ-potential) does not necessarily translate into a successful foam flotation harvesting. This emphasises the importance of bubble in foam flotation process. Unless modified by surfactant, bubbles are naturally negative [100]. After modification, a positively charged bubble becomes capable of electrically attaching to negatively charged algae cells. During this process, the hydrophobic polar end of CTAB attaches to bubble, making them positive and therefore capable of attaching unto negatively charged algae. Alternatively, the positively charged hydrophilic head attaches to negatively charged algae while the hydrophobic tail gets attached to bubbles, [130].

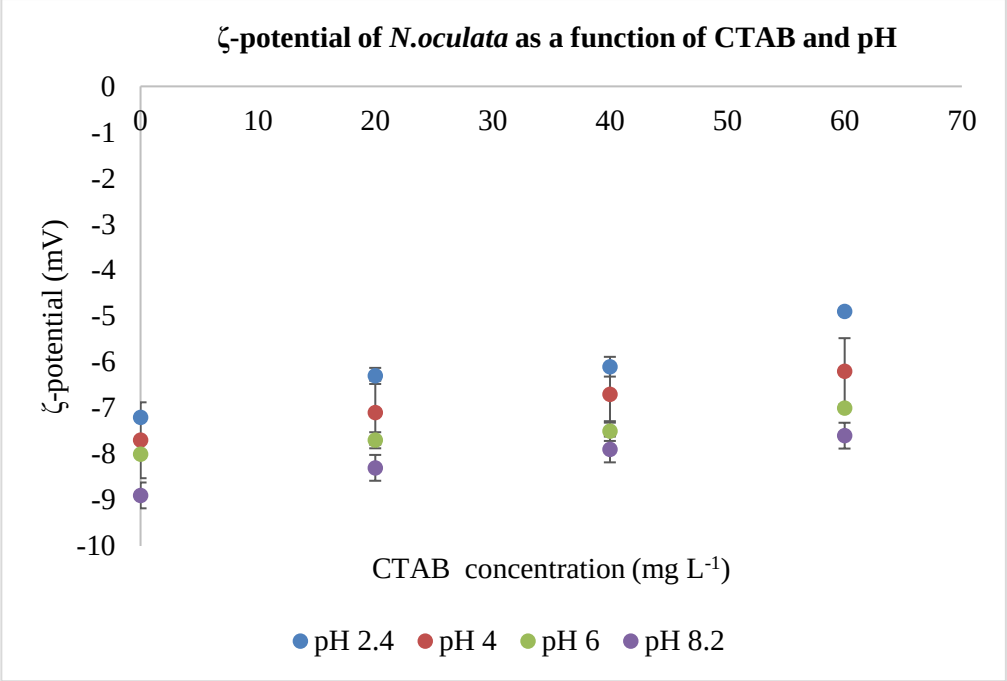

Figure 3.21: Effect of pH on ζ-potential (average ± standard deviation) of *N. oculata* in f/2 media with respect to changes in CTAB concentration

The impact of pH on ζ-potential is presented in Fig 3.21. Fig. 3.21 shows that there was a change towards isoelectric point as pH decreases and CTAB concentration increased. This is because as pH decreases, more H^+ are introduced, leading to the weakening of the electric double layer (repulsive) force that hitherto hinders CTAB - *N. oculata* attachment. However, as already explained, reaching isoelectric point does not necessarily translate into efficient foam flotation.

Similar patterns to the ζ-potential results were observed for the hydrophobicity tests (Fig. 3.22). Although the true value of ζ-potential could not be measured in salt water medium, the influence of acid could be seen on both hydrophobicity and ζ-potential. The interaction between CTAB and salt ions resulted in precipitation of salt ions, which increased with increased CTAB [88].

N. oculata cells owe part of their seemingly hydrophobic nature to algaenan which consists of hydrophobic components [289]. Low charge density means that they are less dispersed in water because of weak repelling forces between individual cells and hence, weak affinity to water. As was seen from ζ-potential measurement, the negative charge of *N. oculata* cells at natural pH (8.2), remain unchanged, indicating lack of CTAB attachment. Therefore, during harvesting, free CTAB molecules would attach to the air-

water interphase, leaving algae cells in the bulk medium.

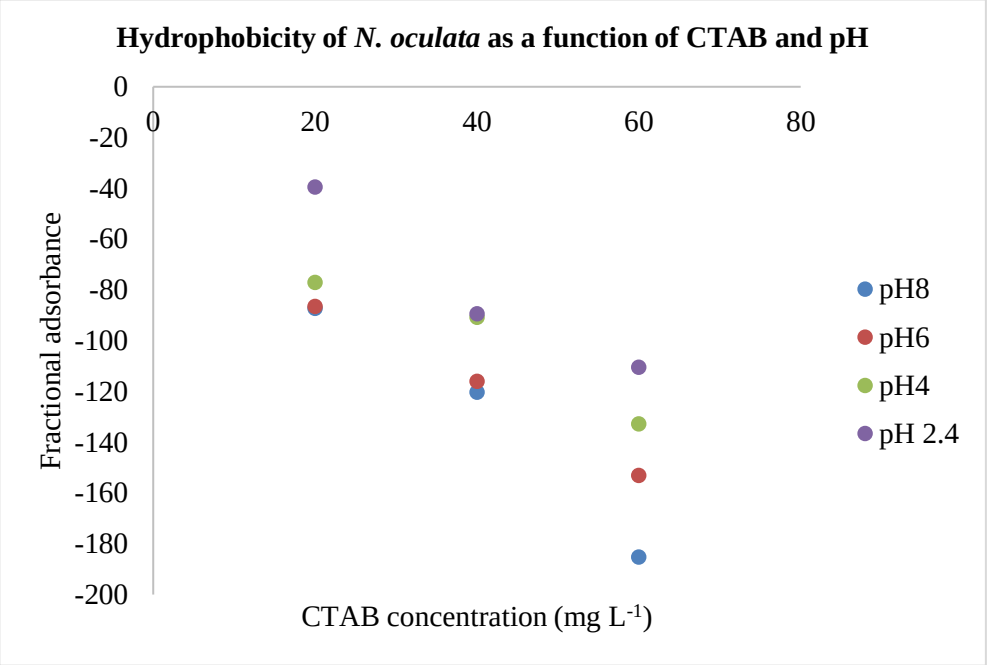

Figure 3.22: Influence of pH on hydrophobicity (average ± standard deviation) of *N. oculata*; fractional distribution is hereby used in order to indicate the interaction between CTAB and salt ions that leaves precipitates that interfere with the absorbance readings

High negative cell charges mean that the cells become more dispersed in solution, indicating a stronger cell-water interaction (hydrophilicity) than cell-cell attraction (hydrophobicity). Figures 3.22 and 3.23, show that the addition of CTAB tends to decrease the hydrophobicity of *N. oculata*. This is because of the presence of salt ions and algaenan. The presence of salt ions could lead to salting out of algae particles so that they flocculate in the presence of CTAB [290]. The higher the CTAB concentration, the more dispersed are the algae cells within the media and hence the higher the absorbance recorded from samples taken from the aqueous layer. Using just 3 mg L^{-1} of CTAB was reported to have increased the hydrophobicity of *C. vulgaris* from 5.3 % to 68 % [92]. However, 5 mg L^{-1} of CTAB was seen to reduce hydrophobicity of *N. oculata*, instead. The more CTAB was added, the less hydrophobic the cells appear to be. It is not clear why *N. oculata* appears hydrophobic or why the addition of CTAB causes reduction in hydrophobicity in *N. oculata*. Nevertheless, the hydrophobic nature of the algaenan covering [289] is a possible culprit. *N.oculata* cells also appear hydrophobic because of highly compressed layer of diffused counterions that reduces the electric double layer force that ensures colloid

stability. The reduced colloid stability means that particles have a high tendency to aggregate (hydrophobic) rather than stay apart (hydrophilic).

The increase in hydrophobicity as pH decreased towards the more acidic zone (Fig. 3.22), is due to the weakening of the stern layer through the attraction of H^+ to Cl^-, thereby weakening the shielding effect of Na^+ on cell particles, allowing them to stay further apart.

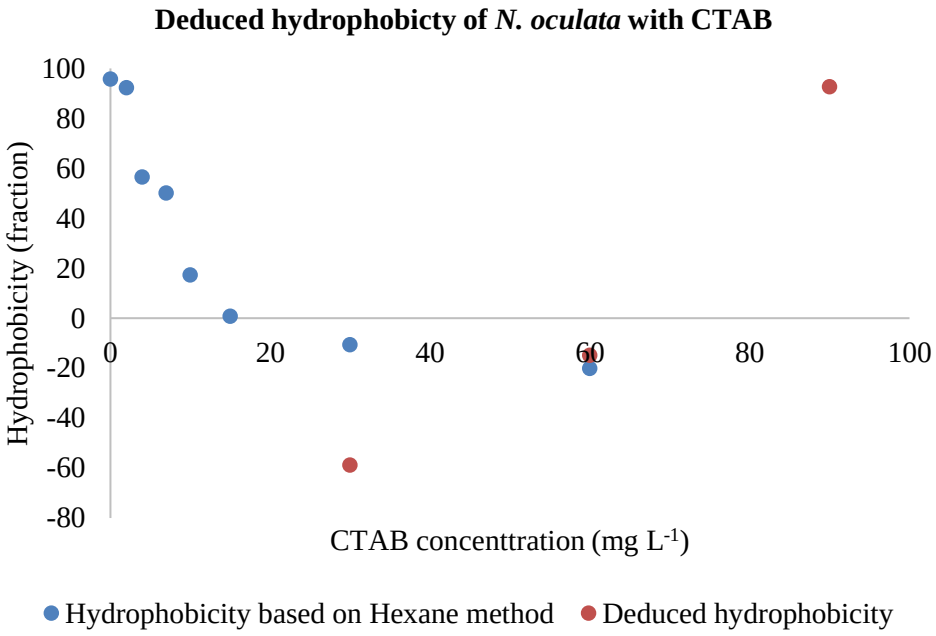

Figure 3.23: Hydrophobicity of *N. oculata* (average ± standard deviation) as a function CTAB; the effect of salt ions was eliminated by subtracting the absorbance when hexane was added from that in which no hexane was added and presented as deduced hydrophobicity

From the corrected hydrophobicity, increasing CTAB concentration from 60 mg L^{-1} to 90 mg L^{-1} was enough to make the cells hydrophobic. This clearly speaks to the difference in morphology between the two cell types. This indicates that hydrophobicity is essential for a successful foam flotation of microalgae to occur.

For a better understanding of the interaction between seawater, CTAB, hexane and *N. oculata*, absorbance of *N. oculata* and seawater with respect to CTAB concentration was measured and as can be seen in Fig. 3.24, there was significant absorbance as measured from the spectrophotometer, even in the absence of cells. The hexane water interface therefore contains CTAB-organic matter.

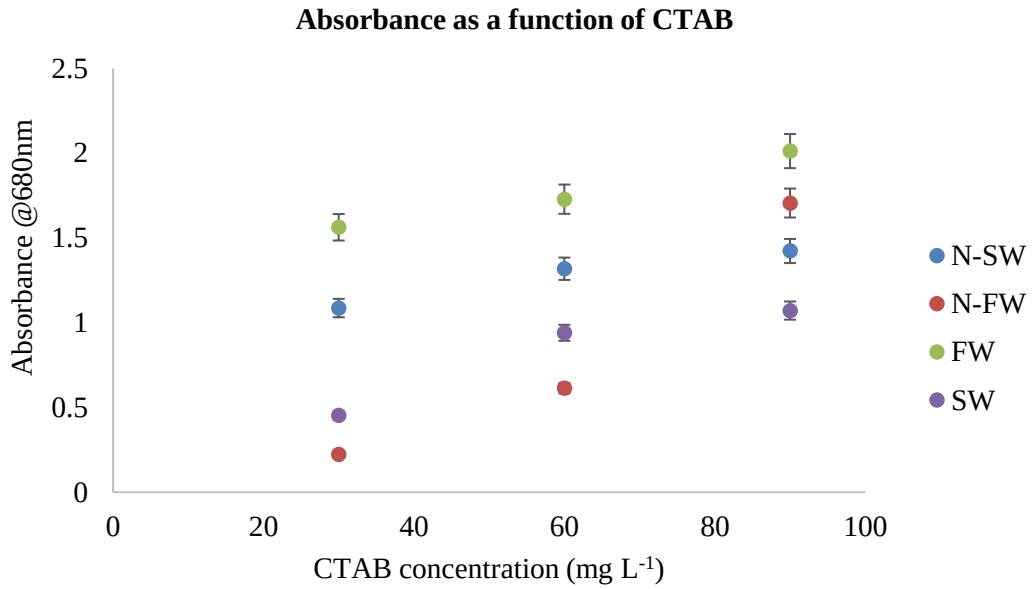

Figure 3.24: Interaction between CTAB and sweater as it affects absorbance (average ± standard deviation); ; N-SW, N-FW, SW, and FW represents mixture of *N. oculata* supernatant and seawater, mixture of *N.oculata* supernatant and freshwater, seawater, and freshwater, respectively

From Fig. 3.24, comparing FW with N-FW, and SW with N-SW, it is obvious that the presence of cells indicated more of absorbance due to pigmentation in the cells. Whereas, in the absence of cells, the values recorded are those of reflectance or scattering of rays, and this could be misunderstood for absorbance but in actual sense it does not mean than absorbance is higher in FW and SW than it is in N-FW and N-SW. Reflectance in FW is higher than in SW because opaque macroemulsion are more likely in freshwater than in seawater due to salt interactions with surfactants [183] and this also explains why recorded absorbance in N-FW increased more with increasing surfactants (compared to N-SW) to the extent that it overtook N-SW at 90 mg L^{-1} of CTAB.

The interaction between surfactants and seawater is a somewhat complex one, during which salt ions could react and form complex with surfactant resulting in suspended particles (macroemulsion) [148]. The presence of hexane (organic solvent) leads to the extraction and or reaction of soluble organic components like polysaccharides and proteins in the seawater, leading to the formation of a thin layer [148] at the water-hexane interface. In particular, the presence of lipid increases the tendency of this thin-layer formation as well as its stability [291]. Therefore, there is a resultant aggregation of complex particles due to the action of CTAB in the highly compressed diffused layer. Consequently, settling

of the complex flocs occurs in the aqueous phase where sampling for absorbance occurs (Fig. 3.25). Hence the explanation for why higher absorbance is recorded in the aqueous layer than the organic layer, during hydrophobicity tests.

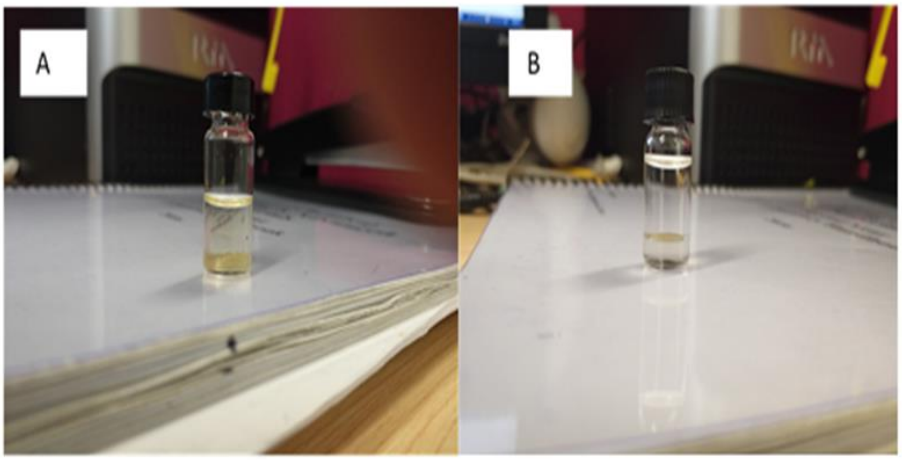

Figure 3.25: Suspended CTAB-organic matter complex; at 90 mg L^{-1} (A), there is higher concentration of the suspension than in B)when CTAB concentration was 30 mg L^{-1}

Surface tension changes in NS (*N. oculata* supernatant), NS-HX (mixture of *N. oculata* supernatant with hexane), SW (seawater), and SW-HX (mixture of seawater with hexane), were measured in presence and absence of CTAB. This was aimed at gaining more insight into the inefficiency of the hexane method of measuring hydrophobicity. It would also provide further explanation of the interaction between CTAB and *N. oculata*.

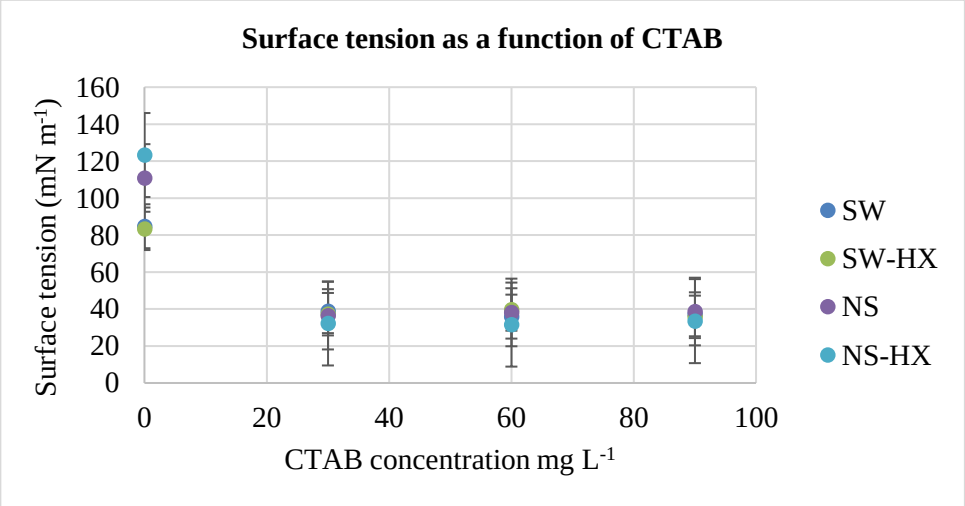

Figure 3.26: Surface tension changes (average ± standard deviation) with CTAB concentration for seawater and *N. oculata* medium; NS, SW-HX, SW, and NS-HX represents *N. oculata* supernatant, mixture of seawater and hexane, seawater, and mixture of *N.oculata* supernatant and hexane, respectively

Fig. 3.26 represent the relationship between surface tension values of the aforementioned media. It shows that the change in surface tension is almost independent of CTAB concentration. This further confirms that CTAB and the resulted complex, remains in the aqueous phase (Fig. 3.25).

Compared to FW, surface tension of SW is higher because of "skin effect" caused by a strong polar attraction existing between Na^+ and Cl^-, even though they displace water molecules which should ordinarily reduce surface tension. The ionic forces increase the interaction between water molecules. With more salt ions in *N. oculata* media than seawater, it is not surprising that, without CTAB treatment, the highest value of surface tension (123.3 ±2 mN m^{-1}) was recorded for NS-HX as seen in Fig. 3.26. It may as well have been as a result of the transfer of extracted components into the aqueous phase thereby forming an extra layer.

The addition of hexane caused a slight reduction in the surface tension of seawater (84.8 – 83.4 ±1 mN m^{-1}). This is expected considering the weaker London forces between hexane molecules, compared to those of seawater molecules. On the contrary, the presence of hexane had led to an increase in the surface tension of NS from 110.9 ±3 mN m^{-1} to 123.3 ±2 mN m^{-1}. This is due to interaction between the hexane and organic components recovered into NS. This interaction becomes even compounded with the introduction of CTAB which leads to particle flocculation as seen in Fig. 3.25.

The overlapping of the NS and NS-HX curves, when CTAB was added, signals the commencement of ionic complexes formation. The closing of the gap between the two curves commenced when 30 mg L^{-1} of CTAB was added. When CTAB concentration increased to 60 mg L^{-1}, the surface tension of NS-HX became lower than NS. This is in agreement with literature [148]. The reason for this is that the air-water surface consisted of less organic matter due to flocculation. Therefore, the hexane method is not recommended for determining hydrophobicity of marine algae.

3.3.6 DLVO explanation of foam flotation of *N. oculata*

The effect of salt concentration can be viewed from the difference in Debye length (κ^{-1}) between freshwater and seawater, calculated in this work as 9.9 nm and 0.43 nm respectively. These values are quite similar to those obtained by Nabweteme et al. [180], which were 9.0 nm and 0.37 nm respectively for freshwater and saltwater medium. The

reduction in Debye length is capable of preventing access to the cells by surfactants and therefore limiting surfactant's ability to capture and recover cells. Note that electrostatic repulsive force is a function of particle radius, distance apart, and the Debye term, which depends on ionic strength. The ionic strength is a very important parameter when it comes to determining this repulsive energy because an increase in ionic strength will shield the charge around the particles and hence a decrease in stabilisation of the colloidal system since the more positive is the overall energy, the more stable. This also means that the true surface charge could not be read using electrophoresis and hence ζ-potential measurements may not be an accurate way of examining the electrostatic interaction between cells and surrounding surfactants, particularly in marine environment. This is because under high salt concentration as stated, there is no colloidal stability as the cells are rather clogged together and this explains the rather hydrophilic behaviour that is observed, even though the cells live in water. The simple explanation is that the perceived hydrophobicity is just an indication of how well the cells would rather stay together than spread evenly within the emulsion system and hence are "water"-phobic. In the presence of surfactants, because this instability is somewhat altered due to ionic interactions between the salt ions and those of the surfactants, there seem to be an increase in hydrophilicity because the cell-cells interaction is becoming less strong while cell-water interactions increases in strength as stated earlier.

The work of Nabweteme et al [180] indicates that the total energy for the flocculation of two strains of microalgae (freshwater Microcystis sp. and marine P. minimum) was mostly controlled by electrostatic repulsive forces in freshwater while in saltwater medium the dominant forces are those associated with acid-base interactions. Estimation of the Van der Waals as well as the electrostatic attractive forces can be easily deployed based on the classical DLVO theory but the addition of the acid-base interactions by the XDLVO involves particle sizes as well as interfacial tension of solids involved (namely, surfactants and algae). Inferring from Nabweteme et al [180], it is safe to say that the acid-base interactions are as applicable to floatation as for flocculation. After all, surfactants in flotation serves a dual purpose of being collectors (similar to flocculants) as well as frothers.

Results from this work, as shown in figures 3.27 and 3.28, indicate that in freshwater medium, the controlling forces are the electrostatic repulsive forces (VD) and

this is in line with the findings of Nabweteme et al [180]. In order to evaluate the prevailing forces in seawater medium, Nabweteme et al. included the acid- base interactions term according to the XDLVO and their conclusion was that the acid-base interfacial forces controls the total energy of the process. Although the XDLVO was not applied in this work, applying the classical DLVO indicated that the Vander Waals attractive force (VH) controlled the total energy of the system in seawater. Without the acid-base term as a third form of energy, it is difficult to say in this case, whether the total energy is controlled by VH or not. Nevertheless, suffice to say that VD is no longer controlling the total energy of the system which agrees with the findings of Nabweteme et al [180]. Figure 3.27 indicates that cells become stable at around 4nm apart as opposed to the complete lack of stability observed in Figure 3.28 across all separation distances.

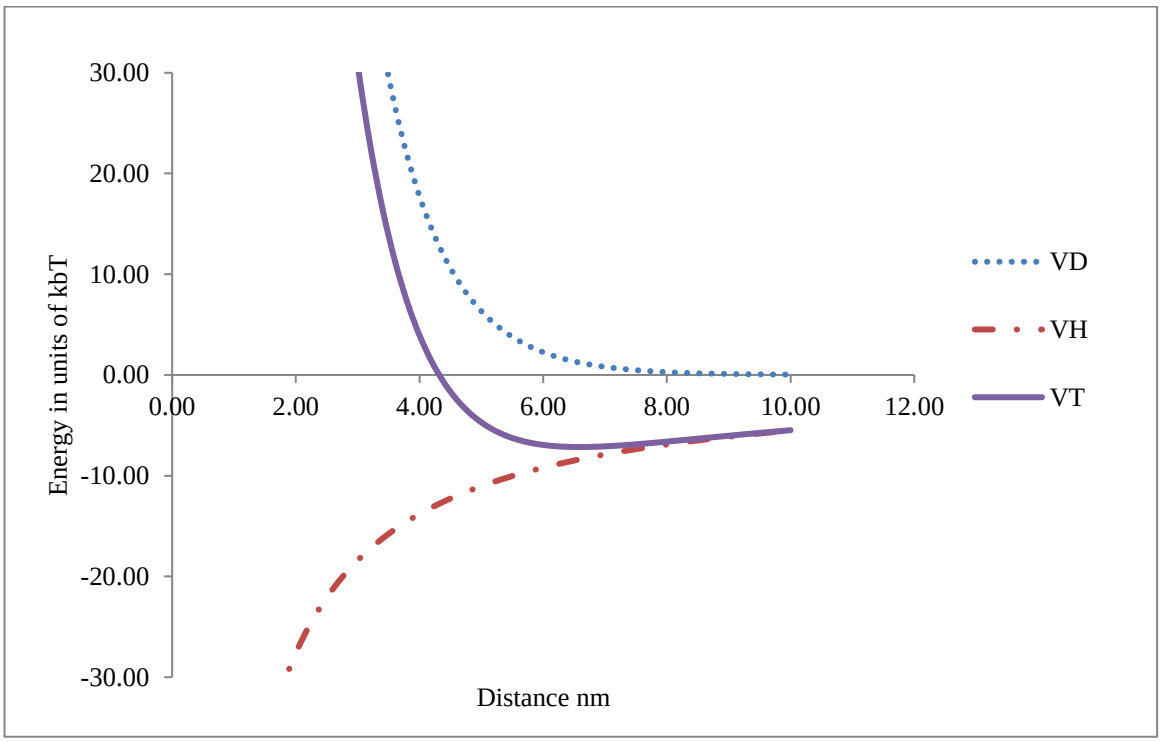

Figure 3.27: DLVO interpretation of Nannochloropsis cells under fresh water conditions; ζ potential of -32mV, pH 7; VD, VH, and VT are electrostatic repulsive forces, Vander Waals attractive forces, and Total system energy or potentials, respectively

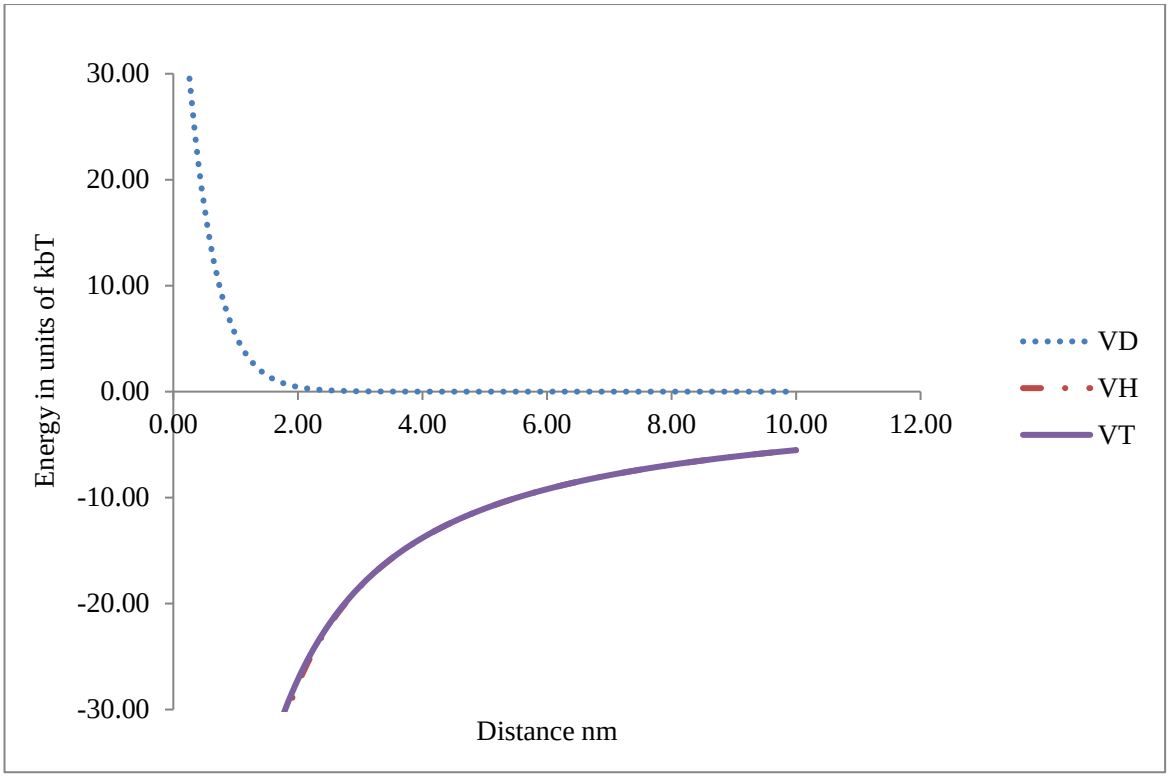

Figure 3.28: DLVO interpretation of *Nannochloropsis* cells in f/2 medium; ζ-potential 0f -8mV, pH 8; VD, VH, and VT are electrostatic repulsive forces, Vander Waals attractive forces, and total system energy or potentials, respectively

As for the components of the cell walls, most of which are negative radicals, the introduction of acidic condition means there is a possible weakness in the surroundings of the cell walls due to the interaction between H^+ ions and these negative elements and hence the increased in surfactants-algae interactions and therefore better recovery by way of attraction.

Because of cells clustering to foam larger and heavier particles, flotation becomes more difficult and hence increasing the airflow was needed to lift the comingled cells. This therefore leads to the conclusion that *N. oculata* recovery by flotation is highly dependent on collision between air bubbles and microalgae cells.

3.4 Conclusion

Recovering *N. oculata* in its natural medium, using 60 mg L^{-1} CTAB, 1 L min^{-1} airflow, 60 mL min^{-1} feed flow, 25 cm liquid height, and 135 cm column height, was not possible. This is due to the limitation of algae-bubble attachment as a result of interference

by seawater ions and protective algaenan layer. Increased airflow can be used to improve recovery by enhancing bubble-algae collision. In this regard, flocculation is a more effective harvesting technology for marine algae than flotation, albeit not as green or cheap.

Increased airflow, increased surfactant concentration, and decreased pH results in increased recovery while a decrease in surfactant concentration and airflow combined with decreased pH, results in higher concentration factor. This is true whether the culture was diluted with freshwater or not. Moreover, the presence of algaenan in *N. oculata* has a negative impact on its harvesting through foam flotation and hence the important role of microalgae strain type on flotation efficiency.

ζ - Potential measurements are not sufficient to determine whether marine microalgae cells can be harvested by foam floatation or not. This is due to the compressed stern layer, which reacts rather sluggishly to applied potential in the measuring device and leading to a smaller potential than the actual value, to be recorded. Furthermore, alternative methods to using hexane as an extractor for organic matter should be avoided when measuring hydrophobicity of *N. oculata* in CTAB, due to the formation of CTAB-organic matter complexes, which interferes with absorbance measurement.

While the combination of SDS and CTAB is capable of improving recovery and concentration of *N. oculata* (20 % at CF=11), the best way to harvest *N. oculata* via foam flotation is to increase the possibility of bubble-cell collision by increasing air flow and pH reduction (pH 6 or 4). By this, more than 80 % cell recovery and CF of 14 can be achieved using CTAB.

This work has demonstrated for the first time, the capability of foam flotation to handle very small algae cells like *N. oculata*, provided other conditions (cell hydrophobicity, surfactant type and strength, and pH), are satisfactory. The process hereby proposed, has some potentials for reduction in production cost, which has been a major obstacle to the success of algal biodiesel beyond laboratory scale.

As a recommendation, the inoculation of algaenan-consuming fungi into the cultivation of *N. oculata* to produce algaenan-free hybrid that will be less problematic to recover should be considered. It is also recommended that the extended DLVO be applied to gain further insight into the interaction forces between microalgae and surfactants particularly under acidic conditions. This will allow for a better understanding of the hydrophobic and hydrophilic forces that are in play within the medium in the presence of

surfactants. Both recommendations should however be carried out independently because a new interaction could be introduced between fungi and surfactant. Besides, if the first option succeeds, there would be no need for the extended DLVO.

Chapter 4

Effective methanol injection - a prerequisite for biodiesel production in a foam column

Abstract

As a prerequisite for biodiesel production from algae in a flotation column, foam stability as well as strong methanol presence in the foamate must be guaranteed. In this chapter, a methanol injection scheme was designed in pursuit of this objective. To this end, methanol distributors were designed, fabricated and used to deliver methanol into the foamate without the foam collapsing. This countercurrent methanol injection system was more effective than cocurrent methanol flow in delivering methanol, while making sure that CTAB and methanol consumptions were minimised while methanol concentration in the foamate was maximised. This strategy combined with contraction sections allowed for methanol accumulation to be equally minimised. However, the cocurrent methanol process allowed for longer contact time between methanol and algae, which could warrant easier cell lysis and oil extraction. Stable foam was possible as long as the percentage of methanol in the mix was not more than 50 vol. %. Seawater was better suited for the process of injecting methanol than freshwater but within the operating conditions of this study, both media were able to deliver the required concentration of methanol appropriate for transesterification.

Keywords: Continuous foam flotation, Methanol distributors, Foam riser, Design of experiments, Methanol accumulation

4.1 Introduction

There is no available literature on the interaction between algae, surfactant and methanol. Although the interplay between water and methanol (as well as other alcohols) is well investigated, the nature of their interaction in foam flotation is not well captured in the literature. The use of surfactant as a cell lysing agent has been reported in biodiesel [277, 292] and DNA extraction processes [293]. In particular, the work of Coward et al [277] indicated the potentials of CTAB to cause cell lysis during foam flotation of microalgae.

Methanol is very popular in biodiesel production through alcoholysis, being the cheapest and most common alcohol. It would be interesting to attempt to integrate the process of biomass recovery and biodiesel production in a single unit, potentially eliminating the drying and hexane extraction steps which accounts for up to 92.2 % of the energy cost of biodiesel production using the conventional transesterification [35]. Besides, drying has to be done within the range of 60 to 80 °C in order to alter the lipid and carbohydrate contents [294]. The objective of this work is to investigate the possibility of adding methanol particularly at the top of the column in order to create the requisite environment for biodiesel production in a foam floatation column. For biodiesel conversion to be achieved, methanol present in the foamate needs to be at least 50 wt. % in order to serve as a reactant and/or oil extractor [295]. Because of the advantage of longer contact time between methanol and microalgae, feeding methanol along with algae would be investigated although the likelihood of achieving the desired concentration is higher when methanol is fed as a separate stream at the column top.

A foam is simply a gas trapped in a liquid or solid when the two surfaces come in contact. To have a liquid foam, gas is bubbled through the liquid, which in turn displaces some liquid molecules, stretching same into thin films that creates boundaries between gas molecules. Simply put, foams are mixtures of gas bubbles, usually of different sizes (disordered) but sometimes of uniform sizes (ordered). Foams can also be regarded as wet or dry depending on liquid content [296], with a liquid volume fraction ranging from much less than 1% to as great as 30%. Where liquid drainage occurs in a rising foam [297] through a column, such foam becomes enriched. The longer the column, the dryer becomes the foam at the top of the column. Foams are stable due to the hydro-aero-dynamics of the system and tend towards rupture because of bubble-to-bubble gas diffusion that reduces the Gibbs free energy of the system [298]. Due to their unique features (including high surface area, large expansion ratio, low interphase slip recovery, and finite yield stress), foams (especially gas-liquid foams) have found usefulness across various industrial applications, such as: petroleum, cosmetics, paints, pharmaceutical, fire safety, water treatment, biomass harvesting, metallurgy, and many more, [299]. The performance of a foam flotation process is dependent on the foam stability which in itself is a function of interdependent physical properties of not just the froth but that of the attaching particles [299].

Surfactants are used in motor oils, lubricants, detergents, soap, pulp, ink etc. because of their ability to reduce the surface tension of water and, in most cases, co-surfactants or additives are applied [242, 300-304] to modify interfacial properties even at low bulk concentrations [238].

CMC of a surfactant in a liquid is that concentration of the surfactant above which, micelles form, and in turn, mediate between the bulk liquid and the gas phases. This concentration is significant for so many reasons. One of such reasons is that it can be used to define the limit for meaningful use of a surfactant since further reduction in surface tension does not occur beyond this concentration. It can also be used to characterise the surface adsorption properties, which is very essential in a flotation process. Although this concentration does not necessarily have to be reached, except for cleaning purposes for example, it is important to know how it is affected by the presence of other substances. This would provide information on how to best use surfactants for the purpose of particle adsorption, for example. Alcohols affect the critical micelle concentration of surfactants in different ways, depending on whether; the surfactant is ionic or not, saturation adsorption is small or large, and interfacial surface tension of the system at CMC (γ_{cmc}) is small or large [240]. Those were the findings of Huang et al. (1998) when they reported that ethanol addition increased the CMC of ionic surfactant in water, but with non-ionic surfactant, a decrease in CMC precedes the increase. They also found that the γ_{cmc} of the system decreased or increased depending on whether the saturation adsorption was small and γ_{cmc} in the absence of methanol was large and vice versa [240]. This is in agreement with earlier reports by Iyota and Motomura (1991) [242], that interfacial interactions play a major role in determining the influence of surface tension. In fact, research along this direction dates back to Ward (1940) [251], where he examined the behaviour of SDS in water and noted that above a certain concentration (C= 0. 00722 N, known today as CMC) micelles were formed with a sudden drop in equivalent conductance (now known as molar conductance). These micelles were affected by the presence of methanol, so much so that when the amount of methanol reached 40%, no micelles formed [251]. Equivalent or molar conductance of a substance is a measure of the ability of the ions of that substance to conduct electricity when one gram is dissolved in an equivalent electrolyte. The unit of equivalent conductivity is $Ohm^{-1}cm^{2}(gm\ equiv)^{-1}$.

Water and methanol mixtures, as a consequence of being the two most abundant

hydrogen-bonded liquids, have been widely studied [305]. The interactions between water and methanol in the presence of surfactants have been investigated by a number of authors [247, 302, 303, 306-308], including foam flotation of metals [252] and polymer wettability [243]. However, the same cannot be said of algae foam flotation. Equally, the process of feeding methanol in a countercurrent direction to the flow of foam in a foam column is not well studied.

Theoretical expressions have been developed to describe the surface tension isotherms of multicomponent aqueous solutions [238], notable among them is the Feinerman and Miller, Szyszkowski, and the Carnors equations: [309-314] all of which are thermodynamic relations between surface excess and bulk concentration, based on Gibbs equation [315] (Eqn. 4.1). Beyond the approach of using thermodynamic relationships that are sometimes based on assumptions, Phan et al. (2016) [247] recently proposed a rather quantitative relationship between molecular arrangement and surface tension of aqueous solutions of alcohols. This work is in line with Langmuir's early findings that molecular arrangement is very important to the variations in surface tension because of the various orientations that are possible and hence the discrepancies between measured surface tensions and theoretically deduced values based on models.

Like salts, alcohols have the tendency to delay bubble coalescence, subject to concentration of NaCl or alcohol in the medium - higher concentrations lead to wetter foams which can improve particle recovery as long as the particles are sufficiently hydrophobic, but if the alcohol concentration exceeds a certain threshold it may cause the detachment of the adsorbed solids [252]. Again, this is a function of the materials involved as well as operating conditions. Beyond the threshold concentration, coalescence time ceases to increase because the film surface has become saturated even as surface tension drops sharply and this is explained by the Gibbs isotherm (Eqn. 4.1).

$$\Gamma = -\frac{1}{RT} * \frac{d\gamma}{d \ln C} \tag{4.1}$$

where γ is the equilibrium surface tension (mN m^{-1}), C is the concentration of surfactant or co-surfactant (mole m^{-3}), R is the gas constant (J mol^{-1} K^{-1}), T is absolute temperature (K), and Γ is the surface excess which is the amount of surfactant or co-surfactant at the interface (mole m^{-2}).

Higher concentrations of surfactants or co-surfactants do not only result in wet

bubbles but they can also reduce stability in bubbles [102].

Adsorption of surface active materials such as surfactants in the presence of methanol have been shown to be a function of the material type and not necessarily dependant on the surface tension of the material [243]. Therefore, whether or not there will be an adsorption to algae cells to surfactant in the presence of methanol is an open question. For methanol to act as both solvent and reactant for the production of biodiesel in a foam column, it is necessary to ensure that they are not only available in the right quantity and quality, but also at the appropriate reaction site within the column. Achieving these targets calls for a careful look at the dynamics of the system vis-à-vis prevailing conditions like airflow, feed flow, surfactant concentration, column height, and methanol feed flow. Because of the limited data on methanol water interaction as it concerns foam flotation, there is no certainty as to how to best introduce methanol into the process, and that is to say should it be mixed with the feed or as a separate stream close to the top of the frothing zone.

In mineralogy for instance, where high-value products are targeted, the process can be expensive, whereas in biodiesel production the economics are more sensitive to process costs. Particularly, in mineralogy, greater attention is paid to recovery because the additional cost that comes with further dewatering or drying can be balanced by the financial value of the minerals being recovered.

The effect of methanol on the surface tension of water and foam stability is studied in this chapter with the aim of enriching methanol at the top of the column where some can be used as both reactant and solvent to produce algal biodiesel within a foam column. CTAB has been chosen as the candidate surfactant, based on previous screening test conducted in chapter 3. The aim of this chapter is to make available methanol at the top of the column, not only in terms of quantity but more importantly in terms of quality. This aim can only be achieved by selecting the appropriate methanol injection route that will allow for foam stability in addition to the desired methanol amount and strength. For an understanding of the influence of methanol on the capacity of CTAB to modify the water-air interface, surface tension measurements will be conducted. Furthermore, flotation experiments will be conducted in the presence of methanol in order to corroborate the surface tension experiments. Batch and continuous flotation runs will be carried out using cocurrent and countercurrent methanol injection modes. During the batch experiments,

effect of airflow, CTAB concentration, and column height on foam stability and methanol concentration will be investigated. In order to account for the impact of feedflow and runtime, continuous experiments will be conducted based on the knowledge gained from batch experiment. The impact of ionic strength will also be studied. Finally, a methanol balance will be carried out over the flotation column to clearly define the fate of methanol in the process. A contraction section will be introduced close to the foam outlet in order to improve concentration of foamate.

4.1.1 Pseudo steady state and methanol balance across a flotation column

In column flotation, the large height-to-width ratio is said to enhance good contact time between bubbles and particles in suspension by eliminating axial mixing [142]. This is however not always true as steady state conditions are usually approximated [316], and in most cases very high airflow, feed flow [142, 317] and sometimes co-surfactants [142] are involved to maintain invariability in process conditions with time. In a flotation system where air and one liquid phase is involved, steady state is said to be when all the air that goes into bubbles formation is equal to the amount of air that is released when the bubbles break [318]. This statement may however not be true in terms of a system involving more than a binary number of elements. In the foam flotation here described, during the countercurrent flotation process, the added stream from the top is consisted of only methanol, which complicates the attainment of steady state because not all the methanol that goes into the column comes out at the beginning of the process. If the process is not allowed to go on long enough for steady state to occur, methanol accumulation occurs. There is a transition from unsteady state to steady state once the system is returned to a one-feed system after the methanol stream was stopped and the process allowed to continue for another 10 minutes. Beyond this time, methanol accumulation equals zero.

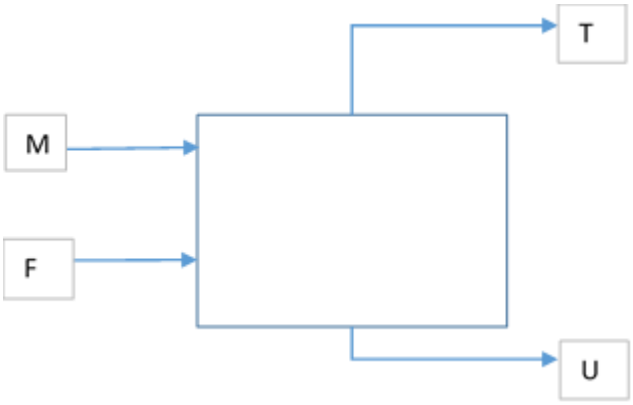

Figure 4.1: Process flow diagram for methanol concentration using foam column; [M]Methanol, [U]Underflow, [F]Feed, and [T]Top

The way to deal with a pseudo-steady-state or non-steady-state system is to do a dynamic material balance, and in this particular case the rate of change or accumulation in the mass of methanol in the system can be calculated based on Eqn. 4.2 below:

$$Rate\ of\ change\ of\ MeOH\ (mass) = Mass\ of\ MeOH\ (in) - Mass\ of\ MeOH\ (out) \quad (4.2)$$

Eqn. 4.2 can be rewritten as:

$$\frac{d(M_f.X_{M,f})}{dt} = FX_{m,F} + MX_{m,M} - TX_{m,T} - UX_{m,U} \quad (4.3)$$

Since there is no methanol in the feed and underflow, the second and last terms becomes zero and hence Eqn. 4.3 can be written as:

$$\frac{d(M_f.X_{M,f})}{dt} = MX_{m,M} - TX_{m,T} \quad (4.4)$$

But $M_f = Q_v \emptyset_l \rho_l$

Where Q_v is the volume of the column (m^3), $\emptyset_l$ is the liquid holdup (fraction), ρ_l is the density of the liquid (kg m^{-3}), and M_f is the mass of methanol in the column (kg).

The liquid fraction can be obtained by measuring the hydrostatic pressure gradient within the foam column, as the pressure gradient is related to the liquid fraction using equation 4.5:

$$\frac{1}{g}\frac{dP}{dZ} = (1 - \emptyset_l)\rho_g + \emptyset_l \rho_l \quad (4.5)$$

Because the density of gas (ρ_g), in this case air, is much less than ρ_l, Eqn. 4.5 can be approximated to:

$$\frac{1}{g}\frac{dP}{dZ} = \emptyset_l \rho_l \quad (4.6)$$

Where g is gravitational acceleration (ms^{-2}) and $\frac{dP}{dZ}$ is the pressure profile along the column, P is pressure in the column (Nm^{-2}), and Z is the height (m) at which the measurement was recorded.

4.2 Materials and methods

Methanol 99.8% (Sigma-Aldrich), CTAB (Sigma-Aldrich) and deionised water were the main chemicals used in this work. A tensiometer (Aqua-Pi Plus by Kibron Inc. Finland) was used to measure static values of surface tension. A refractometer (Refracto 30PX by METLER TOLEDO, Japan) was used and data therefrom was converted to methanol wt. % using a calibration curve of refractive index versus wt. % of known binary mixtures of methanol and water. Density measurements were done with a density meter (METLER TOLEDO Japan, Densito 30PX 15/40). A 3D printer (Form 2) from Formlabs UK was used for 3D printing and methanol recovery was achieved with the aid of a rotary evaporator (Rotavapor R125 from Buchi UK) fitted with a V-70 vacuum pump. The rotavapor system is equipped with automated calibration system and has the ability to perfectly remove water and methanol from solution. Fluke 922 Differential Manometer was used for pressure measurements. Both tensiometer and refractometer have in built calibration system that allows them to be calibrated against known samples.

4.2.1 Measurement of surface tension, refractive index, density, and pressure

In order to understand the role of methanol on the ability of CTAB to reduce water surface tension and eventually foamability, surface tension tests were conducted. CTAB (100 – 400 mg) was weighed and added to 10 mL of water (or a mixture of water and methanol of known volume fraction) in a small glass beaker and mixed with the aid of a magnetic stirrer at 400 rpm until CTAB is fully dissolved. The maximum CTAB concentration of 400 mg L^{-1} was based on the critical micelle concentration (CMC) of 360 mg L^{-1}, used in this work. The solution was then made up to 1 litre of solvent by adding it to water or water-methanol mixture (10 - 90 vol. %), taking the initial 10 mL of water into account, and stirred for 10 minutes before sampling for surface tension. This was to ensure proper dissolution of CTAB in the solvent. Triplicate 3 mL samples were transferred into the sampling cup and allowed to settle before measuring the surface tension, according to the

modified Du Noüy method of Padday et al. (1975) [236]. The ring in the Du Noüy [235] apparatus is hereby replaced with a thin rod which is immersed in the sample and pulled out so that the maximum force is measured and recorded with the aid of a computer interface that allows for automatic control of measurements and data storage. The equipment was first calibrated using deionised water at room temperature where a surface tension of 72.32 of ± 0.05 mN m^{-1} was recorded. Each measurement was done three times to ensure accuracy and repeatability of results while accounting for standard error. The added methanol was recovered using a rotary evaporator.

The refractometer was first calibrated with deionised water (=1.3329 ± 0.0002 nD). This refractometer is robust and quick and error free due to the inbuilt calibration system. It has a measurement range of 1.32 – 1.50 and an accuracy of ± 0.0005 nD, operating within 10 °C – 40 °C. Before every measurement, the glass prism was rinsed with DI water and dried with clean towel. About 2 mL of sample is then poured into the sampling point and the refractive index recorded. In order to draw out a calibration curve, water – methanol samples were prepared on a methanol/water wt./wt. basis of 0/100, 10/90, 20/80, 30/70, 40/60, 50/50, 60/40, 70/30, 80/20, /90/10, and 100/0, for percentages higher than 10. For percentages below 10, the ratios were 0/10, 1/9, 2/8/ 3/7, 4/6, 5/5, 6/4, 7/3, 8/2, and 9/1.

The density meter (Japan, Densito 30PX 15/40) used in this work has an accuracy of ± 0.001 g cm^{-3} and a measurement range of 0 to 2 g cm^{-3}, operating between 5 to 35 °C. This robust equipment can measure density very quickly as soon as the commanded through a button. It accepts sample based on syringe mechanism that allows samples to be suck in and injected. This system also allows for cleaning of the sampler unit. About 3 mL of the sample to be tested is suck and by pressing the ok button, the value of the liquids' density is displayed almost immediately.

For pressure measurements, the inlet side of the manometer is connected to the column via a pipe which allows the pressure at any given point along the column to be measured. The probe is lowered down from the column top to the desired depth. Pressure measurements were taken within a short period along the column, within a period of 15 secs because of the change in pressure along the column with time. Three depths, namely: 60, 90, and 120 cm were chosen for pressure measurements. The quick measurements were possible due to the fast response of the manometer which also has an accuracy of ± 1 N m^{-1}, and can measure up to 41369 N m^{-2} at temperatures up to 50 °C. Pressure measurements

were carried out 12 min into the flotation process during which methanol was been injected.

4.2.2 Foam flotation experiments

The flotation column used in these experiments was described in chapter 3 and for the purpose of this chapter, a process diagram is shown in Fig. 4.3. To ensure better foam stability when methanol is to be injected countercurrently, methanol distributors (Fig. 4.10) were inserted 22.5 cm from the column top. Another peristatic pump was required to accurately pump methanol to the column top. The pump used for methanol feed was calibrated for each distributor size while that for the bottom feed was calibrated once.

To ensure better foam stability when methanol is to be injected countercurrently, methanol distributors (Fig. 4.10) were inserted 22.5 cm from the column top. In order to increase CF, a 15 cm contraction-expansion (riser) section [278] with a 1:5 contraction ratio (Fig. 4.11) was inserted 7.5 cm below the injection point of methanol. A 5 L bucket was used as a feed tank from which various composition (w/w) of water (containing CTAB) and methanol were pumped via a peristaltic pump (Masterflex 7720160 fitted with a Masterflex - 77201-60 head) into the base of the column just above the air chamber while compressed air was supplied into the air chamber through a ¼" hose fitted to the centre of the bottom plate. Between the liquid and air chamber, was a porous (6 µm) polystyrene sparger that diffused air through the liquid and therefore created bubbles that in turn, rose along the column. Foamate was then collected (if available) at the top of the column and analysed for methanol content. The column was provisioned with two feed points, a bottom feed point located 7.5 cm above the air chamber and a top feed point located 22.5 cm from the exit point of the foam. The underflow is manually controlled with the aid of a tap, which is fitted with a flowmeter.

The arrangement of the column with installed distributor and foam riser are shown in fig. 4.2 below.

Methanol feedline is provisioned with another peristatic pump through which flow rates were accurately measured. The pump used for methanol feed was calibrated for each distributor size while that for the bottom feed was calibrated once.

Flotation experiments were carried out in batch and continuous modes. For batch experiments, the required amount of solution to be treated was fed into the column whilst

maintaining around 0.5 L min^{-1} of air to keep the liquids from crossing from the liquid chamber into the gas chamber. Once all the liquid had been fed to the column, the required airflow (capable of forming and raising bubbles) was then set with the aid of flowmeter and the timing of the experiment began. Where runtime was a variable, the process is allowed to continue through the desired period, otherwise it is left to go on until no foamate is available to be collected. To end the process, airflow is reduced to 0.5 L min^{-1}, just enough to prevent liquid in mixing zone from crossing over to the gas chamber. The foamate and bottom residue is then analysed for methanol composition.

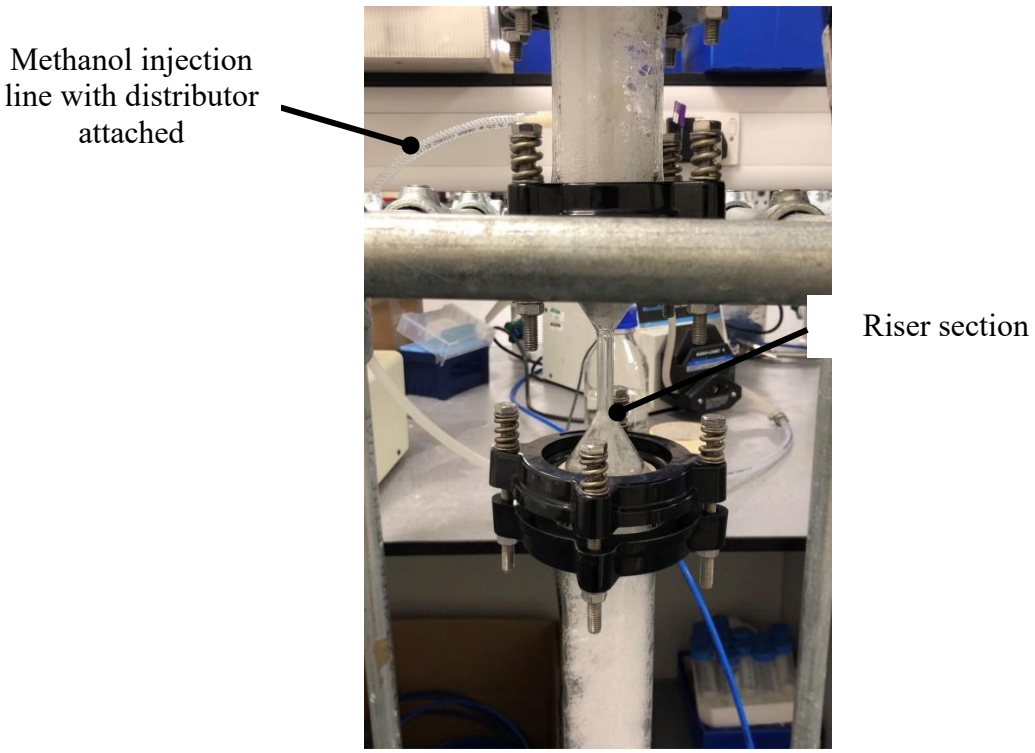

Figure 4.2: Modified flotation column with riser section and methanol injection line; the methanol distributor is connected to methanol feed bottle with the aid of grooves of external diameter equal to the internal diameter of the PVC hose that serves as feed line.

In continuous flotation, once the feed is fed into the column to a desired liquid level, the airflow was then set to the desired value while simultaneously opening the underflow, marking the beginning of the continuous process. Where runtime was a variable, continuous flotation was carried out over a specific time, otherwise the process was allowed to go on until the feed is exhausted. Each process is shut down by reducing airflow to 0.5 L min^{-1}(just to prevent liquid from draining down the sparger) while stopping

the underflow at the same time. Collection of foamate was allowed to stop naturally to ensure that all possible products of a particular process are accounted for. In similar manner to the batch flotations, top and bottom products are analysed for methanol content.

Estimation of methanol accumulation was done based on dynamic methanol balance across the column. Relying on pressure profile measurements, the liquid hold-up in the column was estimated according to Eqn. 4.6. The estimated liquid profile was then used to estimate the rate of accumulation, based on Eqn. 4.4.

Fig. 4.3 below is that of a continuous flotation with or without microalgae cells

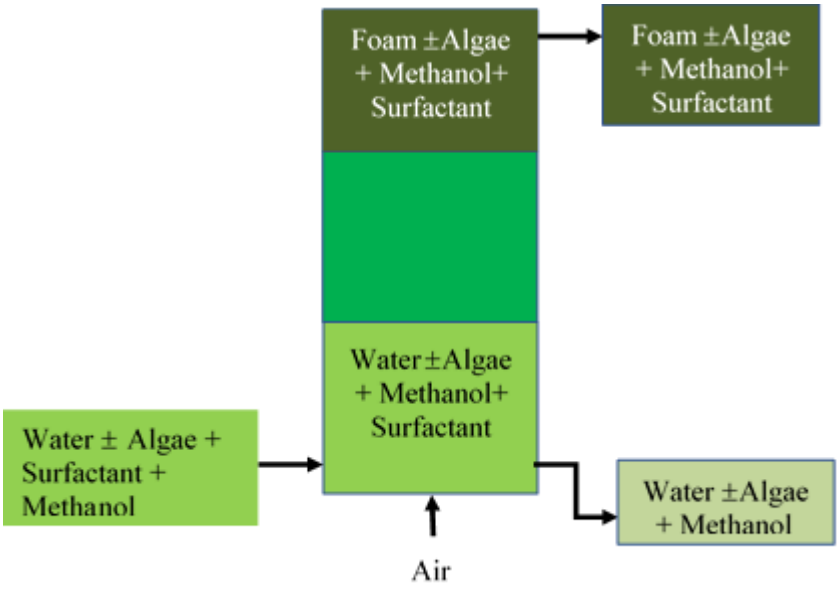

Figure 4.3: Process flowsheet for the flotation system; the example here is that of the cocurrent continuous methanol process and it is assumed that no surfactants are found in the underflow

Foam stability and algae recovery – cocurrent or countercurrent methanol flow

In order to investigate the stability of foam as well as possible harvesting of *C. vulgaris* in the presence of methanol, batch flotations were conducted. Mixtures containing 25, 50, and 75 vol. % of methanol in *C. vulgaris* culture and CTAB (30- 400 mg L^{-1}) were fed to the bottom of the column (Fig. 4.4). The choice of CTAB concentration was based on the CMC of the CTAB used in this work. Feeds were prepared by weighing 30 – 400 mg of CTAB and adding same to 10 mL of water in a small glass beaker (or a mixture of culture

and methanol of known volume fraction in a 1 litre be) and mixed with the aid of a magnetic stirrer at 400 rpm until CTAB is fully dissolved. The CTAB solution is then added to algae culture and mixed for 10 min before the addition of methanol to make up to 1 L mixture, depending on the desired culture-methanol ratio (10 - 90 vol. %). Alternatively, the 10 – 90 % vol. culture – methanol mixture is prepared and mixed first before the addition of CTAB solution. In both cases, the 10 mL of water added to CTAB was accounted for in the final culture – methanol ratio. Measuring cylinders were used for liquid volumes measurements. To avoid evaporation of methanol that could arise from the exothermic process of mixing water and methanol, methanol was gently added to water. Flotation was preceded by at least 10 minutes of slurry mixing.

Separate experiments (1 L min^{-1} airflow, 50 vol. % methanol, 100 cm column height, 400 mL of feed, and 300 mg L^{-1} CTAB) were conducted to estimate the recovery and CF of C. vulgaris in the presence of methanol.

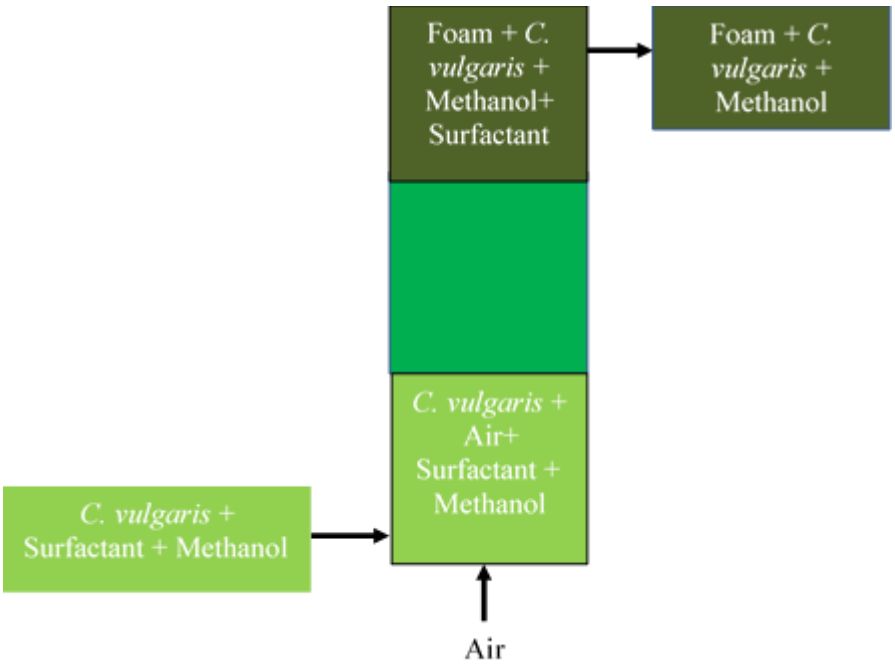

Figure 4.4: Cocurrent recovery of *C. vulgaris* and methanol enrichment in a batch operated column of 100 cm height; methanol concentration in the feed was varied from 25 to 75 vol. % at 30-350 mg L^{-1} CTAB, airflow was 1 L min^{-1}, and feed rate was 50 mL min^{-1}

The choice of 10 min mixing time was made from the results of a set of experiments

to determine the effect of mixing, based on which it was found that 10 min of mixing time was sufficient. In both mixing sequence, foam stability and eventual recoverability of algae (*C. vulgaris*) under the said conditions were investigated. *C. vulgaris* was used in this experiment because its flotation process has been well established both in this work and elsewhere [19, 40, 277]. Although, this project is focused on conversion of oil from marine algae, *C. vulgaris* is hereby used for control purposes. These experiments were conducted in batches of 400 mL of culture per run where airflow was kept at 1 L min^{-1} and the column height was 100 cm. The choice of airflow was based on previous investigations in this work and elsewhere [40].

Injecting methanol from the top (Fig. 4.5) was done with the aid of a separating funnel, mounted at the top of the column. Turning on the tap allowed for methanol to be added to the foamate at a rate of 100 mL min^{-1} depending on the chosen of methanol - culture vol. % (25, 50, or 75). Methanol injection was done once the first foamate reaches the top of the column is about to be collected. Once the right amount of methanol has been injected, the tap on the separating funnel is turned off and the rest of the flotation is allowed to continue in batch foam till the end of the process.

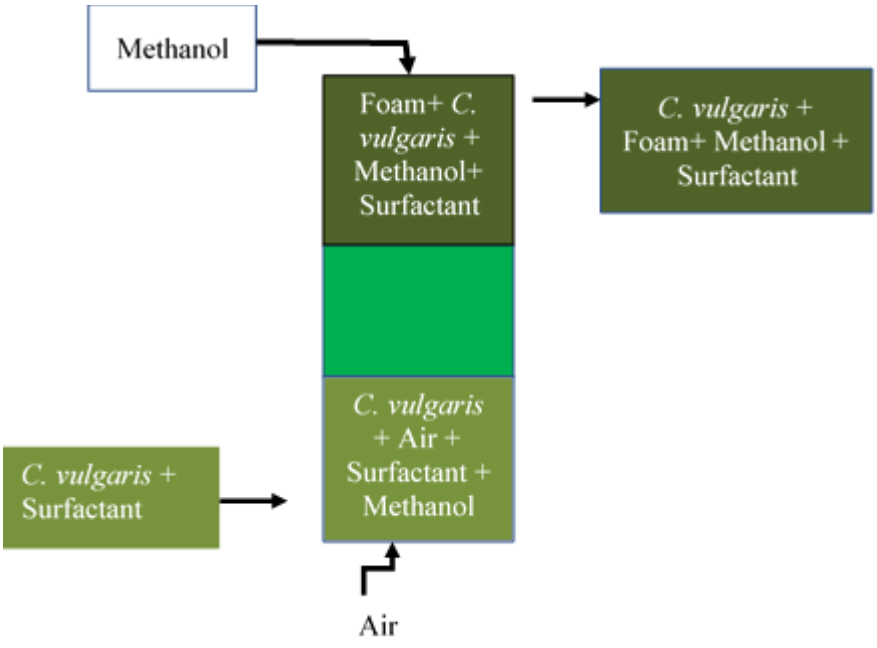

Figure 4.5: Countercurrent recovery of *C. vulgaris* and methanol injection in a batch operated column of 100 cm height; methanol concentration in the feed was varied from 25 to 75 vol. %

at 30-350 mg L^{-1} CTAB, airflow was 1 L min^{-1}, and feed rate was 50 mL min^{-1}

Methanol injection I – cocurrent or countercurrent methanol (using air as a driving tool for methanol in the cocurrent methanol feed process)

1. Batch flotation with water and methanol

Because it is difficult to measure the percentage methanol in a mixture containing algae using refractometry, algae cultures were replaced by water to identify the fate of methanol in the flotation system. For ease of control and better understanding of the role of process parameters, batch operations (Fig. 4.6) were conducted. These batch experiments were based on Minitab composite design of experiments (Table 4.1) to investigate cocurrent and countercurrent methanol injection process. CTAB was added before methanol.

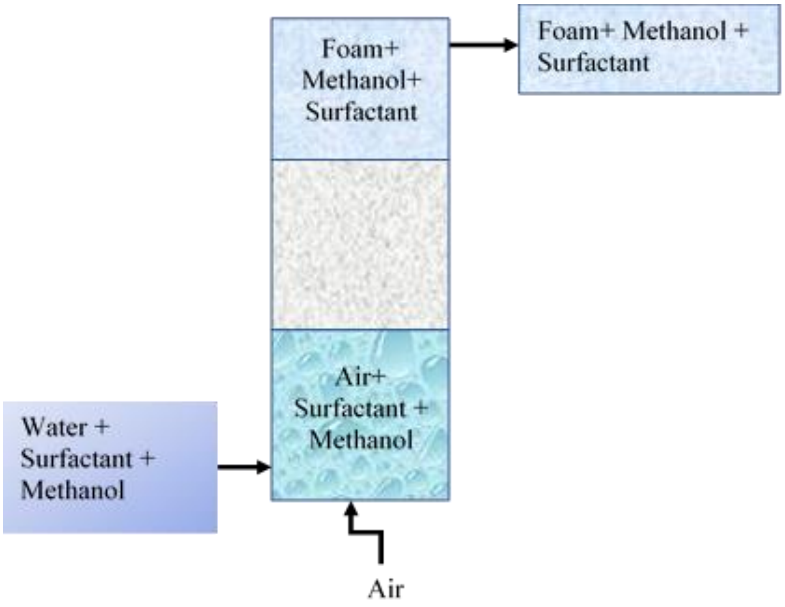

Figure 4.6: Flow diagram for batch flotation of 10 wt. % methanol in water in a cocurrent methanol process; n=2.

Based on the flotation of *C. vulgaris*, foam stability was seen to relied heavily on CTAB concentration. To this end, as high as 400 mg L^{-1} were used, which is not environmentally and economically wise. Therefore, the possibility of reducing CTAB concentrations were investigated using batch operations of cocurrent methanol injection. The concentration of methanol in the feed was also kept at 10 wt. % for economic reasons

and because the impact of methanol concentration of foam stability had already been established. During the process, the role of airflow and column height were also studied.

Although it was intended to use higher airflows to enhance foam stability, being a batch process did not warrant this, as residence time was highly compromised due to the high speed with which the foam travelled. The lack of bottom outlet is mostly responsible for the fast pace of rising foam. Here, and in the following experiments, CTAB concentration is in mg kg^{-1} instead of mg L^{-1}.

Airflow (L min^{-1})	CTAB (mg kg^{-1})	Column height (cm)
0.7	30	90
1.2	30	90
0.7	60	90
1.2	60	90
0.7	45	60
1.2	45	60
0.7	45	120
1.2	45	120
0.95	30	60
0.95	60	60
0.95	30	120
0.95	60	120
0.95	45	90
0.95	45	90
0.95	45	90

Table 4.1: Composite design for batch flotation of 10 wt. % methanol in water in a cocurrent methanol process; n=2

2. Continuous flotation

Continuous flotation has the potential to eliminate the trade-off between recovery efficiency and enrichment than batch and semi-batch flotation [278]. Compared to batch operation, continuous flotation was estimated to cost US$ 0.179 [278], which is less than US$ 0.915 reported for a batch flotation [102]. For these reasons, a set of flotation experiment were conducted in continuous operations (Fig. 4.7). Feed rate and runtime were included in these runs because of the importance of feed rate in a continuous process, and the fact that steady state attainment is a function of time. Therefore, these experiments are also aimed at investigating how long it took to attain steady state flotation. Details of the

½ factorial design using Minitab, is shown in Table 4.2. Being a continuous process also allows for higher airflows (0.7- 2.4 L min-1) compared to 0.7-12. L min-1 that was used in the batch process. The choice of a minimum of 77 g min^{-1} feed rate was based on previous work [40]. The rate of underflow (bottom) rate was adjusted manually to ensure that the liquid pool within the column remans approximately constant at 30 cm above the air chamber. This means that the top and bottom were allowed to vary depending on the airflow, feed flow, column height, runtime, and CTAB concentration. The shortest run time of 15 min was chosen because preliminary tests have revealed that 10 to 12 min was enough for the process to reach steady state during cocurrent methanol flotation. Furthermore, foam stability under the same conditions were attempted based on countercurrent methanol injection. In all the experiments, feed preparation was done by adding CTAB before methanol.

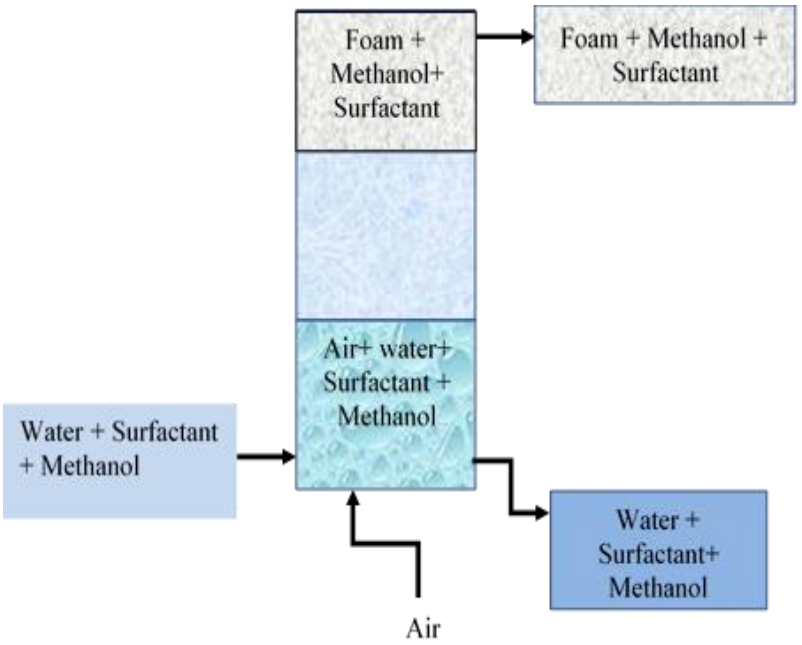

Figure 4.7: Continuous methanol injection in a cocurrent flotation process; Process conditions were varied based on the factorial design in Table 4.2

Airflow ($Lmin^{-1}$)	Feed ($g\ min^{-1}$)	CTAB ($mg\ kg^{-1}$)	Runtime (min)	Column height (cm)
0.7	77	40	15	120
2.4	77	40	15	60
0.7	333	40	15	60

2.4	333	40	15	120
0.7	77	100	15	60
2.4	77	100	15	120
0.7	333	100	15	120
2.4	333	100	15	60
0.7	77	40	45	60
2.4	77	40	45	120
0.7	333	40	45	120
2.4	333	40	45	60
0.7	77	100	45	120
2.4	77	100	45	60
0.7	333	100	45	60
2.4	333	100	45	120
1.55	205	70	30	90
1.55	205	70	30	90

Table 4.2: ½ Factorial design to check the impact of all process parameters on continuous methanol concentration and wt. % in foamate; n=2

Methanol injection II– Countercurrent methanol (replacing separating funnel with methanol distributors in a countercurrent methanol feed process)

Foam stability could not be achieved in the previous batch and continuous flotation when methanol was injected countercurrently, except for when 200 mg L^{-1} CTAB were used during *C. vulgaris* recovery. To this end, it became necessary to device a means by which countercurrent methanol injection can be effectively achieved at CTAB concentrations lower than 200 mg kg^{-1}. Carrying on from cocurrent methanol process, flotations were henceforth conducted in continuous mode. To achieve this purpose, methanol distributors (Fig. 4.10) were fitted in place of a separating funnel, thereby reducing the speed and gravitational impact of oppositely flowing methanol, on rising foam. To achieve this, 26 experiments (13 x 2) were carried out based on a composite design of experiments where distributor holes sizes and CTAB concentration were varied according to Table 4.4. The following experiments were based on composite design as opposed to the factorial design due to the more robust algorithm of the composite design [319]. Column height, feed flow, and the height of the liquid pool were all kept constant at 135 cm, 32 g min^{-1}, and 30 cm, respectively. This means that the top and bottom were allowed to vary depending on the

airflow and CTAB concentration. The choice of a smaller feed rate (32 g min^{-1}) compared to the lowest feed rate of 77 g min^{-1} in previous continuous flotation was borne out of the observation that 32 g min^{-1} federate is capable of supplying enough CTAB, within the chosen concentration range (40 – 60 mg kg^{-1}), needed for foam stability. The schematics of the continuous countercurrent methanol injection process is shown in Fig. 4.8. Before this however, the distributors had to be designed and fabricated.

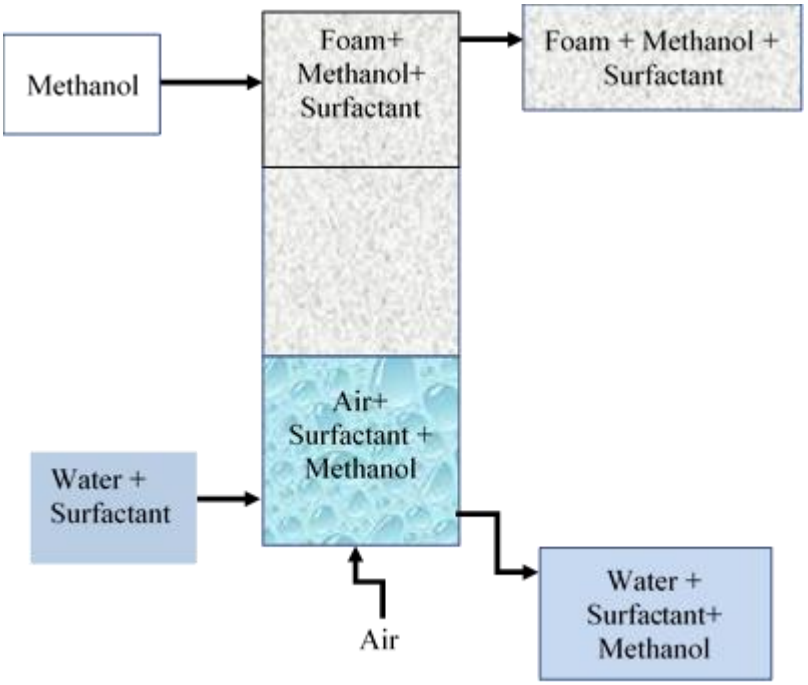

Figure 4.8: : Methanol injection in a countercurrent continuous flotation process; feed rate was 32 g min^{-1}, liquid level was 30 cm, column height was 135 cm, distributor size 0.5 – 3mm, and 40 - 60 mg kg^{-1} CTAB.

4.2.3 Distributor design

It was necessary to design and fabricate distributors that were capable of ensuring that the injection of methanol into the system did not lead to foam collapse. These distributors were made out of transparent plastic resin that is inert to methanol. These 3D – printed distributors were designed using Sketch Up, a licensed graphic design software. The graphic designs were converted to 3D structures with the aid of a Formlabs 3D printer (Fig. 4.9. The form 2 printer is Stereolithography (SLA) compliant, which selectively cures a polymer resin layer-by-layer using an ultraviolet (UV) laser beam. This technology has

very high accuracy in terms of rendering fine details, provides very smooth finish, and is the most cost-effective 3D printing technology.

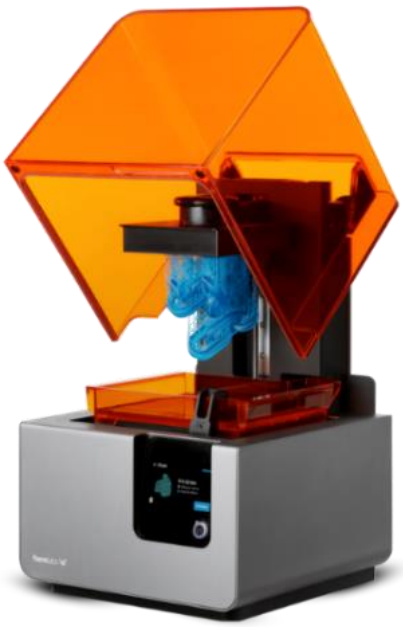

Figure 4.9: Formlabs 3D Desktop printer with Form 2 SLA provisions

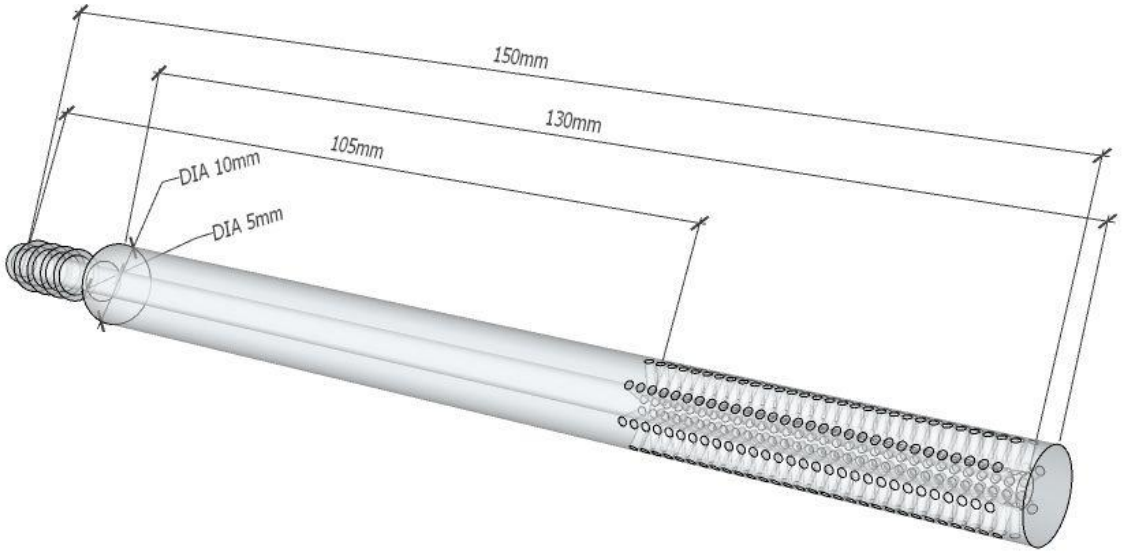

Figure 4.10: Example of methanol distributor (1mm holes)

In order to minimise and control the impact of a countercurrent flow of methanol,

the separating funnel was replaced with distributors (Fig. 4.10). The distributors were fitted with 5 mm X 20 mm grooves to secure the supply hose of equal outer diameter. The external and internal diameters of the distributors were 10 mm and 5 mm respectively. A clearance of 85 cm from the connection groove ensured that methanol did not flow down along the wall of the glass column which could make it slippery, making it difficult for foam to flow upwards along the same streamlines. The diameters of the holes in the distributors were varied from 0.5 mm to 3 mm to determine the hole size or sizes that allows for the best foam stability.

Varying the hole sizes also means that the total area available for flow is varied as following:

- 0.5 mm x 200; 157 mm^2
- 1 mm x 240; 7854 mm^2
- 2 mm x 72; 905 mm^2
- 3 mm x 52; 1470 mm^2

Distributor size (mm)	CTAB concentration (mg Kg^{-1})
1	40
3	40
1	60
3	60
0.5	50
3	50
2	36
2	65
2	50
2	50
2	50
2	50
2	50

Table 4.3: Composite design of experiments for countercurrent methanol stream in a continuous flotation system, feed rate was 32 g min^{-1}, liquid level was 30cm, column height was 120 cm when contraction is involved otherwise it is 135 cm ; n=2

Dynamic Methanol balance - Experimenting with distributors with and without contraction (Estimation of accumulation rate)

Floatation experiments were conducted using 2 mm hole-sized distributors with and

without contraction (Fig. 4.11). Operating conditions were 2 L min^{-1} of airflow, 32 g min^{-1} of feed flow, and column height of 135 cm (120 cm when contraction was attached). Liquid height in the column was maintained at 30 cm, methanol feed rate was varied from 1.5 g min^{-1} to 4.5 g min^{-1}, and CTAB concentration was varied from 100 to 150 mg kg^{-1} of liquid. The objective response was the rate of accumulation of methanol in the column, to be derived through a methanol balance over the flotation column. It was difficult to maintain constant liquid height at high CTAB concentrations and therefore, feed and bottom rates were kept approximately constant throughout (32 g min^{-1} for feed and 16 g min^{-1} for bottom). In order to keep the underflow at 16 g min^{-1}, the tap was calibrated with the aid of the flowmeter that is attached to the tap.

To measure the liquid, holdup, Eqn. 4.6 was used by plotting the pressure profile along the height of the column. Eqn. 4.6 is that of a straight line with slope, $\emptyset_l \rho_l$. Using a density meter ((METLER TOLEDO Japan, Densito 30PX 15/40) ρ_l was recorded for each experiment so that $\emptyset_l$ was calculated. Accumulation rate was estimated between 6 to 7 minutes of flotation, during which the methanol was been fed and this was done very quickly because the rate of accumulation is also changing with time. These measurements were carried out twice and errors were accounted for, based on standard error.

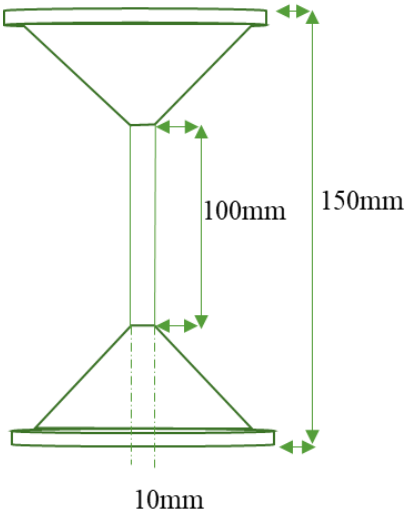

Figure 4.11: Schematics of glass contraction section fitted to increase methanol concentration and reduce accumulation of methanol

Effect of seawater on methanol concentration

Because of the likely difference in foam stability and strength in seawater environment compared to freshwater, flotation experiments were carried out using seawater. The operating conditions (column height of 135cm without contraction, airflow of 2 L min^{-1}, CTAB concentration is 150 mg kg^{-1}, feed flow of 32 g min^{-1}, underflow of 16 g min^{-1}, and methanol flow of 4 g min^{-1}) were chosen for comparison with freshwater. To ensure accuracy, these experiments were done twice.

4.3 Results and discussion

4.3.1 Effect of methanol on surface tension

The effect of methanol and CTAB concentration on the surface tension of a ternary mixture of water-methanol-CTAB is shown in Fig. 4.12. From Fig. 4.12, in agreement with Eqn. 4.1, there is a reduction in surface tension of the mixture with increased CTAB and methanol. This means that the surface excess, i.e. how much of CTAB or methanol is active on the water – air interface is proportional to the concentration of CTAB and methanol. The surface excess in this case depends only on the rate at which the surface tension varies with concentration of CTAB and methanol because constant temperature was maintained. As methanol concentration increased from 0 % to 50 %, there is a reduction in surface tension with respect to each CTAB concentrations. At 60 % methanol and beyond, however, the reduction is surface tension seizes to be a function of CTAB concentration. It is important to note that at CMC of CTAB (360 mg L^{-1}), there should not be further reduction in surface tension caused by CTAB. However, from Fig. 4.12, there is a steady reduction in surface tension, even at 400 mg L^{-1} (beyond the CMC). This further reduction in surface tension can only be possible through the influence of methanol as co-surfactant. Hence, the data suggests that CTAB no longer contributes to lowering of surface tension, once the methanol concentrations had reached 50 wt.%. This results are in agreement with literature [320]. This concentration threshold may also have a strong impact on foam generation and flotation, since foam flotation is dependent on reduction of surface tension in suspension media.

In a methanol-water mixture, molecules of methanol transverse between water surface and the bulk liquid. The hydrophobic CH_3 tail points outwards in a higher proportion than the OH head that lies in the bulk [321] and with increasing methanol, the

amount of water molecules at the surface tends towards zero [247]. The increased presence of methanol at the surface brings about a reduction in the hydrophobicity and adsorption capacity at the water surface [240]. This reduction in hydrophobicity amounts to reduced foaming. Moreover, there is a reduction in H-bond between water molecules due to the presence of methanol [253, 254].

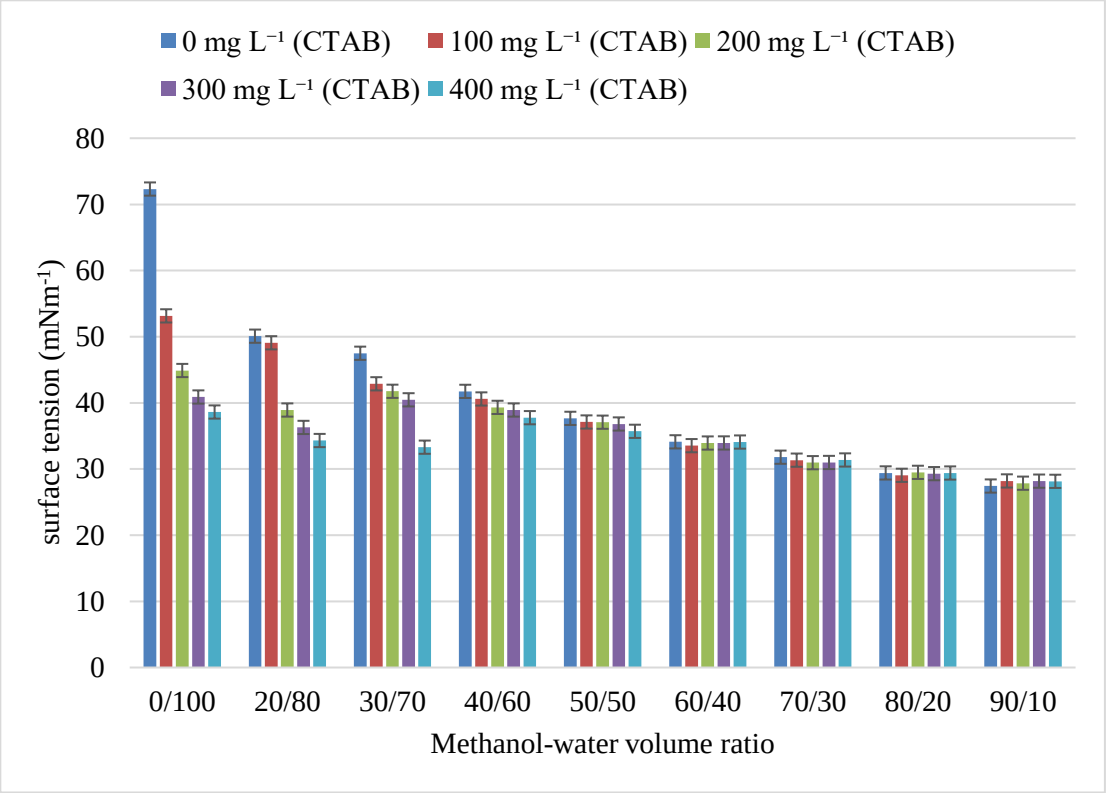

Figure 4.12: Measured surface tension (average ± standard deviation) as a function of volume fraction of methanol in water at different CTAB concentrations; CMC of surfactant is 360 mg L^{-1}

4.3.2 Foam stability and algae recovery as a function CTAB and methanol

From the batch experiments conducted to study the impact of methanol on foam stability and algae recovery, more information was gathered. This information would allow for a better understanding of the practical implication of the surface tension results on the foam flotation of *C. vulgaris*. The results obtained are shown in Table 4.4. The data depicts the impact of methanol and methanol mixing sequence on foam stability. It also highlights the role of flow types (cocurrent or countercurrent) on the stability of foam.

At 75% methanol concentration, no stable foam was generated, irrespective of methanol injection type (cocurrent or countercurrent), even as CTAB was increased beyond the CMC of CTAB (360 mg L^{-1}) to 500 mg L^{-1}. The relationship between methanol concentration and CMC of CTAB in water-methanol mixture is such that, at 60 % methanol, micelles no longer form [322]. This, and the surface tension results in Fig. 4.12, explains why stable foams could not be achieved at 75%. There is also the dependence of foaming on hydrophobicity, which decreases with increased methanol [240].

% Meth	30 mgL^{-1} (CTAB)	40 mgL^{-1} (CTAB)	50 mgL^{-1} (CTAB)	70 mgL^{-1} (CTAB)	80 mgL^{-1} (CTAB)	100 mgL^{-1} (CTAB)	150 mgL^{-1} (CTAB)	200 mgL^{-1} (CTAB)	>360 mgL^{-1} (CTAB)
25A	NS	NS	NS	NS	NS	NS	NS	S	S
25B	NS	NS	NS	S	S	S	S	S	S
25B*	S	S	S	S	S	S	S	S	S
50A	NS	NS	NS	NS	NS	NS	NS	S	S
50B	NS	NS	NS	NS	NS	S	S	S	S
50B*	NS	NS	NS	S	S	S	S	S	S
75A	NS	NS	NS	NS	NS	NS	NS	NS	NS
75B	NS	NS	NS	NS	NS	NS	NS	NS	NS
75B*	NS	NS	NS	NS	NS	NS	NS	NS	NS

Table 4.4: Summary of results of foam flotation harvesting of *C. vulgaris* in the presence of methanol; S and NS stand for stable and nonstable foams respectively: Airflow was 1 L $min^{-1}$and the column height was 100 cm. CMC of CTAB is 360 mg L^{-1}

[A] Adding pure methanol from the top as a separate feed

[B] Adding methanol to culture before the addition of CTAB and fed from bottom

[B*] First mixing CTAB with culture for a while before adding methanol and fed from bottom.

From Table 4.4, when methanol concentration in *C. vulgaris* culture was 50 vol. %, stable foams were generated both in cocurrent and countercurrent methanol injection processes. When CTAB was added to the culture prior to methanol, 70 mg L^{-1} of CTAB was enough to generate stable foams whereas, 100 mg L^{-1} of CTAB was needed to generate stable foams when methanol was added prior to CTAB. These results, in line with Fig. 4.12 and the literature [240, 321], confirms that at 50 vol. % methanol concentration, *C. vulgaris* can be harvested by foam flotation. The role of mixing sequence can be explained in terms of the decrease in hydrophobicity with increased methanol due to steric configuration of water-methanol modules [320]. Similar role is seen to have been played by methanol when methanol concentration was 25 vol. % of *C. vulgaris* culture. However,

when 25 vol. % methanol was involved, less CTAB (30 mg L^{-1}) were needed when CTAB was added first and 70 mg L^{-1} when methanol was added first. In terms of methanol injection type, 200 mg L^{-1} of CTAB was enough to generate stable foams in both cocurrent and countercurrent methanol injection processes, for both 25 vol. % and 50 vol. % methanol in *C. vulgaris*. Indeed, these results are good indications of foam stability but do not necessarily translate to economic and useful methanol supply in the foamate.

In addition to testing for stability, *C. vulgaris* harvesting was investigated. Based on batch flotation conducted with, 1 L min^{-1} airflow, 50 vol. % methanol, 100 cm column height, 400 mL of feed, and 300 mg L^{-1} CTAB, 94 % of cells were recovered at a concentration factor of 18.3. The moisture content (water and methanol) was 156 wt. % more than the cells but no cell lysis was observed and even if there was cell lysis, it is not clear whether or not the methanol in the mix is strong enough to extract, and/or react with, algal oil to produce biodiesel via transesterification. Nevertheless, 50 vol. % methanol is unsustainable. Besides, the aim of this research is to convert marine microalgae to biodiesel.

One of the objectives of this research is to combine the cell lysing capacity of CTAB with the solvent extraction and chemical reaction of methanol with algal oil to produce biodiesel in the flotation column. This however, needs to be achieved within the confines of good economics, of which 25 wt. % methanol does not satisfy. Hence, the need to reduce methanol percentage below 25 %.

4.3.3 Methanol injection in foam flotation – quantitative and qualitative analysis

The use of water as substitute for algae culture became necessary in order to easily measure the quality and quantity of methanol, particularly in the foamate. the process, considering that refractometry was used to quantify methanol composition.

Henceforth, the unit of mg kg^{-1} is used for CTAB concentration as opposed to mg L^{-1} because there is minimum in the partial molar volume of methanol in the water-methanol mix, attributed partially to the hydrophobic CH_3 and the molecular rearrangements [305]. This simply means that adding 80 mL of water to 20 mL is going to be less than 100 mL (96 mL) of mixture due to negative excess volume [323-325], so the above measures were taken to correct that.

Results from these experiments are presented in Figures 4.13 and 4.14 (for cocurrent batch processes where methanol concentration in the feed was 10 wt. %) and 4.15 – 4.26 (for continuous cocurrent and countercurrent methanol process where 99.8% methanol was fed to the top during countercurrent flotation).

Batch flotation

Figures 4.13 and 4.14 represents the response of percentage and mass respectively of methanol, to changes in CTAB concentration (mg L^{-1}), airflow (L min^{-1}), and column height (cm), based on batch operations. In line with the flotation of *C. vulgaris*, 30 mg L^{-1} of CTAB was able to generate stable foams during cocurrent methanol process. However, no stable foams were generated during countercurrent process, although much lesser methanol (10 %) are now involved. The reduction in methanol concentration has also made it possible for smaller CTAB concentrations (30 - 60 mg kg^{-1}) to generate stable foams during cocurrent flotation, compared to as high 200 mg kg^{-1} used in the previous experiments where the minimum methanol concentration was 25 %.

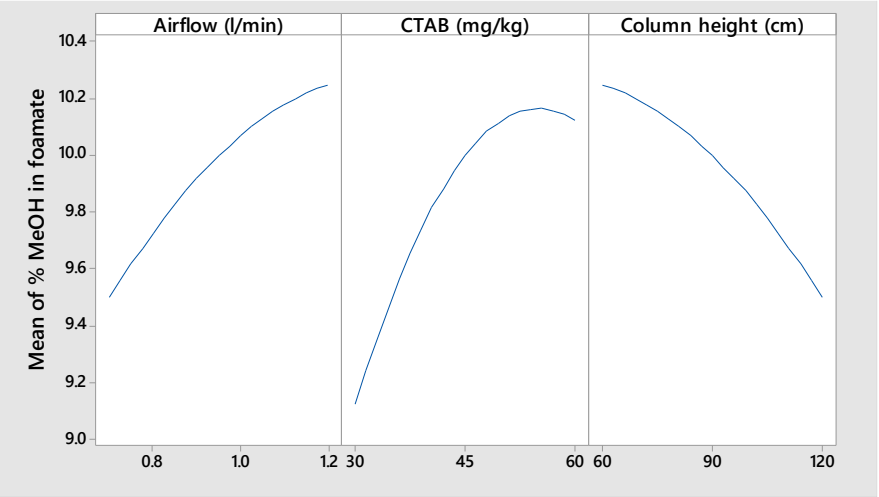

Figure 4.13: Main and interaction effects of major process parameters on the percentage of methanol in the foamate during batch flotation of 10 wt. %; n=2, R^2=0.97

Airflow and CTAB had positive relationship with concentration and mass of methanol while column height affects concentration and mass of methanol in the foamate negatively (Fig. 4.13 and Fig. 4.14). This is because, contrary to CTAB concentration and airflow, foam drainage increases with column height, which leads to less amount of methanol in the foamate. Airflow and CTAB are both drivers of foam stability due to increased rate of bubbles formation and hence the positive impact they both have on

methanol mass and concentration. Increase in CTAB results in smaller bubbles as a result of reduced surface tension, and wetter foams results [40, 102, 298], which means more methanol in the foamate. The range in methanol concentration is small compared to the mass methanol because methanol enrichment is difficult due to intermolecular arrangement between water and methanol. For the same reason, the high positive impact of CTAB and airflow on foam generation, is reflected in the mass of methanol in the foamate as CTAB concentration and airflow increased. The mass of methanol in the foamate increases with time (until the end of flotation), hence the wider range in mass of methanol in the foamate, compared to the concentration. Also, the time taken for foams to become stable, depends on column height. The longer the column height the longer it takes for foam to stabilise and therefore, the higher the chances of foam drainage due to disconnected foams.

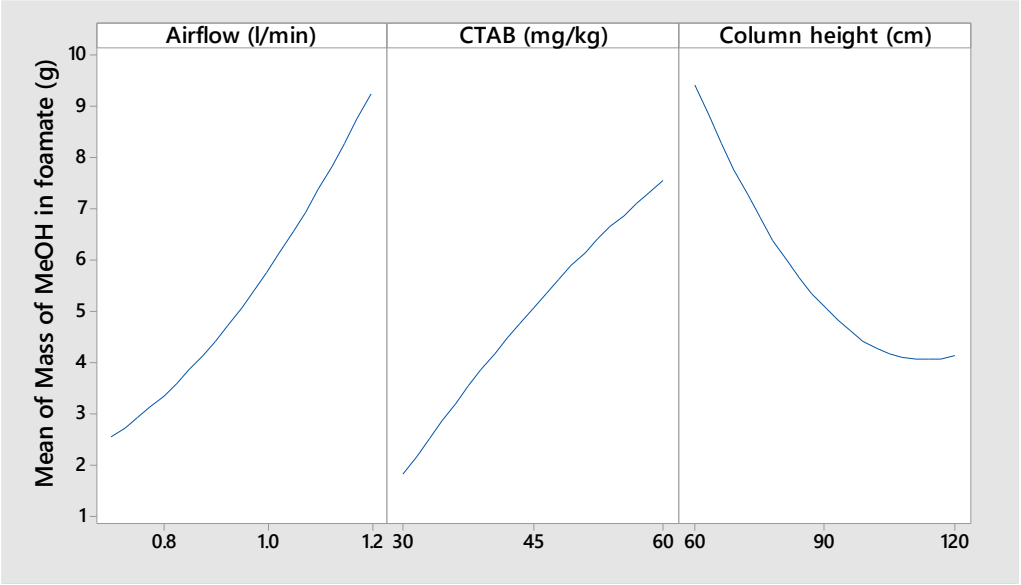

Figure 4.14: Main effects of major process parameters on the mass (g) of methanol in the foamate during batch flotation of 10 wt. % methanol; n=2, R^2=0.99

The combination of increase in CTAB and increase in airflow has positive impact on the mass of methanol in the foamate (Fig. 4.15). Combination of increase in CTAB or increase in airflow with increase in column height, affects the mass of methanol in the foamate negatively. When increase in CTAB or increase in airflow is combined with increased column height, there is a reduction in mass of methanol in the foamate. This is due to the high foam drainage that is associated with high column height. Therefore, very tall columns should be avoided in order to achieve high amount of methanol in the foamate.

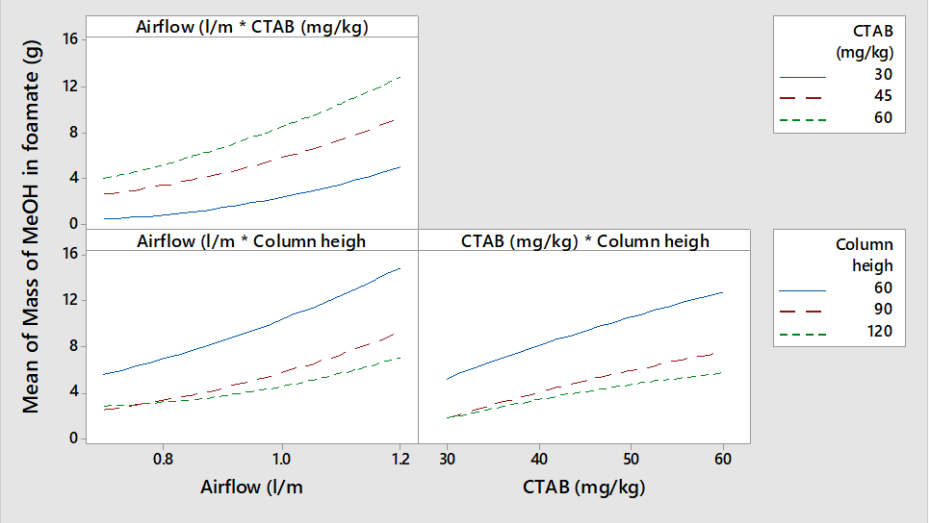

Figure 4.15: Interaction effects of major process parameters on the mass (g) of methanol in the foamate during batch flotation of 10 wt. % methanol; n=2, R^2=0.99

Similar to the main effects, within the operating conditions, the interactions (Fig. 4.16) between CTAB and airflow, airflow and column height, and CTAB and column height, did not show meaningful changes in the concentration of methanol in the foamate. As explained before, this is due to the difficulty of achieving methanol enrichment within the operating conditions.

If for example, the CTAB concentration was kept at 60 mg kg^{-1}, the increase in airflow does not cause any increase in the percentage of methanol beyond the original concentration of 10 %. It should be noted, also, that the range in methanol concentration is very short and hence, within the operating conditions, methanol enrichment is not possible. To achieve the maximum methanol concentration of 10 %, in the foamate when CTAB concentration is kept at 45 mg kg^{-1} of liquid, airflow needs to increase from 0.8 L min^{-1} to 1.2 L min^{-1}. At 30 mg kg^{-1} of CTAB, however, more than 1.2 L min^{-1} of air would be needed. Considering the positive impact of column height on particle enrichment and the fact that increased column height does not necessarily reduce methanol concentration, it might not be necessary to reduce column height on the basis of methanol enrichment.

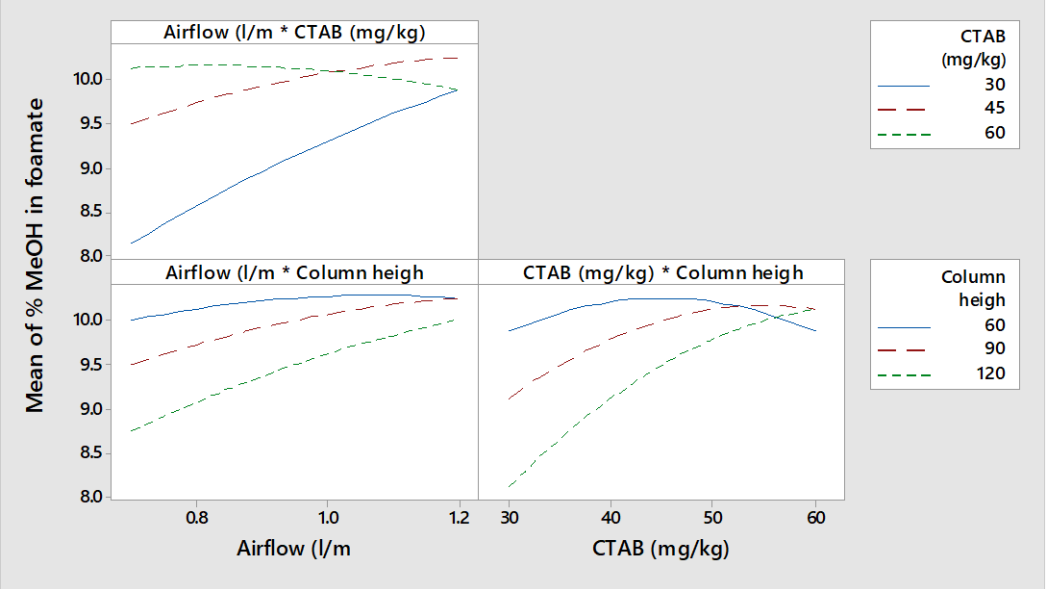

Figure 4.16: Main and interaction effects of major process parameters on the percentage of methanol in the foamate during batch flotation of 10 wt. %; n=2, R^2=0.97

Continuous flotation

Stable foams were generated when continuous flotation was carried out using cocurrent methanol injection strategy, according to results in Fig. 4.17 – 4.20. However, when methanol injection was done countercurrently, foam collapses.

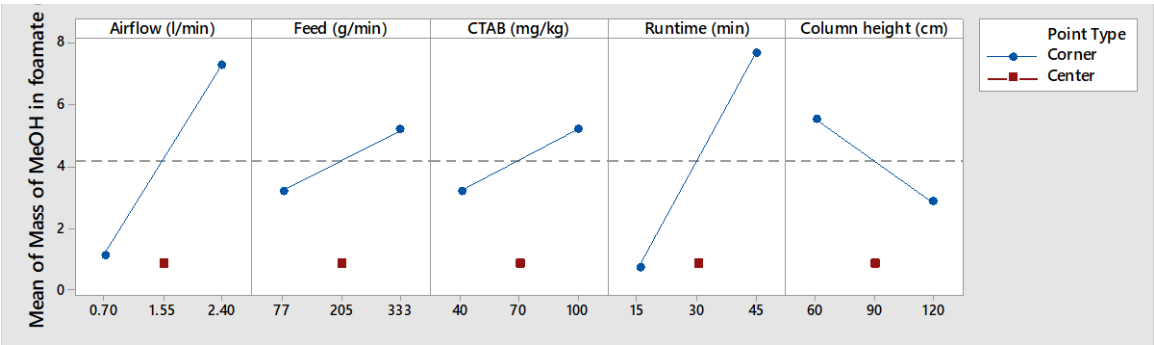

Figure 4.17: Main effects of some major process parameters on the mass of methanol in the foamate during a continuous flotation of 10 wt. % methanol feed; airflow (0.7- 2.4 L min^{-1}), feed (77-333 g min^{-1}), CTAB (40- 100 mg kg^{-1}), runtime (15 - 45 min), and column height (60 -120 cm), n=2, R^2= 1.

Just as in the case of batch flotation, the range of methanol mass is higher than that of methanol concentration (Fig. 4.17 and Fig. 4.18). The results also support the argument that the comparatively larger range in mass of methanol was because mass of methanol in

the foamate was cumulative over time, as opposed to the concentration.

Of the five parameters investigated, only column height had a negative impact on the mass of methanol in the foamate (Fig. 4.17). As earlier explained, this is due to higher amount of drainage as column height increases. The range of methanol mass as a result of CTAB concentration and feed flow is short but the average is as good as airflow and runtime. This is because the feed flow is high enough to supply enough CTAB at a given time and so increase CTAB concentration at this high feed rates, does not make much difference. Therefore, feedflow should be reduced if other process conditions are to remain within the current range. This is to allow for higher residence time of particles which would guarantee better bubble – particle attachment and collision. The highest quantity of 19 g methanol in the foamate was obtained under the following conditions: 2.4 L min^{-1} airflow, 77 g min^{-1} feed flow, 100 mg kg^{-1} CTAB, 45 min runtime, and column height of 60 cm at a corresponding concentration of 10%. Airflow and runtime on the other hand, had a wider range of methanol mass in the foamate. This is because unlike feedflow and CTAB, airflow and runtime are not complementary and individually, they impact positively on foam quantity which is directly linked with methanol quantity, since foam was generated from a given ratio of water to methanol. And as seen from the methanol concentration results, there is no much variation from the original 10 – 90 methanol – water ratio. The plot for the impact of column height on the mass of methanol in continuous process is less steep than it was in batch. This is because there is an underflow in continuous process which reduces the flow rate of the foam and hence reduces foam drainage. Keeping the airflow and runtime within the set ranges is therefore recommended.

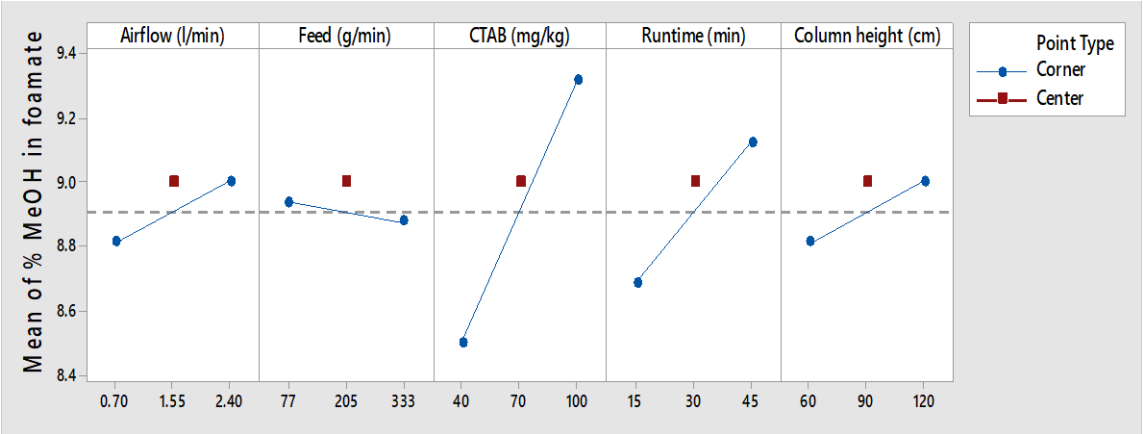

Figure 4.18: Main effects of major process parameters on the percentage of methanol in

the foamate during a continuous flotation of 10 wt. % methanol feed; airflow (0.7- 2.4 L min^{-1}), feed (77-333 g min^{-1}), CTAB (40- 100 mg kg^{-1}), runtime (15- 45 min), and column height (60 -120 cm), n=2, R^2=0.99

From Fig. 4.18, except for CTAB concentration and runtime, concentration of methanol in the foamate had shown very little response to the other three parameters, averaging 8.7 and 9.1 % methanol. The data in figures 4.18 and 4.19 indicates that the average concentration of methanol obtainable from the foamate is 9 %. This level of methanol concentration does not satisfy the objective of this work. The reaction of methanol mass and concentration to feed flow and column height is in line with the trade-off that has been established between recovery and concentration factor [277, 278].

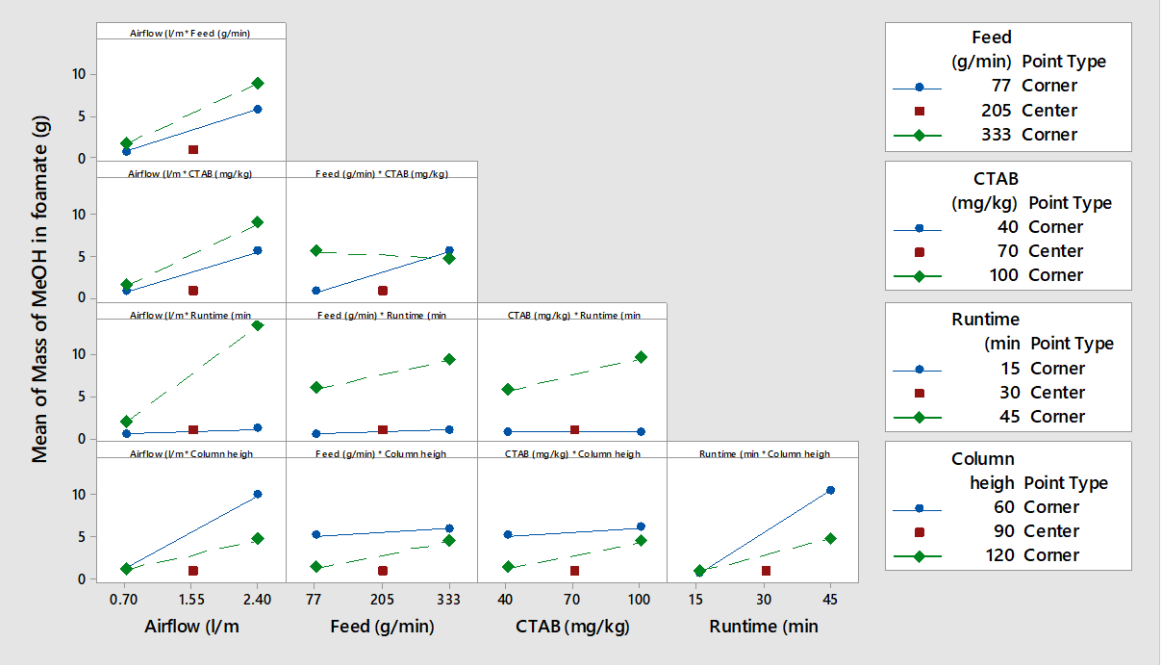

Figure 4.19: Interaction effects of major process parameters on the mass (g) of methanol in the foamate during a continuous flotation of 10 wt. % methanol feed; n=2, R^2=1

From Fig. 4.19, looking at the interactions between airflow, feedflow, and CTAB concentration, with runtime, it is not surprising that the longer the duration of flotation, the more methanol by mass is found in the foamate. Irrespective of airflow, feedflow and CTAB concentration, runtime of 15 min allows only about 1 g of methanol into the foamate. This translates to a foamate rate of 0.07 g min^{-1}, irrespective of federate (77 or 333 g min^{-1}), or CTAB concentration (40 or 100 mg kg^{-1}). The rate of foamate can however rise to as high as 0.3 g min^{-1} if airflow was increased from 0.7 L min^{-1} to 2.4 L min^{-1}, if flotation was allowed to run for 45 min. This is partly because it took between 10 to 12

min for steady state flotation to commence and the higher the airflow, the higher the foam's velocity and hence quantity of foam because a function of time. Similarly, irrespective of feedflow (77 or 333 g min-1) and CTAB (40 or 100 mg kg $^{-1}$), about 5 g of methanol can be found in the foamate as long as the column height is maintained at 60 cm. In order to have similar amount of methanol in the foamate when the column height was 120 cm, feedflow, airflow, CTAB concentrations, and runtime, have to be highest at 333 g min^{-1}, 2.4 L min^{-1}, 100 mg kg^{-1}, and 45 min, respectively. Higher amount (up to 10 g) of methanol can be found in the foamate if column height was kept at 60 cm while airflow and runtime were both highest at 2.4 L min^{-1} and 45 min, respectively. This is because more foams are collected within a shorter time when the column is short. This is however, not the best way to achieve particle enrichment. Therefore, in order to compromise CF, it is wiser to increase airflow and runtime, depending on how much methanol is intended in the foamate. Nonetheless, if 2 L of culture is to be harvested for biodiesel conversion, 5 g of methanol is rather too large.

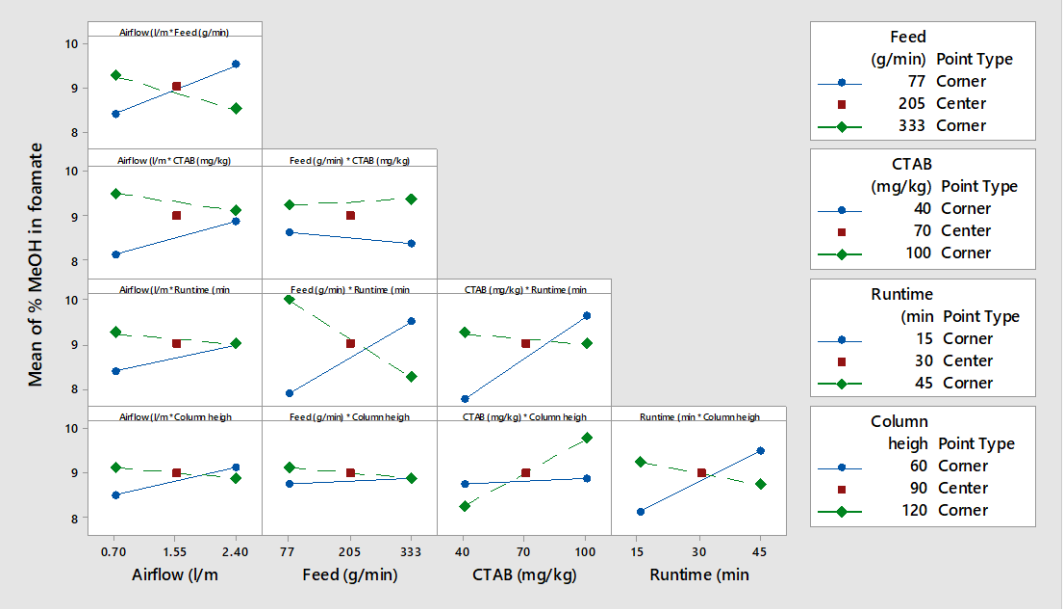

Figure 4.20: Interaction effects of major process parameters on the percentage of methanol in the foamate during a continuous flotation of 10 wt. % methanol feed; n=2, R^2=0.99

From Fig. 4.20, it is obvious that even with combined influence of process parameters, it is not possible to achieve methanol enrichment. Although the combination of airflow and runtime was seen to increase the mass of methanol in the foamate, the

combination of these two parameters had an opposite impact on methanol concentration. Other combinations with negative impacts on methanol concentration, involving these two parameters include: increased air flow and feedflow, increased airflow and CTAB concentration, increased feedflow and runtime, and increased column height and runtime. This is due to the tendency of methanol to evaporate at high airflow and over time.

During unsteady state, the foam is less stable and therefore more methanol and water drainage occurs. The volatility of methanol also surface activity of methanol also means that they are likely to evaporate. Fig. 4.19 also show that when CTAB becomes as high as 80 mg kg^{-1}, percentage methanol reduces from around 10 % to below 9 % as airflow increased, which is essentially an indication that even though independently, they promote increased percentage of methanol at the top, combined, airflow and CTAB concentration increase are detrimental to the concentration of methanol. Overall, there was no significant change in percentage methanol.

Even though the mass of methanol at the top could reach as high 16 g, which is far more than the stoichiometric amount needed to react with the approximately 0.34 g of oil in 2 g of algae (1 g L^{-1}) based on 2 L of water being treated, being in association with over 80 g of water, leaves the methanol very weak and may not be functional as a reactant or even a solvent for oil extraction, as the methanol concentration needs to be 50 % or more [295]. Besides, over 80 % of the methanol supplied per litre of liquids, ends up in the bottom product and require extra energy to recover. The only way to supply methanol effectively through the cocurrent process is to increase the methanol concentration in the feed to 50 %, which is not economical. In essence, these results are still yet to meet the objective of this research to concentrate most, if not all of the methanol in the system at the top where it is required for eventual transesterification of algal oil to biodiesel. Therefore, it is economically wiser to supply methanol from the top because it does not only guarantee better concentration methanol in the foamate, but it also allows for supply of methanol according to need. However, this requires extra measures since the use of a separating funnel failed to deliver the required performance.

It is worthy of note that the small drop in the percentage of methanol in the foamate is not an indication of methanol accumulation. Rather, it could have been due to the loss of methanol to the atmosphere due to methanol's high volatility. There is also the fact that methanol purity was 99.8 % and not 100 % but this is however corrected based on the

calibration curve that was drawn. However, the calibration curves were not based on fractional percentages so it is possible for such little percentages to be unaccounted for especially at the bottom where the ratio of water to methanol mass is much greater than at the top. Nevertheless, there is no indication of the achieving high enough methanol in the foamate using the batch cocurrent flotation, bearing in mind also that countercurrent flotation could not guarantee the first criteria, which is foam stability.

Because the best way to improve the quality of methanol in the foamate is to inject methanol countercurrently, the desired methanol concentration in the foamate without using quantity of the need to achieve stronger methanol at the top using as little methanol as possible, modification of the process was needed.

4.3.4 Improved methanol enrichment using distributors (countercurrent flotation)

When methanol was supplied to the top of the column using a separating funnel, foam stability was not achieved. The results so far obtained from the cocurrent methanol feed process has shown that even though there is high enough quantity of methanol in the foamate the quality (concentrations) of methanol in the foamate is not good enough to achieve transesterification. In order to qualitatively and quantitatively improve on the methanol in the foamate, it was necessary to modify the countercurrent methanol injection scheme. To this end, methanol distributors were used to supply methanol. During cocurrent batch and continuous flotation, there was no methanol accumulation but that was not the case when methanol injection was done countercurrently. The lack of foam stability is in itself an indication of methanol being accumulated during countercurrent methanol flotation. Therefore, countercurrent methanol flotation proceeds under unsteady state conditions. If, however, enough time (10 – 12 min) was allowed after the stoppage of methanol stream, steady state flow is again reached, where methanol accumulation returns to zero.

Flow velocity is indirectly proportional to flow area and therefore it should be expected that the higher the area available for flow, the lower the velocity of methanol in the downwards direction, and hence the less the impact of methanol on the upwards flow of foam. and hence the less the impact on the upwards flow of foam. In order to understand how the area of flow affects the stability of foam, experiments were conducted based on Table 4.3. These experiments were conducted at a constant methanol flow rate of 1.5 g

min^{-1}, airflow of 2.4 L min^{-1}, liquid height of 30 cm and a column height of 135 cm. When contractions (Fig. 4.11) were attached, the total column height was 120 cm. The results shown in Fig 4.21 – Fig 4.26 represents how the change in distributor size and CTAB concentrations had affected the mass and concentration of methanol in the foamate during countercurrent methanol injection.

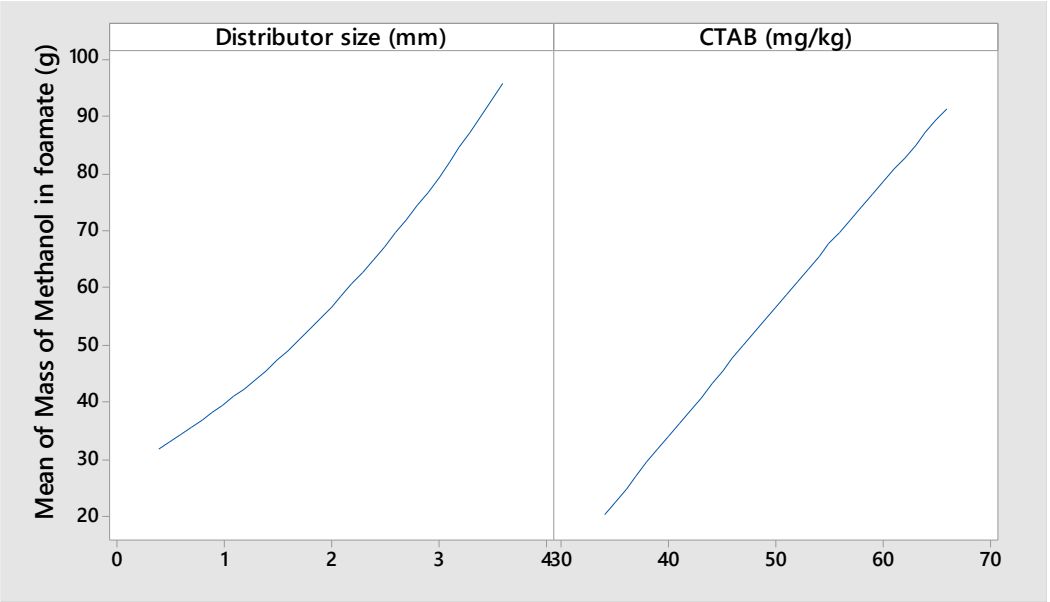

Figure 4.21: Plots of main effects of process parameters on mass of methanol (g) at the top during the continuous flotation using methanol distributors at 1.5 g min^{-1}, airflow of 2.4 L min^{-1}, liquid height of 30cm and a column height of 135cm; R^2=98.7, n=2

In Fig. 4.21, the vertical axis represents the mass of methanol in the foamate while distributor size and CTAB are in the horizontal axes. The diagram shows that there was an increase in the mass of methanol in the foamate as both CTAB concentration and distributor size increased.

From Fig. 4.22, the combined effect of CTAB increase and increase in distributor size lead to a significant increase in the amount of methanol in the foamate. This is because increased CTAB concentration ensured that more bubbles are generated and hence more stable foams are generated. The more stable the foam, the less likely they are the bubbles to be collapsed by the countercurrent methanol. Similarly, the smaller the size of holes in the distributor, the greater the speed with which they inject methanol, which increases the tendency of methanol to be carried upwards by the foam.

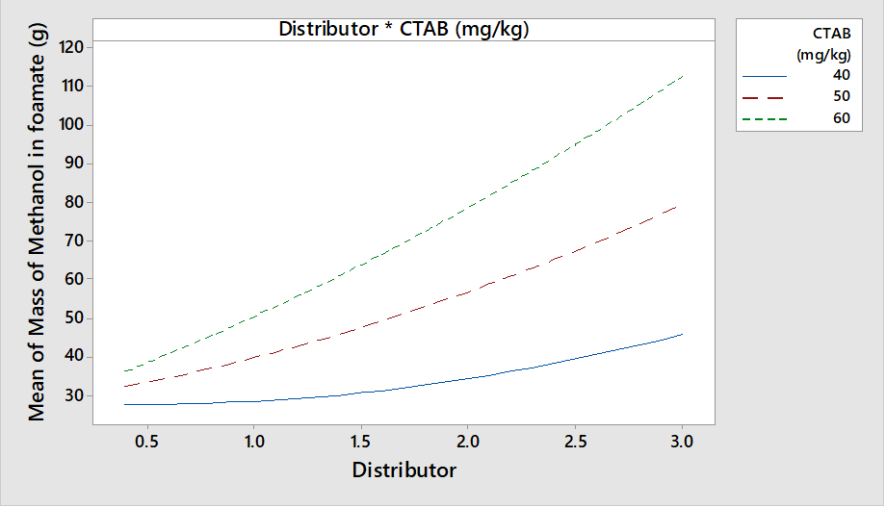

Figure 4.22: Plots of interaction between process parameters on mass (g) of methanol at the top during the continuous flotation using methanol distributors at 1.5 g min^{-1}, airflow of 2.4 L min^{-1}, liquid height of 30cm and a column height of 135cm; R^2=98.7, n=2

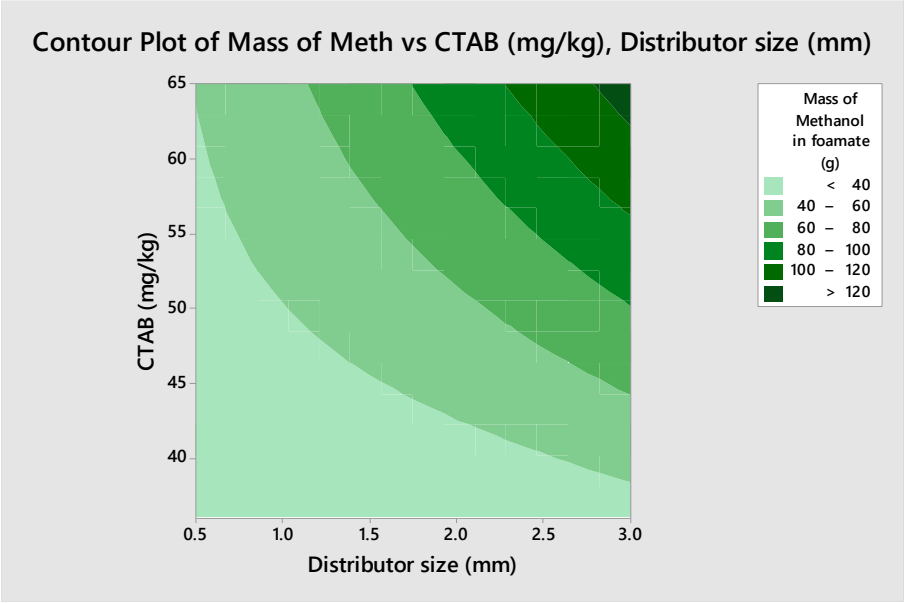

Figure 4.23: Mass of methanol as a function of CTAB concentration and distributor size during continuous flotation using methanol distributors at 1.5 g min^{-1}, airflow of 2.4 L min^{-1}, liquid height of 30 cm and a column height of 135 cm; R^2=98.7, n=2

Fig. 4.23 presents a clearer picture of how the mass of methanol in the foamate is affected by CTAB and distributor size. High CTAB concentration also results is smaller bubbles that are capable to coalesce with methanol without collapsing.

The impact of CTAB concentration and distributor size on the concentration of methanol in the foamate is shown in Fig. 4.24. Both CTAB concentration and distributor

size had positive impacts on the concentration of methanol inn the foamate. There is a greater response as a result of increased distributor size than CTAB concentration. This is because more methanol is injected with respect to foamate. While the rate of methanol injection is controlled by the distributor size, the rate of foamate is controlled by more factors than CTAB concentration. As seen earlier, feed flow and airflow are equally responsible for how much foam is being generated. Since feed flow and airflow are both kept constant, CTAB increase alone was not able to produce foam at the same rate as methanol. However, this is good for the process, because the stronger the stronger is the methanol in the foamate, the better for the intended purpose of achieving transesterification. Overall, the lowest percentage methanol in the foamate was 70 %. This implies that, under the operating conditions, all the distributors are capable of delivering the minimum concentration of methanol required in the process. Also, there is room for using as low as 40 mg kg^{-1} CTAB and still be able to convert algal oil to biodiesel with the methanol in the foamate.

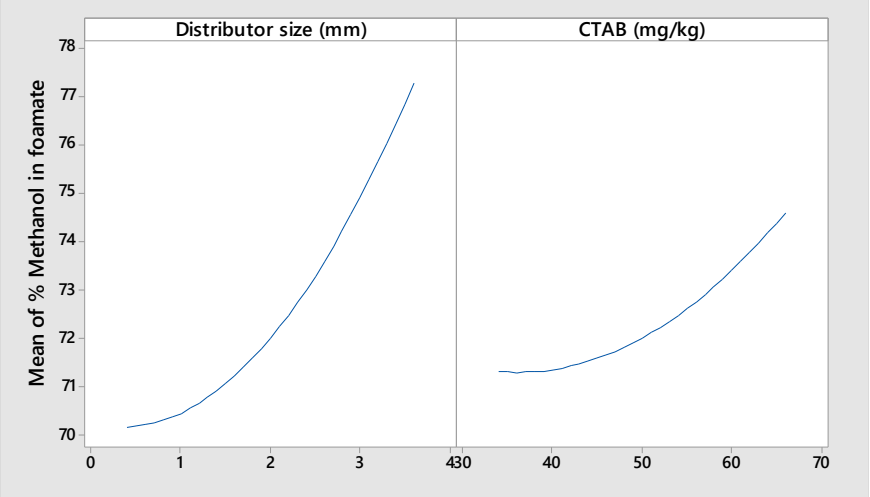

Figure 4.24: Plots of main process parameters on percentage of methanol at the top during the continuous flotation using methanol distributors at 1.5 g min^{-1}, airflow of 2.4 L min^{-1}, liquid height of 30 cm and a column height of 135 cm ; R^2=98.3, n=2

Combined, increased CTAB concentration and distributors size, had positive impact on the concentration of methanol at the top (Fig. 4.25). This is a confirmation of their individual impacts as seen in Fig. 4.24.

Compared to the cocurrent methanol processes, there has been a considerable improvement in the mass and concentration of methanol in the foamate. In particular,

having as high as 76 % in the foamate is in line with the objective of this work. It is therefore, believed that this level of methanol strength will lead to oil extraction as well as transesterification.

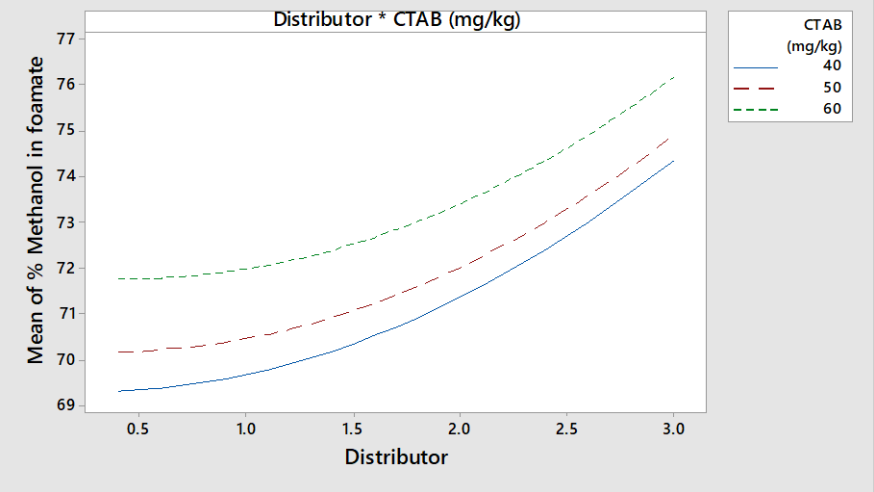

Figure 4.25: Plots of interaction between process parameters on percentage of methanol at the top during the continuous flotation using methanol distributors at 1.5 g min^{-1}, airflow of 2.4 L min^{-1}, liquid height of 30 cm and a column height of 135 cm; R^2=98.3, n=2

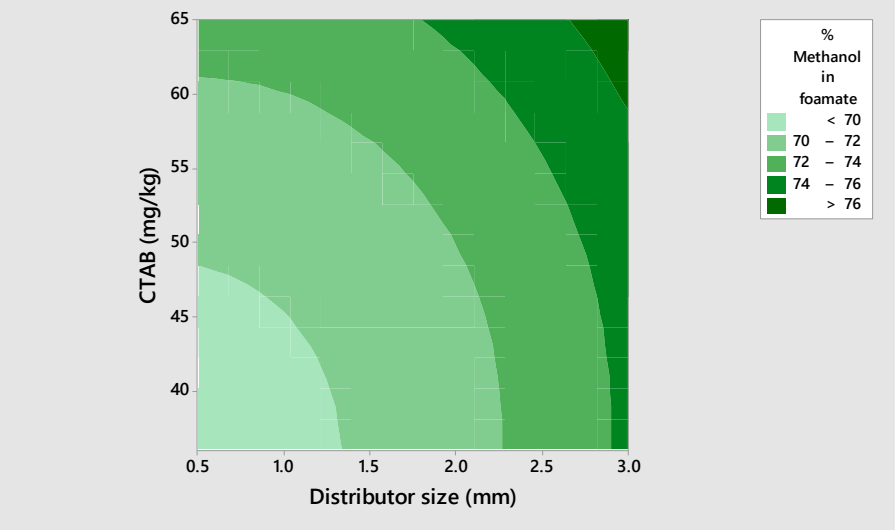

Figure 4.26: Contour plots of the effect CTAB concentration and distributor sizes on percentage of methanol at the top during the continuous flotation using methanol distributors at 1.5 g min^{-1}, airflow of 2.4 L min^{-1}, liquid height of 30 cm and a column height of 135 cm ; R^2=98.3, n=2

With distributors, it was not only possible to increase foam stability, it also allowed for a reduction of feed flow from around 75 g min^{-1} to 32 g min^{-1} which translated to higher residence time and foam drainage which lead to the observed increase in methanol

concentration.

Bubbles generated from seawater behave differently from those generated from freshwater. While comparatively smaller bubbles are synonymous with seawater, larger bubbles tend to form from freshwater. The major contributor to smaller bubbles in seawater is the higher ionic concentration [326-329] due to salt and other metallic ions. Smaller bubbles have a higher tendency to coalesce than larger ones, without collapsing. The lower the chances of foam collapse, the more stable and durable are the foam. The less likely it is for bubbles to coalesce, the higher the rate of accumulation when methanol is fed countercurrently. In order to test this theory, freshwater and seawater flotations were conducted at 4 g min^{-1} methanol injection using the 3 mm sized distributor, 2.4 L min^{-1} of air and 100 mg kg^{-1} of CTAB. As expected, there was a higher foam stability in seawater and hence the ability to hold methanol for a comparatively longer time. While the seawater flotation withstood methanol injection for 17 min, the freshwater flotation lasted 16 min. During seawater flotation, 94 % of the methanol injected was collected in the foamate while 55 % was collected during freshwater flotation. This translates to methanol accumulation of 0.24 g min^{-1} in seawater as opposed to 1.81 g min^{-1} in freshwater. This also meant that methanol was more easily concentrated at the top under seawater conditions, which is also responsible for the lower accumulation rates. Although the same amount of feed was involved at the same feed and bottom rates, the seawater flotation lasted an entire period of 40 min while the freshwater lasted for 30 min. This is an indication that not only higher methanol concentration is possible with seawater, higher CF of particles are equally possible due to the slower foam velocity, which translates to foam drainage.

4.3.5 Methanol balance- effect of contractions on accumulation rate of methanol

Having successfully achieved the minimum level of methanol concentration required in the foamate, it was necessary to estimate the rate of accumulation of methanol as not all the methanol that was supplied during the process is accounted for in the foamate, even when contraction sections were attached. The addition of a foam riser close to the column top was to reduce accumulation rate as well as increase foam drainage and, by extension, algae and methanol concentration.

An example of pressure profile along the column is represented by Fig 4.27 below. The pressure profiles were used to estimate the liquid hold-up within the column during a given time. The rate of accumulation a s a function of time was then estimated based on the liquid holdup, according to Eqn. 4.6. The resulting value of hold-up was then used to calculate the rate of accumulation of methanol. The experimental conditions described are shown in Tables 4.5 and 4.6 for the non-constricted and constricted column units, respectively.

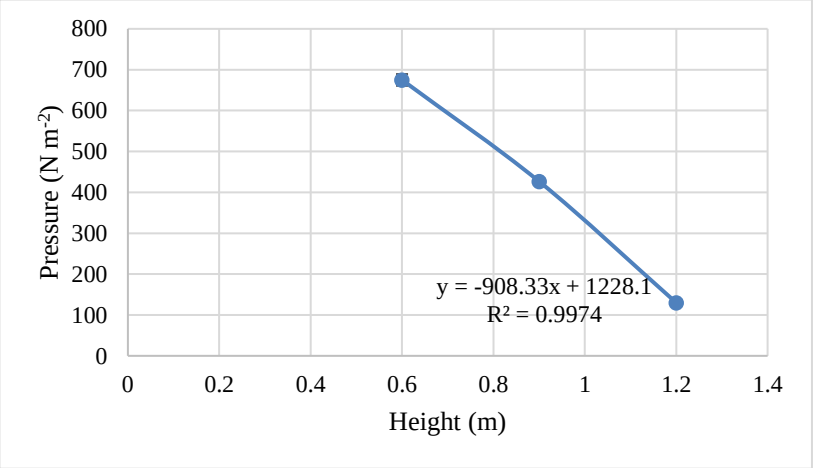

Figure 4.27: Example of a pressure profile measured at 2 L min^{-1} air; 4.5 g min^{-1} methanol; 100 mg kg^{-1} CTAB; 135 cm column height; 32 g min^{-1} and 16 g min^{-1} feed and bottom rates, respectively.

From the slope of the graphs, for each experiment, the liquid hold-up was calculated using Eqn. 4.6 and the values obtained were used to work out the rate of accumulation using Eqn. 4.4.

CTAB (mg $kg^{-1)}$	Feed (g min^{-1})	M (g min^{-1})	U (g min^{-1})	Top (g min^{-1})	Acc. (g min^{-1})
100	32	1.5	18±1	16.1±0.5	0.5±0.1
100	32	3	17±1	19.6±0.5	2.5±0.2
100	32	4.5	15±2	23.7±0.5	3.85±0.1
120	32	1.5	16±1	16.3±0.5	0.35±0.1
120	32	3	15±1	20.5±0.6	1.55±0.1
120	32	4.5	14±1	25±0.5	3.45±0.1
150	32	1.5	12±1	21±0.75	0.25±0.1
150	32	3	11±1	24.8±1	1.3±0.1
150	32	4.5	10±2	27.3±2	3.35±0.2

Table 4.5: Methanol balance (average ± standard deviation) across 135 cm long column at

airflow rate of 2 L min^{-1} under continuous process using 2 mm holes distributors.

^{M}Methanol flow rate, ^{U} Rate of underflow, $^{Acc.}$Rate of methanol accumulation measured at 12 min

CTAB (mg kg^{-1}))	Feed (g min^{-1})	M (g min^{-1})	U (g min^{-1})	Top (g min^{-1})	Acc. (g min^{-1})
100	32	1.5	16.5±0.5	16.1±0.5	0.2±0.1
100	32	3	16±0.5	18.5±0.5	0.75±0.2
100	32	4.5	16±0.5	20.7±0.5	0.95±0.1
120	32	1.5	16±0.5	17.3±0.5	0.15±0.1
120	32	3	16±0.5	19.0±0.5	0.75±0.1
120	32	4.5	16±0.5	21.5±1	2.15±0.1
150	32	1.5	16±0.5	17.1±0.5	0.13±0.1
150	32	3	16±0.5	19.8±0.5	0.81±0.1
150	32	4.5	16±0.5	21.5±0.5	1.5±0.2

Table 4.6: Effect of constriction (1/5) on rate of accumulation (average ± standard deviation) in a 120 cm column with constriction between 90 and 105 cm at airflow rate of 2 L min^{-1} using 2 mm holes distributors.

^{M}Methanol flow rate, ^{U} Rate of underflow, $^{Acc.}$Rate of methanol accumulation measured at 12 min

When contractions were applied, not only did the total flow rate decrease but the rate of accumulation in the frothing zone also decreased under the same operating conditions, which is an indication of higher concentration of methanol at the top. If microalgae were to be present, this would also be an indication that higher concentration factors are achievable with contraction. This is in agreement with similar findings where concentration factors of over 300 were achieved during the flotation of *C. vulgaris* [278]. It is worth noting that with contraction, accumulation of methanol can be reduced to as low as 0 g min^{-1} when CTAB concentration and methanol flow rates were kept at 100 mg kg^{-1} and 1.5 g min^{-1} respectively.

At a given methanol flowrate, the rate of accumulation decreased with increase in CTAB concentration but at low methanol flow rates, while the rate of accumulation increased with increased flow of methanol. This is so because smaller and more stable bubbles are formed with increased surfactant concentration [326] and if the concentration of methanol remains constant whilst the flow of methanol increases, it is only natural that more of the methanol would accumulate. However, when contractions were installed, the rate of accumulation decreased compared to when there were no contractions. This was because the introduction of contraction allowed for a secondary mixing zone that ensured

that downward flow of methanol was limited, as can be seen from Tables 4.5 & 4.6. However, if high airflow was involved and CTAB concentrations were kept low, an eventual depletion in CTAB concentration could occur due to a resultant fast rate of foam movement and that could result in higher accumulation especially if methanol supply is maintained beyond the depletion threshold for CTAB. Although this is a continuous process, and CTAB concentration is expected to remain constant throughout, this is not usually the case because when higher CTAB concentrations and airflow are involved, the foam travels faster than the rate of feed. The contraction section also ensures better concentration of algae, which means additional advantage to using this process for biodiesel production. The side effect of the contraction section however is that the content of the secondary mixing zone is bound to return to the less concentrated primary mixing zone once there is not enough surfactant in the system. Nonetheless, this was corrected by creating a secondary collection point just below the contraction so as to disallow the return of already concentrated foamate back into the mixing zone.

Based on the above results, it is clear that the introduction of contraction decreases the accumulation of methanol in the foam and hence should make most of the methanol supplied available for reaction with algae oil, when made available via cell lysis by the action of CTAB [330]. The introduction of contraction also means that a secondary mixing zone is created at the top of the column and could enhance the transesterification process, considering that mixing has been identified as a condition for favourable transesterification [39, 220, 331]. The introduction of contraction also ensures that the underflow is maintained at an almost constant rate irrespective of CTAB concentration, because of the restriction to the rather faster rate of foamate movement with increased CTAB concentration. Furthermore, with accurate information about how much methanol is fed over time, it is easy to deduce the ratio of methanol to oil that is available for transesterification, when that process step is eventually added to the scheme. This is so because the ratio of methanol to oil is one of importance when it comes to biodiesel production and it would be interesting to see if that ratio can be reduced, taking advantage of the fact that algae cells would have been lysed and the oil content easily accessible.

4.4 Conclusion

Methanol injection in a foam flotation system was successfully achieved through

cocurrent and countercurrent methanol injection schemes. Countercurrent methanol injection is possible with the aid of distributors while enrichment of cocurrent methanol was not possible. Countercurrent methanol injection was capable of delivering the desired methanol concentration for transesterification of algal oil. However, the cocurrent methanol process allows for longer contact time between methanol and algae and hence more likely to bring about cell lysis.

Methanol injection rate and CTAB concentration affected the concentration of methanol in the foamate as well as the rate of accumulation of methanol. While increase in CTAB concentration reduces the rate of methanol accumulation and increases the concentration of methanol in the foamate, increase in methanol flowrate increases the concentration of methanol in the foamate and also the rate of accumulation. Foam risers are useful tools for reducing rate of accumulation, which was an added advantage to its liquid drainage ability.

The interaction between methanol, water, and CTAB with respect to foam stability was such that stable foam is possible as long as the percentage of methanol in the mix was not more than 50%.

In terms of media type, seawater was better suited for the process of enriching methanol but within the operating conditions of this study, both media were able to produce the required level of enrichment appropriate for transesterification.

This work has established a basis for potential reduction in the cost of producing algal biodiesel, provided the cost of separating biodiesel from water does not outweigh the cost of drying.

Chapter 5

Process intensification of biodiesel production: coupling the harvesting and reactive extraction of *Dunaliella salina* within a foam column

Abstract

In situ transesterification has gained popularity in biodiesel research because of the perceived reduction in costs compared with the traditional two-step biodiesel production process; however, cost parity between biodiesel (particularly from microalgae) and fossil diesel has yet to be attained. Drying costs remain one of the economic bottlenecks for algal biodiesel. This work explores the possibility of making algal biodiesel increasingly cost effective by eliminating the drying steps. A 15 cm long foam riser with contraction-expansion ratio of 0.2, as part of a 120 cm long glass flotation column, was used to increase the concentration factor of *Dunaliella salina* from 1.5 ± 0.5 to 4.7 ± 0.5. The operating conditions are: 2.4 L min^{-1} airflow, feed flow of 32 g min^{-1}, bottom flow rate of 16 g min^{-1}, and methanol and acid flow rates of 1.5 g min^{-1}. The transesterification process was conducted for 1 and 24 h with the aim of simultaneously harvesting and converting *D. salina* to biodiesel in situ. Unprecedentedly, biodiesel conversion was achieved, albeit at a low yield (9.3 ± 0.2 and 11.2 ± 0.3% after 1 and 24 h respectively). The low yields were the result of high moisture content, ambient conditions of temperature and pressure, and likely limitations of the transesterifiable lipids in *D. salina.* Nevertheless, this is a clear indication that (through process intensification) significant progress can be made in algal biodiesel production. Cost analysis of the proposed technology has shown some promise of a cost-effective biodiesel in the future.

Keywords: Foam flotation, Foam drainage, Algae biodiesel, Microalgae harvesting, Process intensification, costing, cost effective algal biodiesel.

5.1 Introduction

In situ transesterification or reactive extraction was first investigated using sunflower seeds

in 1985 by Harrington and D'Arcy-Evans [332] as an alternative to the conventional transesterification process where pre-extracted oil is treated with methanol and catalyst, which is essentially a two-step process. In situ transesterification was thought to have advantages such as: reduction of oil losses and improved digestibility of carbohydrates by acid or base catalyst, both of which could improve biodiesel yield. Later in 2004, Hass et al. [333] affirmed the yield improvement capability of reactive extraction based on in situ transesterification of soybean oil. The same has also been said about non-terrestrial biomass like the heterotrophic fungus-like thraustochytrids [256] and the *Mucor circinelloides* fungus [334]. With regards to algae, similar reports are available on different strains such as *Chlorella* [335], *Chaetoceros gracilis, Phaeodactylum tricornutum, Tetraselmis suecica, Neochloris oleoabundans, Chlorella sorokiniana, Synechocystis* sp. PCC 6803, and *Synechococcus elongatus* [257].

In situ transesterification also means that less process time [39] and operating units are involved, thereby improving on the process cost in terms of equipment investment. Although some raw materials like soybean require only little drying (from 2.6 wt.% moisture) [336], the cost of refining oil was estimated to be as high as 88% of the total biodiesel production cost [337]. Lardon and Co [35] reported that 92.2 % of biodiesel production energy from microalgae can be associated to drying and hexane-oil-extraction, out of which 84.2 % is for drying alone. The recommended water content in biomass feedstock for transesterification of algae oil is < 0.5 % [338]. Therefore, in terms of algal biodiesel, the drying cost is of great importance and needs to be drastically reduced since it cannot be eliminated completely.

To overcome the challenges posed by the drying cost, efforts have been directed at converting wet biomass to biodiesel via in situ transesterification. Velasquez-Orta et al. [32] reported the feasibility of producing algal biodiesel using *Chlorella vulgaris* and *Nannochloropsis oculata* biomass with 10% water content. Similarly, Kamoru et al. [292] reported a successful biodiesel conversion with *C. vulgaris* and *N. oculata* at a maximum water content of 30%. According to Kim et al. [231], biodiesel production was achieved using *N. gaditana* with 80 % moisture content. Using *Schizochytrium limacinum* of similar moisture content (80 w/w. %), a similar outcome was reported, although the traditional two-step process, outperformed the in situ wet process [339]. This argument is also supported by Velasquez-Orta [32], where changing the moisture content from 0 to 10%

reduced the yield from 92 % to 60 %. Kamoru et al. [340] reported that there was no significant change in biodiesel yield between 0 and 20 wt. % moisture, until 30 wt. % moisture content was reached. In order to prevent saponification at 20 wt. % moisture, excess methanol (600:1 methanol to oil ratio), was needed. Even more methanol (1277:1 methanol to oil ratio) was needed in order to withstand a 30 wt. % moisture content. water. It was also reported that the addition of a surfactant (sodium dodecyl sulphate; SDS) increased the biodiesel yield from wet *C. vulgaris* and *N. oculata* in the H_2SO_4-catalysed process.

It is hard to say if wet processing is more economically viable without a proper cost analysis. However, literature [255] tends to suggest that there is a greater chance of achieving near cost parity if wet processing technology is combined with advanced processes like microwave, ultrasound, or supercritical conditions, as long as the costs of installing equipment are reduced. It is important to note that these advanced technologies are not only expensive but are based on extreme and sometimes dangerous conditions such as the involvement of hexane and phenol as co-solvents.

With respect to acid catalysis, in situ transesterification has been reported within the following conditions: moisture content (0 – 400 %), heat (65 – 90 ^oC), H_2SO_4 :oil ratio (0.093:1 – 0.797:1), HCl to oil ratio (0.186:1), Mg-Zr oxide (1.65:1), NaOH (0.15:1), and methanol to oil ratio (154:1 – 3460:1). Based on these range of conditions, 40 – 98 % biodiesel conversion, in reaction times of 1.25 to 20 h has been reported [340]. Within a shorter period (30 min), *C. gracilis* containing 400 % moisture was said to have been converted to FAME [257].

To avoid acid overload, which may result in side reactions (especially the polymerisation of unsaturated fatty acids with one or more double bonds), 0.2M to 0.3M concentration of acid is recommended [341]. Moreover, the use of 0.4M H_2SO_4 has been reported to result in black precipitates [258]. Nonetheless, the work of Velasquez-Orta et al. [342], which reported a 97 % FAME conversion under these conditions: 20 h of reactive extraction of dry *C. vulgaris*, 600:1 methanol to oil, 0.35:1 acid to oil, and 60 ^oC, suggested that the high acid strength may have assisted cell lysis, and hence the high yield. Similar results could not be achieved with *N. oculata* cells due to the acid resistance of the of algaenan covering of the cell walls.

In virtually all of the cases reported for wet biomass conversion to biodiesel, the starting feedstock was sourced as dried microalgae and therefore crucially does not eliminate the original drying and harvesting costs. Between 20 to 30 % of harvesting and dewatering costs are associated with increasing the total solids suspension (TSS) to between 5 and 37% (5 % representing pre-concentration), depending on the technology for dewatering (centrifugation, vacuum filtration, or pressure filtration) [343]. Nevertheless, there is no universal technology for biomass recovery as in most cases, achieving a 37 % TSS required a combination of more than one process technology [344], which calls for improvement in terms of universality and efficiency of microalgae harvesting technology for biodiesel.

Among the available technologies, foam flotation is receiving increased attention due to the comparative cost reduction [19]. Foam flotation can reduce moisture content to between 93 and 98 % [345], which is far more than the recommended < 0.5 % for successful biodiesel conversion [338], although as high as 400 % moisture was reported as mentioned earlier. In terms of total solids suspension, a TSS of 14.6 % was reported for the flotation of *C. vulgaris*, consuming 0.052 kWh of power per m^3 of culture [346]. In spite of these progresses, the harvesting of marine microalgae via flotation technology still suffers from a major setback as it is not yet well developed. As far as we know, the only available literature on harvesting marine algae via flotation, are those reported by Garg et al. [92, 347], and more recently that by Alkarawi et al [278] where diluted (lowered ionic strength) cultures were used. The major bottleneck is the interference of salt and other ions present in seawater. This phenomenon and how to manage it, has been thoroughly dealt with in chapter 3.

It is noteworthy that marine algae tend to produce wetter foam than freshwater species and this could lead to reduced enrichment. With low enrichment comes the difficulty of further processing, especially biodiesel conversion. Whether or not the negative effect of excess water on biodiesel conversion would be outweighed by a reduced cost of drying, is a question that needs to be answered. In an attempt to answer this question, this work seeks to produce biodiesel from algae by combining the harvesting, oil extraction, and transesterification steps of algal biodiesel, in a foam column, under ambient temperature and pressure conditions.

Selection of microalgae for biofuel production can be based on three main conditions, namely: growth rate, cell morphology, and lipid (mainly triacylglyceride - TAG) accumulation [260]. Given the difficulties encountered in lysing *N. oculata* cells (Chapter 3), *Dunaliella salina* was chosen as the demonstration strain for this Chapter as it lacks a true cell wall [348] which allows the cells to be easily lysed by surfactants such as CTAB. In addition, *D. salina* has been identified as a potential biodiesel feedstock [348] with fast growth rate [349]. It also has a high salt tolerance of up to 350 g L^{-1} [350], meaning that it can be grown in brackish water, which confers on them the low tendency of contamination and attack by predators, in addition to sustainability.

Process intensification refers to the reduction of process steps and unit operations with the aim of making them smaller, safer, more efficient, more sustainable, and cheaper, through the use of new and/or modified technologies. An example of intensification is the in-situ transesterification of vegetable oil to produce biodiesel. In this work, in situ transesterification would be further intensified to include algae harvesting, oil extraction, and biodiesel production in one process unit (the foam flotation column).

5.2 Materials and method

5.2.1 Cultivation of *Dunaliella salina*

Dunaliella salina (CCAP 18/19) was cultivated in batch for four weeks in F/2-Si media [275] in a 20 L polycarbonate Nalgene carboy under a 16 L: 8 D photoperiod (2200–2800 lux) using a mixture of warm and cold fluorescent tubes. Mixing and gas exchange were facilitated by bubbling HEPA filtered (0.2 µm) air through the culture. Details of the culture media is as described in chapter 3 for F/2-Si.

5.2.2 Flotation harvesting of *Dunaliella salina*

As a first stage in the intensification scheme, the possibility of, as well as the most favourable conditions for, recovering *D. salina* were sought. Based on results from chapter 4, the operating conditions with the least methanol accumulation rate (Feed flow, underflow, column height with riser, and CTAB concentrations of 32 g min^{-1}, 16 g min^{-1}, 120 cm, and 150 mg L^{-1}, respectively) were applied. Under these conditions, the performance of the flotation as a harvester for *D salina* was investigated in the presence of 1.5 g min^{-1} and 0 g min^{-1} methanol flow rates. In addition, a combination of 20 and 30 mg

L^{-1} of chitosan and saponin respectively [93], were used in place of CTAB. Furthermore, the performance of the flotation column to harvest *D. salina* in the presence of methanol was investigated using a combination of chitosan, saponin, and CTAB. These trials were necessary because there was no prior knowledge on how the flotation column performs in the presence of methanol when marine microalgae are involved. Although flotation experiments were conducted to check the impact of saltwater, the impact of suspended particles in salt environment is not established, neither was the unique morphology of *D. salina* as opposed to *C. vulgaris* and *N. oculata*. After the preliminary investigation, the performance of the flotation harvesting of *D. salina* was then investigated according to conditions described in Table 5.1

The performance of the foam flotation process was tested on the basis of both recovery and concentration factor. To achieve this aim, mixing sequence, airflow, CTAB concentration, dilution and contraction sections were varied according to Tables 5.1 below.

Material stream composition	Airflow (L min^{-1})	Constriction
Normal	3.6	No
Normal	3.6	yes
Normal	3.6	yes
CTAB added before saponin	3.6	yes
Undiluted culture	3.6	yes
50% dilution	3.6	yes
30 mg L^{-1} of CTAB	2.4	yes
30 mg L^{-1} of CTAB	3.6	yes
Normal	3.6	yes
Normal	2.4	yes

Table 5.1: Effect of constriction presence on flotation harvest performance; column height was 120 cm with constriction and 135 cm without, feed and bottom rates were 32 and 16 g min^{-1} respectively. Normal material stream compositions were: 20 mg L^{-1} chitosan, 30 mg L^{-1} saponin, 50 mg L^{-1} CTAB, and 1.5 g L^{-1} methanol.

Because it is difficult to count cells after the addition of CTAB due to cell rapture that occur as a result, a calibration curve was first defined to describe cell concentration as a function of optical density, e.g. Fig. 5.1.

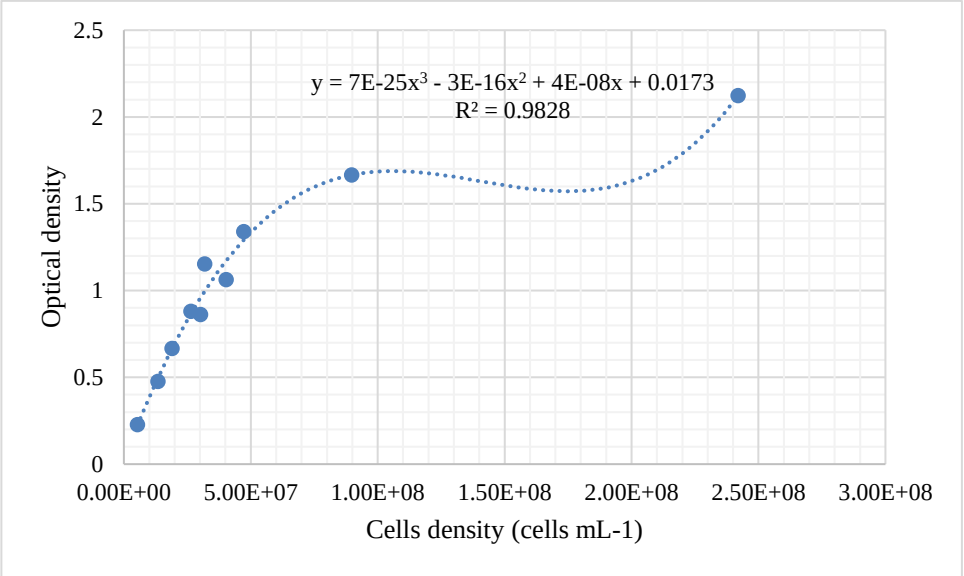

Figure 5.1: Calibration curve for optical density as a function of *D. salina* cell concentration @ 670 nm wavelength: initial cell concentration was 256 mg L^{-1} of culture and was concentrated to 256 mg in 50 mL (20 X) through mild centrifugation @ 1000 rev for 1 minute; the final concentration and 1L of initial sample were diluted serially. The least dilution was obtained at 5 X dilution of initial culture

5.2.3 Quantification of lipid in *D. salina* and determination of maximum biodiesel yield

To determine the lipid content of *D. salina*, 100 and 200 mg of dry biomass (in triplicates) were treated according to a modified Bligh and Dyer method [351]. Briefly, 1 mL of a 2:1:0.8 v/v/v mixture of methanol (99.8 %, Sigma Aldrich), chloroform (Sigma Aldrich), and deionised water were added to dry cells in a glass test tube to form a paste. The paste was transferred to a centrifuge tube and another 1 mL of the extraction mixture was used to wash what was left in the glass tube into the centrifuge tube and topped up to 5.7 mL, capped and centrifuged (SIGMA type 2-6) at 400 G for 10 minutes. The supernatant was carefully transferred into a glass tube using an automatic pipette and capped to avoid evaporation. A second extraction was performed by adding another 5.7 mL of the extraction mixture to the pellet in the centrifuge tube and resuspended by vortex (Heidolph, type REAX top) and centrifuged the second time to collect a second supernatant that added to a total volume of 11.4 mL. 3 mL of water was then added followed by 3 mL of chloroform, each time ensuring mixing by vortex. The top layer containing water and methanol was carefully removed leaving behind the chloroform and lipid layer. Toluene

(Sigma Aldrich) was added (6-8 drops) to the chloroform layer to remove any leftover water. The chloroform layer was then transferred to a pre-weighed vial and quickly placed under a stream of pure N_2 (BOC) to remove the chloroform at 38 ^oC in a fume cupboard, leaving behind lipid. The vial containing lipid was then transferred to a desiccator (Bel-art) under KOH (Sigma Aldrich) overnight and weighed to determine the mass of the lipid extracted. The quantity of lipid was presented according to standard deviations of three values.

5.2.4 Analysis of cell lysis by CTAB treatment

Cell lysis by surfactant has the advantage of increasing the chances and quantity of oil being extracted, as well as biodiesel yield. Cultures of *D. salina* were treated with 50 mg L^{-1} CTAB and shaken for 2 min and allowed to stay for another 10 min. Samples were then taken and examined under the microscope at x100 magnification to ascertain whether or not the cells remained intact after surfactant treatment. Similarly, samples of fresh *D. salina* culture was viewed under the same magnification for comparison.

5.2.5 Combined harvesting and reactive extraction of D. salina using foam flotation

Using the flotation column, *D. salina* cells were harvested and converted to biodiesel via reactive extraction. The collector was also used as a reaction vessel for biodiesel conversion. The chosen harvesting conditions were decided based on the best flotation conditions (2.4 L min^{-1} of air, 1.5 g min^{-1} of 1.6 M acid in methanol, feed and bottom rates of 32 g min^{-1} and 16 g min^{-1} respectively) determined from trials. The column height was maintained at 120 cm (with foam riser). The methanol stream now contains 1.6 M H_2SO_4, prepared in a 500 mL bottle with 98.9 % methanol and 98 % sulphuric acid (Sigma Aldrich). Acid solution was prepared by gently adding methanol along the walls of the bottle at constant mixing with the aid of a magnetic stirrer to prevent methanol evaporation as a result of the exothermic energy of mixing between methanol and sulphuric acid. The density of the acid was 1.84 g mL^{-1} and molecular weight of 98.08 g mol^{-1}. 16 mL of sulphuric acid was added to 200 mL, which is the equivalent of 86 wt. % methanol. The volume fraction of acid to methanol is 0.074 and the methanol to oil molar ration is 7455:1. Due to difference in density, the pump was recalibrated. The position on the pump that

corresponded to 1.5 g L^{-1} of methanol is now 1.2 g L^{-1} of acid in methanol solution.

The methanol stream containing H_2SO_4 (1.6 M) was fed at 1.5 g min^{-1} for 6 min, so that a top product of the interaction between algae, surfactant, acid and methanol was collected in a plastic bucket. The final acid concentration was approximately 0.2 M (which is ideal for biodiesel conversion) based on the final foamate composition of approximately 400 g of liquids per litre of culture fed into the column. In order to avoid the return of cells back to the bulk liquid in the mixing zones at the expiration of feed supply, a secondary collection point was introduced just above the riser to ensure that concentrated cells were collected before the last stream of feed enters the column. Products collected from this secondary point were transferred into the main plastic collector at the column top. The content of the plastic bucket was then transferred to a freezer to quench the biodiesel production process. Quenching was done after 1h and 24 h of the last foam collection in order to investigate the effect of reaction time on biodiesel production. The storage temperature was -20 ^{O}C. Before biodiesel analysis, excess water was driven off using a rotary evaporator (Buchi Rotavapor R- 215), fitted with V 70 vacuum pump, operated at 40 ^{O}C and 72 mbar for 2h. The final samples were approximately 5 mL per litre of biodiesel mix (approximately 375 mg algae).

5.2.6 Analysis of biodiesel production

After the removal of excess methanol and water by evaporation, analysis of the remaining liquid mix for FAME was carried out using gas chromatograph (Hewlett-Packard - HP 6890), equipped with a fused silica capillary column (15QC3/BPX5-0.25, SGE Analytics, UK) of 0.25 μm in film thickness, 15 m in length and 0.32 mm in diameter. The GC oven was held at an initial temperature of 140 °C for 1 min and then heated at 8 °C min^{-1} to 210 °C, 2 °C min^{-1} to 260 °C, and then to a final temperature of 280 °C at a rate of 30 °C min^{-1}, held for 1 min. The total run time was 36.42 min. The injector temperature was 250 °C while the temperature of the detector was 230 °C. Helium gas was used as the carrier at a flow rate of 1 mL min^{-1}. The analysis with flame ionisation detector was carried out at the following conditions: helium as carrier gas, electron energy of 70 eV and mass range from 10 to 400.

Using Eqn. 5.1 below, it was possible to compute the concentration of FAME in a given sample.

$$C = \frac{\sum A - A_{Ei}}{A_{Ei}} X \frac{C_{Ei} V_{Ei}}{m} X100\% \quad (5.1)$$

Where $\sum A$ is the total area under the peaks corresponding to C8:1 – C20:1

A_{Ei} is the area under the standard FAME peak

V_{Ei} is the volume of the standard (mL)

C_{Ei} is the concentration of the standard (mg mL^{-1})

m is the sample weight (mg)

The concentration of FAME obtained from Eq. 5.1 was then multiplied by the total mass of filtrate from the experiment containing all the products, according to Eq. 5.2.

$$mass\ of\ FAME = C(\%)\ X\ W \quad (5.2)$$

Where W is the weight of filtrate (mg)

Mass of filtrate was obtained by filtering out the solid components of the biodiesel product collected after quenching the reaction. Filtration was achieved through vacuum filtration using a combination of Buchner funnel, filter paper, and a side-arm flask connected to a pump. Once the liquid was separated from solid, the liquid was weighed in an empty centrifuge tube and set aside for GC analysis.

Finally, the FAME yield was calculated from Eq. 5.3.

$$Yield\ (\%\ W/W) = \frac{mass\ of\ FAME\ (mg)}{weight\ of\ Lipid\ (mg)} X100\% \quad (5.3)$$

Standard solution of C_{17} was prepared by dissolving 100 mg of 99 % heptadecanoic acid (Sigma Aldrich) in 10 mL of methanol and was stored in the fridge for storage. 1 mL of the standard solution was added to 50 mg of biodiesel sample in a 2 mL vial. once water was eliminated the remaining sample was filtered to remove solid particles and the filtrate was analysed for biodiesel. Sampling was done in triplicates for each of the investigated reaction times.

5.2.7 Cost analysis and process economy

Based on a batch flotation, Coward and Co [102] had estimated the cost of harvesting 1 m^3 of algae to be US$ 0.915. In a related work, the cost of harvesting the same volume of algae culture under continuous flotation was estimated at US$ 0.179 by Al – Karawi [346]. The operating condition of airflow in both cases was 1 L min^{-1}. Being a continuous flotation, the work of Al- Karawi, took into recognition, the feedflow, which was 0.1 L min^{-1}. Both

estimates were based on the cost of air compression and surfactant dosage, and was irrespective of algae specie.

Air compression is necessary in order to overcome the pressure - drop across the sparger, the hydrostatic pressure of the liquid pool, and the pressure - drop due to friction between foam and the column wall. This compression work represents the work done by the flotation column in generating bubbles. According to Stevenson and Li [299], the power (W_{comp}) required for an isentropic compression of an ideal gas can be estimated using Eqn. 5.4.

$$W_{comp} = \frac{RT_o}{\eta_{is}} \frac{\gamma-1}{\gamma} \left[\left(\frac{P_1}{P_0} \right)^{\frac{\gamma-1}{\gamma}} - 1 \right] \quad (5.4)$$

where: W_{comp} is the compressor work (J mol^{-1}); R is the universal gas constant (8.314 J mol^{-1} K^{-1}); T_o is the absolute initial temperature (298 ºK); η_{is} is compressor efficiency; γ is the ratio of the isobaric to isochoric heat capacities (1.4 for dry air); P_0 is the pressure upstream of the compressor (kPa); and P_1 is the pressure of the compressed gas (kPa).

Pressure of the compressed air was measured with the aid of a pressure gauge connected to the air line. A 70 % compressor efficiency is assumed in this work because compressor efficiencies are generally within the range of 65 – 90 % [352]. The air compression cost model was based on the flotation conditions of 2.4 L min^{-1} airflow and 0.05 L min^{-1}.

In addition to compression work, is the cost of surfactants used in the process. For ease of comparison, the unit of power in J mol^{-1} of algae will be converted to kWh m^{-3} of algae. The ideal gas Eqn. 5.5 will be used to convert from mole basis to volume basis. The costs of surfactants based on information from vendors, would also be in same unit. The energy cost in monetary terms would be based on the May 2020 data from the US Energy Information and Administration (eia) [353].

$$\frac{n}{v} = \frac{P}{RT} \quad (5.5)$$

where: P (Pa) and T (ºK) are the same as P_1 and $T_{O,}$ above.

Based on the work of Lardon at al., an estimate of the process economy would be made.

5.3 Results and discussion

5.3.1 Foam flotation: Effect of column design, CTAB, and airflow

When feed flow, underflow, column height with riser, and CTAB concentrations were 32 g min^{-1}, 16 g min^{-1}, 120 cm, and 150 mg L^{-1}, respectively, stable foam could not be achieved in the presence of methanol. This is mainly due to the difference in algae species and media type between *C. vulgaris* and *D. salina*. The fact that this is the first time an attempt was made at harvesting marine algae in the presence of methanol also leaves room for uncertainties. To this end, flotation experiments were conducted under the same conditions without the methanol stream but even then, only 64 % recovery at CF of 1.7 was recorded (Table 5.2). When a combination of 20 and 30 mg L^{-1} of chitosan and saponin respectively [93], were used in place of CTAB, in the absence of methanol, recovery and CF of 81 ± 1 % and 14.3 ± 0.2, respectively were recorded. Increasing the concentration of saponin to 50 mg L^{-1} saw only a slight increase in process performance (recovery and CF of 84 ± 1 % and 14.2 ± 0.2, respectively) (Table 5.2). However, when methanol injection was introduced, foam stability could not be achieved, even when airflow was increased to 3.6 L min^{-1}. Therefore, in order to keep foam stable in the presence of methanol, CTAB was needed. When the combination of chitosan, saponin, and CTAB were used, *D salina* recovery was achieved in the presence of methanol. The mechanism of algae capture is such that the higher molecular weight chitosan has less binding energy than CTAB and hence is capable of creating stronger adsorption on to algae cells. The use of chitosan as flocculants has been reported for freshwater [354, 355] and marine [356] algae alike. Due to salt ions however, saponin was needed to counter the influence of Na^+ in the diffused layer, where access to algae cells were difficult as result of the neutralisation of the charge on chitosan head group by Na^+ [357]. Although non-ionic, saponin would assume a negative charge just like most particles in suspension, creating some electrostatic attraction with oppositely charged Na^+, especially when added first. Saponin also serves as a frothing agent and contains hydrophilic functional groups. Although chitosan is hydrophilic, its adsorption capacity is not as strong as CTAB and often require enhancement by CTAB [358]. The respond to surface tension reduction in chitosan is also very slow [359] and hence its function as a foam stabiliser can easily be compromised by countercurrent flow of methanol. Moreover, neither saponin or chitosan or combination of both are as able as CTAB in reducing surface

tension[360].

Surfactant	Recovery (%)	C.F
150 mg L^{-1} CTAB	64 ± 2	1.7 ± 0.5
20 mg L^{-1} Chitosan. + 30 mg L^{-1} Saponin	81. ± 1	14.3 ± 0.2
20 mg L^{-1} Chitosan + 50 mg L^{-1} Saponin	84 ± 1	14.2 ± 0.2

Table 5.2: Recovery and CF (average ± standard deviation) from trial experiments on *D. salina* using a 135 cm height column without a riser and a 120 cm with riser (0.2); airflow of 2.4 L min^{-1}.

The results obtained based on flotation experiments conducted in the presence of methanol, are presented in Tables 5.3 – 5.7 below.

Airflow (L min^{-1})	Constriction	Recovery %	CF
3.6	No	89 ± 2	1.5 ± 0.5
3.6	Yes	80 ±1	3.3 ± 0.5

Table 5.3: Effect of contraction on the recovery % and concentration factor (CF) (average ± standard deviation) of *D. salina.* Operating conditions of 20 mg L^{-1} chitosan, 30 mg L^{-1} saponin, 50 mg L^{-1} CTAB and 1.5 g L^{-1} methanol.

From Table 5.3, it is clear that the introduction of foam riser allowed for better concentration of microalgae in the foamate. Because it was intended to not further dry the biomass, greater importance was attached to concentration factor than recovery, although both recovery and CF are important. Due to making and breaking of bubbles that take place along the neck of the riser section, more liquid was drained off the foam, leading to an increase in particles (algae) enrichment. Once CTAB was depleted in the secondary mixing zone (above the riser), the collected cells began to fall back in to the primary mixing zone, a situation made worse by the downward flow of methanol [252], and hence the reduced recovery in the case of constricted columns. The use of constriction in the flotation of *C. vulgaris* has been reported to produce microalgae biomass 722 times more concentrated than the fed culture, representing a 4.2 times higher concertation factor than when no contractions were used [346]. Although there is a 2.2-fold increase in concentration factor based on the above results, the difference in media culture, microalgae strain, CTAB concentration and other process parameters would have been responsible for the lower scale of increment observed. In order to correct the reduced recovery as a result of the riser,

a secondary outlet was provided, 7.5 cm above the riser where collected cells are manually transferred into the main collection point.

Mixing pattern	Recovery %	CF
Saponin preceded CTAB	80 ± 1	3.3 ± 0.5
CTAB preceded saponin	79 ± 1	3.1 ± 0.5

Table 5.4: Effect of mixing pattern with contraction on the recovery and concentration factor (CF) (average ± standard deviation) of *D. salina*. Operating conditions: airflow of 3.6 L min^{-1} with constriction, 20 mg L^{-1} chitosan, 30 mg L^{-1} saponin, 50 mg L^{-1} CTAB and 1.5 g L^{-1} methanol.

From Table 5.4, the effect of mixing sequence is such that there was a slightly higher concentration factor when saponin addition preceded the addition of CTAB to the chitosan-treated culture. This is because the stronger impact of Na^+ on CTAB as opposed to chitosan [357] would have disrupted the bridging created by saponin between algae and chitosan. The interference by Na^+ is however reduced once an electrostatic attraction has been established between the now positively charged cells and the negatively charged saponin [93]. Nonetheless, the difference in impacts is not so significant because the lowering of CTAB adsorption properties of CTAB by Na^+ is strong therefore leaving CTAB to act as a mere frothing agent.

Dilution	Recovery %	CF
No	62 ± 1	2.6 ± 0.4
50/50	85	14.3 ± 1

Table 5.5: Effect of dilution on recovery and concentration factor (CF) (average ± standard deviation) of *D. salina* at a reduced CTAB concentration. Operating conditions*:* airflow of 3.6 L min^{-1} with constriction, 20 mg L^{-1} chitosan, 30 mg L^{-1} saponin, 30 mg L^{-1} CTAB and 1.5 g L^{-1} methanol.

From Table 5.5, 30 mg L-1 of CTAB was chosen because it was intended to keep CTAB as minimum as possible so that the impact of salt ions can be better felt. Earlier results have confirmed that salt and other ions present in the marine medium are strong inhibitors to the successful use of foam flotation in the recovery of marine algae. An analysis of the results in Table 5.5 translates to only about 100 mg of cells being recovered from the diluted culture as opposed to 146 mg from the undiluted culture, meaning that about 25 % fewer cells are recovered from diluted than the undiluted stream, even though

concentration of the final cells were lower and more appropriate for further processing. However, this would not be considered as a practical solution due to the negative economy of the process.

Airflow (L min^{-1})	Recovery %	CF
2.4	50 ±1	3.5 ± 0.7
3.6	62 ±1	2.6 ± 0.4

Table 5.6: Effect of airflow at low CTAB concentration with constriction on the recovery % and concentration factor (CF) (average ± standard deviation) of *D. salina.* Operating conditions*:* 20 mg L^{-1} chitosan, 30 mg L^{-1} saponin, 30 mg L^{-1} CTAB and 1.5 g L^{-1} methanol.

As expected, the higher the airflow the lower was the concentration factor, but the higher the recovery (Table 5.6). This implies that higher CTAB concentrations are needed to increase both recovery and concentration factor. As stated above, CTAB may not necessarily be acting as a collector but because it helps to strengthen the foam, it can reduce the detachment of already adsorbed cells [252], especially in the presence of countercurrent methanol.

Airflow (L min^{-1})	Recovery (%)	CF
3.6	80 ± 1	3.3 ± 0.5
2.4	73 ± 1	4.7 ± 0.4

Table 5.7: Effect of airflow at high CTAB with constriction on recovery and concentration factor (CF) (average ± standard deviation) of *D. salina*. Operating conditions*:* 20 mg L^{-1} chitosan, 30 mg L^{-1} saponin, 50 mg L^{-1} CTAB and 1.5 g L^{-1} methanol.

The increase in CTAB concentration (from 30 to 50 mg L^{-1}) was to see whether there will be an improvement in process response (Recovery and CF). Compared to Table 5.6, better responses were obtained when CTAB concentration was increased from 30 to 50 mg L^{-1} (Table 5.7). However, care must be taken not to use too much CTAB as this may cause the foam to become wetter, more so in the presence of methanol [252, 299]. The choice of CTAB concentration was to ensure there was high enough cell recovery. Therefore, the recommended airflow is 2.4 $Lmin^{-1}$ while CTAB concentration is kept at 50 mg L^{-1}.

5.3.2 Lipid content of *D. salina*

The harvested cells had 16 ± 1 % of lipid. Although this is in agreement with the literature [348], depending on the prevailing conditions (moisture content, temperature, time, pressure, alcohol, and co-solvents), some of the lipid may not be transesterifiable. For example, the moisture content could affect the solubility of lipids in methanol as well as the digestibility by the H_2SO_4 acid. Furthermore, even though triacyl glycerides (TAGs) form of natural lipids are considered as markers for biodiesel, it has been proven that polar lipids such as phospholipids and glycolipids can be converted to biodiesel [257]. A large percentage of *D. salina* is comprised of mildly volatile components under ambient conditions [348] , and may not be transesterifiable.

5.3.3 Cell lysis: Effect of CTAB

In addition to being a frother, CTAB also served as a cell lysing agent to facilitate the eventual and important steps of converting *D. salina* lipids to biodiesel. Fig. 5.2 shows *D. salina* before and after surfactant treatment.

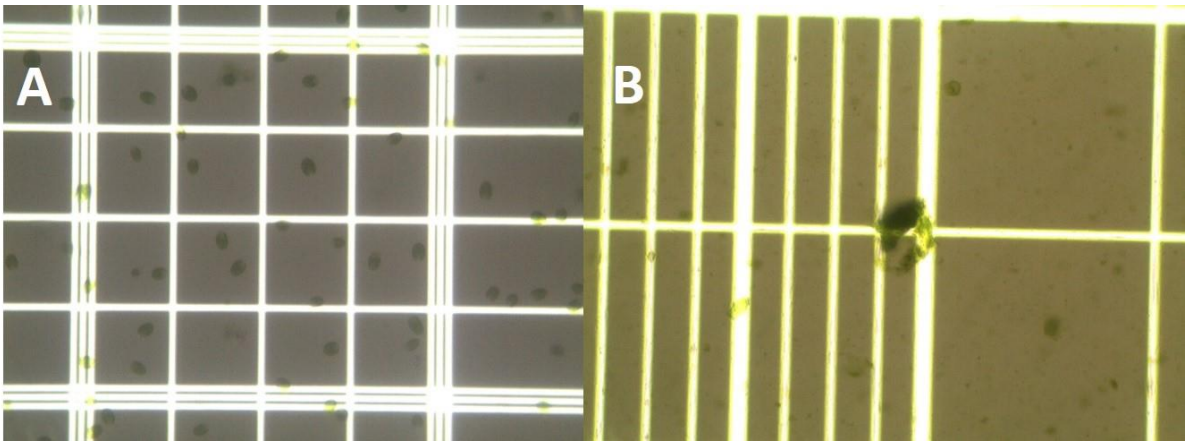

Figure 5.2: *Dunaliella salina* cells (A) without and (B) after treatment with 50 mg L^{-1} CTAB. X100 magnification.

Fig. 5.2 shows that the cells were no longer intact after being treated with 50 mg L^{-1} of CTAB for 10 min. From the background colour in Fig 5.2B, it is evident that the cell contents were released into the medium and aggregated cell debris can be seen in form of green patches. With cell lysis achieved, access to the lipid content of *D. salina* becomes less difficult and so is transesterification of lipids. If such cells are recovered via a foam flotation where methanol is injected at the top, conversion of algal lipids to biodiesel can

be achieved.

5.3.4 Biodiesel production: Effect of reaction time

Having achieved cell lysis, the next objective was to take advantage of available access to algal lipids, by converting them to biodiesel via in situ transesterification. Based on the flotation results, an airflow of 2.4 L min^{-1} and 50 mg L^{-1} CTAB were chosen. Although recovery was higher with greater airflow, the difference was marginal, hence with energy savings in mind 2.4 L min^{-1} of air was chosen. Based on these operating conditions, approximately 73 % of the cells (172 mg or 0.0312 mole of oil) per litre of culture, is expected to be available for transesterification. The amount of methanol plus acid supplied was 9 g per litre of culture. Therefore, the methanol to oil ratio in the reaction was 7455:1. Other conditions were room temperature of approximately 19 ^{O}C and atmospheric pressure, without mixing.

According to Ehimen et al. [335], the important process parameters in biodiesel production are: alcohol volume, reaction temperature, reaction time, moisture content, and rate of agitation. With regards to acid catalysed transesterification, the acid concentration or volume is very important [340]. Combining the counter current methanol feed system with a foam-riser- mounted column as described in Chapter 4, it was possible to convert *D. salina* lipids to biodiesel without any additional dewatering processes within a process time of one hour. After 1 h and 24 h, respectively, the biodiesel yield was 9.3 ± 0.2 and 11.2 ± 0.3 %. The decision to run the process for up to 24 h was informed by the fact that acid transesterification usually takes between four hours [332] to over a day [361, 362] or two [363] to complete due to slow reaction rates, although reaction times of 2 and 0.33 h have been reported elsewhere [257, 364]. Therefore, if temperatures were elevated and moisture contents were lowered, increasing reaction time could have led to a better yield than what has been recorded.

Although in one literature, [231] 80 wt. % moisture was reported, which essentially meant that microalgae formed 20 % of the reaction medium. The rest 80 % was arrived at based on all moisture contents including acid, alcohol, and added water. In comparison, only 0.093 % of the reaction medium in this case were *D. salina* cells. Hence, it is safe to say that if the cost saving as a result of using such highly wet microalgae is compared with the shortfall in yield compared to the reported cases in literature, this process has a higher

cost saving opportunity. In order to reduce moisture content, this technology can be applied to freshwater strains of *Dunaliella* like *D. acidophila* [365] where higher concentration factors are likely due to lack of salt effect. An example is Table 5.4 where concentration factor was increased by 17 – fold as a result of diluting the *D. salina* culture by 50% using freshwater. Water content is a major determinant of a successful biodiesel production. The efficiency and yield of oil extraction is affected by water content [35], just like temperature. The work of Salami et al, for example revealed that biodiesel yield began to decline once the moisture content was greater than 30 % [292]. Reduced moisture content also meant that methanol strength and consequently reaction rate, would increase. In order to arrive at a conclusion as to whether this technology is economically reasonable or not, a cost analysis is needed.

Even when where extreme conditions (supercritical/subcritical fluids, hydrothermal liquefaction, microwave irradiation, co-solvents, high temperatures reaching 300 ^{O}C, high speed centrifugal systems, etc). were involved, the water contents were usually around 60 to 80 % [366], including when enzymes (lipase) [230] or cellulase [367] were involved. Therefore, if this technology could be combined with an additional dewatering strategy that could reduce the moisture contents to these recognised limits, higher biodiesel yield could be achieved. This will help to bring algal biodiesel closer to cost effectiveness than ever before.

Contrary to literature, where temperatures were between 65 and >200 ^{o}C [363, 368], pressures as high as 1700 bar has been used [189], and sometimes involving supercritical fluids [233, 369], this work is based on ambient temperature and pressure. It is also important to note that in all of the cases cited above, moisture contents were less than 90%. Temperature is very essential to the success of biodiesel production as increasing temperature increase the fate of mass transfer and hence the rate of oil extraction and consequently, increase in biodiesel yield especially for acid catalysed process [370]. In a similar manner, solvent dosage is less while oil extraction rate is higher at increased pressure [370]. For a 20 hr reaction time, using 0.2 M H_2SO_4, the yield of FAME increased from 44.8 % to 74.5% to 85.1 % to 96.8 % when the temperature was increased from 40 to 50 to 60 to 70 ^{o}C, respectively [258], in a process involving 1:20 biomass to methanol (w/v) ratio. The impact of temperature is however, felt in the early stage of the process [370]. The heat requirement of oil extraction is however, reduced by

wet processing [35]. To this end, it is safe to say that with improvement on the current process (such as provisioning the column with a heating jacket), the reaction rate and indeed yield can be scaled up.

The lipid content of *D. salina* was calculated herein to be 16 ± 1 %, which agrees with the 5 – 25 % range in literature [344]. Elsewhere, more than 50 % of *D. salina* cell was said to be comprised of lipids and that over 30 % of the total lipids are aliphatic hydrocarbons [348]. However, whether or not the lipids were transesterifiable is another question. It is also possible that other reactions like the hydrolysis of polysaccharides during acid catalysis may have taken place. To this end, the effect of reaction time is less significant and hence other process parameters such as methanol to oil ratio, catalyst concentration, and mixing are potential culprits. Nevertheless, the successful biodiesel conversion achieved in a period of one hour is comparable with conventional processes where dried biomass were involved, in the sense of reaction time.

Although the effect of other process parameter like temperature, pressure, methanol to oil ratio, and catalyst concentration were not investigated in this work, there is a basis for comparison with other reported cases in the literature with respect to time. For example, after one hour of reaction time, 15 and 17 % yields were reported by Kamoru [340] from *N. oculata* and *C. vulgaris* respectively. Keeping other parameters i.e. methanol to oil ratio of 600:1, mixing rate of 450 rpm, temperature of 60 ^{o}C, and 8.5:1 acid to oil molar ratio, the maximum yield was 57.5 ± 3.6 % for *C. vulgaris* and 53.8 ± 8 % for *N. oculata* respectively at 24 h. However, within the same 24 h timeframe, when the acid concentration was increased from 0.087 to 0.15 μL per (mg algae), a 17 % and 62 % increase in FAME yield was recorded for *C. vulgaris* and *N. oculata*, respectively. These results are also in agreement with Velasquez-Orta et al. where dry biomass of *N. oculata* yielded a FAME conversion of 14 ± 2 % after 19 h in situ transesterification process at 60 ^{o}C using H_2SO_4: lipid molar ratio of 0.35:1 and a methanol: lipid molar ratio of 600:1.

Density of the 86 wt.% methanol solution (1.6 M H_2SO_4 in methanol) was 0.997 kg L^{-1}. Therefore, the volume of methanol needed per g of algae was 8.4 mL of methanol. In comparison to literature [257], where 69 % biodiesel yield was reported from *C. gracilis* at 400 % moisture content, using 7 mL of methanol, the achievement of 11 % biodiesel yield under extremely high water content of 10800 %, suggests a less amount of methanol per volume of water. Therefore if yield was a function of moisture content as alluded to in

the literature [292], biodiesel yield could be greatly enhanced by increasing CF amidst a heating source. In a related work, Sathish and Co [371], reported 83 % biodiesel yield after 30 min transesterification of a mixture of *Chlorella* and *Scenedesmus*, using 40 mL of a 5 % (v/v) H_2SO_4 in methanol. Thus, implying that 38 mL of methanol was needed to overcome the interference caused by the 84 % moisture content. Compared to this work, if the amount of methanol, temperature, time, and water content are assumed to be proportional to biodiesel yield, 38 mL of methanol consumption alone, would amount to 4 times the current yield (44 %). Unlike in literature [257, 292] and a lot more, the feedstock used in this work, was not prepared by dissolving freeze-dried algae in liquids (water and/or alcohol and/or homogenous catalyst). Nevertheless, only a cost analysis can justify the economic advantage of this work.

5.3.5 Cost analysis

The cost of air compression was modelled according to the air flow rate and feed flow rate of 2.4 L min^{-1} and 0.05 L min^{-1} (0.0024 and 0.00005 m^3 min^{-1}), respectively, used in harvesting *D. salina*. Therefore, the ratio of the volumetric flow rate of gas to the volumetric flow rate of microalgae feed was 48.

A summary of how the cost of air compressions and surfactants were arrived at is shown in Table 5.8.

R (J mol^{-1})	8.314
T_o (K)	293.15
η_{is}	0.7
P_1 (kPa)	113.4
P_0 (kPa)	101.3
$\gamma\ (air)$	1.4
W_{comp} (J mol^{-1} of gas)	399.27
W_{comp} (kWh mol^{-1} of gas)	$1.11*10^{-4}$
W_{comp} (kWh m^{-3} of gas)	$5.16*10^{-4}$
W_{comp} (kWh m^{-3} of algae)	0.248 [a]
Energy cost (US $ kWh^{-1})	0.017 [b]
Chemical cost (US$ m^{-3})	0.191 [c]
Total cost of harvesting 1 m^3 of algae (US$)	0.208

Table 5.8: Cost estimation of harvesting 1 m^3 of *D. salina* through foam flotation. The

airflow and feedflow were 2.4 L min^{-1} and 0.05 L min^{-1} (32 g min^{-1})

[a] The energy cost per m^3 of algae was calculated based on the ration of airflow to feedflow
[b] The cost in US dollars per kWh of electricity was calculated according to the latest data (6.70 Cents Kwh^{-1}) from the US Energy Information Administration May 2020 [353].
[c] The cost of chemicals namely: CTAB, chitosan, and saponin were calculated based on current bulk prices of US \$1 kg^{-1} (min order of 1 ton), US \$ 1.6 kg^{-1} (min order of 1 ton), and US \$ 3 kg^{-1} (min order of 7 tons), respectively (www.alibaba.com)

From Table 5.8, the cost of harvesting 1 kg of *D. salina* is US \$ 1.209, based on the cost of processing 1 m^3 of culture. This has taken into consideration, the 73 % recovery of the 235 mg L^{-1} culture. From the work of Lardon et al., the energy cost of culturing and harvesting is 7.5 MJ [35]. Minowa and Sawayama had estimated the energy cost of culturing alone to be 2.5 MJ [372]. If the cost of cultivation is 2.15 MJ, then the value in terms of electricity is 0.597 kWh or 0.04 US \$ kg^{-1} of *D. salina*. Therefore, the cost of cultivation and harvesting is \$ 1.249 kg^{-1}, which according Lardon et al., represents 6.99 % of the production energy. The remainder of the costs is distributed into 8.01 % for oil extraction, 84.16 % for drying, and 0.84 % for transesterification. Conversion from kWh to \$ is based on the conversion rates as obtainable from the latest energy review by BP (2019) [373].

In the work of Lardon et al, the cost of oil extraction was based on heat (22.4 MJ), hexane loss (55 g), and electricity (8.2 MJ) for wet algae. The energy cost of transesterification was based on heat (0.9 MJ) and methanol (114 g). In this work, however, none of the energy processes (heat or electricity), nor hexane losses were involved. Therefore, the cost of oil extraction is zero. The energy share of transesterification was based on heating and since heating was not involved in transesterification, this cost will be associated with methanol recovery. Therefore, the energy cost of drying (including cost of water and methanol removal) is 93 % of the production energy. Based on the energy cost of harvesting and culturing, the energy cost of production is \$18.64 kg^{-1} and the cost of drying is \$17.34 kg^{-1}, assuming 100 % of the water was driven off during drying. This figures are a bit lower than the estimates of \$ 20.53 $gallon^{-1}$ by Davis et al [374]. It should be noted however, that the cost of methanol recovery is not included.

During wet processing, 80 % of the biodiesel conversion cost was said to be related to material recovery such as methanol, catalysts, and co solvents, at operating temperatures

above 200 ^{O}C [366]. And when temperatures are ≤ 100 ^{O}C, the share of the costs associated with materials recover is 95 %. This temperature is high enough to recover both water and methanol. Using a 95 % recovery cost, based on the work of Lardon et al, the cost of materials recovery would be 0.86 MJ which is $ 0.016 kg^{-1} of algae. To this end, the cost of production would be $18.66 kg^{-1}. But if only 40 % of the initial water is to be driven off then the cost of drying would be $ 6.94 kg^{-1} and hence the total cost in energy terms of processing 1 kg of algae would be $ 8.19 kg^{-1}. Consequently, based on the current technology, the cost reduces to $ 8.21 kg^{-1}. This estimate is not only lower than $ 10.08 kg^{-1} proposed by Chisti [26], it is also lower than the average estimates of $10.87 gallon^{-1} to $13.32 gallon^{-1} by Davis et al [374], , and even much lower than the estimates of $ 20.53 gallon^{-1} by the same authors, regarding photo-bioreactor-cultured algae. However, considering the low yield of 11%, this process cannot be said to be competitively productive. Also, considering the fact that the quantity of biodiesel is proportional to the quantity of lipid [344], reworking current estimates for higher culture concentrations, would lead to availability of more lipid and hence more biodiesel, which is good for the overall economy of the process. Therefore, in order to improve on the cost implications of this technology, moisture content has to be further reduced as well operating at temperatures above ambient conditions. Beyond this, an LCA should be conduct to further establish the overall energy balance of the system.

5.4 Conclusions

By combining harvesting and transesterification, without drying steps, *D. salina* was successfully converted into biodiesel in a foam flotation column at ambient conditions of temperature and pressure. This is a positive deviation from reported cases of biodiesel production. Achieving biodiesel conversion in such an unprecedented manner is a huge improvement from the conventional in situ transesterification process and all other reported cases of wet biomass to biodiesel conversion. Besides the novelty of this process, it also has potential for huge reductions in cost of production.

The low biodiesel yield experienced is as a result of very high moisture content and low (room) temperatures. Therefore, in order to enhance the process economics, water contents must be reduced further and heating should be provided.

Cost analysis has shown that, with some improvement, this technology has the

potentials to render algal biodiesel cost effective.

It is expected that the concept demonstrated by this work will rekindle hope that was once associated with algal biodiesel as an alternative to liquid fossil fuels. Besides biodiesel, the presence of a wide range of lipid class in *D. salina* could see this technology been deployed for a variety of valuable biotechnological products. This is achievable by introducing the concept of biorefining into this technology.

Experimenting with lower airflow rates in collaboration with the use of freshwater strains like *C. vulgaris* which potentially guarantees lower moisture contents, is hereby recommended. The use of freshwater microalgae also returns higher concentration factors, thereby reducing the heavy impact of water on the biodiesel yield from this technology. However, lysing of *C. vulgaris* cell walls would require more acid than what has been used in the present work.

Chapter 6

Conclusion and recommendations for future work

6.1 Conclusions

For algal biodiesel to be commercially viable, the major process steps, namely: cultivation; harvesting; drying; transesterification of oil (two-step or in situ); and refining, needs to undergo some improvements in terms of process economy. By manipulating the microbiology of potential algal feedstock, growth media requirements and organic composition can be engineered to reduce water utilisation and oil contents. To this end, less energy would be expended in the cultivation of microalgae as biodiesel feedstock. The focus of this work is on the processing steps that proceed cultivation, which currently accounts for most of the process cost. Because of the importance of strain selection to biodiesel, this project handled three strains of microalgae; freshwater *C. vulgaris* and two marine species, *N. oculata* and *D. salina*. Although this work did not particularly target cost reduction from cultivation processes, it involved the use of a more sustainable feedstock in the form of marine microalgae, which implies a cost reduction in terms of environmental footprint.

The need to improve the foam floatation technology as a means for harvesting microalgae has been emphasised based on the cost reduction potential carried by the technology. To this end, this project aims to build on an earlier attempt to harvest *C. vulgaris* cells in a continuous foam flotation process. This means that foam flotation can now handle higher production volumes in shorter timescales in addition to other advantages like lowered unit cost as well as energy savings. In this work, the aforementioned advantages have been further extended to the flotation of marine algae.

This work has, for the for the firsts time, successfully achieved the foam floatation of marine algae using flotation column without mechanical components. In this regard, two marine species, *N. oculata* and *D. salina*, were harvested via foam flotation. Marine algae can be recovered by leveraging on increased bubble-particle attachment probability through the use of high airflow. Airflow of 3.6 L min^{-1} was enough to recover 86 % of *N. oculata* cells fed into the column at the rate of 100 mL min^{-1} when the culture pH was 6.

In order to increase the enrichment of *N. oculata* from 4 to 14, both airflow and CTAB concentrations were reduced to 2.4 L min^{-1} and 20 mg L^{-1}, respectively. Therefore, airflow, pH, and surfactant concentration are important factors to consider in order to successfully harvest marine algae. While increase surfactant concentrations and airflows favour algae recovery, lowered pH is good for both recovery and CF. CF is also favoured by reduced airflow and surfactant concentration. The presence of Na^+ in saltwater is capable of neutralising the Br^- head group in CTAB, thereby limiting the ability of CTAB to adsorb onto algae cells. This impact by Na^+ is however reduced by the introduction of H+ ions, which further compresses the diffused layer and facilitate better algae-surfactant attachment.

Also important are, surfactant type, cell properties (morphology and surface charge).Contrary to what is obtainable with freshwater species of microalgae, the knowledge of ζ - potential values measured under marine conditions, are not sufficient to determine whether microalgae cells can be harvested by foam flotation or not due to the condensed stern layer in seawater, which resists the electrophoretic mobility of the cells. The measured ζ - potential in this case, reflects a smaller value of potential difference compared to the actual difference in potential. Furthermore, relying on the preferential transfer of organic matter into the hexane phase in a water-hexane system, as a measure of hydrophobicity should be avoided as this method could be misleading when marine microalgae are involved. For example, in measuring the hydrophobicity of *N. oculata* in CTAB, formation of CTAB-organic matter complexes was observed, which interferes with absorbance measurement. The presence of algaenan in *N. oculata* does not only reduce the effect of CTAB as a collector, but it also prevents cell lysis by CTAB, even under acidic conditions. This project has demonstrated the capability of foam flotation to handle very small microalgae cells therefore increasing the versatility of foam flotation as a harvesting technology, in addition to the capacity to handle a mixed culture.

A simple cost analysis on the cost of air compression reveals that this process has better economic advantages than the only available literature where marine algae were harvested via foam flotation. In this work, 2.4 L min^{-1} was used as opposed to 5 L min^{-1} used in literature. The involvement of a Jameson's cell (mechanical device) in literature gives additional advantage to this work in terms of process economy. Furthermore, in terms of deliverables, the potentials for lipids are higher in this this work (20-56 %) than literature

(20-30 %), and therefore better suited for algal biodiesel. The use of foam flotation to harvest *N. oculata* can easily be scaled up compared to literature.

In order to achieve transesterification of algal oil in the flotation column, adequate supply of methanol in essential. To this end, this research has made it possible for a countercurrent injection of methanol into the column. This effective methanol supply made possible with the aid of distributors, capable of ensuring that methanol was supplied in the right concentration fit for transesterification reaction. Between 1.5 to 4.5 g L^{-1} of methanol injection is possible with the aid of distributors with hole sizes ranging from 0.5 to 3 mm. Therefore, monitoring and regulating the amount of methanol available for transesterification is possible in a combined harvesting-methanol injection system. Foam stability is a function of methanol flow rate and concentration in the bulk phase (mixing zone), surfactant concentration, airflow, column height, and operating mode (batch or continuous). The concentration and mass of methanol in the foamate vary in continuous flotation while only very little variation in methanol concentration is possible in batch flotation. Unlike mass of methanol in the foamate, the concentration is a functional of time, irrespective of flotation mode. This provides a means for controlling and regulating the amount of methanol in the foamate. Contrary to batch flotation, there is a significant increase in the concentration of methanol in the foamate over time. This intensification is capable of facilitating algal oil extraction and eventual biodiesel production in a foam flotation column. The final concentration of methanol in the foamate was between 70 and 76 %. A methanol balance reveals that methanol accumulation occurs but can be reduced by increasing airflow and CTAB concentration, in addition to the introduction of foam riser. The introduction of foam riser also increased particle enrichment by encouraging bubble coalescence. The positioning of the riser close to the column top made both foam enrichment and reduced methanol accumulation possible because of the separation distance between the bulk liquid and foam.

The cocurrent methanol feed process without distributors allow for longer contact time between algae and methanol. The critical concentration of methanol in CTAB solution is 50 %, beyond which generation of stable foams are not possible, and this is an important point to note if it is desired to foam a ternary system containing water-methanol-CTAB. Compared to freshwater media, seawater allowed for better concentration of methanol because smaller bubbles are less prone to the collapse and coalescence that could result

from methanol infusion. Using a 50 % methanol in *C. vulgaris* culture, foam floatation with methanol enrichment was used to successfully recover 98 % of algae with a CF of 18.3 where liquid content (water and methanol) was 156 wt. %.

Based on the intensified technology, transesterification of algal oil to biodiesel was achieved. Before proceeding with transesterification, harvesting of *D. salina* was investigated under different conditions of airflow, surfactant type and concentration. The brackish nature of the *D. salina* media was responsible for the low performance (Recovery and CF) compared to *N. oculata.* Performance of the floatation column was better with *N. oculata* than was with *D. salina*. This is because the concentration of Na^+ in *D. salina* media is higher than that in *N. oculata*. The lack of cell walls in *D. salina*, however, made it a better candidate for this work. Consequently, cell lysis was achieved in *D. salina* as opposed to *N. oculata*, when 50 mg L^{-1} of CTAB was used. This made it possible to combine the methanol injection process with harvesting of *D. salina*, which ultimately gave for transesterification at the top of the column. 73 % of cells were recovered and converted to biodiesel with 9 and 11 % yields, after a reaction time of 1 hr and 24 h, via H_2SO_4 catalyst. Achieving transesterification was possible due to the effective availability of methanol in terms of amount and concentration. This reactive extraction was carried out at ambient conditions of temperature and pressure. Biodiesel conversion was achieved at 108000 % moisture content in *D. salina*. The low yield of biodiesel can be corrected if the operating temperatures and water content are modified. Increased temperature and reduced moisture contents in the foamate are capable of increasing the biodiesel yield.

To justify the potential cost savings of this work, a cost analysis was carried out. The cost of production was estimated to be less than current literature values, mainly due to the reduced drying duty by 60 %. To this end, at least $ 3.21 can be saved per kg of biodiesel produced. If algae concentrations of approximately 1 g L^{-1} were used, the cost savings could be higher than current estimates. Although current operating conditions present lower cost of production as a result of the combined process, only an increase in current yields would guarantee the cost effectiveness of the technology. It is expected that the concept proven by this work would rekindle the hope that was once associated with algal biodiesel as an alternative to liquid fossil fuels.

Compared to the highest amount of moisture (400 %) so far reported in literature, this work has further narrowed down the offset in cost of additional methanol volume as a

function of increased moisture content in algal biodiesel production.

The technology hereby proposed can be deployed in the form of floating rigs that allow for a combined capture of marine blooms and the conversion of same into useful products like pharmaceutical raw materials, food supplements, and biodiesel, on site. Such environmental and water sanitation strategy is priceless. The potential for high value products is also of great economic importance.

6.2 Recommendations

In order to improve upon the low biodiesel yields, efforts should be made to reduce the moisture contents below the current values. In addition, the provision of a source of heat would greatly increase the reaction rate and therefore increase biodiesel yield. To increase the enrichment of cells, foam flotation can be combined with other methods like filtration, although this could mean that the transesterification process is going to be done in as separate unit.

The inoculation of algaenan-consuming fungi into the cultivation of *N. oculata* to produce algaenan-free hybrid that will be less problematic to recover and lyse should be looked into. This would be a great addition to the numerous microbiological and genetic modifications currently aimed at sustainable algal biodiesel as well as other products from algae, e.g. biocomposites.

The use of XDLVO theory is hereby recommended to allow for better understanding and estimation of the hydrophobic and hydrophilic forces that are in play within the colloidal system of algal culture, in the presence of surfactants, which has been proven to be highly acid-base interaction dependant in marine environments. This would bring about a more efficient deployment of foam flotation technology as a tool for harvesting marine microalgae. The XDLVO allows for the interfacial forces of solids and liquid components to be measured, making it possible for the acid-base component of the total colloid energy to be estimated.

Experimenting with lower airflow rates along with the use of freshwater strains like *C. vulgaris* is equally recommended. *C. vulgaris* has a higher growth rate and density than *D. salina* which means more oil for the same quantity, and hence higher biodiesel yield. The use of freshwater microalgae also guarantees higher concentration factors, thereby reducing the heavy impact of water on the biodiesel yield from this technology. Increased

acid concentration is also recommended with *N. oculata* as a measure for cell lysis.

The use of foam floatation as both a harvesting and conversion unit can be harnessed towards the cleaning of contaminated water, especially in countries like China where marine blooms seem to have become a major environmental issue. On one hand, rivers and lakes can be made useful as a source of drinking and other domestic use, and on the other, the algae bloom is converted to energy. This would require the mounting of a rig like the one used in this experiment on a buoy. Because this process is multi-feed compatible, it means that no sorting of the bloom will be required, thereby giving the process an additional cost benefit.

Detailed life cycle analysis (LCA) is required to establish whether or not the cost savings from elimination of drying steps, in this novel technology, has affected the overall process cost, particularly the refining process which has not been investigated in this work.

The intensification process hereby proposed can be carried out using flocculation as the harvesting technology instead of flotation. This is because flocculation is better suited for harvesting marine algae due to the action of salt ions in support of flocculation rather than flotation.

References

1. Musa, S.D., T. Zhonghua, A.O. Ibrahim, and M. Habib, *China's energy status: A critical look at fossils and renewable options.* Renewable and Sustainable Energy Reviews, 2018. **81**: p. 2281-2290.
2. BP. *Statistical review of world energy 2020*. 2020 [cited 2020 28/08]; Available from: https://www.bp.com/en/global/corporate/energy-economics/statistical-review-of-world-energy.html.
3. Bartlett, A.A., *Forgotten fundamentals of the energy crisis.* American Journal of Physics, 1978. **46**(9): p. 876-888.
4. LiveScience. *We will not run out of fossil fuels*. 2013 [cited 2016 17, April]; Available from: http://www.livescience.com/37469-fuel-endures.html.
5. Wikipedia. 2015; Available from: https://en.wikipedia.org/wiki/Paris_Agreement.
6. UN. *Sustainable development goals*. 2019; Available from: http://www.un.org/sustainabledevelopment/energy/.
7. Muntean, M., Guizzardi, D., Schaaf, E., Crippa, M., Solazzo, E., Olivier, J.G.J., Vignati, E. , *Fossil co2 emissions of all world countries - 2018 report*, in *EUR 29433 EN*. 2018: Publications Office of the European Union, Luxembourg.
8. Rafael Luque, J.C. and a.J. Clark, *Handbook of biofuels production - processes and technologies*, ed. J.C. Rafael Luque and a.J. Clark. 2011: Woodhead Publishing Series in Energy. 659.
9. Fernandes, S.D., N.M. Trautmann, S.D. G, C.A. Roden, and T.C. Bond., *Global biofuel use, 1850–2000.* Global Biogeochemical Cycles, 2007. **Vol 21**.
10. Webb, A. and D. Coates. *Biofuels and biodiversity. Secretariat of the convention on biological diversity montreal, technical series no. 65, 69 pages*. 2012.
11. Radich, A., *Biodiesel performance, costs, and use.* Combustion., 1998. **24**(2): p. 131-132.
12. Kovarik, B., *Henry ford, charles f. Kettering and the fuel of the future.* Automotive History Review 1998. **32**: p. 7–27.
13. EBTP. *Advanced biofuels in europe*. 2016 [cited 2016 30 September]; Available from: http://www.biofuelstp.eu/advancedbiofuels.htm.
14. Ma, F. and M.A. Hanna, *Biodiesel production: A review1*. Bioresource Technology, 1999. **70**(1): p. 1-15.
15. IRENA, E., *Renewable energy prospects for the european union*, A.Z. Amin, Editor. 2018. p. 120.
16. Lee, R.A.L., Jean-Michel, *From first- to third-generation biofuels: Challenges of producing a commodity from a biomass of increasing complexity.* Animal Frontiers, 2013. **3**: p. 6-11.
17. Scott, S.A., M.P. Davey, J.S. Dennis, I. Horst, C.J. Howe, D.J. Lea-Smith, and A.G. Smith, *Biodiesel from algae: Challenges and prospects.* Curr Opin Biotechnol, 2010. **21**(3): p. 277-86.
18. Roessler, J.S.T.D.J.B.P., *A look back at the u.S. Department of energy's aquatic species program: Biodiesel from algae*. 1998, National Renewable Energy Laboratory: Golden, Colorado 80401-3393. p. 1–328.
19. Coward, T., *Foam fractionation : An effective technology for harvesting microalgae biomass*, in *School of Chemical, Engineering Advanced, Materials*. 2012, Newcastle University: Newcastle upon Tyne. p. 200.
20. Demirbasa, A. and M.F. Demirbasb, *Importance of algae oil as a source of biodiesel.* Energy Conversion and Management, 2011: p. 163–170.
21. Ghasemi, Y., S. Rasoul-Amini, Naseri, A T, N. Montazeri-Najafabady, M.A. Mobasher, and F. Dabbagh, *Microalgae biofuel potentials (review).* Applied Biochemistry and Microbiology 2012: p. 126-144
22. Pittman, J.K., A.P. Dean, and O. Osundeko, *The potential of sustainable algal biofuel production using wastewater resources.* Bioresource Technology, 2011: p. 17-25.

23. Leite, G.B., A.E. Abdelaziz, and P.C. Hallenbeck, *Algal biofuels: Challenges and opportunities.* bioresource technology, 2013: p. 134-141.
24. Kim, J., G. Yoo, H. Lee, J. Lim, K. Kim, C.W. Kim, M.S. Park, and J.W. Yang, *Methods of downstream processing for the production of biodeisel from microalgae.* Biotechnol Adv, 2013: p. 862-876.
25. NRE, A.D., *Recent and current research & roadmapping activities: Overview*, N.R.E.L. (U.S.), Editor. 2008.
26. Chisti, Y., *Biodiesel from microalgae.* Biotechnol Adv, 2007. **25**(3): p. 294-306.
27. Chisti, Y., *Biodiesel from microalgae.* Biotechnology Advances, 2007. **25**(3): p. 294–306.
28. James, W.R., L.O. Joe, and A. Marc, *The economics of microalgae oil.* 2009. **13**(2).
29. Sun, A., R. Davis, M. Starbuck, A. Ben-Amotz, R. Pate, and P.T. Pienkos, *Comparative cost analysis of algal oil production for biofuels.* Energy, 2011. **36**(8): p. 5169-5179.
30. Suna, A., R. Davisb, M. Starbuckc, A. Ben-Amotze, R. Patea, and P.T. Pienkos, *Comparative cost analysis of algal oil production for biofuels.* Energy, 2011. **36**(8): p. 5169-5179.
31. Davis, R., A. Aden, and P.T. Pienkos, *Techno-economic analysis of autotrophic microalgae for fuel production.* Applied Energy, 2011. **88**(10): p. 3524–3531.
32. Velasquez-Orta, S.B., J.G.M. Lee, and A.P. Harvey, *Evaluation of fame production from wet marine and freshwater microalgae by in situ transesterification.* Biochemical Engineering Journal, 2013. **76**: p. 83-89.
33. Šoštarič, M., D. Klinar, M. Bricelj, J. Golob, M. Berovič, and B. Likozar, *Growth, lipid extraction and thermal degradation of the microalga chlorella vulgaris.* New Biotechnology, 2012. **29**(3): p. 325-331.
34. Molina Grima, E., E.H. Belarbi, F.G. Acién Fernández, A. Robles Medina, and Y. Chisti, *Recovery of microalgal biomass and metabolites: Process options and economics.* Biotechnology Advances, 2003. **20**(7–8): p. 491-515.
35. Lardon, L., A. Hélias, B. Sialve, J.-P. Steyer, and O. Bernard, *Life-cycle assessment of biodiesel production from microalgae.* Environmental Science & Technology, 2009. **43**(17): p. 6475-6481.
36. Xu, L., D.W.F. Brilman, J.A.M. Withag, G. Brem, and S. Kersten, *Assessment of a dry and a wet route for the production of biofuels from microalgae: Energy balance analysis.* Bioresource Technology, 2011. **102**(8): p. 5113-5122.
37. Salam, K.A., S.B. Velasquez-Orta, and A.P. Harvey, *A sustainable integrated in situ transesterification of microalgae for biodiesel production and associated co-product-a review.* Renewable and Sustainable Energy Reviews, 2016. **65**: p. 1179-1198.
38. Coward, T., J.G.M. Lee, and G.S. Caldwell, *Harvesting microalgae by ctab-aided foam flotation increases lipid recovery and improves fatty acid methyl ester characteristics.* Biomass and Bioenergy, 2014. **67**: p. 354-362.
39. Salam, K.A., S.B. Velasquez-Orta, and A.P. Harvey, *Kinetics of fast alkali reactive extraction/in situ transesterification of chlorella vulgaris that identifies process conditions for a significant enhanced rate and water tolerance.* Fuel Processing Technology, 2016. **144**: p. 212-219.
40. Coward, T., J.G.M. Lee, and G.S. Caldwell, *Development of a foam flotation system for harvesting microalgae biomass.* Algal Research, 2013. **2**(2): p. 135-144.
41. Kanhaiya Kumar, S.K.M., Gang-Guk Choi, and Ji-Won Yang, *Bottlenecks in the algal biomass production*, in *Algal biorefinery*, D. Das, Editor. 2015. p. 44-48.
42. Rawat, I., R. Ranjith Kumar, T. Mutanda, and F. Bux, *Dual role of microalgae: Phycoremediation of domestic wastewater and biomass production for sustainable biofuels production.* Applied Energy, 2011. **88**(10): p. 3411-3424.
43. Danquah, M.K., B. Gladman, N. Moheimani, and G.M. Forde, *Microalgal growth characteristics and subsequent influence on dewatering efficiency.* Chemical Engineering Journal, 2009. **151**(1): p. 73-78.

44. Barros, A.I., A.L. Gonçalves, M. Simões, and J.C.M. Pires, *Harvesting techniques applied to microalgae: A review.* Renewable and Sustainable Energy Reviews, 2015. **41**(Supplement C): p. 1489-1500.
45. Brennan, L.O., Philip, *Biofuels from microalgae—a review of technologies for production, processing, and extractions of biofuels and co-products.* Renewable and Sustainable Energy Reviews, 2010. **14**(2): p. 557-577.
46. Taylor, R.L., J.D. Rand, and G.S. Caldwell, *Treatment with algae extracts promotes flocculation, and enhances growth and neutral lipid content in nannochloropsis oculata-a candidate for biofuel production.* Marine Biotechnology, 2012. **14**(6): p. 774-781.
47. Weschler, M.K., W.J. Barr, W.F. Harper, and A.E. Landis, *Process energy comparison for the production and harvesting of algal biomass as a biofuel feedstock.* Bioresource Technology, 2014. **153**: p. 108-115.
48. Chen, C.-L., J.-S. Chang, and D.-J. Lee, *Dewatering and drying methods for microalgae.* Drying Technology, 2015. **33**(4): p. 443-454.
49. Brennan, L. and P. Owende, *Biofuels from microalgae—a review of technologies for production, processing, and extractions of biofuels and co-products.* Renewable and Sustainable Energy Reviews, 2010. **14**(2): p. 557-577.
50. Henderson, R., S.A. Parsons, and B. Jefferson, *The impact of algal properties and pre-oxidation on solid–liquid separation of algae.* Water Research, 2008. **42**(8): p. 1827-1845.
51. Liu, J.C., Y.M. Chen, and Y.-H. Ju, *Separation of algal cells from water by column flotation.* Separation Science and Technology, 1999. **34**(11): p. 2259-2272.
52. Chen, C.-Y., K.-L. Yeh, R. Aisyah, D.-J. Lee, and J.-S. Chang, *Cultivation, photobioreactor design and harvesting of microalgae for biodiesel production: A critical review.* Bioresource Technology, 2011. **102**(1): p. 71-81.
53. Granados, M.R., F.G. Acién, C. Gómez, J.M. Fernández-Sevilla, and E. Molina Grima, *Evaluation of flocculants for the recovery of freshwater microalgae.* Bioresource Technology, 2012. **118**: p. 102-110.
54. Singh, G. and S.K. Patidar, *Microalgae harvesting techniques: A review.* Journal of Environmental Management, 2018. **217**: p. 499-508.
55. Lee, A.K., D.M. Lewis, and P.J. Ashman, *Harvesting of marine microalgae by electroflocculation: The energetics, plant design, and economics.* Applied Energy, 2013. **108**: p. 45-53.
56. Dassey, A.J. and C.S. Theegala, *Reducing electrocoagulation harvesting costs for practical microalgal biodiesel production.* Environmental Technology, 2014. **35**(6): p. 691-697.
57. Vandamme, D., S.C.V. Pontes, K. Goiris, I. Foubert, L.J.J. Pinoy, and K. Muylaert, *Evaluation of electro-coagulation–flocculation for harvesting marine and freshwater microalgae.* Biotechnology and Bioengineering, 2011. **108**(10): p. 2320-2329.
58. Knuckey, R.M., M.R. Brown, R. Robert, and D.M.F. Frampton, *Production of microalgal concentrates by flocculation and their assessment as aquaculture feeds.* Aquacultural Engineering, 2006. **35**(3): p. 300-313.
59. Pezzolesi, L., C. Samorì, and R. Pistocchi, *Flocculation induced by homogeneous and heterogeneous acid treatments in desmodesmus communis.* Algal Research, 2015. **10**: p. 145-151.
60. Christenson, L. and R. Sims, *Production and harvesting of microalgae for wastewater treatment, biofuels, and bioproducts.* Biotechnology Advances, 2011. **29**(6): p. 686-702.
61. Wu, Z., Y. Zhu, W. Huang, C. Zhang, T. Li, Y. Zhang, and A. Li, *Evaluation of flocculation induced by ph increase for harvesting microalgae and reuse of flocculated medium.* Bioresource Technology, 2012. **110**: p. 496-502.
62. Vandamme, D., I. Foubert, I. Fraeye, B. Meesschaert, and K. Muylaert, *Flocculation of chlorella vulgaris induced by high ph: Role of magnesium and calcium and practical implications.* Bioresource Technology, 2012. **105**: p. 114-119.

63. García-Pérez, J.S., A. Beuckels, D. Vandamme, O. Depraetere, I. Foubert, R. Parra, and K. Muylaert, *Influence of magnesium concentration, biomass concentration and ph on flocculation of chlorella vulgaris.* Algal Research, 2014. **3**: p. 24-29.
64. Lee, A.K., D.M. Lewis, and P.J. Ashman, *Microbial flocculation, a potentially low-cost harvesting technique for marine microalgae for the production of biodiesel.* Journal of Applied Phycology, 2009. **21**(5): p. 559-567.
65. Frølund, B., R. Palmgren, K. Keiding, and P.H. Nielsen, *Extraction of extracellular polymers from activated sludge using a cation exchange resin.* Water Research, 1996. **30**(8): p. 1749-1758.
66. Toeda, K. and R. Kurane, *Microbial flocculant from alcaligenes cupidus kt201.* Agricultural and Biological Chemistry, 1991. **55**(11): p. 2793-2799.
67. Yokoi, H., T. Yoshida, S. Mori, J. Hirose, S. Hayashi, and Y. Takasaki, *Biopolymer flocculant produced by an enterobacter sp.* Biotechnology Letters, 1997. **19**(6): p. 569-573.
68. Salehizadeh, H., M. Vossoughi, and I. Alemzadeh, *Some investigations on bioflocculant producing bacteria.* Biochemical Engineering Journal, 2000. **5**(1): p. 39-44.
69. Zajic, J.E. and A. LeDuy, *Flocculant and chemical properties of a polysaccharide from pullularia pullulans.* Applied microbiology, 1973. **25**(4): p. 628-635.
70. Kurane, R., K. Toeda, K. Takeda, and T. Suzuki, *Culture conditions for production of microbial flocculant by rhodococcus erythropolis.* Agricultural and Biological Chemistry, 1986. **50**(9): p. 2309-2313.
71. Salim, S., M.H. Vermuë, and R.H. Wijffels, *Ratio between autoflocculating and target microalgae affects the energy-efficient harvesting by bio-flocculation.* Bioresource Technology, 2012. **118**: p. 49-55.
72. Japar, A.S., M.S. Takriff, and N.H.M. Yasin, *Harvesting microalgal biomass and lipid extraction for potential biofuel production: A review.* Journal of Environmental Chemical Engineering, 2017. **5**(1): p. 555-563.
73. Dassey, A.J. and C.S. Theegala, *Harvesting economics and strategies using centrifugation for cost effective separation of microalgae cells for biodiesel applications.* Bioresource Technology, 2013. **128**: p. 241-245.
74. Petruševski, B., G. Bolier, A.N. Van Breemen, and G.J. Alaerts, *Tangential flow filtration: A method to concentrate freshwater algae.* Water Research, 1995. **29**(5): p. 1419-1424.
75. Hwang, T., S.-J. Park, Y.-K. Oh, N. Rashid, and J.-I. Han, *Harvesting of chlorella sp. Kr-1 using a cross-flow membrane filtration system equipped with an anti-fouling membrane.* Bioresource Technology, 2013. **139**: p. 379-382.
76. Show, K.-Y., D.-J. Lee, and A.S. Mujumdar, *Advances and challenges on algae harvesting and drying.* Drying Technology, 2015. **33**(4): p. 386-394.
77. Abdelaziz, A.E.M., G.B. Leite, and P.C. Hallenbeck, *Addressing the challenges for sustainable production of algal biofuels: Ii. Harvesting and conversion to biofuels.* Environmental Technology, 2013. **34**(13-14): p. 1807-1836.
78. Esen, I.I., K. Puskas, I.M. Banat, and R. Al-Daher, *Algae removal by sand filtration and reuse of filter material.* Waste Management, 1991. **11**(1): p. 59-65.
79. Brink, J. and S. Marx, *Harvesting of hartbeespoort dam micro-algal biomass through sand filtration and solar drying.* Fuel, 2013. **106**: p. 67-71.
80. Lin, C.-C. and P.K.A. Hong, *A new processing scheme from algae suspension to collected lipid using sand filtration and ozonation.* Algal Research, 2013. **2**(4): p. 378-384.
81. Ahmad, A.L., N.H. Mat Yasin, C.J.C. Derek, and J.K. Lim, *Crossflow microfiltration of microalgae biomass for biofuel production.* Desalination, 2012. **302**: p. 65-70.
82. Gerardo, M.L., D.L. Oatley-Radcliffe, and R.W. Lovitt, *Integration of membrane technology in microalgae biorefineries.* Journal of Membrane Science, 2014. **464**: p. 86-99.
83. Zacharof, M.-P. and R.W. Lovitt, *The filtration characteristics of anaerobic digester effluents employing cross flow ceramic membrane microfiltration for nutrient recovery.* Desalination, 2014. **341**: p. 27-37.

84. Gerardo, M.L., D.L. Oatley-Radcliffe, and R.W. Lovitt, *Minimizing the energy requirement of dewatering scenedesmus sp. By microfiltration: Performance, costs, and feasibility.* Environmental Science & Technology, 2014. **48**(1): p. 845-853.
85. Uduman, N., Y. Qi, M.K. Danquah, G.M. Forde, and A. Hoadley, *Dewatering of microalgal cultures: A major bottleneck to algae-based fuels.* Journal of Renewable and Sustainable Energy, 2010. **2**(1): p. 012701.
86. Heasman, M., J. Diemar, W. O'Connor, T. Sushames, and L. Foulkes, *Development of extended shelf-life microalgae concentrate diets harvested by centrifugation for bivalve molluscs – a summary.* Aquaculture Research, 2000. **31**(8‐9): p. 637-659.
87. L., G., *Microalgae as a feedstock for biofuels.* 2011, Berlin, Heidelberg: Springer. 76.
88. Matis, K.A. and P. Mavros, *Recovery of metals by ion flotation from dilute aqueous solutions.* Separation and Purification Methods, 1991. **20**(1): p. 1-48.
89. Phoochinda, W. and D.A. White, *Removal of algae using froth flotation.* Environmental Technology, 2003. **24**(1): p. 87-96.
90. Chen, Y.M., J.C. Liu, and Y.-H. Ju, *Flotation removal of algae from water.* Colloids and Surfaces B: Biointerfaces, 1998. **12**(1): p. 49-55.
91. Phoochinda, W., D.A. White, and B.J. Briscoe, *Comparison between the removal of live and dead algae using froth flotation.* Journal of Water Supply: Research and Technology - AQUA, 2005. **54**(2): p. 115-125.
92. Garg, S., Y. Li, L. Wang, and P.M. Schenk, *Flotation of marine microalgae: Effect of algal hydrophobicity.* Bioresource Technology, 2012. **121**(Supplement C): p. 471-474.
93. Kurniawati, H.A., S. Ismadji, and J.C. Liu, *Microalgae harvesting by flotation using natural saponin and chitosan.* Bioresource Technology, 2014. **166**: p. 429-434.
94. Garg, S., L. Wang, and P.M. Schenk, *Effective harvesting of low surface-hydrophobicity microalgae by froth flotation.* Bioresource Technology, 2014. **159**: p. 437-441.
95. Xu, L., F. Wang, H.Z. Li, Z.M. Hu, C. Guo, and C.Z. Liu, *Development of an efficient electroflocculation technology integrated with dispersed ‐air flotation for harvesting microalgae.* Journal of Chemical Technology & Biotechnology, 2010. **85**(11): p. 1504-1507.
96. Csordas, A. and J.-K. Wang, *An integrated photobioreactor and foam fractionation unit for the growth and harvest of chaetoceros spp. In open systems.* Aquacultural Engineering, 2004. **30**(1-2): p. 15-30.
97. Levin, G.V., J.R. Clendenning, A. Gibor, and F.D. Bogar, *Harvesting of algae by froth flotation.* Applied Microbiology, 1962. **10**(2): p. 169-175.
98. Choi, S.J. and K.H. Kim, *The improvement of the removal efficiency of foam flotation by the synergistic effect of mixed surfactant solutions.* Environmental Technology, 1998. **19**(11): p. 1151-1156.
99. Henderson, R.K., S.A. Parsons, and B. Jefferson, *The potential for using bubble modification chemicals in dissolved air flotation for algae removal.* Separation Science and Technology, 2009. **44**(9): p. 1923-1940.
100. Henderson, R.K., S.A. Parsons, and B. Jefferson, *Surfactants as bubble surface modifiers in the flotation of algae: Dissolved air flotation that utilizes a chemically modified bubble surface.* Environmental Science & Technology, 2008. **42**(13): p. 4883-4888.
101. Garg, S., L. Wang, and P.M. Schenk, *Flotation separation of marine microalgae from aqueous medium.* Separation and Purification Technology, 2015. **156**: p. 636-641.
102. Coward, T., J.G. Lee, and G.S. Caldwell, *The effect of bubble size on the efficiency and economics of harvesting microalgae by foam flotation.* J Appl Phycol, 2015. **27**(2): p. 733-742.
103. Hanotu, J., H.C.H. Bandulasena, and B. Zimmerman William, *Microflotation performance for algal separation.* Biotechnology and Bioengineering, 2012. **109**(7): p. 1663-1673.
104. Laamanen, C.A., G.M. Ross, and J.A. Scott, *Flotation harvesting of microalgae.* Renewable and Sustainable Energy Reviews, 2016. **58**(Supplement C): p. 75-86.

105. Henderson, R.K., S.A. Parsons, and B. Jefferson, *The impact of differing cell and algogenic organic matter (aom) characteristics on the coagulation and flotation of algae.* Water Research, 2010. **44**(12): p. 3617-3624.
106. Rubio, J., M.L. Souza, and R.W. Smith, *Overview of flotation as a wastewater treatment technique.* Minerals Engineering, 2002. **15**(3): p. 139-155.
107. Bennett, N.K.S.a.G.F., *Principles of air flotation technology*, in *Handbook of environmental engineering: Flotation technologyedited*, L.K.W.e. al., Editor. 2010, Springer Science and Business Media, LLC. p. 694.
108. Prakash, R., S.K. Majumder, and A. Singh, *Flotation technique: Its mechanisms and design parameters.* Chemical Engineering and Processing - Process Intensification, 2018. **127**: p. 249-270.
109. Alhattab, M. and M.S.-L. Brooks, *Dispersed air flotation and foam fractionation for the recovery of microalgae in the production of biodiesel.* Separation Science and Technology, 2017: p. 1-15.
110. Wiley, P.E., K.J. Brenneman, and A.E. Jacobson, *Improved algal harvesting using suspended air flotation.* Water Environment Research, 2009. **81**(7): p. 702-708.
111. Kwak, D.-H. and M.-S. Kim, *Flotation of algae for water reuse and biomass production: Role of zeta potential and surfactant to separate algal particles.* Water Science and Technology, 2015. **72**(5): p. 762.
112. Zimmerman, W.B., V. Tesař, and H.C.H. Bandulasena, *Towards energy efficient nanobubble generation with fluidic oscillation.* Current Opinion in Colloid & Interface Science, 2011. **16**(4): p. 350-356.
113. Zimmerman, W.B., B.N. Hewakandamby, V. Tesař, H.C.H. Bandulasena, and O.A. Omotowa, *On the design and simulation of an airlift loop bioreactor with microbubble generation by fluidic oscillation.* Food and Bioproducts Processing, 2009. **87**(3): p. 215-227.
114. William, B.Z., T. Vaclav, B. Simon, and C.H.B. Himiyage, *Microbubble generation.* Recent Patents on Engineering, 2008. **2**(1): p. 1-8.
115. Kim, J., B.-G. Ryu, B.-K. Kim, J.-I. Han, and J.-W. Yang, *Continuous microalgae recovery using electrolysis with polarity exchange.* Bioresource Technology, 2012. **111**: p. 268-275.
116. Andrade, M., *Heavy metal removal from bilge water by electrocoagulation treatment*. 2019.
117. Zouboulis, A.I., K.A. Matis, and G.A. Stalidis, *Flotation techniques in waste water treatment*, in *Innovations in flotation technology*, P. Mavros and K.A. Matis, Editors. 1992, Springer Netherlands: Dordrecht. p. 475-497.
118. Zhang, H. and X. Zhang, *Microalgal harvesting using foam flotation: A critical review.* Biomass and Bioenergy, 2019. **120**: p. 176-188.
119. Gerardo, M.L., S. Van Den Hende, H. Vervaeren, T. Coward, and S.C. Skill, *Harvesting of microalgae within a biorefinery approach: A review of the developments and case studies from pilot-plants.* Algal Research, 2015. **11**: p. 248-262.
120. Okada, K., Y. Akagi, M. Kogure, and N. Yoshioka, *Effect on surface charges of bubbles and fine particles on air flotation process.* The Canadian Journal of Chemical Engineering, 1990. **68**(3): p. 393-399.
121. Banerjee, C., S. Ghosh, G. Sen, S. Mishra, P. Shukla, and R. Bandopadhyay, *Study of algal biomass harvesting through cationic cassia gum, a natural plant based biopolymer.* Bioresource Technology, 2014. **151**: p. 6-11.
122. Aulenbach, D.B., N.K. Shammas, L.K. Wang, and R.C. Marvin, *Algae removal by flotation*, in *Flotation technology: Volume 12*, L.K. Wang, et al., Editors. 2010, Humana Press: Totowa, NJ. p. 363-399.
123. Schlesinger, A., D. Eisenstadt, A. Bar-Gil, H. Carmely, S. Einbinder, and J. Gressel, *Inexpensive non-toxic flocculation of microalgae contradicts theories; overcoming a major hurdle to bulk algal production.* Biotechnology Advances, 2012. **30**(5): p. 1023-1030.
124. Ahmad, A.L., N.H. Mat Yasin, C.J.C. Derek, and J.K. Lim, *Optimization of microalgae coagulation process using chitosan.* Chemical Engineering Journal, 2011. **173**(3): p. 879-882.

125. Pragya, N., K.K. Pandey, and P.K. Sahoo, *A review on harvesting, oil extraction and biofuels production technologies from microalgae.* Renewable and Sustainable Energy Reviews, 2013. **24**: p. 159-171.
126. Kim, S.G., A. Choi, C.Y. Ahn, C.S. Park, Y.H. Park, and H.M. Oh, *Harvesting of spirulina platensis by cellular flotation and growth stage determination.* Letters in Applied Microbiology, 2005. **40**(3): p. 190-194.
127. Barrut, B., J.-P. Blancheton, A. Muller-Feuga, F. René, C. Narváez, J.-Y. Champagne, and A. Grasmick, *Separation efficiency of a vacuum gas lift for microalgae harvesting.* Bioresource Technology, 2013. **128**: p. 235-240.
128. Shahbazi, B., B. Rezai, and S.M. Javad Koleini, *Bubble–particle collision and attachment probability on fine particles flotation.* Chemical Engineering and Processing: Process Intensification, 2010. **49**(6): p. 622-627.
129. Basařová, P. and M. Hubička, *The collision efficiency of small bubbles with large particles.* Minerals Engineering, 2014. **66-68**: p. 230-233.
130. Shen, Z., Y. Li, H. Wen, X. Ren, J. Liu, and L. Yang, *Investigation on the role of surfactants in bubble-algae interaction in flotation harvesting of chlorella vulgaris.* Scientific Reports, 2018. **8**(1): p. 3303.
131. Laurila, H., Karesvuori, J., Tiili, O., *Strategies for instrumentation and control of flotation circuits. Mineral processing plant design, practise and control*. Vol. Volume 1. 2002.

.
132. deSousa, S.R., K.F. Oliveira, C.S. Souza, B.V. Kilikian, and C. Laluce, *Yeast flotation viewed as the result of the interplay of supernatant composition and cell-wall hydrophobicity.* Colloids and Surfaces B: Biointerfaces, 2003. **29**(4): p. 309-319.
133. Rosen, M.J. and J.T. Kunjappu, *Surfactants and interfacial phenomena*. 2012, Hoboken, New Jersey Published simultaneously in Canada: John Wiley & Sons, Inc.
134. Ruen-ngam, D., P. Wongsuchoto, A. Limpanuphap, T. Charinpanitkul, and P. Pavasant, *Influence of salinity on bubble size distribution and gas–liquid mass transfer in airlift contactors.* Chemical Engineering Journal, 2008. **141**(1): p. 222-232.
135. Vandamme, D., I. Foubert, and K. Muylaert, *Flocculation as a low-cost method for harvesting microalgae for bulk biomass production.* Trends in Biotechnology, 2013. **31**(4): p. 233-239.
136. Davies, J.T., A. Haydon Denis, and K. Rideal Eric, *Surface behaviour of bacterium coli - i. The nature of the surface.* Proceedings of the Royal Society of London. Series B - Biological Sciences, 1956. **145**(920): p. 375-383.
137. Douglas, H.W. and D.J. Shaw, *Electrophoretic studies on model particles. Part 1. Mobility, ph and ionic strength relations for droplets having protein, lipid or polysaccharide surfaces, and for certain complexes.* Transactions of the Faraday Society, 1957. **53**(0): p. 512-522.
138. Adams, D.M. and E. Rideal, *The surface behaviour of mycobacterium phlei.* Transactions of the Faraday Society, 1959. **55**(0): p. 185-189.
139. Viehweg, H. and K. Schügerl, *Cell recovery by continuous flotation.* European journal of applied microbiology and biotechnology, 1983. **17**(2): p. 96-102.
140. Nguyen, T.L., D.J. Lee, J.S. Chang, and J.C. Liu, *Effects of ozone and peroxone on algal separation via dispersed air flotation.* Colloids and Surfaces B: Biointerfaces, 2013. **105**: p. 246-250.
141. B. Grieves, R. and S.L. Wang, *Foam separation of bacteria with a cationic surfactant*. Vol. 9. 1967. 187-194.
142. Husband, D.L., J.H. Masliyah, and M.R. Gray, *Cell and surfactant separation by column flotation.* The Canadian Journal of Chemical Engineering, 1994. **72**(5): p. 840-847.
143. McTaggart, H.A., *Xxxviii. On the electrification at the boundary between a liquid and a gas.* The London, Edinburgh, and Dublin Philosophical Magazine and Journal of Science, 1922. **44**(260): p. 386-395.

144. Henderson, R.K., S.A. Parsons, and B. Jefferson, *Successful removal of algae through the control of zeta potential.* Separation Science and Technology, 2008. **43**(7): p. 1653-1666.
145. Henderson, R.K., S.A. Parsons, and B. Jefferson, *Polymers as bubble surface modifiers in the flotation of algae.* Environmental Technology, 2010. **31**(7): p. 781-790.
146. Yap, R.K.L., M. Whittaker, M. Diao, R.M. Stuetz, B. Jefferson, V. Bulmus, W.L. Peirson, A.V. Nguyen, and R.K. Henderson, *Hydrophobically-associating cationic polymers as micro-bubble surface modifiers in dissolved air flotation for cyanobacteria cell separation.* Water Research, 2014. **61**: p. 253-262.
147. Zutic, V., Cosovic, B., Marcenko, E., Bihari, N. and Krsinic, F, *Surfactant production by marine-phytoplankton.* Marine Chemistry, 1981. **10**(6): p. 505-520.
148. Guzmán, E., E. Santini, A. Benedetti, F. Ravera, M. Ferrari, and L. Liggieri, *Surfactant induced complex formation and their effects on the interfacial properties of seawater.* Colloids and Surfaces B: Biointerfaces, 2014. **123**(Supplement C): p. 701-709.
149. Lin, Z., Y.L. Kuang, and Y.W. Leng, *Harvesting microalgae biomass by instant dissolved air flotation at batch scale.* Advanced Materials Research, 2011. **236-238**: p. 146-150.
150. Eldridge, R.J., D.R.A. Hill, and B.R. Gladman, *A comparative study of the coagulation behaviour of marine microalgae.* Journal of Applied Phycology, 2012. **24**(6): p. 1667-1679.
151. Clayton, R., G.J. Jameson, and E.V. Manlapig, *The development and application of the jameson cell.* Minerals Engineering, 1991. **4**(7): p. 925-933.
152. Molaei, A. and K.E. Waters, *Aphron applications — a review of recent and current research.* Advances in Colloid and Interface Science, 2015. **216**: p. 36-54.
153. Jauregi, P., G.R. Mitchell, and J. Varley, *Colloidal gas aphrons (cga): Dispersion and structural features.* AIChE Journal, 2000. **46**(1): p. 24-36.
154. Parmar, R. and S.K. Majumder, *Mineral beneficiation by ionic microbubble in continuous plant prototype: Efficiency and its analysis by kinetic model.* Chemical Engineering Science, 2016. **142**: p. 42-54.
155. Das, A. and J.D. Miller, *Swirl flow characteristics and froth phase features in air-sparged hydrocyclone flotation as revealed by x-ray ct analysis.* International Journal of Mineral Processing, 1996. **47**(3): p. 251-274.
156. Jarvis, P., P. Buckingham, B. Holden, and B. Jefferson, *Low energy ballasted flotation.* Water Research, 2009. **43**(14): p. 3427-3434.
157. Ometto, F., C. Pozza, R. Whitton, B. Smyth, A.G. Torres, R.K. Henderson, P. Jarvis, B. Jefferson, and R. Villa, *The impacts of replacing air bubbles with microspheres for the clarification of algae from low cell-density culture.* Water Research, 2014. **53**: p. 168-179.
158. Matis, K.A., G.P. Gallios, and K.A. Kydros, *Separation of fines by flotation techniques.* Separations Technology, 1993. **3**(2): p. 76-90.
159. Zhang, J., Z. Liu, S. Wang, and P. Jiang, *Characterization of a bioflocculant produced by the marine myxobacterium nannocystis sp. Nu-2.* Applied Microbiology and Biotechnology, 2002. **59**(4): p. 517-522.
160. Liu, W., W. Liu, X. Wang, D. Wei, H. Zhang, and W. Liu, *Effect of butanol on flotation separation of quartz from hematite with n-dodecyl ethylenediamine.* International Journal of Mining Science and Technology, 2016. **26**(6): p. 1059-1063.
161. Cheng, Y.-S., Y. Zheng, J.M. Labavitch, and J.S. VanderGheynst, *The impact of cell wall carbohydrate composition on the chitosan flocculation of chlorella.* Process Biochemistry, 2011. **46**(10): p. 1927-1933.
162. Huang, C. and Y. Chen, *Coagulation of colloidal particles in water by chitosan.* Journal of Chemical Technology & Biotechnology, 1996. **66**(3): p. 227-232.
163. Marshall, K.C., R. Stout, and R. Mitchell, *Selective sorption of bacteria from seawater.* Canadian Journal of Microbiology, 1971. **17**(11): p. 1413-1416.
164. Levin, G.V., Gibor, A., Clendenning, J. R. and Bogar, F. D. , *Harvesting of algae by froth flotation.* Applied Microbiology, 1962. **10**(2): p. 169-75.

165. Micheau, C., P. Bauduin, O. Diat, and S. Faure, *Specific salt and ph effects on foam film of a ph sensitive surfactant.* Langmuir, 2013. **29**(27): p. 8472-8481.
166. Gao, S., M. Du, J. Tian, J. Yang, J. Yang, F. Ma, and J. Nan, *Effects of chloride ions on electro-coagulation-flotation process with aluminum electrodes for algae removal.* Journal of Hazardous Materials, 2010. **182**(1): p. 827-834.
167. Lim, D.K.Y., H. Schuhmann, S.R. Thomas-Hall, K.C.K. Chan, T.J. Wass, F. Aguilera, T.C. Adarme-Vega, C.G.O. Dal'Molin, G.J. Thorpe, J. Batley, D. Edwards, and P.M. Schenk, *Rna-seq and metabolic flux analysis of tetraselmis sp. M8 during nitrogen starvation reveals a two-stage lipid accumulation mechanism.* Bioresource Technology, 2017.
168. Bondioli, P., L. Della Bella, G. Rivolta, G. Chini Zittelli, N. Bassi, L. Rodolfi, D. Casini, M. Prussi, D. Chiaramonti, and M.R. Tredici, *Oil production by the marine microalgae nannochloropsis sp. F&m-m24 and tetraselmis suecica f&m-m33.* Bioresource Technology, 2012. **114**: p. 567-572.
169. Lim, D.K.Y., S. Garg, M. Timmins, E.S.B. Zhang, S.R. Thomas-Hall, H. Schuhmann, Y. Li, and P.M. Schenk, *Isolation and evaluation of oil-producing microalgae from subtropical coastal and brackish waters.* PLOS ONE, 2012. **7**(7): p. e40751.
170. Sukarni, Sudjito, N. Hamidi, U. Yanuhar, and I.N.G. Wardana, *Potential and properties of marine microalgae nannochloropsis oculata as biomass fuel feedstock.* International Journal of Energy and Environmental Engineering, 2014. **5**(4): p. 279-290.
171. Derjaguin, B.V., N.V. Churaev, and V.M. Muller, *The derjaguin—landau—verwey—overbeek (dlvo) theory of stability of lyophobic colloids*, in *Surface forces*, B.V. Derjaguin, N.V. Churaev, and V.M. Muller, Editors. 1987, Springer US: Boston, MA. p. 293-310.
172. Derjaguin, B. and L. Landau, *Theory of the stability of strongly charged lyophobic sols and of the adhesion of strongly charged particles in solutions of electrolytes.* Progress in Surface Science, 1993. **43**(1): p. 30-59.
173. Verwey, E.J.W., *Theory of the stability of lyophobic colloids.* The Journal of Physical and Colloid Chemistry, 1947. **51**(3): p. 631-636.
174. Cui, Y., W. Yuan, and J. Cheng, *Understanding ph and ionic strength effects on aluminum sulfate-induced microalgae flocculation.* Applied Biochemistry and Biotechnology, 2014. **173**(7): p. 1692-1702.
175. Van Oss, C.J., R.J. Good, and M.K. Chaudhury, *The role of van der waals forces and hydrogen bonds in "hydrophobic interactions" between biopolymers and low energy surfaces.* Journal of Colloid and Interface Science, 1986. **111**(2): p. 378-390.
176. Fonte, P., F. Andrade, F. Araújo, C. Andrade, J.d. Neves, and B. Sarmento, *Chapter fifteen - chitosan-coated solid lipid nanoparticles for insulin delivery*, in *Methods in enzymology*, N. Düzgüneş, Editor. 2012, Academic Press. p. 295-314.
177. Krstić, M., Đ. Medarević, J. Đuriš, and S. Ibrić, *Chapter 12 - self-nanoemulsifying drug delivery systems (snedds) and self-microemulsifying drug delivery systems (smedds) as lipid nanocarriers for improving dissolution rate and bioavailability of poorly soluble drugs*, in *Lipid nanocarriers for drug targeting*, A.M. Grumezescu, Editor. 2018, William Andrew Publishing. p. 473-508.
178. Oss, C.J.v., *Interfacial forces in aqueous media*. 2nd Edition ed. 2006: CRC Press. 456.
179. van Oss, C.J., *Aspecific and specific intermolecular interactions in aqueous media.* Journal of Molecular Recognition, 1990. **3**(3): p. 128-136.
180. Nabweteme, R., M. Yoo, H.-S. Kwon, Y.J. Kim, G. Hwang, C.-H. Lee, and I.-S. Ahn, *Application of the extended dlvo approach to mechanistically study the algal flocculation.* Journal of Industrial and Engineering Chemistry, 2015. **30**: p. 289-294.
181. van Oss, C.J., *Long-range and short-range mechanisms of hydrophobic attraction and hydrophilic repulsion in specific and aspecific interactions.* Journal of Molecular Recognition, 2003. **16**(4): p. 177-190.

182. van Oss, C.J., L.L. Moore, R.J. Good, and M.K. Chaudhury, *Surface thermodynamic properties and chromatographic and salting-out behavior of iga and other serum proteins.* Journal of Protein Chemistry, 1985. **4**(4): p. 245-263.
183. van Oss, C.J., M.K. Chaudhury, and R.J. Good, *Monopolar surfaces.* Advances in Colloid and Interface Science, 1987. **28**: p. 35-64.
184. Stephen L. Pahl , A.r.K.L., Theo Kalaitzidis , Peter J. Ashman , Suraj Sathe , and David M. Lewis, *Harvesting, thickening and dewatering microalgae biomass*, in *Algae for biofuels and energy*, M.A.B.a.N.R. Moheimani, Editor. 2013, Springer: Dordrecht. p. 165-185.
185. Park, J.-Y., M.S. Park, Y.-C. Lee, and J.-W. Yang, *Advances in direct transesterification of algal oils from wet biomass.* Bioresource Technology, 2015. **184**: p. 267-275.
186. Halim, R., T.W.T. Rupasinghe, D.L. Tull, and P.A. Webley, *Modelling the kinetics of lipid extraction from wet microalgal concentrate: A novel perspective on a classical process.* Chemical Engineering Journal, 2014. **242**: p. 234-253.
187. Guldhe, A., B. Singh, I. Rawat, K. Ramluckan, and F. Bux, *Efficacy of drying and cell disruption techniques on lipid recovery from microalgae for biodiesel production.* Fuel, 2014. **128**: p. 46-52.
188. Kamoru A. Salam, S.B.V.-O., Adam P. Harvey *In situ transesterification of wet marine and fresh water microalgae for biodiesel production and its effect on the algal residue.* Journal of Sustainable Bioenergy Systems, 2016. **06**(2): p. 17-30.
189. Lai, Y.S., P. Parameswaran, A. Li, M. Baez, and B.E. Rittmann, *Effects of pulsed electric field treatment on enhancing lipid recovery from the microalga, scenedesmus.* Bioresource Technology, 2014. **173**: p. 457-461.
190. Florentino de Souza Silva, A.P., M.C. Costa, A. Colzi Lopes, E. Fares Abdala Neto, R. Carrhá Leitão, C.R. Mota, and A. Bezerra dos Santos, *Comparison of pretreatment methods for total lipids extraction from mixed microalgae.* Renewable Energy, 2014. **63**: p. 762-766.
191. Yoo, G., Y. Yoo, J.-H. Kwon, C. Darpito, S.K. Mishra, K. Pak, M.S. Park, S.G. Im, and J.-W. Yang, *An effective, cost-efficient extraction method of biomass from wet microalgae with a functional polymeric membrane.* Green Chemistry, 2014. **16**(1): p. 312-319.
192. Lee, Y.-C., Y.S. Huh, W. Farooq, J. Chung, J.-I. Han, H.-J. Shin, S.H. Jeong, J.-S. Lee, Y.-K. Oh, and J.-Y. Park, *Lipid extractions from docosahexaenoic acid (dha)-rich and oleaginous chlorella sp. Biomasses by organic-nanoclays.* Bioresource Technology, 2013. **137**: p. 74-81.
193. Lee, Y.-C., Y.S. Huh, W. Farooq, J.-I. Han, Y.-K. Oh, and J.-Y. Park, *Oil extraction by aminoparticle-based h2o2 activation via wet microalgae harvesting.* RSC Advances, 2013. **3**(31): p. 12802-12809.
194. Steriti, A., R. Rossi, A. Concas, and G. Cao, *A novel cell disruption technique to enhance lipid extraction from microalgae.* Bioresource Technology, 2014. **164**: p. 70-77.
195. Huang, Y., A. Hong, D. Zhang, and L. Li, *Comparison of cell rupturing by ozonation and ultrasonication for algal lipid extraction from chlorella vulgaris.* Environmental Technology, 2014. **35**(8): p. 931-937.
196. Nurra, C., C. Torras, E. Clavero, S. Ríos, M. Rey, E. Lorente, X. Farriol, and J. Salvadó, *Biorefinery concept in a microalgae pilot plant. Culturing, dynamic filtration and steam explosion fractionation.* Bioresource Technology, 2014. **163**: p. 136-142.
197. Park, J.-Y., Y.-K. Oh, J.-S. Lee, K. Lee, M.-J. Jeong, and S.-A. Choi, *Acid-catalyzed hot-water extraction of lipids from chlorella vulgaris.* Bioresource Technology, 2014. **153**: p. 408-412.
198. Park, J.-Y., B. Nam, S.-A. Choi, Y.-K. Oh, and J.-S. Lee, *Effects of anionic surfactant on extraction of free fatty acid from chlorella vulgaris.* Bioresource Technology, 2014. **166**: p. 620-624.
199. Lee, I., J.-Y. Park, S.-A. Choi, Y.-K. Oh, and J.-I. Han, *Hydrothermal nitric acid treatment for effectual lipid extraction from wet microalgae biomass.* Bioresource Technology, 2014. **172**: p. 138-142.

200. Choi, S.-A., J.-Y. Jung, K. Kim, J.-S. Lee, J.-H. Kwon, S.W. Kim, J.-W. Yang, and J.-Y. Park, *Acid-catalyzed hot-water extraction of docosahexaenoic acid (dha)-rich lipids from aurantiochytrium sp. Krs101.* Bioresource Technology, 2014. **161**: p. 469-472.
201. Halim, R., M.K. Danquah, and P.A. Webley, *Extraction of oil from microalgae for biodiesel production: A review.* Biotechnology Advances, 2012. **30**(3): p. 709-732.
202. Halim, R., R. Harun, M.K. Danquah, and P.A. Webley, *Microalgal cell disruption for biofuel development.* Applied Energy, 2012. **91**(1): p. 116-121.
203. Deshmukh, S., R. Kumar, and K. Bala, *Microalgae biodiesel: A review on oil extraction, fatty acid composition, properties and effect on engine performance and emissions.* Fuel Processing Technology, 2019. **191**: p. 232-247.
204. Bligh, E.G. and W.J. Dyer, *A rapid method of total lipid extraction and purification.* Canadian Journal of Biochemistry and Physiology, 1959. **37**(8): p. 911-917.
205. Folch, J., M. Lees, and G.H. Sloane Stanley, *A simple method for the isolation and purification of total lipides from animal tissues.* J Biol Chem, 1957. **226**(1): p. 497-509.
206. Emilio Molina Grima , M.J.I.G., and Antonio Giménez Giménez, *Solvent extraction for microalgae lipids*, in *Algae for biofuels and energy, developments in applied phycology 5*, M.A.B.a.N.R. Moheimani, Editor. 2015, Springer.
207. Halim, R., B. Gladman, M.K. Danquah, and P.A. Webley, *Oil extraction from microalgae for biodiesel production.* Bioresource Technology, 2011. **102**(1): p. 178-185.
208. Chen, M., X. Chen, T. Liu, and W. Zhang, *Subcritical ethanol extraction of lipid from wet microalgae paste of nannochloropsis sp.* Journal of Biobased Materials and Bioenergy, 2011. **5**(3): p. 385-389.
209. Zhukov, A.V. and A.G. Vereshchagin, *Current techniques of extraction, purification, and preliminary fractionation of polar lipids of natural origin*, in *Advances in lipid research*, R. Paoletti and D. Kritchevsky, Editors. 1981, Elsevier. p. 247-282.
210. Huang, W.-C. and J.-D. Kim, *Cationic surfactant-based method for simultaneous harvesting and cell disruption of a microalgal biomass.* Bioresource Technology, 2013. **149**: p. 579-581.
211. Fujita, K., D. Kobayashi, N. Nakamura, and H. Ohno, *Direct dissolution of wet and saliferous marine microalgae by polar ionic liquids without heating.* Enzyme and Microbial Technology, 2013. **52**(3): p. 199-202.
212. Demirbas, A. and M. Fatih Demirbas, *Importance of algae oil as a source of biodiesel.* Energy Conversion and Management, 2011. **52**(1): p. 163-170.
213. Tsaousis, P., Y. Wang, A.P. Roskilly, and G.S. Caldwell. *Algae to energy: Engine performance using raw algal oil*. in *Energy Procedia*. 2014.
214. Lin, L., Z. Cunshan, S. Vittayapadung, S. Xiangqian, and D. Mingdong, *Opportunities and challenges for biodiesel fuel.* Applied Energy, 2011. **88**(4): p. 1020-1031.
215. Knothe, G., *Production and properties of biodiesel from algal oils*, in *Algal biofuels and energy*, M.A.B.a.N.R. Moheimani, Editor. 2013, Springer Science+Business Media: Dordrecht.
216. Aguado, R., M. Olazar, B. Gaisán, R. Prieto, and J. Bilbao, *Kinetic study of polyolefin pyrolysis in a conical spouted bed reactor.* Industrial & Engineering Chemistry Research, 2002. **41**(18): p. 4559-4566.
217. Cornelissen, T., J. Yperman, G. Reggers, S. Schreurs, and R. Carleer, *Flash co-pyrolysis of biomass with polylactic acid. Part 1: Influence on bio-oil yield and heating value.* Fuel, 2008. **87**(7): p. 1031-1041.
218. Eterigho, E.J., J.G.M. Lee, and A.P. Harvey, *Triglyceride cracking for biofuel production using a directly synthesised sulphated zirconia catalyst.* Bioresource Technology, 2011. **102**(10): p. 6313-6316.
219. Lima, D.G., V.C.D. Soares, E.B. Ribeiro, D.A. Carvalho, É.C.V. Cardoso, F.C. Rassi, K.C. Mundim, J.C. Rubim, and P.A.Z. Suarez, *Diesel-like fuel obtained by pyrolysis of vegetable oils.* Journal of Analytical and Applied Pyrolysis, 2004. **71**(2): p. 987-996.

220. Eze, V.C., *The use of mesoscale oscillatory baffled reactors for rapid screening of heterogeneously catalysed biodiesel production reactions*. 2014, Newcastle University. p. 204.
221. Wellert, S., M. Karg, H. Imhof, A. Steppin, H.J. Altmann, M. Dolle, A. Richardt, B. Tiersch, J. Koetz, A. Lapp, and T. Hellweg, *Structure of biodiesel based bicontinuous microemulsions for environmentally compatible decontamination: A small angle neutron scattering and freeze fracture electron microscopy study.* Journal of Colloid and Interface Science, 2008. **325**(1): p. 250-258.
222. Fukuda, H., A. Kondo, and H. Noda, *Biodiesel fuel production by transesterification of oils.* Journal of Bioscience and Bioengineering, 2001. **92**(5): p. 405-416.
223. Bertoldi, C., C. da Silva, J.P. Bernardon, M.L. Corazza, L.C. Filho, J.V. Oliveira, and F.C. Corazza, *Continuous production of biodiesel from soybean oil in supercritical ethanol and carbon dioxide as cosolvent.* Energy & Fuels, 2009. **23**(10): p. 5165-5172.
224. M. Canakci, J.V.G., *Biodiesel production viaacid catalysis.* American Society of Agricultural Engineers, 1999. **0001**(42): p. 1203-1210.
225. Wang, Y., S. Ou, P. Liu, F. Xue, and S. Tang, *Comparison of two different processes to synthesize biodiesel by waste cooking oil.* Journal of Molecular Catalysis A: Chemical, 2006. **252**(1–2): p. 107-112.
226. Patil, P., S. Deng, J. Isaac Rhodes, and P.J. Lammers, *Conversion of waste cooking oil to biodiesel using ferric sulfate and supercritical methanol processes.* Fuel, 2010. **89**(2): p. 360-364.
227. Wan Omar, W.N.N., N. Nordin, M. Mohamed, and N.A.S. Amin, *A two-step biodiesel production from waste cooking oil: Optimization of pre-treatment step.* Journal of Applied Sciences, 2009. **9**(17): p. 3098-3103.
228. Singh, A.K. and S.D. Fernando, *Preparation and reaction kinetics studies of na-based mixed metal oxide for transesterification.* Energy & Fuels, 2009. **23**(10): p. 5160-5164.
229. Haas, M.J. and K. Wagner, *Simplifying biodiesel production: The direct or in situ transesterification of algal biomass.* European Journal of Lipid Science and Technology, 2011. **113**(10): p. 1219-1229.
230. Tran, D.-T., K.-L. Yeh, C.-L. Chen, and J.-S. Chang, *Enzymatic transesterification of microalgal oil from chlorella vulgaris esp-31 for biodiesel synthesis using immobilized burkholderia lipase.* Bioresource Technology, 2012. **108**: p. 119-127.
231. Kim, B., H. Im, and J.W. Lee, *In situ transesterification of highly wet microalgae using hydrochloric acid.* Bioresource Technology, 2015. **185**: p. 421-425.
232. Teixeira, R.E., *Energy-efficient extraction of fuel and chemical feedstocks from algae.* Green Chemistry, 2012. **14**(2): p. 419-427.
233. Patil, P.D., V.G. Gude, A. Mannarswamy, S. Deng, P. Cooke, S. Munson-McGee, I. Rhodes, P. Lammers, and N. Nirmalakhandan, *Optimization of direct conversion of wet algae to biodiesel under supercritical methanol conditions.* Bioresource Technology, 2011. **102**(1): p. 118-122.
234. Sills, D.L.P., V. Franke, M. J. Johnson, M. C. Akabas, T. M. Greene, C. H. Tester, J. W., *Quantitative uncertainty analysis of life cycle assessment for algal biofuel production.* Environ Sci Technol, 2013. **47**(2): p. 687-94.
235. Du Noüy, P.L., *An interfacial tensiometer for universal use.* The Journal of General Physiology, 1925. **7**(5): p. 625.
236. Padday, J.F., A.R. Pitt, and R.M. Pashley, *Menisci at a free liquid surface: Surface tension from the maximum pull on a rod.* Journal of the Chemical Society, Faraday Transactions 1: Physical Chemistry in Condensed Phases, 1975. **71**(0): p. 1919-1931.
237. Suomalainen, P., C. Johans, T. Söderlund, and P.K.J. Kinnunen, *Surface activity profiling of drugs applied to the prediction of blood−brain barrier permeability.* Journal of Medicinal Chemistry, 2004. **47**(7): p. 1783-1788.

238. Zdziennicka, A. and B. Jańczuk, *Behavior of cationic surfactants and short chain alcohols in mixed surface layers at water–air and polymer–water interfaces with regard to polymer wettability. I. Adsorption at water–air interface.* Journal of Colloid and Interface Science, 2010. **349**(1): p. 374-383.
239. SALTON, M.R.J., *The adsorption of cetyltrimethylammonium bromide by bacteria, its action in releasing cellular constituents and its bactericidal effects.* Microbiology, 1951. **5**(2): p. 391-404.
240. Huang, J.B., M. Mao, and B.Y. Zhu, *The surface physico-chemical properties of surfactants in ethanol–water mixtures.* Colloids and Surfaces A: Physicochemical and Engineering Aspects, 1999. **155**(2–3): p. 339-348.
241. Bielawska, M., B. Jańczuk, and A. Zdziennicka, *Behavior of cetyltrimethylammonium bromide and triton x-100 mixture at solution–air interface in presence of short-chain alcohols.* Colloids and Surfaces A: Physicochemical and Engineering Aspects, 2014. **454**: p. 65-73.
242. Iyota, H. and K. Motomura, *Miscibility of ethanol and 2-(octylsulfinyl)ethanol in the adsorbed film at the water/air interface and in the micelle.* Journal of Colloid and Interface Science, 1992. **148**(2): p. 369-374.
243. Zdziennicka, A. and B. Jańczuk, *Behavior of cationic surfactants and short-chain alcohols in mixed surface layers at water–air and polymer–water interfaces with regard to polymer wettability: Ii. Wettability of polymers.* Journal of Colloid and Interface Science, 2010. **350**(2): p. 568-576.
244. Szymczyk, K., A. Zdziennicka, B. Jańczuk, and W. Wójcik, *The properties of mixtures of two cationic surfactants in water at water/air interface.* Colloids and Surfaces A: Physicochemical and Engineering Aspects, 2005. **264**(1–3): p. 147-156.
245. Zdziennicka, A. and B. Jańczuk, *Adsorption of cetyltrimethylammonium bromide and propanol mixtures with regard to wettability of polytetrafluoroethylene. I. Adsorption at aqueous solution–air interface.* Journal of Colloid and Interface Science, 2008. **317**(1): p. 44-53.
246. Zdziennicka, A. and B. Jańczuk, *The adsorption of cetyltrimethylammonium bromide and propanol mixtures with regard to wettability of polytetrafluoroethylene: Ii. Adsorption at polytetrafluoroethylene–aqueous solution interface and wettability.* Journal of Colloid and Interface Science, 2008. **318**(1): p. 15-22.
247. Phan, C.M., C.V. Nguyen, and T.T.T. Pham, *Molecular arrangement and surface tension of alcohol solutions.* The Journal of Physical Chemistry B, 2016. **120**(16): p. 3914-3919.
248. Jańczuk, B., A. Zdziennicka, and W. Wójcik, *Adsorption of sodium dodecyl sulphate and propanol mixtures at aqueous solution–air interface.* Colloids and Surfaces A: Physicochemical and Engineering Aspects, 2004. **244**(1–3): p. 1-7.
249. Bielawska, M., B. Jańczuk, and A. Zdziennicka, *Behavior of cetyltrimethylammonium bromide, tert-octylphenol (9.5 eo) ethoxylate and ethanol mixtures at the water–air interface.* Journal of Surfactants and Detergents, 2013. **16**(2): p. 203-212.
250. Hardy, W.B., *The tension of composite fluid surfaces and the mechanical stability of films of fluid.* Proceedings of the Royal Society of London. Series A, 1912. **86**(591): p. 610.
251. Ward, A.F.H., *The influence of the solvent on the formation of micelles in colloidal electrolytes. I. Electrical conductivities of sodium dodecyl sulphate in ethyl alcohol-water mixtures.* Proceedings of the Royal Society of London. Series A. Mathematical and Physical Sciences, 1940. **176**(966): p. 412.
252. Bournival, G., R.J. Pugh, and S. Ata, *Examination of nacl and mibc as bubble coalescence inhibitor in relation to froth flotation.* Minerals Engineering, 2012. **25**(1): p. 47-53.
253. Chang, T.-M. and L.X. Dang, *Liquid−vapor interface of methanol−water mixtures: A molecular dynamics study.* The Journal of Physical Chemistry B, 2005. **109**(12): p. 5759-5765.

254. Paul, S. and A. Chandra, *Hydrogen bond properties and dynamics of liquid−vapor interfaces of aqueous methanol solutions.* Journal of Chemical Theory and Computation, 2005. **1**(6): p. 1221-1231.
255. Park, J.-Y.P., Min S. Lee, Young-Chul Yang, Ji-Won, *Advances in direct transesterification of algal oils from wet biomass.* Bioresource Technology, 2015. **184**: p. 267-275.
256. Lewis, T., P.D. Nichols, and T.A. McMeekin, *Evaluation of extraction methods for recovery of fatty acids from lipid-producing microheterotrophs.* Journal of Microbiological Methods, 2000. **43**(2): p. 107-116.
257. Wahlen, B.D., R.M. Willis, and L.C. Seefeldt, *Biodiesel production by simultaneous extraction and conversion of total lipids from microalgae, cyanobacteria, and wild mixed-cultures.* Bioresource Technology, 2011. **102**(3): p. 2724-2730.
258. Liu, B. and Z. Zhao, *Biodiesel production by direct methanolysis of oleaginous microbial biomass.* Journal of Chemical Technology & Biotechnology, 2007. **82**(8): p. 775-780.
259. Sitepu, E.K., D.B. Jones, Y. Tang, S.C. Leterme, K. Heimann, W. Zhang, and C.L. Raston, *Continuous flow biodiesel production from wet microalgae using a hybrid thin film microfluidic platform.* Chemical Communications, 2018. **54**(85): p. 12085-12088.
260. Hu, Q., M. Sommerfeld, E. Jarvis, M. Ghirardi, M. Posewitz, M. Seibert, and A. Darzins, *Microalgal triacylglycerols as feedstocks for biofuel production: Perspectives and advances.* The Plant Journal, 2008. **54**(4): p. 621-639.
261. Roselet, F., J. Burkert, and P.C. Abreu, *Flocculation of nannochloropsis oculata using a tannin-based polymer: Bench scale optimization and pilot scale reproducibility.* Biomass and Bioenergy, 2016. **87**: p. 55-60.
262. Shen, Y., Y. Cui, and W. Yuan, *Flocculation optimization of microalga nannochloropsis oculata.* Applied Biochemistry and Biotechnology, 2013. **169**(7): p. 2049-2063.
263. Zheng, H., Z. Gao, J. Yin, X. Tang, X. Ji, and H. Huang, *Harvesting of microalgae by flocculation with poly (γ-glutamic acid).* Bioresource Technology, 2012. **112**: p. 212-220.
264. Coward, T., *Foam fractionation : An effective technology for harvesting microalgae biomass*, E. University of Newcastle upon Tyne. School of Chemical, M. Advanced, and T. University of Newcastle upon, Editors. 2012, Thesis (Ph. D.)--University of Newcastle upon Tyne, 2012.: Newcastle upon Tyne.
265. Mari, X. and M. Robert, *Metal induced variations of tep sticking properties in the southwestern lagoon of new caledonia.* Marine Chemistry, 2008. **110**(1): p. 98-108.
266. Vadstein, O., G. Øie, and Y. Olsen. *Particle size dependent feeding by the rotifer brachionus plicatilis*. in *Rotifer Symposium VI*. 1993. Dordrecht: Springer Netherlands.
267. Flint, L.R. and W.J. Howarth, *The collision efficiency of small particles with spherical air bubbles.* Chemical Engineering Science, 1971. **26**(8): p. 1155-1168.
268. Reay, D. and G.A. Ratcliff, *Experimental testing of the hydrodynamic collision model of fine particle flotation.* The Canadian Journal of Chemical Engineering, 1975. **53**(5): p. 481-486.
269. Collins, G.L. and G.J. Jameson, *Double-layer effects in the flotation of fine particles.* Chemical Engineering Science, 1977. **32**(3): p. 239-246.
270. Derjaguin, B.V. and N.D. Shukakidse, *Dependence of the floatability of antimonite on the value of zeta-potential.* Progress in Surface Science, 1993. **43**(1): p. 267-272.
271. Fukui, Y. and S. Yuu, *Collection of submicron particles in electro-flotation.* Chemical Engineering Science, 1980. **35**(5): p. 1097-1105.
272. Okada, K. and Y. Akagi, *Method and apparatus to measure the ξ-potential of bubbles.* Journal of Chemical Engineering of Japan, 1987. **20**(1): p. 11-15.
273. Derjaguin, B.V., S.S. Dukhin, and N.N. Rulyov, *Kinetic theory of flotation of small particles*, in *Surface and colloid science: Volume 13*, E. Matijević and R.J. Good, Editors. 1984, Springer US: Boston, MA. p. 71-113.
274. Yoon, R.-H. and J.L. Yordan, *Zeta-potential measurements on microbubbles generated using various surfactants.* Journal of Colloid and Interface Science, 1986. **113**(2): p. 430-438.

275. Guillard, R.R.L., *Culture of phytoplankton for feeding marine invertebrates*, in *Culture of marine invertebrate animals: Proceedings — 1st conference on culture of marine invertebrate animals greenport*, W.L. Smith and M.H. Chanley, Editors. 1975, Springer US: Boston, MA. p. 29-60.
276. Rippka, R., J. Deruelles, J.B. Waterbury, M. Herdman, and R.Y. Stanier, *Generic assignments, strain histories and properties of pure cultures of cyanobacteria.* Microbiology, 1979. **111**(1): p. 1-61.
277. Coward, T., J.G.M. Lee, and G.S. Caldwell, *Harvesting microalgae by ctab-aided foam flotation increases lipid recovery and improves fatty acid methyl ester characteristics.* Biomass & Bioenergy, 2014. **67**: p. 354-362.
278. Alkarawi, M.A.S., G.S. Caldwell, and J.G.M. Lee, *Continuous harvesting of microalgae biomass using foam flotation.* Algal Research, 2018. **36**: p. 125-138.
279. Clasen, J., U. Mischke, M. Drikas, and C. Chow, *An improved method for detecting electrophoretic mobility of algae during the destabilisation process of flocculation: Flocculant demand of different species and the impact of doc.* Journal of Water Supply: Research and Technology-Aqua, 2000. **49**(2): p. 89-101.
280. Kim, T.-i., H. Park, and M. Han, *Development of algae removal method based on positively charged bubbles.* KSCE Journal of Civil Engineering, 2017.
281. Cheng, G., C.L. Shi, X.K. Yan, Z.J. Zhang, H.X. Xu, and Y. Lu, *A study of bubble-particle interactions in a column flotation process.* Physicochemical Problems of Mineral Processing, 2017. **53**(1): p. 18-33.
282. Bulatovic, S.M., *Handbook of flotation reagents: Chemistry, theory and practice: Flotation of sulphides ores*. Vol. vol. 1. 2007: Elsevier, Amsterdam. 448.
283. Sun, J., J. Cheng, Z. Yang, K. Li, J. Zhou, and K. Cen, *Microstructures and functional groups of nannochloropsis sp. Cells with arsenic adsorption and lipid accumulation.* Bioresour Technol, 2015. **194**: p. 305-11.
284. Rijnaarts, H.H.M., W. Norde, J. Lyklema, and A.J.B. Zehnder, *Dlvo and steric contributions to bacterial deposition in media of different ionic strengths.* Colloids and Surfaces B: Biointerfaces, 1999. **14**(1): p. 179-195.
285. Chattoraj, D.K. and K.S. Birdi, *Adsorption and the gibbs surface excess.* 1984.
286. Hofmeister, F., *Zur lehre von der wirkung der salze.* Archiv für experimentelle Pathologie und Pharmakologie, 1888. **24**(4): p. 247-260.
287. Wen H, L.Y.P., Shen Z, Ren X Y, Zhang W J, Liu J., *Surface characteristics of microalgae and their effects on harvesting performance by air flotation.* Int J Agric & Biol Eng,, 2017. **10**(1): p. 125–133.
288. Huang, W.-J., H.-H. Tsai, and W.-F. Lee, *Preparation and properties of thermosensitive organic-inorganic hybrid gels containing modified nanosilica.* Polymer Composites, 2010. **31**(10): p. 1712-1721.
289. Scholz, M.J., T.L. Weiss, R.E. Jinkerson, J. Jing, R. Roth, U. Goodenough, M.C. Posewitz, and H.G. Gerken, *Ultrastructure and composition of the nannochloropsis gaditana cell wall.* Eukaryotic Cell, 2014. **13**(11): p. 1450-1464.
290. Gulyaeva, N., A. Zaslavsky, A. Chait, and B. Zaslavsky, *Measurement of the relative hydrophobicity of organic compounds without organic solvent. Effects of salt composition and ph on organic acids and nonionic compounds.* Journal of Pharmaceutical Sciences, 2001. **90**(9): p. 1366-1374.
291. Frka, S., Z. Kozarac, and B. Ćosović, *Characterization and seasonal variations of surface active substances in the natural sea surface micro-layers of the coastal middle adriatic stations.* Estuarine, Coastal and Shelf Science, 2009. **85**(4): p. 555-564.
292. Kamoru A. Salam, S.B.V.-O., Adam P. Harvey, *In situ transesterification of wet marine and fresh water microalgae for biodiesel production and its effect on the algal residue.* Journal of Sustainable Bioenergy Systems, 2016. **6**(2): p. 17-30.

293. Tamari, F., C.S. Hinkley, and N. Ramprashad, *A comparison of DNA extraction methods using petunia hybrida tissues.* Journal of biomolecular techniques : JBT, 2013. **24**(3): p. 113-118.
294. Hosseinizand, H., S. Sokhansanj, and C.J. Lim, *Studying the drying mechanism of microalgae chlorella vulgaris and the optimum drying temperature to preserve quality characteristics.* Drying Technology, 2018. **36**(9): p. 1049-1060.
295. Osmić, S., S. Begić, and V. Mićić. *The effect of concentration of methanol as a solvent on the antioxidative activity of sage extract*. in *New Technologies, Development and Application*. 2019. Cham: Springer International Publishing.
296. Denis Weaire, S.T.T., Aaron J. Meagher and Stefan Hutzler, *Foam morphology,* in *Foam engineering: Fundamentals and applications*, P. Stevenson, Editor. 2012, John Wiley & Sons, Ltd. p. 6-7.
297. Koehler, S.A., *Foam drainage*, in *Foam engineering: Fundamentals and applications,*, P. Stevenson, Editor. 2012, John Wiley & Sons, Ltd: Chichester. p. 27-58.
298. Paul Stevenson, X.L., *Foam fractionation principles and process design*. 1st ed. 2014, Boca Raton: CRC Press. 206.
299. Stevenson, P., *Gas–liquid foam in products and processes*, in *Foam engineering fundamentals and applications*, P. Stevenson, Editor. 2012, John Wiley & Sons, Ltd. p. 1-2.
300. Flockhart, B.D., *The critical micelle concentration of sodium dodecyl sulfate in ethanol-water mixtures.* Journal of Colloid Science, 1957. **12**(6): p. 557-565.
301. Shinoda, K., *The effect of alcohols on the critical micelle concentrations of fatty acid soaps and the critical micelle concentration of soap mixtures.* The Journal of Physical Chemistry, 1954. **58**(12): p. 1136-1141.
302. Shirahama, K. and T. Kashiwabara, *The cmc-decreasing effects of some added alcohols on the aqueous sodium dodecyl sulfate solutions.* Journal of Colloid and Interface Science, 1971. **36**(1): p. 65-70.
303. Nishikido, N., Y. Moroi, H. Uehara, and R. Matuura, *Effect of alcohols on the micelle formation of nonionic surfactants in aqueous solutions.* Bulletin of the Chemical Society of Japan, 1974. **47**(11): p. 2634-2638.
304. Manabe, M. and M. Koda, *The effect of poly(oxyethylene) alkyl ethers, alkanediols, and alkanols on the critical micelle concentration of sodium dodecyl sulfate.* Bulletin of the Chemical Society of Japan, 1978. **51**(6): p. 1599-1601.
305. Soetens, J.-C. and P.A. Bopp, *Water–methanol mixtures: Simulations of mixing properties over the entire range of mole fractions.* The Journal of Physical Chemistry B, 2015. **119**(27): p. 8593-8599.
306. Niraula, T.P., S.K. Shah, S.K. Chatterjee, and A. Bhattarai, *Effect of methanol on the surface tension and viscosity of sodiumdodecyl sulfate (sds) in aqueous medium at 298.15–323.15 k.* Karbala International Journal of Modern Science, 2018. **4**(1): p. 26-34.
307. Hayase, K. and S. Hayano, *Effect of alcohols on the critical micelle concentration decrease in the aqueous sodium dodecyl sulfate solution.* Journal of Colloid and Interface Science, 1978. **63**(3): p. 446-451.
308. Zdziennicka, A. and B. Jańczuk, *Behavior of anionic surfactants and short chain alcohols mixtures in the monolayer at the water–air interface.* Journal of Surfactants and Detergents, 2011. **14**(2): p. 257-267.
309. Khossravi, D. and K.A. Connors, *Solvent effects on chemical processes. 3. Surface tension of binary aqueous organic solvents.* Journal of Solution Chemistry, 1993. **22**(4): p. 321-330.
310. Fainerman, V.B., R. Miller, and E.V. Aksenenko, *Simple model for prediction of surface tension of mixed surfactant solutions.* Advances in Colloid and Interface Science, 2002. **96**(1–3): p. 339-359.
311. Miller, R., E.V. Aksenenko, and V.B. Fainerman, *The elasticity of adsorption layers of reorientable surfactants.* Journal of Colloid and Interface Science, 2001. **236**(1): p. 35-40.

312. Fainerman, V.B., S.V. Lylyk, E.V. Aksenenko, A.V. Makievski, J.T. Petkov, J. Yorke, and R. Miller, *Adsorption layer characteristics of triton surfactants: 1. Surface tension and adsorption isotherms.* Colloids and Surfaces A: Physicochemical and Engineering Aspects, 2009. **334**(1–3): p. 1-7.
313. Lavi, P. and A. Marmur, *Adsorption isotherms for concentrated aqueous-organic solutions (caos).* Journal of Colloid and Interface Science, 2000. **230**(1): p. 107-113.
314. Connors, K.A. and J.L. Wright, *Dependence of surface tension on composition of binary aqueous-organic solutions.* Analytical Chemistry, 1989. **61**(3): p. 194-198.
315. Guggenheim, E.A. and N.K. Adam, *The thermodynamics of adsorption at the surface of solutions.* Proceedings of the Royal Society of London. Series A, 1933. **139**(837): p. 218.
316. Rocha e Silva, F.C.P., N.M.P. Rocha e Silva, J.M. Luna, R.D. Rufino, V.A. Santos, and L.A. Sarubbo, *Dissolved air flotation combined to biosurfactants: A clean and efficient alternative to treat industrial oily water.* Reviews in Environmental Science and Bio/Technology, 2018. **17**(4): p. 591-602.
317. F. P, P., M. M. V, and G. Massarani, *Modelling of the dispersed air printed in brazil flotation process applied to dairy wastewater treatment*. Vol. 21. 2004.
318. Bikerman, J.J., *Surface chemistry for industrial research.* 1947.
319. Xu, G., C. Liang, P. Huang, Q. Liu, Y. Xu, C. Ding, and T. Li, *Optimization of rice lipid production from ultrasound-assisted extraction by response surface methodology.* Journal of Cereal Science, 2016. **70**: p. 23-28.
320. Bielawska, M., A. Chodzińska, B. Jańczuk, and A. Zdziennicka, *Determination of ctab cmc in mixed water+short-chain alcohol solvent by surface tension, conductivity, density and viscosity measurements.* Colloids and Surfaces A: Physicochemical and Engineering Aspects, 2013. **424**: p. 81-88.
321. Pascal, T.A. and W.A. Goddard, *Hydrophobic segregation, phase transitions and the anomalous thermodynamics of water/methanol mixtures.* The Journal of Physical Chemistry B, 2012. **116**(47): p. 13905-13912.
322. Anderson, M.T., J.E. Martin, J.G. Odinek, and P.P. Newcomer, *Effect of methanol concentration on ctab micellization and on the formation of surfactant-templated silica (sts).* Chemistry of Materials, 1998. **10**(6): p. 1490-1500.
323. Lee, H., W.-H. Hong, and H. Kim, *Excess volumes of binary and ternary mixtures of water, methanol, and ethylene glycol.* Journal of Chemical & Engineering Data, 1990. **35**(3): p. 371-374.
324. Xiao, C., H. Bianchi, and P.R. Tremaine, *Excess molar volumes and densities of (methanol+water) at temperatures between 323 k and 573 k and pressures of 7.0 mpa and 13.5 mpa.* The Journal of Chemical Thermodynamics, 1997. **29**(3): p. 261-286.
325. Yilmaz, H. and S. Güler, *Excess properties of methanol-water binary system at various temperatures.* Il Nuovo Cimento D, 1998. **20**(12): p. 1853-1861.
326. Winkel, E.S., S.L. Ceccio, D.R. Dowling, and M. Perlin, *Bubble-size distributions produced by wall injection of air into flowing freshwater, saltwater and surfactant solutions.* Experiments in Fluids, 2004. **37**(6): p. 802-810.
327. Zieminski, S.A. and R.C. Whittemore, *Behavior of gas bubbles in aqueous electrolyte solutions.* Chemical Engineering Science, 1971. **26**(4): p. 509-520.
328. Keitel, G. and U. Onken, *Inhibition of bubble coalescence by solutes in air/water dispersions.* Chemical Engineering Science, 1982. **37**(11): p. 1635-1638.
329. Slauenwhite, D.E. and B.D. Johnson, *Bubble shattering: Differences in bubble formation in fresh water and seawater.* Journal of Geophysical Research: Oceans, 1999. **104**(C2): p. 3265-3275.
330. Brown, R.B. and J. Audet, *Current techniques for single-cell lysis.* Journal of The Royal Society Interface, 2008. **5**(Suppl 2): p. S131-S138.
331. Zakaria, R. and A.P. Harvey, *Kinetics of reactive extraction/in situ transesterification of rapeseed oil.* Fuel Processing Technology, 2014. **125**: p. 34-40.

332. Harrington, K.J. and C. D'Arcy-Evans, *A comparison of conventional and in situ methods of transesterification of seed oil from a series of sunflower cultivars.* Journal of the American Oil Chemists Society, 1985. **62**(6): p. 1009-1013.
333. Haas, M.J., K.M. Scott, W.N. Marmer, and T.A. Foglia, *In situ alkaline transesterification: An effective method for the production of fatty acid esters from vegetable oils.* Journal of the American Oil Chemists' Society, 2004. **81**(1): p. 83-89.
334. Vicente, G., L.F. Bautista, R. Rodríguez, F.J. Gutiérrez, I. Sádaba, R.M. Ruiz-Vázquez, S. Torres-Martínez, and V. Garre, *Biodiesel production from biomass of an oleaginous fungus.* Biochemical Engineering Journal, 2009. **48**(1): p. 22-27.
335. Ehimen, E.A., Z.F. Sun, and C.G. Carrington, *Variables affecting the in situ transesterification of microalgae lipids.* Fuel, 2010. **89**(3): p. 677-684.
336. Haas, M.J. and K.M. Scott, *Moisture removal substantially improves the efficiency of in situ biodiesel production from soybeans.* Journal of the American Oil Chemists' Society, 2007. **84**(2): p. 197-204.
337. Haas, M.J., A.J. McAloon, W.C. Yee, and T.A. Foglia, *A process model to estimate biodiesel production costs.* Bioresource Technology, 2006. **97**(4): p. 671-678.
338. Canakci, M. and J. Van Gerpen, *Biodiesel production viaacid catalysis.* Transactions of the ASAE, 1999. **42**(5): p. 1203-1210.
339. Johnson, M.B. and Z. Wen, *Production of biodiesel fuel from the microalga schizochytrium limacinum by direct transesterification of algal biomass.* Energy & Fuels, 2009. **23**: p. 5179-5183.
340. Salam, K.A., *Reactive extraction of microalgae for biodiesel production*, E. University of Newcastle upon Tyne. School of Chemical, M. Advanced, and T. University of Newcastle upon, Editors. 2015, Thesis (Ph. D.)--University of Newcastle upon Tyne, 2015.: Newcastle upon Tyne.
341. Erhan, S.Z. and M.O. Bagby, *Polymerization of vegetable oils and their uses in printing inks.* Journal of the American Oil Chemists' Society, 1994. **71**(11): p. 1223-1226.
342. Velasquez-Orta, S.B., J.G.M. Lee, and A. Harvey, *Alkaline in situ transesterification of chlorella vulgaris.* Fuel, 2012. **94**: p. 544-550.
343. Grima, M.M., Acien Fernandez, F.G. and Robles Medina, A., *Downstream processing of cell-mass and products*, in *Handbook of microalgal culture*. 2004. p. 215-252.
344. Mata, T.M., A.A. Martins, and N.S. Caetano, *Microalgae for biodiesel production and other applications: A review.* Renewable and Sustainable Energy Reviews, 2010. **14**(1): p. 217-232.
345. Barros, A.I., A.L. Gonçalves, M. Simões, and J.C.M. Pires, *Harvesting techniques applied to microalgae: A review.* Renewable and Sustainable Energy Reviews, 2015. **41**: p. 1489-1500.
346. Al-karawi, M.A.S., *Development and intensification of a foam flotation system in harvesting microalgae for biofuel*, E. University of Newcastle upon Tyne. School of Chemical, M. Advanced, and T. University of Newcastle upon, Editors. 2018, Thesis (Ph. D.)--Newcastle University, 2018.: Newcastle upon Tyne, England.
347. Garg, S., L. Wang, and P.M. Schenk, *Effective harvesting of low surface-hydrophobicity microalgae by froth flotation.* Bioresource Technology, 2014. **159**(Supplement C): p. 437-441.
348. Tornabene, T.G., G. Holzer, and S.L. Peterson, *Lipid profile of the halophilic alga, dunaliella salina.* Biochemical and Biophysical Research Communications, 1980. **96**(3): p. 1349-1356.
349. D'Alessandro, E.B. and N.R. Antoniosi Filho, *Concepts and studies on lipid and pigments of microalgae: A review.* Renewable and Sustainable Energy Reviews, 2016. **58**: p. 832-841.
350. Bonnefond, H., N. Moelants, A. Talec, P. Mayzaud, O. Bernard, and A. Sciandra, *Coupling and uncoupling of triglyceride and beta-carotene production by dunaliella salina under nitrogen limitation and starvation.* Biotechnology for Biofuels, 2017. **10**(1): p. 25.
351. Moheimani, N.R., M.A. Borowitzka, A. Isdepsky, and S.F. Sing, *Standard methods for measuring growth of algae and their composition*, in *Algae for biofuels and energy*, A.M.

Borowitzka and R.N. Moheimani, Editors. 2013, Springer Netherlands: Dordrecht. p. 265-284.
352. Campbell, J.M., L.L. Lilly, and R.N. Maddox, *Gas conditioning and processing : Volume 2 : The equipment modules.* 1984.
353. Administartion, U.E.I. *Electric power monthly*. Electricity 2020 [cited 2020 26 July]; Available from: https://www.eia.gov/electricity/monthly/.
354. Gerchman, Y., B. Vasker, M. Tavasi, Y. Mishael, Y. Kinel-Tahan, and Y. Yehoshua, *Effective harvesting of microalgae: Comparison of different polymeric flocculants.* Bioresource Technology, 2017. **228**(Supplement C): p. 141-146.
355. Xu, Y., S. Purton, and F. Baganz, *Chitosan flocculation to aid the harvesting of the microalga chlorella sorokiniana.* Bioresource Technology, 2013. **129**: p. 296-301.
356. Farid, M.S., A. Shariati, A. Badakhshan, and B. Anvaripour, *Using nano-chitosan for harvesting microalga nannochloropsis sp.* Bioresource Technology, 2013. **131**: p. 555-559.
357. Qazi, M.J., S.J. Schlegel, E.H.G. Backus, M. Bonn, D. Bonn, and N. Shahidzadeh, *Dynamic surface tension of surfactants in the presence of high salt concentrations.* Langmuir, 2020. **36**(27): p. 7956-7964.
358. Guo, J., S. Chen, L. Liu, B. Li, P. Yang, L. Zhang, and Y. Feng, *Adsorption of dye from wastewater using chitosan–ctab modified bentonites.* Journal of Colloid and Interface Science, 2012. **382**(1): p. 61-66.
359. Calero, N., J. Muñoz, P. Ramírez, and A. Guerrero, *Flow behaviour, linear viscoelasticity and surface properties of chitosan aqueous solutions.* Food Hydrocolloids, 2010. **24**(6): p. 659-666.
360. Santini, E., E. Jarek, F. Ravera, L. Liggieri, P. Warszynski, and M. Krzan, *Surface properties and foamability of saponin and saponin-chitosan systems.* Colloids and Surfaces B: Biointerfaces, 2019. **181**: p. 198-206.
361. Kumar Tiwari, A., A. Kumar, and H. Raheman, *Biodiesel production from jatropha oil (jatropha curcas) with high free fatty acids: An optimized process.* Biomass and Bioenergy, 2007. **31**(8): p. 569-575.
362. Lotero, E., Y. Liu, D.E. Lopez, K. Suwannakarn, D.A. Bruce, and J.G. Goodwin, *Synthesis of biodiesel via acid catalysis.* Industrial & Engineering Chemistry Research, 2005. **44**(14): p. 5353-5363.
363. Marchetti, J.M., V.U. Miguel, and A.F. Errazu, *Possible methods for biodiesel production.* Renewable and Sustainable Energy Reviews, 2007. **11**(6): p. 1300-1311.
364. Li, P., X. Miao, R. Li, and J. Zhong, *In situ biodiesel production from fast-growing and high oil content chlorella pyrenoidosa in rice straw hydrolysate.* Journal of biomedicine & biotechnology, 2011. **2011**: p. 141207-141207.
365. Gimmler, H., M. Schieder, M. Kowalski, U. Zimmermann, and U. Pick, *Dunaliella acidophila: An algae with a positive zeta potential at its optimal ph for growth*.* Plant, Cell & Environment, 1991. **14**(3): p. 261-269.
366. Kim, B., H.Y. Heo, J. Son, J. Yang, Y.-K. Chang, J.H. Lee, and J.W. Lee, *Simplifying biodiesel production from microalgae via wet in situ transesterification: A review in current research and future prospects.* Algal Research, 2019. **41**: p. 101557.
367. He, Y., T. Wu, X. Wang, B. Chen, and F. Chen, *Cost-effective biodiesel production from wet microalgal biomass by a novel two-step enzymatic process.* Bioresource Technology, 2018. **268**: p. 583-591.
368. Miao, X., R. Li, and H. Yao, *Effective acid-catalyzed transesterification for biodiesel production.* Energy Conversion and Management, 2009. **50**(10): p. 2680-2684.
369. Reddy, H.K., T. Muppaneni, P.D. Patil, S. Ponnusamy, P. Cooke, T. Schaub, and S. Deng, *Direct conversion of wet algae to crude biodiesel under supercritical ethanol conditions.* Fuel, 2014. **115**: p. 720-726.
370. Zakaria, R., *Reactive extraction of rapeseed for biodiesel production*, E. University of Newcastle upon Tyne. School of Chemical, M. Advanced, and T. University of Newcastle

upon, Editors. 2010, Thesis (Ph. D.)--University of Newcastle upon Tyne, 2010.: Newcastle upon Tyne.
371. Sathish, A., B.R. Smith, and R.C. Sims, *Effect of moisture on in situ transesterification of microalgae for biodiesel production.* Journal of Chemical Technology & Biotechnology, 2014. **89**(1): p. 137-142.
372. Minowa, T. and S. Sawayama, *A novel microalgal system for energy production with nitrogen cycling.* Fuel, 1999. **78**(10): p. 1213-1215.
373. BP. *Statistical review of world energy 2019*. 2019 [cited 2019 10/07/2019]; Available from: https://www.bp.com/en/global/corporate/energy-economics/statistical-review-of-world-energy.html.
374. Davis, R., A. Aden, and P.T. Pienkos, *Techno-economic analysis of autotrophic microalgae for fuel production.* Applied Energy, 2011. **88**(10): p. 3524-3531.

Appendices

Appendix A - Calibration curve for methanol wight percentage in binary mixtures

Appendix B - Calibration curve for peristatic pumps

Appendix C - Material flow during the combined harvesting and transesterification process

Appendix A: Calibration curve for methanol wight percentage in binary mixtures

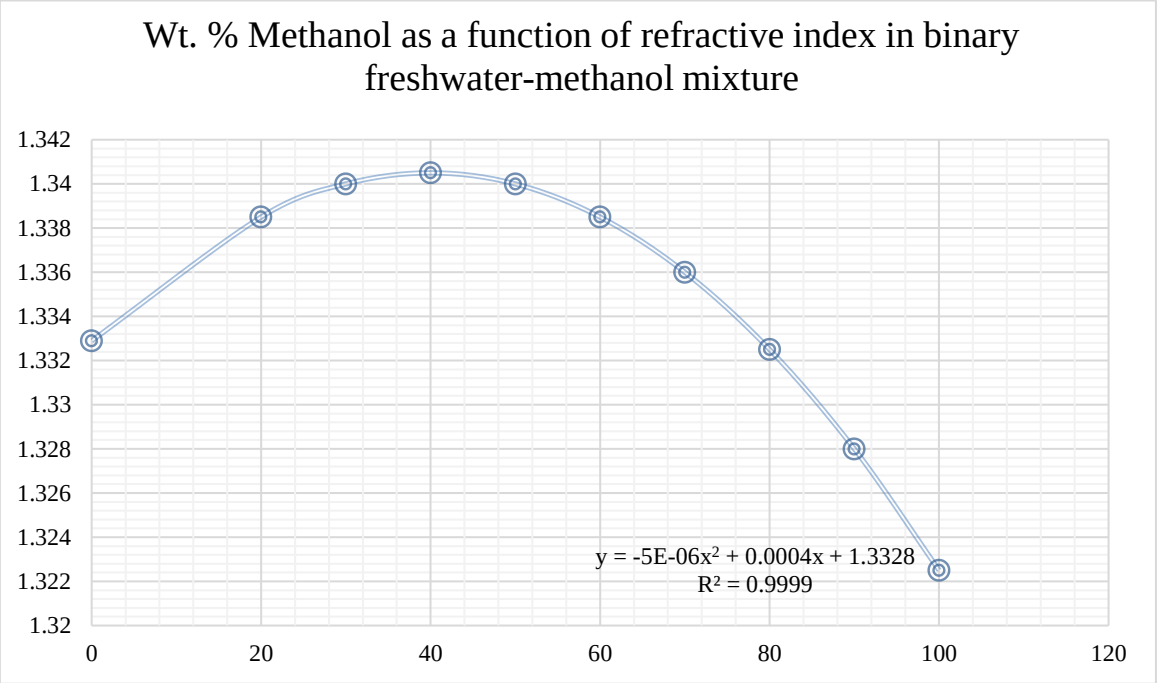

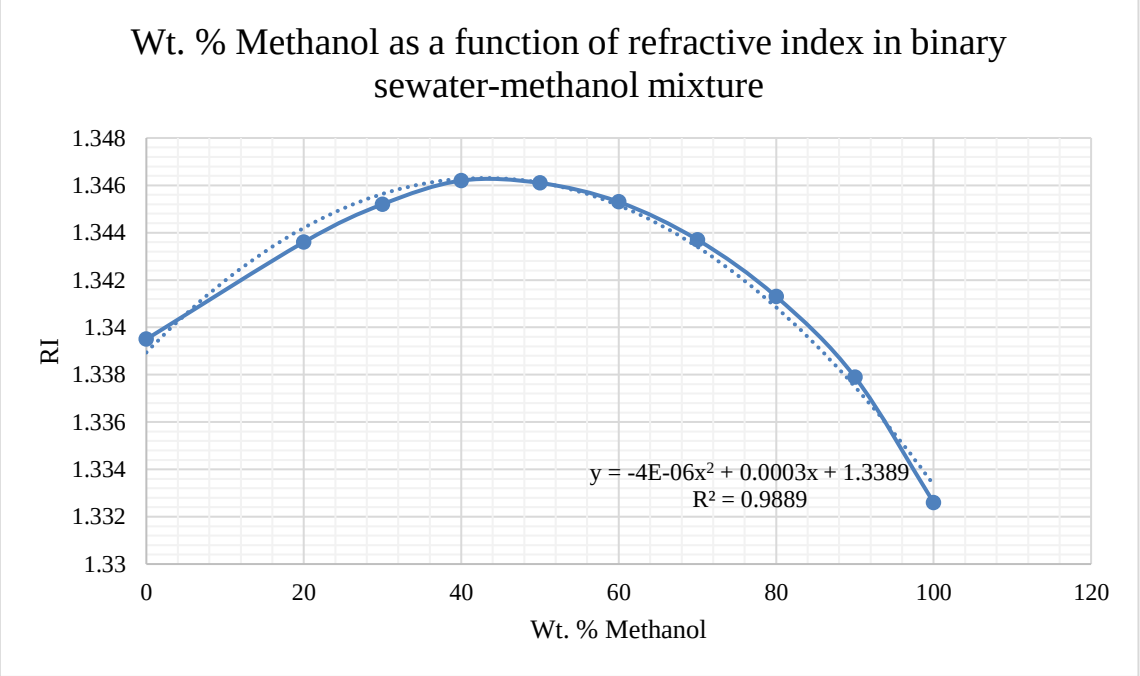

Appendix B: Calibration curve for peristatic pumps

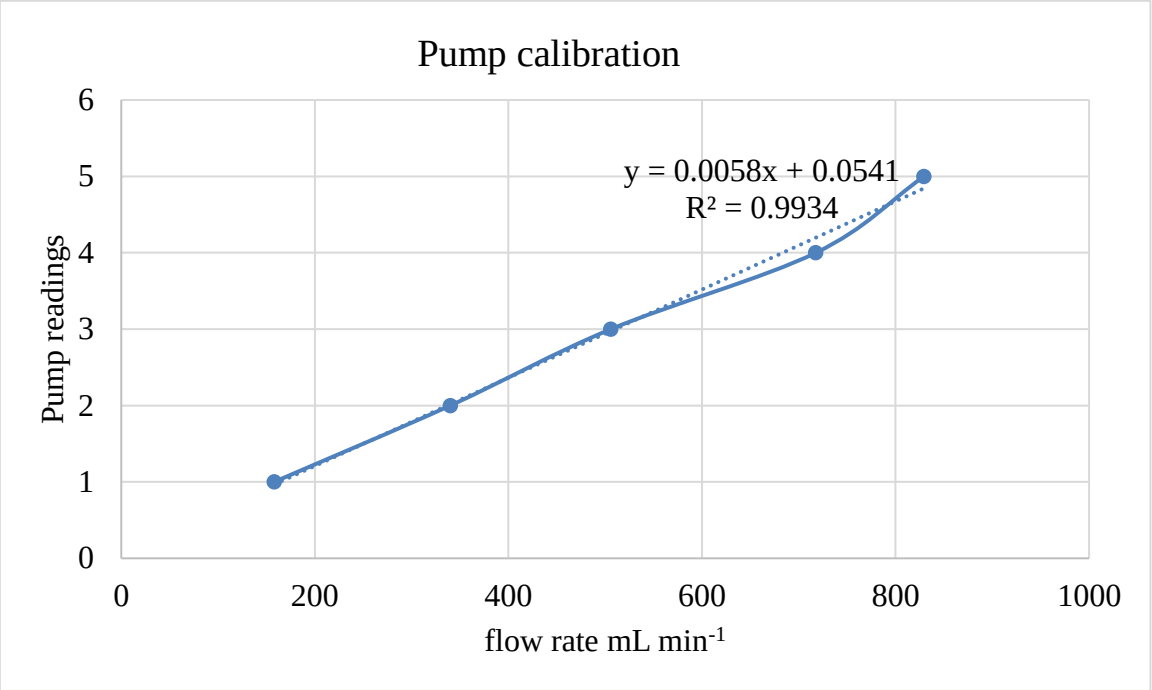

Appendix C: Material flow during the combined harvesting and transesterification process

Mass of algae (g m^{-3})	171.5500
Mass of oil (g m^{-3})	27.4480
Number of moles of oil (mol m^{-3})	0.0312
number of moles of methanol (mol m^{-3})	0.1872
Mass of methanol used (g m^{-3})	5.9961
Mass of methanol + acid supplied (g m^{-3})	8964.0340
Mass of methanol supplied (g m^{-3})	7571.7075
Mass of acid supplied (g m^{-3})	1392.3285
Excess methanol (g m^{-3})	7565.7113
Excess acid (g m^{-3})	1392.3285
Excess methanol (m^3 m^{-3} of culture)	0.00945
Excess acid (m^3 m^{-3} of culture)	0.0008
Excess methanol + acid (m^3 m^{-3} of culture)	0.0102